LEABHARLANN CHOLÁISTE NA TRÍONÓIDE, BAILE ÁTHA CLIATH | TRINITY COLLEGE LIBRARY DUBLIN
Ollscoil Átha Cliath | The University of Dublin

Terms and Conditions of Use of Digitised Theses from Trinity College Library Dublin

Copyright statement

All material supplied by Trinity College Library is protected by copyright (under the Copyright and Related Rights Act, 2000 as amended) and other relevant Intellectual Property Rights. By accessing and using a Digitised Thesis from Trinity College Library you acknowledge that all Intellectual Property Rights in any Works supplied are the sole and exclusive property of the copyright and/or other IPR holder. Specific copyright holders may not be explicitly identified. Use of materials from other sources within a thesis should not be construed as a claim over them.

A non-exclusive, non-transferable licence is hereby granted to those using or reproducing, in whole or in part, the material for valid purposes, providing the copyright owners are acknowledged using the normal conventions. Where specific permission to use material is required, this is identified and such permission must be sought from the copyright holder or agency cited.

Liability statement

By using a Digitised Thesis, I accept that Trinity College Dublin bears no legal responsibility for the accuracy, legality or comprehensiveness of materials contained within the thesis, and that Trinity College Dublin accepts no liability for indirect, consequential, or incidental, damages or losses arising from use of the thesis for whatever reason. Information located in a thesis may be subject to specific use constraints, details of which may not be explicitly described. It is the responsibility of potential and actual users to be aware of such constraints and to abide by them. By making use of material from a digitised thesis, you accept these copyright and disclaimer provisions. Where it is brought to the attention of Trinity College Library that there may be a breach of copyright or other restraint, it is the policy to withdraw or take down access to a thesis while the issue is being resolved.

Access Agreement

By using a Digitised Thesis from Trinity College Library you are bound by the following Terms & Conditions. Please read them carefully.

I have read and I understand the following statement: All material supplied via a Digitised Thesis from Trinity College Library is protected by copyright and other intellectual property rights, and duplication or sale of all or part of any of a thesis is not permitted, except that material may be duplicated by you for your research use or for educational purposes in electronic or print form providing the copyright owners are acknowledged using the normal conventions. You must obtain permission for any other use. Electronic or print copies may not be offered, whether for sale or otherwise to anyone. This copy has been supplied on the understanding that it is copyright material and that no quotation from the thesis may be published without proper acknowledgement.

A MID TO LATE HOLOCENE ENVIRONMENTAL HISTORY OF MUNSA ARCHAEOLOGICAL SITE, UGANDA

Thesis submitted for the Degree of Doctor of Philosophy
in Trinity College, University of Dublin
Department of Geography

Julius Lejju Bunny
BSc, PGDE, MSc. (MUK)

April 2005

TRINITY COLLEGE
0 5 AUG 2005
LIBRARY DUBLIN
THESIS
7702

Declaration

I hereby declare that:

This thesis has not been submitted for a degree at this or any University, and except where acknowledged, it is entirely my own work.

I agree that the library of the University of Dublin, Trinity Collge, may lend or copy this thesis on request.

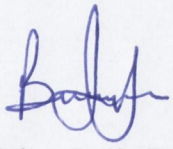

Julius Lejju Bunny

Trinity College, Dublin

January, 2005

Acknowledgments

This research was made possible with financial assistance from the National Geographic Society (NGS) through a research grant, the British Institute in Eastern Africa (BIEA) for logistical support, American Society for Stratigraphic Palynologist (ASSP) for small grants, and Trinity College, University of Dublin (TCD) for a scholarship award. This funding and support is sincerely acknowledged.

I am indebted to my supervisor Professor David Taylor for his tireless effort, support and encouragement throughout the period of the research. Special thanks also go to Ms Poonam and Sky for the hospitality rendered to me during my initial periods of stay in Dublin. Thanks are due to Professor Peter Robertshaw of California State University for his assistances in the area of archaeology and history. I am also grateful to Messer Moses Mafabi, Dismas Ongwen and Ssenfuma for their field assistance during the filed work.

I am grateful to the administration of Mbarara University of Science and Technology for the permission given to me to persue my research. Thanks are due to staff Faculty of Science with Education. The help received from staff Botany Department, Makerere University especially from Professor Ziraba-Bukenya, Professor Oryem-Origa and Dr. Patrick Muchunguzi is highly appreciated. Thanks are due to staff of National Herbarium at Makerere University for assistance with identification of plant specimens.

I would like to thank the staff of Geography and Botany Departments, Trinity College, University of Dublin for their support during my research. Thanks are due to Ms Mabel Denniston, Mr. Terry Dunne, Ms Sheila MacMorrow. Special thanks go to Ms Tara Nolan for the technical assistance rendered to me during the laboratory work. Thanks are also due to Mr. Robert Legg, and Dr. Raila Manel for the technical assistance rendered to me during my research. Many thanks also go to those who contributed in one way or another.

Thanks are due to the staff at Centre for Microscopy and Analysis (CMA) at Trinity College Dublin, The Royal Museum of Central Africa, Tervuren and Catholic University of Luven, Belgium for the permission to use their SEM facilities. Special thanks go to Dr. Luc Vrydaghs for his assistance with the identification of Musaceae phytoliths.

Finally I would like to thank Esther, Hope, Robinah and Sam for their continued encouragement throughout the period of the research. Special thanks are due to Freea Hzstein-Davey for her valuable comments.

Dedication

To Esther

Table of contents

Contents	Page
Declaration	i
Acknowledgments	ii
Dedication	iv
List of figures	xi
List of tables	xviii
List of plates	xix
List of abbreviations and acronyms	xxi
Summary	xxii

PART ONE: BACKGROUND TO THE THESIS AND STUDY AREA

Chapter one

Introduction to the thesis

1.1	Introduction	1
1.2	Aims of the thesis	1
1.3	Guiding research questions	3
1.4	Scope of the thesis	4
1.5	Structure of the thesis	4

Chapter two

Present–day environmental conditions of the Interlacustrine highlands

2.1	Introduction	6
2.2	The Interlacustrine highlands	6
	2.2.1 Geographical location	6

2.2.2 Geology, topography and drainage 8
2.2.3 Climate 10
2.2.4 Vegetation 11
2.2.4i Swamp vegetation 17

Chapter three

Background to the study

3.1 Introduction 18
3.2 Sources of evidence 18
3.2.1 Sedimentary sources of evidence 19
3.2.2 Documentary records 28
3.2.3 Linguistics and oral history 31
3.3 Environmental history of the Interlacustrine highlands, ca. 5000 yr. BP to present 33
3.3.1 Description of palaeoenvironmental sites 35
3.3.2 A summarised sediment-based mid to late Holocene environmental history for the Interlacustrine highlands based on published evidence 42
3.4 The rise and fall of pre-colonial states in the Interlacustrine highlands 45

Chapter four

Munsa archaeological site: description and field-based sampling

4.1 Introduction 51
4.2 Munsa archaeological site 51
4.2.1 Geographical location 51
4.2.2 Topography, geology and drainage 51
4.2.3 Local climatic conditions 53
4.2.4 Local vegetation 56
4.2.5 Agricultural activities 61
4.2.6 Occupation of Munsa archeological site 61
4.3 Sedimentary environments at Munsa 63
4.3.1 Location of Munsa swamps 63

4.3.2 Swamp vegetation 65
4.3.3 Munsa II swamp 65
4.4 Sampling of sediments 67
4.5 Collection and analysis of voucher specimens 70

PART TWO: METHODS AND RESULTS

Chapter five

Methods

Laboratory based analysis of sediment cores for microfossil

5.1 Introduction 72
5.2 Sediment description 72
5.3 Estimation of organic matter by loss on ignition (LOI) 73
5.4 Sediment chronology and radiocarbon dating 74
5.5 Construction of age-depth curves 75
5.6 Methods for investigating charcoal content in Munsa II sediments 76
5.6.1 Estimation of charcoal content by chemical assay method 78
5.6.2 Estimation of charcoal surface area by point count method 79
5.7 Preparation and analysis of fossil pollen and spores 83
5.7.1 Pollen identification and counting 83
5.7.2 Descriptions of fossil pollen and spores 84
5.7.3 Relative absolute abundance of pollen 95
5.8 Construction and zonation of pollen assemblage diagrams 97
5.9 Identification and enumeration of fungal spores 98
5.9.1 Descriptions of fossil fungal spores 99
5.10 Analysis of phytoliths 105
5.10.1 Extraction of voucher specimens of phytoliths from plant materials 105
5.10.2 Comparision of cross-shaped phytolith morphotypes extracted from maize (*Zea mays*) and wild grasses 106
5.10.3 Morphological characteristics of Musaceae phytoliths 112
5.10.4 Extraction of phytoliths from soil sediment 112
5.10.5 Phytolith classification and counting 113

5.10.6 Descriptions of phytolith morphotypes 115
5.19.7 Vegetation indices 124
5.10.8 Principle correspondence analysis (PCA) 126

Chapter six

Results

Results of sediment stratigraphy and chronology analysis

6.1 Introduction 127
6.2 Sediment stratigraphy of Munsa II cores 127
6.3 Results of sediment chronology and age-depth curves for Munsa II cores 129
6.3.1 Age-depth curve for M2C1 131
6.3.2 Age-depth curve for M2C2 133
6.3.3 Age-depth curve for M2C3C 133
6.3.4 Extrapolating and interpolating the ages of depths 134
6.4 Loss on ignition (LOI) results for Munsa II cores 134
6.4.1 Core M2C1 138
6.4.2 Core M2C2 138
6.4.3 Core M2C3C 139
6.5 Results of $\delta^{13}C$ isotope analysis 143
6.6 Summary of sediment stratigraphy and chronology for Munsa II 144

Chapter seven

Results of pollen and fungal spores analysis

7.1 Introduction 149
7.2 Results of pollen analysis 149
7.2.1 Pollen stratigraphy for M2C1 sediment core 149
7.2.2 Pollen stratigraphy for M2C2 sediment core 158
7.2.3 Pollen stratigraphy for M2C3C sediment core 167

7.3 Inter-core comparison of pollen data for Munsa II sediments 176
7.4 Results of fungal spore analysis 177
7.4.1 Fungal spore stratigraphy for M2C1 sediment core 177
7.4.2 Fungal spore stratigraphy for M2C2 sediment core 180
7.4.3 Fungal spore stratigraphy for M2C1 sediment core 182

Chapter eight

Results of phytolith analysis

8.1 Introduction 185
8.2 Distribution of modern phytolith morphotypes 185
8.3 Morphological characteristics used for distinguishing Musa from Ensete phytoliths 187
8.4 Fossil phytolith assemblages 188
8.4.1 Fossil phytolith stratigraphy for M2C1 189
8.4.2 Fossil phytolith stratigraphy for M2C2 198
8.4.3 Fossil phytolith stratigraphy for M2C3C 205
8.5 Inter-core comparison of phytolith data from Munsa II sediments 213

Chapter nine

Results of charcoal analysis

9.1 Introduction 215
9.2 Results of charcoal analysis for Munsa II sediment cores 215
9.2.1 Charcoal results for M2C1 215
9.2.1i Results of chemical assay method 215
9.2.1ii Results of point count method 216
9.2.2 Charcoal results for M2C2 220

9.2.2i Results of chemical assay method 220

9.2.2ii Results of point count method 220

9.2.3 Charcoal results for M2C3C 224

9.2.3i Results of chemical assay method 224

9.2.3ii Results of point count method 224

9.3 Summary of charcoal results for Munsa II 225

PART THREE: DISCUSSION AND CONCLUSSIONS

Chapter ten

Discussion

Dynamics of Munsa II, ca. 5000 yr. BP to the present

10.1 Introduction 228

10.2 Sedimentary conditions at Munsa II, ca. 5000 yr. BP to present 228

10.3 Vegetation dynamics at Munsa II, and their likely causes 231

10.4 Vegetation dynamics at Munsa, ca. 5000 yr. BP to present, within a regional context 246

Chapter eleven

Conclusions

11.1 Introduction 253

11.2 Summary of sedimentary and vegetation dynamics at Munsa II catchement ca. 5000 yr. BP to present 253

11.3 Implications of the multi-proxy records in palaeoenvironments of central and eastern Africa 258

References 260

List of Figures

		Page
Figure 2.1	Map showing location of the Interlacustrine highlands in central Africa	7
Figure 2.2	Map of Interlacustrine highlands showing topography and drainage system	9
Figure 2.3	Generalised altitudinal and moisture relationships of montane, medium and low land forest vegetation in central Africa (Adapted from Langdale-Brown *et al.*, 1964)	12
Figure 3.1	Water level fluctuations (m) of the Nile minimum summer levels since 622 AD based on decadal average and representative of long-term fluctuations of Lake Victoria due to variations in rainfall in the Interlacustrine highlands of central Africa and Ethiopian highlands (Adapted from Herring, 1979 and Nicholson, 1998)	30
Figure 3.2	Fluctuations of Lake Victoria water levels from 1890 to 2001 AD. The records are based on modern measurements at Jinja Gauge (0.5^0 N, 33^0E) (Data provided by Yin, X. 2003)	32
Figure 3.3	Comparison of major droughts and famines recorded in oral tradition with documented water levels for Lake Naivasha and the Nile River summer minimum levels (Adapted from Nicholson, 1998 and Verschuren *et al.*, 2000)	34
Figure 3.4	map showing the location of major archaeological and palaeoenvironmental sites in the Interlacustrine highlands Mentioned in the text	36
Figure 3.5	Map showing the location of major pre-colonial states in the Interlacustrine highlands of central Africa (Adapted from Sutton, 1993)	50

Figure 4.1	Location of Munsa study site and the earthwork systems (trenches) surrounding Bikegete	52
Figure 4.2	Mean annual rainfall distributions in the study area. Isohyets are in inches (Adapted from Langdale-Brown *et al.*, 1964; Atlas of Uganda, 1967)	57
Figure 4.3	Mean monthly rainfall (mm) and temperature for Mubende District for the period 1910-1970	58
Figure 4.4	Location of Munsa swamps within the earthwork systems. Inset is Munsa II swamp	64
Figure 4.5	Location of Munsa II sediment cores along a transect cut across Munsa II swamp. The stratigraphies for M2C1, M2C2 and M2C3C are illustrated	69
Figure 5.1	Construction of age-depth cures	77
Figure 5.2	Dimensions of cross-shaped phytoliths used to distinguish the Longer axis (length) from shorter axis (width), with measurements of N by N (**a**) or N by (N+2) (**b**), where N = 4.58μm (see 5.10.2)	107
Figure 5.3	Cross-shaped variants adapted from Piperno (1984) and Pearsall (1978; 2000)	111
Figure 6.1	Sediment stratigraphy for cores M2C1, M2C2 and M2C3C	128
Figure 6.2	M2C1, Age-depth curve. A linear relationship between age and depth is assumed between contiguous AMS ^{14}C dates	132
Figure 6.3	M2C2, Age-depth curve. A linear relationship between age and depth is assumed between contiguous AMS ^{14}C dates	135
Figure 6.4	M2C2, Age-depth curve. A linear relationship between age and depth is assumed between contiguous AMS ^{14}C dates	136

Figure 6.5 Extrapolated and interpolated ^{14}C age (ca. yr. BP) for cores M2C1, M2C2 and M2C3C 137

Figure 6.6 M2C1, Percentage organic matter calculated from LOI 140

Figure 6.7 M2C2, Percentage organic matter calculated from LOI 141

Figure 6.8 M2C3C, Percentage organic matter calculated from LOI 142

Figure 6.9 M2C1, dilution factor calculated from phytoliths of C_4 (Cyperaceae + Poaceae) versus sum of C_4 and C_3 (trees/shrubs) 146

Figure 6.10 M2C2, dilution factor calculated from phytoliths of C_4 (Cyperaceae + Poaceae) versus sum of C_4 and C_3 (trees) 147

Figure 6.11 M2C3C, dilution factor calculated from phytoliths of C_4 (Cyperaceae + Poaceae) versus sum of C_4 and C_3 (trees) 148

Figure 7.1 M2C1, Distribution of pollen samples for core M2C1 according to DCA axes 1 and 2. The grouping of pollen samples according to the three pollen zones discussed in the text are shown and labelled 151

Figure 7.2 M2C1, Distribution of non-local pollen types used in numerical zonation of M2C1 according to DCA axes 1 and 2 152

Figure 7.3 M2C1, down-core variations in abundances of non-local subfossil pollen taxa. A total of 32 samples were analysed, with total pollen counts ranging from 503 to 746 (mean = 544) 155

Figure 7.4 M2C1, down-core variations in abundances of local subfossil pollen and spores 156

Figure 7.5 Distribution of pollen samples for core M2C2 according to DCA axes 1 and 2. The groupings of pollen samples according to the three pollen zones discussed in the text are shown and labelled 161

Figure 7.6 M2C2, distribution of non-local pollen types used in numerical zonation M2C2 according to DCA axes 1 and 2 162

Figure 7.7 M2C2, down-core variations in abundances of non-local subfossil pollen taxa. A total of 49 samples were analysed, with local pollen counts ranging from 495 to 525 (mean = 510) 165

Figure 7.8 M2C2, down-core variations in abundances of local subfossil pollen and spores 166

Figure 7.9 Distribution of pollen samples for core M2C3C according to DCA axes 1 and 2. The grouping of pollen samples according to the three pollen zones discussed in the text are shown and labelled 169

Figure 7.10 Distribution of non-local pollen types used in numerical zonation of M2C3C according to DCA axes 1 and 2 170

Figure 7.11 M2C3C, down-core variations in abundances of non-local subfossil pollen taxa. A total of 32 samples were analysed for their contents, with counts ranging from 496 to 1849 (mean = 585) 174

Figure 7.12 M2C3C, down-core variations in abundances of local subfossil pollen and spores 175

Figure 7.13 M2C1, down-core variations in abundances of subfossil fungal spores.A total of 32 samples were analysed for their fungal spore content, with counts ranging from 205 to 211 (mean = 209) 179

Figure 7.14 M2C2, down-core variations in abundances of subfossil fungal spores. A total of 49 samples were analysed for their fungal spore content, with counts ranging from 210 to 223 (mean = 205) 181

Figure 7.15 M2C3C, down-core variations in abundances of subfossil fungal

spores. A total of 32 samples were analysed for their fungal spore content, with counts ranging from 200 to 340 (mean = 271) 184

Figure 8.1 M2C1, Biplot distribution of principle component analysis (PCA) loadings of fossil phytolith morphotypes showing the separation of C_3 plants from C_4 tall and short Poaceae 191

Figure 8.2 M2C1, Biplot distribution of principle component analysis (PCA) of fossil phytolith assemblages showing the relative distribution of forest (C_3 plants) and grassland (C_4 Poaceae) morphotypes in the three zones 192

Figure 8.3 M2C1, down-core variations in abundances of subfossil phytoliths. 32 samples were analysed for their phytolith contents and counts ranged from 503 to 582 (mean = 544) 195

Figure 8.4 M2C1, Phytolith indices, D/P = tree cover density (ligneous dicotyledons / Poacaeae morphotypes) and % Iph = aridity index (Chloridoid / Chloridoid + Panicoid). A minimum value of 30% distinguishes tall C_3/C_4 Poaceae from short C_4 Poaceae (Alexandre *et al.*, 1997) 196

Figure 8.5 M2C2, Biplot distribution of principle component analysis (PCA) loadings of fossil phytolith morphotypes showing the separation of C_3 plants from C_4 tall and short Poaceae 200

Figure 8.6 M2C2, Biplot distribution of principle component analysis (PCA) of fossil phytolith assemblages showing the distribution of forest (C_3 plants) and grassland (C_4 Poaceae) morphotypes in the three zones 201

Figure 8.7 M2C2, down-core variations in abundances of subfossil phytoliths. 57 samples were analysed for their phytolith contents and counts

ranged from 506 to 759 (mean = 577) 203

Figure 8.8 M2C2, Phytolith indices, D/P = tree cover density (ligneous dicotyledons/Poacaeae morphotypes) and % Iph = aridity index (Chloridoid / Chloridoid + Panicoid). A minimum value of 30% distinguishes tall C_3/C_4 Poaceae from short C_4 Poaceae (Alexandre *et al.*, 1997) 204

Figure 8.9 M2C3C, Biplot distribution of principle component analysis (PCA) loadings of fossil phytolith morphotypes showing the separation of C_3 plants from C_4 tall and short Poaceae 207

Figure 8.10 M2C3C, Biplot distribution of principle component analysis (PCA) scores for fossil phytolith assemblages, showing the distribution of forest (C_3 plants) and grassland (C_4 Poaceae) in the three zones 208

Figure 8.11 M2C3C, down-core variations in abundances of subfossil phytoliths. 32 samples were analysed for their phytolith content and counts ranged from 540 to 1180 (mean = 573) 211

Figure 8.12 M2C3C, Phytolith indices, D/P = tree cover density (ligneous dicotyledons / Poacaeae morphotypes) and % Iph = aridity index (Chloridoid / Chloridoid + Panicoid). A minimum value of 30% distinguishes tall C_3/C_4 Poaceae from short C_4 Poaceae (Alexandre *et al.*, 1997) 212

Figure 9.1 Comparison of charcoal results for M2C1 218

Figure 9.2 M2C1, number of charcoal particles per gram dry weight of sediment recorded for different size-classes 219

Figure 9.3 Comparison of charcoal results for M2C2 222

Figure 9.4 M2C2, number of charcoal particles per gram dry weight of sediment recorded for different size-classes 223

Figure 9.5 Comparison of charcoal results for M2C3C 226

Figure 9.6 M2C3C, number of charcoal particles g^{-1} dry weight of sediment recorded for different size-classes 227

List of tables

		Page
Table 4.1	Voucher plant materials collected at Munsa study area	71
Table 5.1	Voucher plant materials -analysed for cross-shaped phytolith morphotypes	109
Table 6.1	AMS radiocarbon dates and $^{13}C/^{12}C$ ratios ($\delta^{13}C$ ‰) values for M2C1, M2C2 and M2C3C. The AMS dates were calibrated using Calib 4.4 and calibration curve INTCAL 98 Radiocarbon Age Calibration and presented as 2-sigma calibrated age (BC/AD) at 95% probability	130
Table 8.1	The percentage distribution of cross-shaped phytoliths in each size-class category for the eleven species analysed	186

List of Plates

		Page
Plate 4.1	Bikegete surrounded by dense grass cover, mainly dominated by *Penisetum purepurium* (a) and tussock grasses (*Cympopogon afronudus, Hypherrinia rufa* and *Aspera cylindrica*) (b). Scattered tress of *Albizia* spp, *Sapium elipticum* and *Ficus* spp occur in the background	54
Plate 4.2	Rock shelters at Bikekete containing burial grounds. The area outside the rock-shelters has been cleared for agricultural purposes, and planted mainly with cassava, maize and bananas. The rocks contain a number of burial sites that have been excavated (see text for details)	55
Plates 4.3	Distribution of local vegetation at Munsa, interspersed with patches of cultivated fields (i) and (iii). In the centre of the photograph (ii) is Munsa II swamp	60
Plate 4.4	Munsa II swamp is dominated by papyrus (*Cyperus papyrus*) (a). The swamp is surrounded by agricultural land (b) mainly planted with bananas, cassava and maize	66
Plate 4.5	Sediment coring at Munsa II site during July 2001 field work. The swamp is dominated by dense papyrus (*Cyperus papyrus*) vegetation cover	68
Plate 5.1	Fossil pollen and spores extracted from Munsa II sediments	92
Plate 5.2	Fossil fungal spores extracted from Munsa II sediments	102
Plate 5.3	Characteristic features of phytoliths used to distinguish maize cross-shaped morphotype (1) from a dumbbell-shaped morphotype (2)	107
Plate 5.4	Phytolith morphotypes extracted from plant materials and fossil	

records 124

Plate 8.1 Characteristic features of Musaceae phytoliths used to distinguish *Musa* (1) from *Ensete* (2) 188

List of abbreviations and acronyms

AD	*anno Domini*
AMS	accelerated mass spectrometer
BP	radiocarbon years before present (1950)
a.s.l.	above sea level
ca.	*circa*
cal	calibrated
cm	centimetre
DCA	detrended correspondence analysis
ENSO	El Niño-Southern Oscillation
g	gram
ICPN	International Code for Phytolith Nomenclature
km	kilometre
Mt	mount
SEM	scanning electron microscope
SST	sea surface temperature
PCA	principal component analysis
yr.	year

Summary

Multi-proxy palaeoenvironmental data in the form of microfossil pollen, fungal spores, phytoliths and charcoal have provided a means of reconstructing the mid to late Holocene environmental history of the Munsa archaeological site, Uganda. The palaeoenvironmental data are discussed within a chronological framework provided by fifteen AMS ^{14}C dates; eleven of the dates are for plant macrofossils, while the other four are for bulk sediment samples. The data were extracted from sediment cores obtained from Munsa II, which is today a papyrus-dominated swamp, located within an area described by earthworks that form part of the archaeological site at Munsa.

The sediment-based data from Munsa II provide a record of environmental history at the site dating to ca. 5000 yr. BP. The sediments cored consist of accumulations of rich deposits of organic material dating to at least ca. 1000 yr. BP, which mark the onset of a sedge-dominated swamp at Munsa II. The sediment record is characterised by at least one major hiatus, which may have occurred during a period of increased discharge between ca. 3000 and 1000 yr. BP.

Evidence from plant microfossils (pollen and phytoliths) indicates the presence of medium altitude evergreen and semi-deciduous forest in the catchment for Munsa II prior to ca. 900 yr. BP (cal 1032 - 1217 AD). Both pollen and phytolith microfossil records suggest that the period from at least ca. 900 yr. BP (cal 1032- 1217 AD) marked the onset of forest decline in the catchment, while fungal spores indicate the possible presence of increased numbers of herbivores during the post-deforestation period.

Charcoal also increased in abundance, suggesting an increase in burning was associated with forest decline. Indicators of deforestation and increased herbivore numbers and vegetation fires broadly accord with the archaeological evidence for major expansions in human population levels at Munsa, from cal 1000-1200 AD.

Evidence for forest recovery and reduced herbivore numbers locally from ca. 200 yr. BP (cal 1647-1948 AD) could reflect abandonment of the archaeological site and again accord with the archaeological record, possibly during or following a period of reduced precipitation experienced in the Interlacustrine highlands of central Africa and/or a period of political upheaval in the region.

Microfossil fungal spores and phytoliths provide evidence of agricultural activities at Munsa that are not often registered in pollen records, thus supporting the case for the use of multi-proxies in palaeoenvironmental reconstruction, while inter-core differences between the three sediment cores analysed confirm the benefits of a multi-core approach. Possible evidence for the very early presence of *Musa* (edible banana) would appear to indicate that the plant or its close relative was growing in the catchment of Munsa II pre-dating ca. 4000 yr. BP, and therefore well before the date that archaeologists have presumed the plant was first introduced to Africa. This evidence also suggests that people were living around the site at Munsa long before the construction of earthworks during the second millennium AD.

PART ONE: BACKGROUND TO THE THESIS AND STUDY AREA

CHAPTER ONE

INTRODUCTION TO THE THESIS

1.1 Introduction

This chapter presents the major aims of the thesis. It outlines the guiding research questions and describes the structure adopted in the thesis.

1.2 Aims of the thesis

The primary aim of this thesis is to present the environmental history of Munsa archaeological site, Uganda, over the last ca. 5000 years. The last ca. 5000 years, and more especially the last 1000 years in what is now Uganda are associated with significant environmental (including climatic) and socio-economic changes (Sutton, 1993; Robersthaw, 1997; Schoenbrun, 1998). Notable among the variations are a transition to drier, possibly more seasonal, climatic conditions (Robertshaw & Taylor, 2000; Taylor *et al*, 2000) and the introduction of agricultural and iron smelting technologies (Sutton, 1993; Robertshaw, 1997; Schoenbrun, 1998). The first food producers in the region grew grains, mainly sorghum and millet, and herded cattle (Robertshaw, 1997; Schoenbrun, 1998), and because of their low density, left little evidence of their activities. Profound changes in socio-economic conditions, at least so far as their environmental impacts are concerned, occurred in Uganda and neighbouring parts of the wider region of the Interlacustrine highlands of central Africa from about

1000 yr. BP, and the onset of the Late Iron Age (Schoenbrun, 1993a; 1998; Sutton, 1993; 2000; Robersthaw, 1997; Schmidt, 1997).

Significant changes in land use, substantial increases in population and development of large, permanent settlements surrounded by earthworks, and the introduction of cattle rearing to an agricultural economy formerly dominated by cultivation of grains characterize the last ca. 1000 years in the Interlacustrine highlands (Sutton, 1993; Robertshaw, 1997; Schoenbrun, 1998). These changes in settlement and economic activities have been associated with the rise of states and kingdoms (Robertshaw & Taylor, 2000), which entered a period of decline towards the end of the second millennium AD (Sutton, 1993; Robertshaw, 1997; Schoenbrun, 1998; Robertshaw & Taylor, 2000). Hence, the second aim of this thesis is to utilize the available evidence to examine the extent to which the changes in settlement and related socio-economic activities, suggested for the wider region in general, are recorded at Munsa. According to the archaeological record for Munsa, the site was first occupied from around 1200 to 1300 AD and abandoned around 1500 to 1700 AD (Robertshaw, 1997). The abandonment of Munsa may have been part of major economic, political and social upheavals that brought about a shift in settlement patterns from nucleated villages to dispersed homesteads.

It has been speculated, based on evidence from other parts of the Interlacustrine highlands, that collapse of the pre-colonial states and kingdoms in the region was in part caused by environmental changes (Sutton, 1993). The environmental drivers of collapse may have included environmental degradation, arising from the over-exploitation of

natural resources locally, and climate change, notably the repeated incidence of prolonged droughts (Robertshaw & Taylor, 2000). A third aim of the thesis therefore is to determine the possible role of environmental changes in the rise, period of occupation and fall of the settlement at Munsa. As human activities are likely to have been intimately linked to environmental conditions at Munsa, through a range of interrelationships, the research presented here also examines the extent to which these activities affected local environmental conditions.

1.3 Guiding research questions

The major questions that this thesis addresses are:

- How has vegetation at Munsa changed over the last ca. 5000 years and particularly since ca. 1000 years ago?
- To what extent are environmental changes, including climatic variations, likely to have influenced changes in settlement and socio-economic conditions at Munsa?
- Is it possible to identify and date significant changes on the basis of food production at Munsa based on sedimentary evidence, and can these changes be related to processes, such as climate variation and the spread of food technologies through the Interlacustrine highlands?

1.4 Scope of the thesis

The primary focus on this thesis is to reconstruct the mid- to late-Holocene environmental history of Munsa archaeological site, Uganda, within a context of the Interlacustrine highlands of central Africa. The research on which this thesis is based integrates a range of sources of evidence. Sedimentary cores from a small papyrus–dominated swamp within the earthworked perimeter of the archaeological site at Munsa yielded multi-proxy evidence, in the form of sub-fossil pollen and spores, charcoal, phytoliths, fungal spores and AMS ^{14}C radiocarbon dates. Other sources of evidence consulted include archaeological information, historical documents and instrumental records.

1.5 Structure of the thesis

This thesis is arranged into three parts. Part one comprises the introduction and background to the thesis and the study area. Part two contains the methods and results chapters. The discussion and conclusions chapter form part three. The first chapter in part one contains the aims and objectives of the research, the guiding research questions, scope of the thesis and the structure of the thesis. The second chapter describes the present-day environment of the Interlacustrine highlands of central Africa in terms of geology, topography, drainage, climate and flora. Chapter three presents the past environmental conditions of the Interlacustrine highlands over the mid to late Holocene. It describes the sources of evidence used in this study for reconstructing the past environmental conditions in the region. Within this chapter, the socio-cultural changes in

the region during the pre-colonial period are described. Chapter four describes the present day environmental conditions of Munsa archaeological site and the field based sediment sampling.

Part two is arranged into three chapters containing the laboratory based methods, and results of the study. The procedures for sediment analysis, including dating of core sediments, are also described in the methods chapter. The third part contains two chapters comprising the discussion of the results and the thesis conclusions.

CHAPTER TWO

PRESENT–DAY ENVIRONMENTAL CONDITIONS OF THE INTERLACUSTRINE HIGHLANDS

2.1 Introduction

This chapter examines the geographical location of the Interlacustrine highlands in central Africa. Within this chapter the contemporary environment of the Interlacustrine highlands is described.

2.2 The Interlacustrine highlands

2.2.1 Geographical location

For the purpose of this study, the geographical boundary of the regional context incorporates the Interlacustrine highlands of central Africa and extends from Burundi, Rwanda and the northern part of Tanzania to northeastern Democratic Republic of Congo (DRC) and eastwards from the western rift valley into western and central Uganda to the shores of Lake Victoria (Figure 2.1). The highlands lie between $4^{0}20'$ S and $2^{0}20'$ N and $30^{0}30'$ W and $32^{0}30'$ E, and form part of the western plateau of central Africa between the eastern and western arms of the Great Rift Valley system.

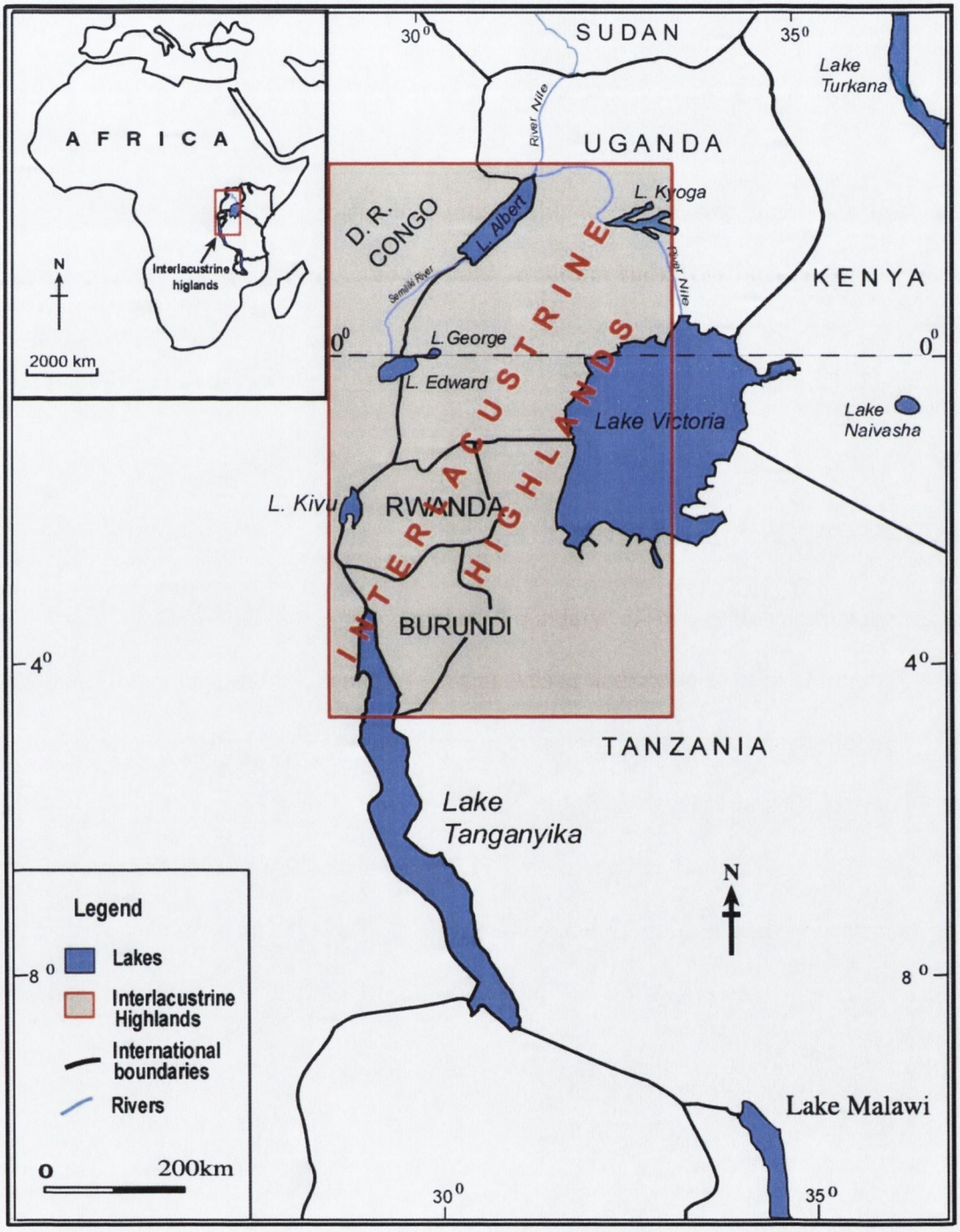

Figure 2.1 Map showing the location of the Interlacustrine highlands in central Africa.

2.2.2 Geology, topography and drainage

The Interlacustrine highlands of central Africa are generally characterised by broad similarities in topography, geology and drainage (Summerfield, 1996). The region consists largely of high plateau, and warped, denuded, uplifted Palaeozoic basement rocks, intruded by Quaternary volcanics associated with the Great Rift Valley (Nyamweru, 1996; Summerfield, 1996; Tiercelin & Lezzar, 2002). The plateau generally lies within an altitudinal range of 1000 to 2000 m a.s.l (Figure 2.2). The Great Rift Valley was formed by tectonic activity that occurred during the Mesozoic Period (Tiercelin & Lezzar, 2002) and reaches its maximum during the mid-Tertiary Period (Grove, 1986). The major tectonic events that occurred during this period resulted in the formation of the Western Rift Valley, followed by development of the Virunga volcanic mountains (Figure 2.2) during the Quaternary Period (Tiercelin & Lezzar, 2002).

One of the characteristic features of the rifting process was the development of numerous lakes along the Western Rift Valley system (Walling, 1996; Tiercelin & Lezzar, 2002). In the Kivu-Rusizi region in the south, the lakes include Tanganyika and Kivu, while in the Albertine rift region in the north, the lakes comprise George, Edward and Albert (Figure 2.2). Uplift along the shoulders of the Western Rift Valley resulted in the reversal of the previously west-flowing rivers (such as Kagera, Katonga, Kafu and Muzizi) and the creation of the basin now occupied by Lake Victoria (Hamilton, 1982; Tiercelin & Lezzar, 2002). The Nile River, which forms the eastern boundary of the Interlacustrine highlands, is the major outlet of Lake Victoria, flowing northwards from Lake Victoria through Lakes Kyoga and Albert.

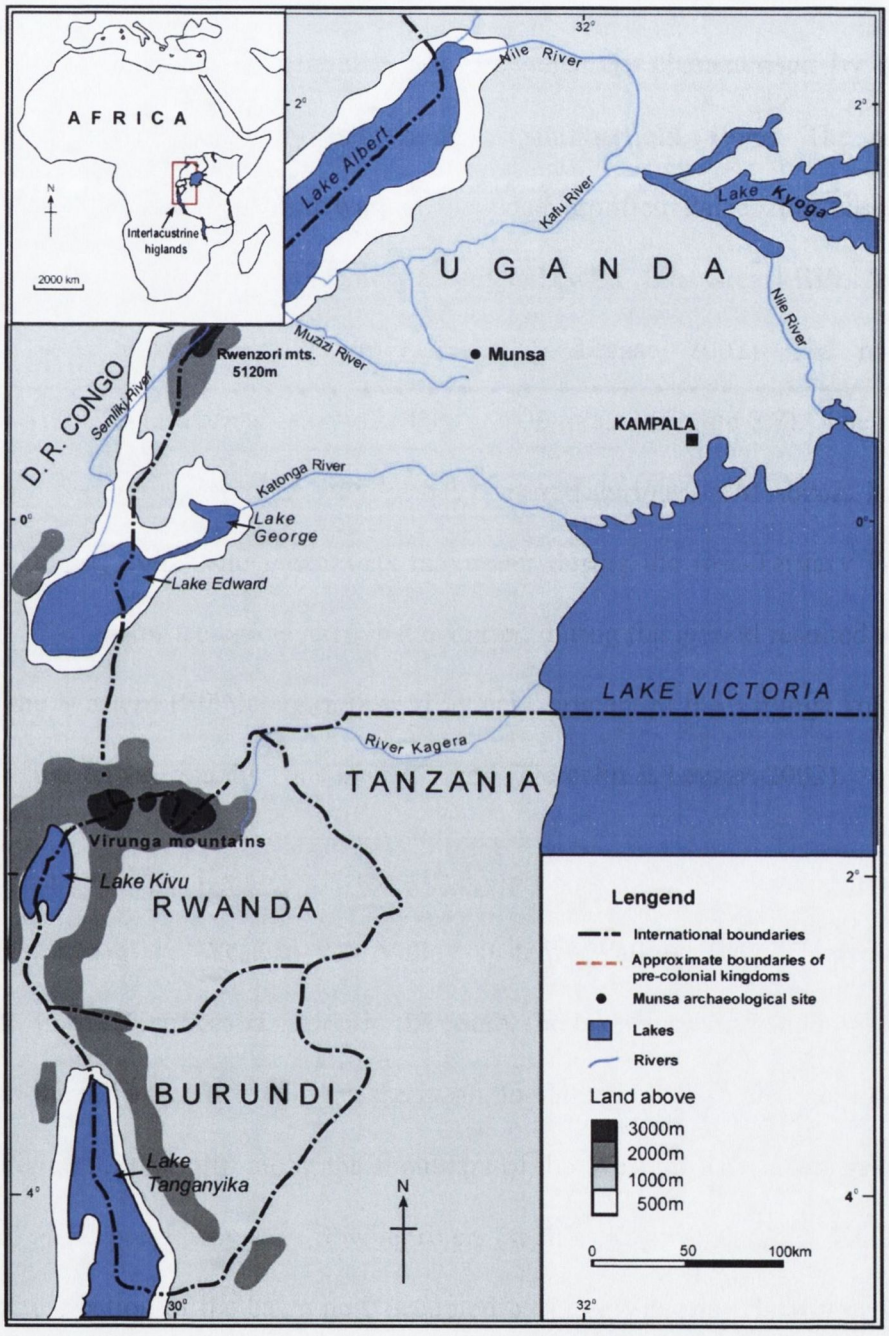

Figure 2.2 Map of Interlacustrine highlands showing topography and drainage system.

2.2.3 Climate

The climate of the Interlacustrine highlands is varied and ranges from humid through to seasonally arid conditions (Goudie, 1996; Nicholson, 1996a; b). Precipitation in the region is dependent largely upon the southern monsoon and is associated in part with the Inter-Tropical Convergence Zone (ITCZ) (Goudie, 1996; Hume, 1996; Nicholson, 1996a; b; Hume *et al.*, 2000). The movement of the ITCZ follows the position of maximum surface heating associated with the overhead position of the sun (Goudie, 1996; Nicholson, 1996b; Mistry & Conway, 2003). Climatic conditions are further modified by topography, and the proximity of the large central African lakes (Lind & Morrison, 1974).

Another important factor responsible for inter-annual variations in rainfall is the El Niño-Southern Oscillation (ENSO) (Nicholson & Entekhapi, 1986; Conway, 2002; Mistry & Conway, 2003). ENSO events are associated with exceedingly high sea-surface temperatures (SSTs) in the tropical Indian and Atlantic Oceans (Nicholson & Kim, 1997; Nicholson, 2000). Generally warm SST anomalies lead to enhanced production of rainfall in the region (Conway, 2002). The typical rainfall anomalies associated with ENSO events are intense and prolonged high levels of precipitation, as occurred between 1960 and 1963 (Flohn, 1987; Conway, 2002) and 1997-1998 (Conway, 2002), resulting in extremely wet conditions over the region. The anomalously heavy rains during the early 1960s led to rapid rises in water levels of most central African lakes. Lake Victoria, for instance, rose by 2 m in one year, causing widespread

flooding and significant outflow into the White Nile (Flohn & Nicholson, 1980; Flohn, 1987; Conway, 2002).

Much of the heavy rainfall in the southern-most parts of the Interlacsutrine highlands occurs from December to April, while north of the equator the wettest period is from March to May (Nicholson, 1994, 1996a; Stager, 2002). Temperature variability in the region is mainly influenced by changes in altitude (Davis *et al.*, 1977; Lind & Morrison, 1974). The region generally experiences a mean annual temperature of about 25^0C, with a small annual temperature range of 4^0C (Lind & Morrison, 1974; Goudie, 1996). The diurnal range in temperature, however, exceeds the annual range and the fluctuations are particularly strong at high altitudes (Davis *et al.*, 1977).

2.2.4 Vegetation

The distribution of vegetation in the Interlacustrine highlands is mainly dependent on altitude, levels of precipitation and human activities (Langdale-Brown *et al.*, 1964; Lind & Morrison, 1974). Due to human pressure, cultivated and grazed land with fragments of broad-leafed forests occupies a large part of the Interlacustrine highlands (Jolly *et al.*, 1997). Much of the region lies within a phytogeographical zone known as the Lake Victoria Regional Mosaic (White, 1983), where five distinct floras meet, namely; the Afromontane, Guineo-Congolian, Somalia-Masai, Sudanian, and Zambazian Regional Centres of Endemism. The general distribution of the vegetation types that occur in the region is presented in Figure 2.3.

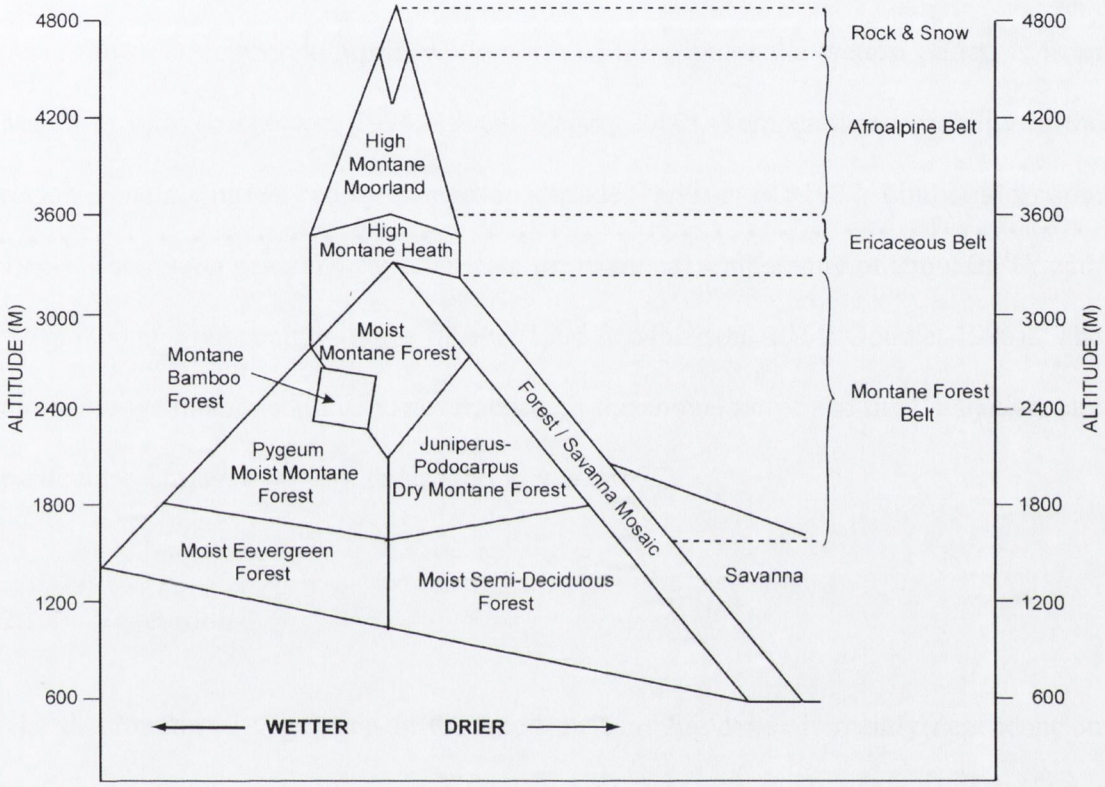

Figure 2.3 Generalised altitudinal and moisture relationships of montane, medium and low land forest vegetation in central Africa (Adapted from Langdale-Brown *et al.*, 1964).

The Afromontane Regional Centre of Endemism is composed of vegetation communities that occur mainly above 2000 m a.s.l (Hamilton, 1982; White, 1983). Hamilton (1982) describes three distinct vegetation belts within the Afromontane phytochoria of White (1983), namely; Afroalpine, Ericaceous and Montane Forest Belts. The Afroalpine Belt occurs mainly above 3600 m a.s.l on the high mountains of the region that include Mt Elgon, Virunga volcanic mountains and Mt Rwenzori (Hamilton (1982). The Afroalpine Belt, also referred to as Moorland by Langdale-Brown *et al.* (1964), is characterised by open woodland dominated by low shrubs and herbs, mainly giant *Senecio* spp and *Helichrysum* spp. in association with giant *Lobelia telekii* and *Festuca* spp. The Ericaceous Belt (Montane health) occurs below the Afroalpine Belt, mainly between 3000 and 3600 m. It is characterised by ericaceous shrubs and montane grasslands, in which members of the Ericaceae family, such as *Agauria salisfolia, Erica arborea, Philippia johnstonii* and *Vaccinium* sp. dominate along with other taxa, such as *Anthospermum*, *Artemisia afra, Cliffortia nitidula* and *Stoebe kilimandscharica.* Trees, particularly *Hagenia abyssinica*, are occasionally present.

Hamilton (1982) categorized the Montane Forest Belt into; Upper Montane Forest Zone, Bamboo Forest Zone, Lower Montane Forest Zone, and Dry Lower Montane Forest Zone. These zones are equivalent to those described by Langdale-Brown *et al.* (1964), respectively as *Hagenia-Rapanea* Moist Montane Forest, *Arundinaria*,

Montane Bamboo Forest, *Pygium* (now *Prunus*) Moist Montane Forest and *Juniperus-Podcarpus* Dry Montane Forest (Figure 2.3). In the Moist Montane Forest Zone, *Rapanea rhododendroides* and *Hagenia abyssinium* are abundant. Other common species include *Afrocrania volkensii*, *Dombeya goetzenii*, *Hypericum lanceolatum* and *Prunus africana*. The Bamboo (*Arundinaria alpina*) Forest Zone occurs between 2200 and 3000 m a.s.l on moist mountain sites and is absent in drier locations (Hamilton, 1982).

The Lower Forest Zone occurs between 1500 and 2700 m a.s.l in wetter parts of the region, and its composition bears some similarities to lowland forests (Hamilton, 1982). Vegetation in this zone is characterised by evergreen trees that include *Aningeria adolfi-friederici*, *Enandrophragma* excelsum, *Ficalhoa laurifolia*, *Olea capensis*, *Parinari excelsa*, *Podocarpus latiforlius*, *Prunus Africana* and *Syzygium guineense* (Hamilton, 1982; White, 1983). In areas where farming has been abandoned, regenerating forests are characterised by taxa such as *Hagenia abyssinica*, *Macaranga capensis*, *Neoboutonia macrocalyx* and *Polyscias fulva* (Jolly *et al.*, 1997).

The Dry Lower Montane Forest extends from 1500 m a.s.l to the boundary of the Upper Montane Forest Belt about 2700 m a.s.l, and is mainly composed of *Juniperus procera* and *Podocarpus graciliar*. Other common species include *Celtis africana*, *Ilex mitis*, *Olea africana*, and *Diospyrus abyssinica (*Langdale-Brown *et al.*, 1964; Hamilton, 1982).

To the west of the Lake Victoria Regional Mosaic, forests of Guineo-Congolian affinity are common. The mosaic includes Medium Altitude Moist Evergreen Forests and Medium Altitude Moist Semi-deciduous Forests (Langdale-Brown *et al.*, 1964; Lind & Morrison, 1974; White, 1983). The former occurs at altitudes between 1000 and 1500m a.s.l, and extends from the shores of Lake Victoria to the escarpments of the western Great Rift Valley (Langdale-Brown *et al.*, 1964). The vegetation is associated with members of the genera *Albizia*, *Celtis*, *Parinari*, *Piptadeniastrum* and *Uapaca.* Medium Altitude Moist Semi-deciduous Forests have some characteristics features of evergreen forest, but they are mainly associated with areas of reduced precipitation. They constitute members of the genera *Albizia*, *Celtis*, *Chlorophora*, *Chrysophyllum*, *Cynometra* and *Markhamia*. On the lower parts of the western escarpment of the Great Rift Valley, *Cynometra alexandria* is the dominant species, while *Chrysophyllum* and *Juniperus* are common at higher altitudes (Langdale-Brown *et al.*, 1964).

Within the Lake Victoria Regional Mosaic, areas of forest/savanna mosaic are present, extending into higher altitudes (Figure 2.3). On drier mountains sites, patches of savanna shrubs are mainly associated with fires (Langdale-Brown *et al.*, 1964). Among the common trees and shrubs are *Agauria salicifolia*, *Erythrina abyssinica*, *Faurea saligna*, *Hagenia abyssinica* and *Protea gaguedi*. The grass layer is dominated by *Andropogon dictachysus, Cymbopogon validus, Exotheca abyssinica* and *Hyparrhenia cymbaria.* At medium altitudes, the mosaic is composed of forest remnants and grass savannas dominated by *Pennisetum purpurem* (Elephant grass) (Langdale-Brown *et al.*, 1964; Lind & Morrison, 1974).

Extensive areas of savanna mosaic occur in central and south-western parts of the Lake Victoria Regional Mosaic (Langdale-Brown *et al.*, 1964). The mosaic is composed of a complex distribution of wooded and grass savannas, which has been attributed to contrasting edaphic, relief and drainage conditions (Adams, 1996) and levels of burning. To the northwest of the Lake Victoria Regional Mosaic, the forest/savanna mosaic extends into the Sudanian Regional Centre of Endemism. The latter phytochoria is characterised by woodlands composed of *Albizia zygia, Combretum binderanum*, *C. molle*, and *Terminalia glaucescens*; these woodlands are replaced by grass savanna, with *Hyparrhenia* occurring in the drier areas (Langdale-Brown *et al.*, 1964), usually as a result of human activities.

In central and south-western parts of the Lake Victoria Regional Mosaic, species of *Acacia polyacantha*, *A sieberana*, and *Albizia coriaria* dominate the woodlands, while grass savanna is dominated by *Hyperrhenia dissolute*, *H. filipendula*, *Loudetia kagerensis* and *Themedia triandra*, (Langdale-Brown, 1960; Langdale-Brown, *et al.*, 1964; Lind & Morrison, 1974). The savanna mosaic extends to the south of Lake Victoria, joining the Zambezian Centre of Endemism, in which members of the Caesalpiniaceae, such as *Brachystegia speciformis* and *B. boehmii*, are common. Other taxa represented include members of the genera *Albizia, Burkea*, *Erthrophloem, Parinari*, *Pterocarpus* and *Uapaca* (White, 1983). Large areas of these savanna mosaics currently form habitats for wildlife management, while some areas are used by pastoralists for livestock grazing.

2.2.4i Swamp vegetation

A wide range of wetland vegetation exists in poorly drained valleys, around lake margins and within depressions (Thompson & Hamilton, 1983; Hughes, 1996). Most swamps are characterised by sedges and grasses (Thompson & Hamilton, 1983). At higher altitudes the tussock forming species of sedge *Carex ruwenzoriensis* dominates the vegetation, and is replaced by the sedge *Pycerus nigricans* at lower altitudes (Morrison, 1968; Hamilton, 1982). At mid-altitudes, the sedge species *of Cyprus denudatus* and *C. latifolius* are common. Medium and low land altitude swamp vegetation is mainly characterised by dense stands of papyrus (*Cyperus papyrus*) (Lind, 1956; Morrison, 1968). In some swamps, where flooding is less common the vegetation is dominated by *Phragmites mauritianus* (Thompson & Hamilton, 1983), while in other swamps, where water is not a limiting factor, *Mischanthus violaceum, Cyperus latifolia* and *Typha australis* dominate the vegetation (Langdale-Brown *et al.*, 1964; Lind & Morrison, 1974; Thompson & Hamilton, 1983).

In areas of little human activity, swamp forest vegetation is found in some locations below 2000 m a.s.l. Swamp forests in the Interlacustrine highlands are characterised by a wide variety of species, including *Myrica kandtiana* and *Syzygium guineense* (Lind & Morrison, 1974). *Rapanea rhododendroides*, which is mainly found in mountain forests between 2300 to 3500 m, also occurs in swamp forests in central and western Uganda, in Kigezi and in lowland areas along the Lake Victoria shoreline in Masaka (Hamilton, 1991). Swamp forests species such as *Phoenix reclinata* and *Neoboutonia macrocalyx* are also common in wetlands associated with Lake Victoria.

CHAPTER THREE

BACKGROUND TO THE STUDY

3.1 Introduction

This chapter reviews the background to the thesis, placing the study within the context of the current literature. The chapter evaluates the various sources of evidence that are used in the reconstruction of the past environments and that are derived from sedimentary, archaeological, historical linguistic / oral traditions and documentary sources. Within this chapter, the environmental, cultural and socio-economic changes that are believed to have occurred during the pre-colonial and colonial periods in the wider region of interest (the Interlacustrine highlands) are described as are the most important sites where sediment-based palaeoenvironmental studies have been carried out in the past.

3.2 Sources of evidence

Environmental histories of the Interlacustrine highlands have been reconstructed mostly from sediment-based records (e.g., Livingstone, 1967; Morrison, 1968; Kendall, 1969; Morrison & Hamilton, 1974; 1982; Hamilton, 1982; Hamilton *et al*, 1986; Haberyan & Hecky, 1987; Taylor, 1988; 1990; 1993; Vincens, 1989; Casanova & Hillaire-Marcel, 1992; Marchant, 1997; Marchant *et al*., 1997; Jolly *et al*., 1994; 1997; Marchant & Taylor, 1998; Taylor *et al*., 1999; Bonnefille & Chalie, 2000; Vincens *et al*., 2003; Alin, & Cohen, 2003). However, recent interest in the use of other proxy records, such as archaeology (Reid, 1990; 1993; Robertshaw, 1997; Schmidt, 1997), historical

linguistics, oral traditions (Sutton, 1993) and meteorological data (Nicholson, 1998) offer the promise of additional and complementary information, are potentially new perspectives, especially given the possible close associations between environmental and human histories in the region (Robertshaw & Taylor, 2000; Taylor *et al.*, 2000).

3.2.1 Sedimentary sources of evidence

Sediment-based material is one of the archives that allow the reconstruction of past environmental conditions. Sedimentary materials comprise a range of proxies of past environmental conditions, including microfossils, among which pollen and spores are the most abundant (Lowe & Walker, 1997). Other microfossils include charcoal, fungal spores and phytoliths. The chemical composition, including isotopic content, of sediments can also be used to reconstruct past environmental conditions. Initially pollen analysis was the most vital tool used in the reconstruction of Quaternary environments in the Interlacustrine highlands (e.g., Livingstone, 1967; Kendall, 1969; Hamilton, 1982; Hamilton *et al.*, 1986; Taylor, 1988; Marchant, 1997; Ssemmanda & Vincens, 2002; Ssemmanda *et al.*, in press). However, the use of pollen data, in conjunction with other proxies, such as diatoms, isotopes and charcoal records, together with improved dating control (Stager *et al.* 1997, 2003; Alin *et al.*, 2003; Russell *et al.*, 2003; Thevenon *et al.*, 2003), has led to an improved understanding of long-term environmental changes and opened-up the possibility of carrying out detailed studies of relatively recent environmental histories.

Interpretation of pollen data is, however, influenced by a number of inherent and environmental factors. For instance, pollen production, preservation and dispersal often tend to affect the representation of each pollen taxa in an assemblage (Birks & Birks, 1980; Faegri & Iverson, 1989; Lowe & Walker, 1997). Some plants, for example, produce pollen grains, while others, such as bananas, rely primarily on vegetative reproduction. Plants that produce pollen are either wind-pollinated or insect-pollinated. The former often produce abundant pollen and therefore they are likely to be over-represented in the pollen assemblage compared to the latter, which produce minimal amounts of pollen. Some pollen grains are not resistant to preservation, but deteriorate as a result of physical, chemical or biological attacks on their exines, resulting in under representation in the pollen record (Lowe & Walker, 1997). Another problem in the use of pollen is the inability to identify some pollen grains beyond the family level, for example pollen produced by the Poaceae and Cyperaceae families. Some of these problems can, however, be circumvented through recourse to additional sediment-based proxies of the former environmental conditions.

Among these additional proxies, the use of remains of fungal spores to enhance palaeoenvironmental studies has been limited (e.g. van Geel *et al.* 1982-83; van Geel, 1986; 2001; Davis, 1987; Innes & Black, 2003), particularly in equatorial Africa where, the initial attempts to analyse fungal spores in lake sediments was conducted by Wolf (1966). Fungal spores are often noted in pollen slides (van Geel, 1978; 1986; 2001). The parent taxa of some fungal spores can be associated with relatively precise ecological conditions. For instance, Gaeumannomyce is associated with sedges (Cyperaceae) such as *Carex*, while *Ustulina* is associated with forest habitats (van Geel, 1986; 2001). Some

fungal species, however, and therefore the presence of their spores are indicative of the levels of moisture, while others indicate the influence of human activities, such as burning, deforestation, animal keeping (herbivore dung) and eutrophication (van Geel, *et al.* 1982-83; van Geel, 1986; Davis, 1987; van Geel, 1986; van Geel, 2001). For example, fungal spores of the dung fungi *Sporormiella* and *Cercopora* are reported to be associated with the dung of herbivores, as well as decaying wood (Ahmed & Cain, 1972; van Geel, 1986; Davis, 1987; Innes & Black, 2003). Spores of the fungus *Neurospora* indicate the occurrence locally of burning, while those of *Chaetomium* are associated with human settlements (van Geel, 1978; van Geel, 2001). However, major problems in the use of fungal spores lie in their identification and in determining their ecological indicator value. This is particularly the case in those locations where relatively little is known about the taxonomy and ecological requirements of species of fungi, as is throughout much of equatorial Africa.

As with fungal spores, phytoliths have been rarely used in the reconstruction of past environments in the Interlacustrine highlands, although when they have been used (e.g. Runge, 1995; 1999; Maitima, 1997; Wooller, 2002), they have provided useful information, especially in those locations (e.g. semi-arid environments) where other plant derived microfossils are absent or have low abundances.

Phytoliths are biogenic mineral deposits of silica ($SiO_2.H_2O$) that precipitate in and between the cells of living plants tissues (Geis, 1973; Piperno, 1988; Fearn, 1998). They occur in stems, leaves, roots and inflorescences of higher plants (Pearsall & Trimble, 1984; Piperno, 1988; Runge, 1999; Pearsall, 2000), and are abundant in the Poaceae

family, ranging from less than 1% to more than 5% of the total dry weight of an individual plant (Johnston *et al.*, 1966; Pearsall, 2000). Phytoliths have diverse and distinctive morphological characteristics (Twiss *et al.*, 1969; 1992; Piperno, 1988; Pearsall, 2000). Their sizes range from less than 2 μm to about 1000 μm (Rovner, 1971; Piperno, 1988; Alexandre & Muenier, 1994, 1999; Runge, 1995, 1999), but the majority occur within the 20-100 μm range (Alexandra, 2001).

Since its first application as a tool of environmental reconstruction in the 1970s and 1980s (e.g., Rovner, 1971; 1988; Pearsall, 1978; 1984; Piperno, 1985; 1988), phytolith analysis has become increasingly important and widely used in the field of archeology (e.g., Piperno, 1985; 1988; Bowdery, 1998; Pearsall, 2000; Elbaum & Weiner, 2003) and palaeoecology (Kealhofer, 1996; Alexandre *et al.*, 1997; 1999; Kealhofer & Penny, 1998; Barboni *et al.*, 1999). Earlier archaeological studies (e.g. Pearsall, 1978; Pearsall & Trimble 1984; Piperno, 1985) successfully applied phytoliths to identifying the presence of cultivated crops. In recent years, the application of phytoliths has enhanced the recovery of data pertaining to human and plant relationships (e.g., Mbida, 2000; 2001; Mercader, 2000; Pearsall, 2000; Boyd, 2002), and enabled the identification of the remains of plants, such as bananas, in sedimentary records that would otherwise not have been possible using pollen. Phytolith analysis thus offers additional information where the preservation of biological material is otherwise poor, and enables the reconstruction of vegetation history, for instance, in areas where arid and humid grass associations cannot be discriminated through pollen alone. For instance, it is possible to discriminate between forest (C_3 plants) and grasslands (C_3/C_4 grasses) in a sediment-based phytolith record (Alexandre *et al.*, 1997; Barboni *et al.*, 1999). Among the C_4

grasses, phytoliths can also be used to distinguish between members of the subfamily Chloridoideae (short grasses), which are adapted to warm and dry environments, members of the subfamily Panicoideae, which are adapted to warm and wet environments and members of the Festucoideae (C_3 grasses), which are adapted to cool temperate and high altitude environments (Twiss, 1992; Alexandre *et al.*, 1997; Pearsall, 2000).

The application of phytolith analysis to the reconstruction of past environments also poses a challenge, because of difficulties in enumerating, identifying, and interpreting phytolith remains. Unlike pollen and fungal spores that are part of specific reproductive structures, silica accumulating species produce different types of phytoliths, which may be shared by related or unrelated taxa (Rovner, 1971). According to Rovner (1971), different plant structures from one species may produce different shapes of phytoliths, and many plants may produce a single phytolith type, hence leading to redundancy in phytolith counts. Only a limited number of taxa are reported to be capable of producing distinctive phytolith types (Piperno, 1988; Pearsall, 2000). Furthermore, some plant taxa do not accumulate silica (Piperno, 1988; Alexandre *et al.*, 1994; Runge, 1995) and therefore their presence in the phytolith assemblages may not be detectable. In addition, as stated earlier in the text, phytoliths occur in different sizes, which often range from less than 2 μm to over 1000 μm (Rovner, 1971; Piperno, 1988; Alexandre & Muenier, 1999). During the extraction process, phytoliths are sieved through small-sized sieves to make counting easier under the microscope. As a result, rod-like bodies and sand-sized phytoliths that are greater than 7 μm may be broken into smaller particles during sample preparation, and therefore the fragments may be counted as different bodies (Runge,

1999). Finally, unlike pollen and other microfossils that can be transported over large distances, and therefore may reflect regional vegetation patterns and changes, phytoliths are often from plants found close to the site of deposition (Piperno, 1988; Pearsall, 2000). As such they are good indicators of local vegetation. However, phytoliths can under exceptional circumstances be transported over long distances, thus proving regional vegetation signal (Kurmann, 1985; Piperno, 1988). Thus the use of phytoliths, in conjunction with other plant microfossils such as pollen, can facilitates the reconstruction of past environmental conditions, particularly in those areas where ecologically or anthropogenically important plant taxa are otherwise invisible in the sedimentary record, and where variations in local vegetation have palaeoenvironmental significance.

The use of charcoal analysis has also played an important role in the reconstruction of fires histories in the Interlacustrine highlands (e.g., Maitima, 1997; Thevenon, *et al.*, 2003). Charcoal is an amorphous inorganic carbon compound, which results from the incomplete oxidation of organic plant materials (Clark, 1984; Patterson *et al.*, 1987; Bird & Gröcke, 1997). Charcoal fragments are often deposited and preserved in sediments along with other microfossils, and can be used as a basis for reconstructing past fire regimes, including the frequency, intensity and, in some cases, the location of fires, as well as the type of plant material being combusted (Waddington, 1969; Winkler, 1985; Morrison, 1994; Nichols *et al.* 2000; Scott *et al.,* 2000; Whitlock & Larsen, 2001). The amount of charcoal that accumulates at a site is, however, potentially influenced by a range of complex taphonomic factors, such as dispersal, deposition and preservation

(Clark, 1984; Patterson *et al.*, 1987; Clark, 1988a; Scott *et al.,* 2000). Many inter-related factors, which include the size of charcoal particles and wind speed, also affect the influx of charcoal to a site of deposition (Patterson *et al.*, 1987; Clark, 1988b; 1996; Morrison, 1994).

Wind and water are the primary agents responsible for transporting charcoal from source to sink (Patterson *et al.*, 1987; Clark, 1988a; Morrison, 1994; Clark & Hussey, 1996; Scott *et al.,* 2000). Small fragments of charcoal (< 50 μm) tend to be transported for longer distances by wind than large fragments (> 50 μm), which tend to be deposited closer to the source (Patterson *et al.*, 1987; Clark, 1988a; Scott *et al.,* 2000). Scott *et al.* (2000) noted that larger fragments of charcoal are mainly water borne, a fraction of which may have been mobilised through the erosion of existing sediments, and hence be secondary in origin. The size of the charcoal particles may therefore reflect the source of its origin and the mode of transport. Indeed Patterson *et al.* (1987) and Clark (1988a) noted that the size of charcoal fragments in sediments is inversely related to the distance from its source of origin. Clark (1984) noted that laboratory preparation procedures used for concentrating pollen and charcoal in sediment samples, where they involve severe chemical and physical treatments, are likely to increase the breakage of charcoal fragments. Therefore reconstructing fire histories using sedimentary charcoal can best be interpreted in conjunction with other charcoal data, which include charcoal weight, size and area, and other related proxies, such as pollen data (Whitlock & Larsen, 2001).

The chemical residue of plants preserved in sediments also have potential in the reconstruction of past environments, and one such residue, the stable carbon isotope

(^{13}C), has been used in several studies in the region (e.g., Hillaire-Marcel *et al.*, 1989; Talbot & Livingstone, 1989; Ficken *et al.* 2002). The ^{13}C isotope is an important component of organic and inorganic material (Bird & Grocke, 1997; Boutton *et al.*, 1998; Kelly *et al.,* 1998). According to Smith & Epstein (1971) and Kelly *et al.* (1998), $\delta^{13}C$ values are calculated during radiocarbon dating to correct for isotopic fractionation. Isotopic fractionation is caused by variations in metabolic incorporation of carbon and nitrogen into living tissues during photosynthesis (Bender, 1971). In the process of photosynthesis, isotopic fractionation favours the fixation of lighter ^{12}C isotopes into plants, with the result that all plants contain relatively less ^{13}C than the atmosphere (Park & Epstein, 1960). The fractionation lowers the $\delta^{13}C/\delta^{12}C$ ratio by 20 per mil for terrestrial plants and 10 per mil for marine plants (Smith & Epstein, 1971). According to Bender (1971) and Smith & Epstein (1971), photosynthetic fixation of CO_2 by terrestrial plants produces changes in the $\delta^{13}C/\delta^{12}C$ ratio because of discrimination against the heavier C isotope, resulting in the formation of C_3 and C_4 photosynthetic pathways in plants (Bender, 1971; Smith & Epstein, 1971; Cerling, 1999).

Measurements of $\delta^{13}C$ values, which are routinely carried out during ^{14}C (radiocarbon) dating, indicate that plants with the C_3 pathway, which initially fix CO_2 to a 3-C acid by carboxylation of ribulose biphosphate (Calvin Cycle), have $\delta^{13}C$ values ranging from –37‰ to –21‰, while those with the C_4 pathway, which initially fix CO_2 to 4-C acids by carboxylation of phosphoenopyruvate, have $\delta^{13}C$ values ranging from –19‰ to –8‰ (Smith & Epstein, 1971; Cerling, 1999). Plants that utilise Crassulacean acid metabolism (CAM) in the fixing of carbon are found to be functionally equivalent to C_3 plants if

they fix carbon during the day or to C_4 plants if they fix it during the night (Boutton *et al.*, 1998). Their $\delta^{13}C$ values therefore cover the range of C_3 and C_4 plants, including intermediate ratios and depend to an extent on local environmental conditions.

The distribution of C_3, C_4 and CAM-types is to some extent influenced by environmental conditions such as temperature, precipitation and levels of atmospheric CO_2 concentration (Ehleringer *et al.*, 1997; Collatz *et al.*, 1998). According to Ehleringer *et al.* (1997) and Collatz *et al.* (1998), plants using the C_4 photosynthesis pathway predominate in areas with less moist conditions or in areas with low CO_2 concentrations, whereas the C_3 pathway dominates in cool, moist conditions with high CO_2 concentrations. According to Twiss (1992), C_3 plants are widely distributed both in the tropics and temperate regions, while C_4 plants are mainly restricted to the tropics. However, within the tropics, C_4 plants tend to occur at lower altitudes, mainly below 1300 m a.s.l (Tieszen *et al.*, 1979; Livingstone & Clayton, 1980; Young *et al.*, 1983). CAM plants are typically tropical or warm temperate succulents, particularly adapted to arid or semi-arid climates (Tinga & Gibbs, 1982).

The relationship between $\delta^{13}C$ values and photosynthesis is, however, complex. Aquatic taxa such as algae and submerged higher plants yield high $\delta^{13}C$ values, being similar to those of C_4 plants. According to $\delta^{13}C$ values published by Smith & Epstein, (1971), Hillaire-Marcel *et al.* (1989) and Aucour *et al.* (1994), algae possess values ranging between –12‰ to –23‰, while some aquatic monocotyledons, including members of the Potamogetonaceae, have values between –10‰ to –5.6‰. Swamp taxa in tropical

regions such as *Cyperus papyrus* typically have high values ranging from –9.5‰ to –15.9‰ (Hillaire-Marcel *et al.*, 1989; Aucour *et al.* (1994).

In view of the potential problems associated with each of the proxy records described above, environmental reconstruction can best be conducted using multi-proxy sources to eliminate the deficiencies in the use of any one technique. Even with a multi-proxy approach, however, problems of interpretation may arise because of poor dating control. Possible reasons for poor dating control include an inadequate number of reliable radiometric dates, contamination of samples for dating either naturally or during samples collection and/ or pre-treatment, and deficiencies in the calibration procedure. Unfortunately, many of the early studies of Quaternary environmental changes in the Interlacustrine highlands were severely weakened by poor chronological control.

3.2.2 Documentary records

Long term records of water level fluctuations have provided a useful means of reconstructing the climatic history of the Interlacustrine highlands (Flohn, 1987; Nicholson, 1996a; 1998; Conway, 2002). These records are available from the Nile River and from several of the Rift Valley lakes, including Victoria, Naivasha, Tanganyika, and Rudolf. The Nile River provides the longest record of reliable measurements, covering more than the last 1000 years (Nicholson, 1996a, 1998).

Available reliable records of water levels in the Nile system date back to the early part of the seventh century AD (Figure 3.1). The measurements, which comprise minimum

and maximum water levels, have been recorded at Rodah Islands, near Cairo in Egypt, from 622 AD (Riiehl & Meltin, 1979; Hassan, 1981). The Nile River receives its water from two major sources; the White Nile, which drains most of its water from Lake Victoria, and the Ethiopian tributaries (Atbara and the Blue Nile), which drains water from the Ethiopian highlands. The maximum flood levels are reported to be indicators of precipitation in the Ethiopian highlands, while the minimum levels which relate to the early part of the Northern Hemisphere summer are though to reflect, to a degree, equatorial rainfall (Herrings, 1979; Nicholson, 1996).

The records of Nile River levels have been criticized by historians on several grounds. For example, the records at times in the past may have been modified, since the rulers of Egypt levied taxes according to river levels; periods of high levels resulted in agricultural surpluses, while low flows were associated with reduced agricultural productivity (Butzer, 1984). Another problem is that deposition of sediments in the Nile River channel at the measuring station is likely to have influenced water levels. Indeed, Riehl & Meltin (1979) noted that the Nile River bed rose by an average of 10 to 15% per century as a result of sedimentation. However, geological and archaeological evidence (Butzer, 1984; Hassan, 1981; 1986; 1997), suggest that the records are reasonably accurate. For instance, the low summer minimum levels of the Nile from about 1500 to 1600 AD and in the early 1800s AD (Figure 3.1), correspond to reduced amount of rainfall in the catchment areas of lake Victoria, as this evidence is also registered in water levels from Lake Naivasha (Verschuren *et al.*, 2000).

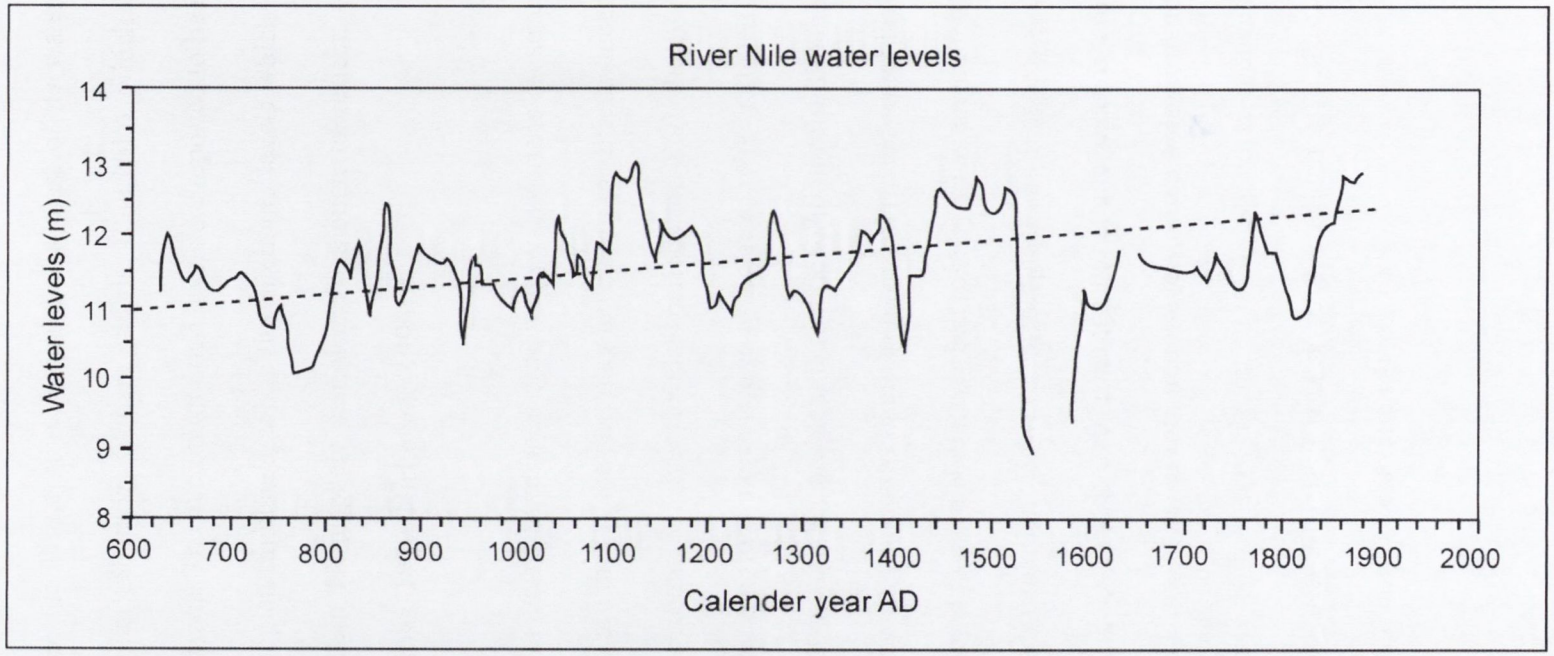

Figure 3.1 Water level fluctuations (m) of the Nile River minimum summer levels since 622 AD based on decadal average and believed to be representative of long-term fluctuations of Lake Victoria due to variations in rainfall in the Interlacustrine highlands of central Africa and in the Ethiopian highlands (Adapted from Herring, 1979 and Nicholson,1998).

Measurements of Lake Victoria water levels have been conducted at Jinja Gauge (0.5^0 N, 33^0E) since 1890 (Figure 3.2). The fluctuations in the water levels have been attributed to the variability in the amount of rainfall received in the surrounding areas (Nicholson, 1998, 2000). The records indicate that Lake Victoria maintained generally low levels from the early to mid 1900s AD, but increased sharply thereafter, reaching maximum levels in the early 1960s. The peak levels attained in the early 1960s are attributed to extremely high rainfall that occurred in the Lake Victoria catchment during 1961 and 1962 (Flohn, 1987; Nicholson, 1998; Conway, 2002). Lake Victoria levels remained high during the late 1900s, with a sharp rise between 1997 and 2000 AD, attributed to widespread rainfall that occurred in the region during 1997-1998 associated with a strong El Niño (Conway, 2002).

3.2.3 Linguistics and oral history

Accounts of major droughts recounted in oral histories have been used as a basis for climate reconstruction in the Interlacustrine highlands (Cohen, 1974; Herring, 1979; Webster, 1979; Nicholson, 1998) The accounts have, however, been criticized by many historians (e.g., Robertshaw *et al.*, 2005) for uncritical use of oral traditions in reconstructing East African climate and demographic history. However, comparisons with lake level based evidence of periods of prolonged drought in the region appears to show some commonalities (Figure 3.3), while an association in some of the oral histories of drought with famine (e.g., Webster, 1979) would appear to indicate an awareness of the vulnerability of some communities at least to past reduction in precipitation.

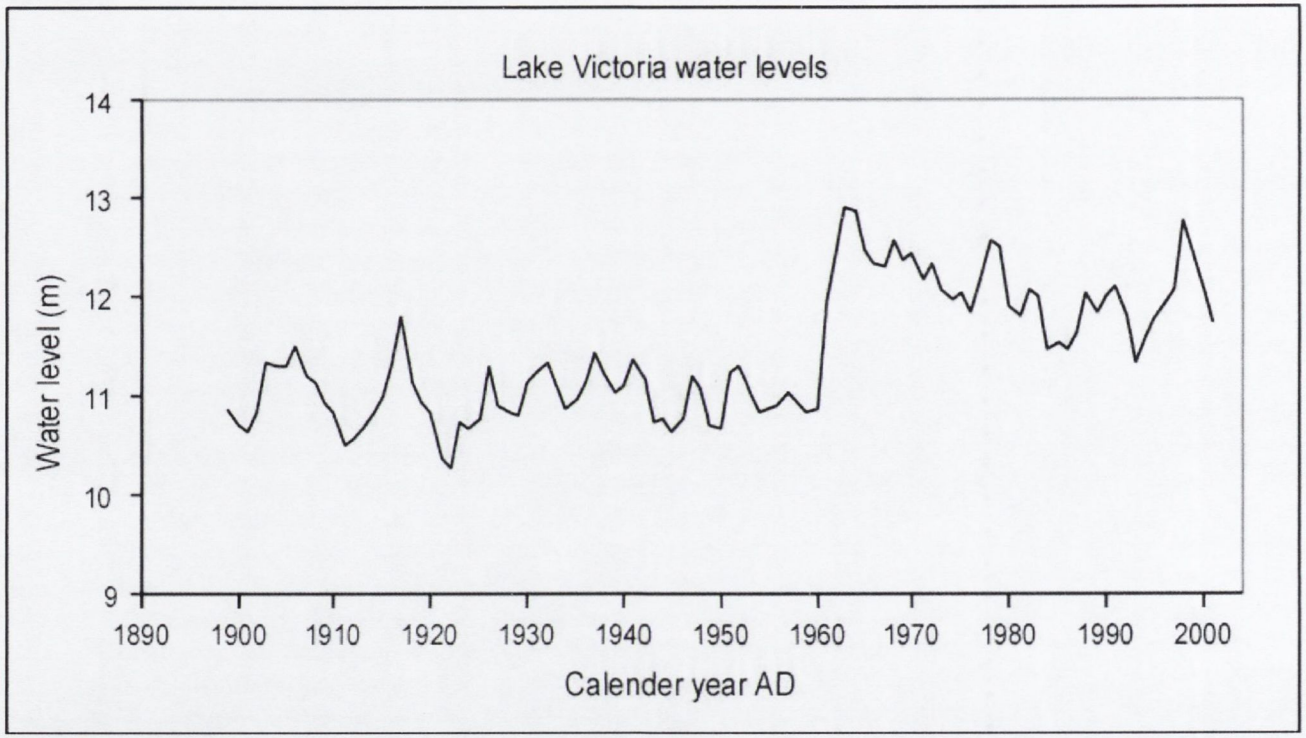

Figure 3.2 Fluctuations of Lake Victoria water levels from 1890 to 2001 AD. The records are based on modern measurements at Jinja Gauge (0.5^0 N, 33^0E) (Data provided by Yin, X., 2003)

According to oral traditions (Webster, 1979), evidence for drought induced famine, political unrest, and large scale migration of indigenous inhabitants are believed to have occurred from around 1390-1420 AD (the Wamara famine), 1560-1625 AD (the Nyarubanga famine), and 1760-1840 AD (the Lapanarat-Mahlatule famine). These famines have been found to match the reconstructed sequence of Lake Naivasha low stands (Verschuren *et al.*, 2000) and also correlate well with reconstructed Nile River summer minimum levels (Figure 3.3). The Nile levels at the period from 1390 to 1420 AD and 1560 to 1625 AD were low, suggesting a continuous period of low precipitation, with the most extreme conditions occurring in the later part of the 1500s AD and early 1600s AD (Herring, 1979).

3.3 Environmental history of the Interlacustrine highlands, ca. 5000 yr. BP to present

Late Quaternary environmental histories for the Interlacustrine highlands have been reconstructed from sediment-based records comprising swamp and lake sediments. Relatively high resolution sediment-based records of the mid to late Holocene period are of greatest interest to this thesis. Sediment-based records are documented from several sites in the Interlacustrine highlands (see Figure 3.4). including Lake Victoria (e.g., Kendall, 1969; Stager *et al.*, 1997; 2003; Ssemmanda & Vincens, 2002) and the Rift Valley lakes such as Albert (Beuning, 1997), Edward (Russell *et al.*, 2003), Kivu (Haberyan & Hecky, 1987) and Tanganyika (Casanova & Hillaire-Marcel, 1992; Alin & Cohen, 2003). Sedimentary records from permanently and seasonally-inundated bogs

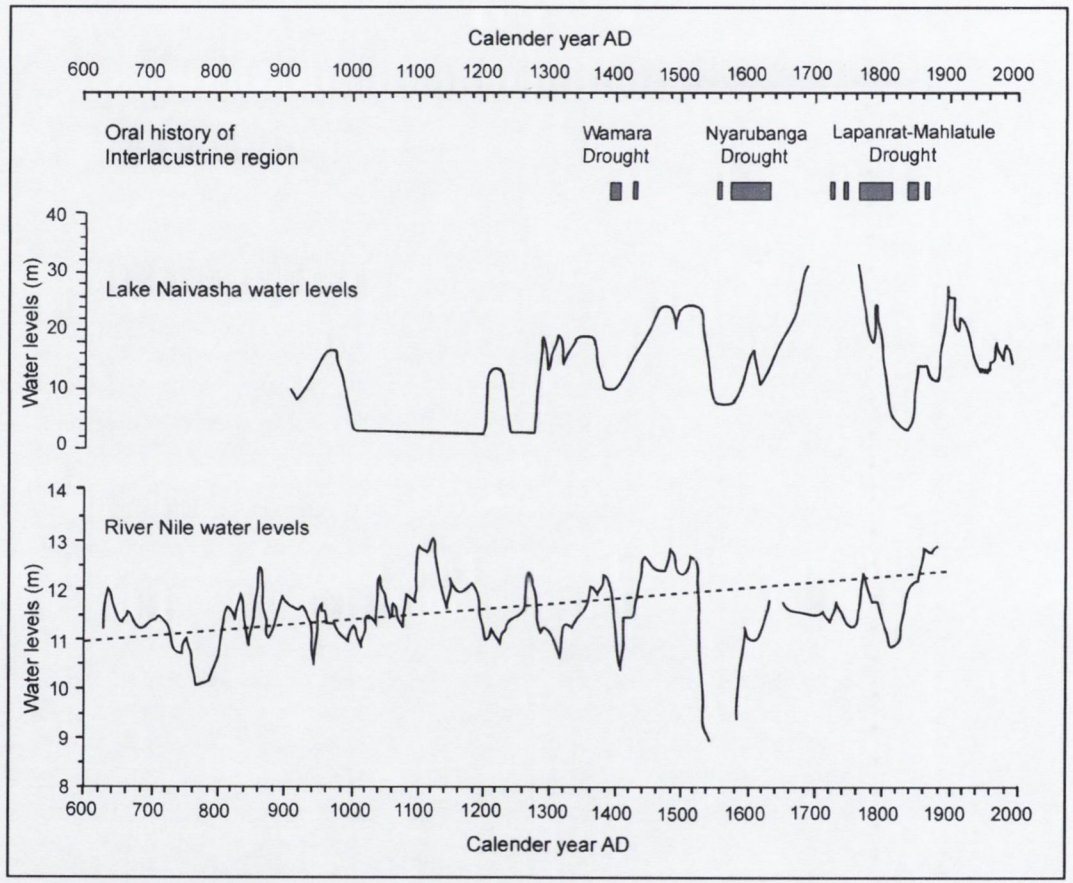

Figure 3.3 Comparison of major droughts and famines recorded in oral histories with documented water levels for Lake Naivasha and the Nile River summer minimum levels (Adapted from Webster, 1979; Nicholson, 1998 and Verschuren *et al.*, 2000).

and swamps are available from Ahakagyezi, Kabata and Muchoya (Hamilton *et al.*, 1986; Taylor, 1988; 1992; 1993; Taylor *et al.*, 1999), Kuruyange (Jolly *et al.*, 1994; 1997), Rusaka and (Bonnefille *et al.*, 1991; 1995). Brief descriptions of these sites from which, relatively highly resolved and tightly chronologically-constrained sediment-based records of mid to late Holocene environmental histories are provided below.

3.3.1 Description of palaeoenvironmental sites

Figure 3.4 illustrates the location of the sites (generally bogs, lakes and swamp) in the Interlacustrine highlands that have guided sedimentary records that are particularly relevant to this thesis because they cover, in some details, the mid to late Holocene period and because they are relevantly well-dated. The sites are described below. The descriptions are based on the location, altitude, drainage, topography and present day vegetation of the sites, and general information on the sedimentary sequence(s) obtained.

(a) Lake Victoria (altitude: 1135 m a.s.l; 1^0 S, 30^0 E to 4^0 35' E)

(i) Core P-2 (0^0 18' N, 33^0 20' E)

Core P-2 is fully described in Kendall (1969). It was obtained from Pilkington Bay (about 40 km^2) in the northern part of Lake Victoria at a depth of 19.5 m. The core was analysed for microfossil pollen data. A total of twenty eight radiocarbon dates were obtained for this core, fifteen of these dates relate to the mid to late Holocene period, with the youngest date of 860 ± 120 yr. BP. Lake Victoria covers a surface area of about 69,000 km2 and is approximately 40 to 80 m deep (Kendall, 1969). The vegetation

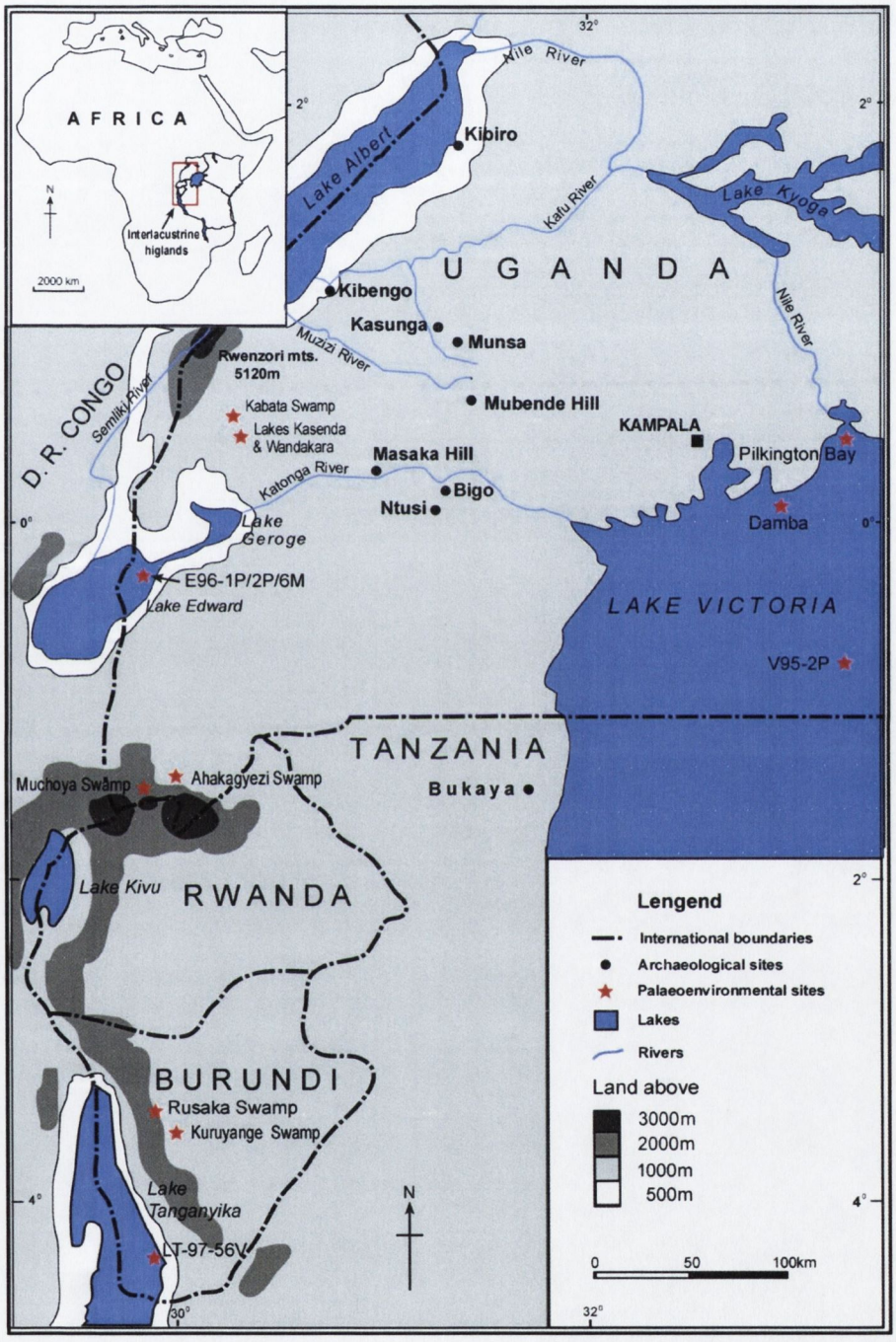

Figure 3.4 Map showing the location of major archaeological and palaeoenvironmental sites in the Interlacustrine highlands mentioned in the text.

of the basin is described by Langdale-Brown *et al.* (1964) and Kendall (1969) as comprising savanna woodland, swamp and forest mosaics. The savannas consists of members of the genera *Acacia, Albizia, Butyrospermum, Combretum*, while *Cymbopogon, Hyparrhenia* and *Loudetia* dominate among the grasses (Kendall, 1969). The swamps are dominated by the *Cyperus papyrus*.

(ii) Core 64-2 (0^0 18' N, 33^0 20' E)

Core 64-2 was collected near the mouth of Pilkington Bay in northern end of Buvuma Island, Uganda from a depth of 11 m. The detail of this core is described in Stager *et al.* (2003). The core was analysed for its diatom content. A total of thirty one ^{14}C dates were obtained from this core, fifteen of these dates relate to the mid to late Holocene period, with recent most date of 385 ± 60 yr. BP. The vegetation of the shoreline near the coring site is reported to be dominated by papyrus swamps (Stager *et al.*, 2003). Lake Victoria is reported to be sensitive to regional climatic changes (Kendall, 1969; Stager *et al.*, 1997; 2003), and these changes are often registered in the water levels. A change in lake level is reported to affect the chemical and degree of turbulence of the water, and thus the distribution of diatom species in the lake (Stager *et al.*, 1997; 2003).

(iii) Core V95-29 (0^0 58' N, 33^0 27' E)

Core 95-2P is fully described in Ssemmanda & Vincens (2002). The core was recovered from Lake Victoria at a depth of 67 m. Pollen data were obtained from the upper part (3.78 m) of the core to interpret human activities and climate in the region (Ssemmanda

& Vincens, 2002). Five radiocarbon dates were obtained for this core, three of these dates relate to the mid to late Holocene period, with most recent date of 1450 ± 61 yr. BP.

(b) Lakes Kasenda and Wandakara (altitude: 1170 m and 1260 m a.s.l; 0^0 5' S, 30^0 15' E)

Lakes Kasenda and Wandakara are described in Ssemmanda *et al.* (2005), and are small crater lakes located within the western arm of the Great Rift Valley in western Uganda. The catchment areas of these two lakes are reported to be largely cultivated with crops that include bananas (*Musa* spp), yams (*Dioscorea* spp), maize (*Zea mays*), and also contain non-cultivars associated with agriculture, such as with commons weeds such as castor oil (*Ricinus communis*). The catchment is characterised by vegetation that includes *Teclea nobilis*, *Diospyros sp.*, *Croton sp.*, *Celtis sp.*, *Polyscias fulva*, and *Ficus brachylesis*, and *Acalypha.* A total of four AMS radiocarbon dates were obtained from the sediment cores extracted from the two lakes. All these dates relate to the late Holocene, the oldest being 1250 ± 50 yr. BP.

(c) Lake Edward (altitude: 912m a.s.l; 0^0 40 S', 29^0 20' - 29^0 50' E)

(i) Cores E96-1/2P, E96-5/6M

Lake Edward is described in Laerdal *et al.* (2002) and Russell *et al.* (2003). The lake has a surface area of abound 2325km^2 and a maximum depth of 117 m a.s.l. Four sediment cores (E96-1, E96-2P, E96-5M and E96-6M) were collected from this lake at depths ranging from 12 cm to 60 cm (Russell *et al.*, 2003). The cores were analysed for diatom

content. A total of twenty nine ^{14}C dates were obtained from the cores, with twenty seven dates relating to the mid to late Holocene period. The vegetation of the area lies within the phytogeographical region of Lake Victoria Regional Mosaic (White, 1983). The vegetation around the area is composed of moist thickets of savanna mosaic dominated by acacia woodland (Langdale-Brown *et al.*, 1964).

(d) Lake Tanganyika, LT-97-56 (altitude: 700 m a.s.l; 5^0 46' S, 29^0 56' E)

(i) Core LT-97 (5^0 46' N, 29^0 56' E)

Lake Tanganyika is a large lake covering a surface area of about 32,600 km^2 and is ca. 1470 m deep at its deepest point (Alin & Cohen, 2003). The surface level of the lake is reported to fluctuate in response to both climatic and geomorphic factors (Haberyan & Hecky, 1987; Alin & Cohen, 2003). According to the vegetation description map of Africa (White, 1983), Lake Tanganyika lies with the Zambezian Regional Centre of Endemism. The vegetation of the area is composed of miombo woodland dominated by species of *Brachystegia* (Caesalpiniaceae). Core LT-97-56 of 356 cm long was collected from a water depth of 56 m. A total of ten radiocarbon dates were obtained from this core. Nine of these dates relate to the mid to late Holocene period, with the youngest radiocarbon date of 323 ± 46 yr. BP. Samples for the core were analysed for their ostracodes content in order to reconstruct lake level history (Alin & Cohen, 2003).

(e) Kabata swamp (altitude: 1370 m a.s.l; 0^0 29' N, 30^0 16' E)

Kabata swamp is fully described in Taylor (1999). The swamp is reported to be a small, in-filled volcanic crater with a very limited catchment set within an area of settled agricultural land in western Uganda. The vegetation is reported to be dominated by sedges, ferns and *Miscanthus violaceus*. A fringing band of *Cyperus papyrus* with a few isolated shrubs of *Myrica kandtiana* is also reported as occurring at the site. Most of the land surrounding the swamp is under cultivation (Taylor *et al.*, 1999). Six radiocarbon dates (5 AMS) were obtained from a 5.97m long core of the sediment (Ka) collected from the centre of the swamp. Five of the radiocarbon dates relate to the last mid to late Holocene period, with most recent being 400 ± 50 yr. BP.

(f) Ahakagyezi Swamp (altitude: 1830 m a.s.l; 1^0 5' S, 29^0 54' E)

Ahakagyezi swamp, which covers an area of approximately 1.5km^2, is located in the Rukiga Highlands of southwestern Uganda (Taylor, 1988; 1993). It is part of a large basin set within a mosaic of intensively cultivated fields, planted wood-lots and regenerating shrubs (Taylor, 1993). Before much of the swamp was drained and converted into pasture and agricultural land (Taylor, 1993), vegetation on the swamp would have been composed of *Miscanthus violaceus*, *Cyperus papyrus* and *Typha* sp. Remnants of swamp forest exist at the site and *Myrica kandtiana* and *Syzygium cordatum* are common components of these remnants. Two cores (AH1 and AH2) were collected from Ahakagyezi swamp. A total of 10 radiocarbon dates have been obtained

from core, AH2 (Taylor, 1993). Five of the ^{14}C dates relate to mid to late Holocene, with most recent being 1080 ± 70 yr. BP.

(g) Muchoya Swamp (altitude: 2260 m a.s.l; 1^0 15' S, 29^0 48' E)

Muchoya swamp is described by Taylor (1988; 1992; 1999). It is situated within Euchoya Forest, which is dominated by mountain bamboo (*Arundinaria alpine*) and scattered montane forest tress such as *Macaranga capensis*, *Neoboutonia macrocalyx* and *Polyscias fulva*. The swamp is located in a valley that occupies an area of approximately $8km^2$. Much of Muchoya swamp is reported to be prone to frequent fires that occur in the area (Taylor, 1992). The swamp surface is dominated by the tussock-forming sedge *Pycreus nigricans*, which regenerate rapidly following burning. The northern part of the swamp, where fires are believed to be less common, supports woodland containing tree heathers (*Erica kingaensis*), giant lobelia (*Lobelia mildbraedii*) and *Myrica kandtiana.* Four cores were collected from Muchoya swamp and fourteen radiocarbon dates were obtained from the longest (M2C1) of these cores. Five of the ^{14}C relate to the mid to late Holocene, with the most recent being modern.

(h) Rusaka Swamp (altitude: 2070 m a.s.l; 3^0 26' S, 29^0 37' E)

Rusaka is described by Bonnefille *et al.* (1995) as a small swamp with a catchment area of about 1 km^2. The adjacent hill slopes are reported to be covered by crops and the swamp has been drained for agricultural land. The swamp is located on the south-eastern slopes of the Burundi highlands, and lies within the montane forest belt, which is

characterised by *Entandrophragma, Macaranga*, *Neoboutonia*, *Parinari*, *Polysia* and *Prunus*. A 10m core (Ru-3) was taken from the swamp using a Russian corer (Bonnefille *et al.* (1995) and a total of 15 radiocarbon dates were obtained, all of which relate to the mid- to late Holocene period.

(i) Kuruyange Swamp (altitude: 2000 m a.s.l; 3^0 35' S, 29^0 41' E)

Kuruyange swamp is described in Bonnefille *et al.* (1991) and Jolly *et al.* (1994; 1997). The swamp is situated in eastern Burundi with a poorly drained valley. The vegetation within the adjacent hills is reported to be characterised by remnants of broad-leaved trees, and part of the swamp has been drained for agricultural land (Jolly *et al.*, 1994). Three cores (Ku1, Ku2 and Ku3) were collected from the swamp (Jolly *et al.*, 1994). A total of twelve ^{14}C dates were obtained form core Ku2, with seven dates relating to the mid to late Holocene period.

3.3.2 A summarised sediment-based mid to late Holocene environmental history for the Interlacustrine highlands based on published evidence

The climate history of the region from ca. 5000 yr. BP to the present is registered in all the sediment cores described above, and in the instrumental records of variations in the levels of the Nile River (Adamson *et al.*, 1980) and lakes such as Victoria (Nicholson, 1998). Some of the evidence of past climates, for instance in the form of records of past water levels in lake basins and river channels, is relatively direct. In other cases, such as in the case of vegetation histories, the evidence is in the form of ecological and

ecosystem responses to climate changes in the past. Some of these ecological and ecosystem response to climate change, however, will have been increasingly influenced by human activity during the Holocene, and thus become increasingly difficult to disentangle from anthropogenic signals in the sedimentary record (see Taylor & Robertshaw, 2001).

Sedimentary records from Lake Tanganyika (Haberyan & Hecky, 1987; Cohen *et al.*, 1997; Alin, & Cohen, 2003), Lake Victoria (Stager *et al.*, 1997, 2003), Lakes Edward and George (Laerdal *et al.*, 2002; Russell *et al.*, 2003) suggest a period of relatively drier climatic conditions between ca. 5000 and 2000 yr. BP. Water levels in lakes Kivu and Tanganyika are reported to have dropped to relatively low levels between ca. 3500 and 2000 yr. BP (Haberyan & Hecky, 1987; Casanova & Hillaire-Marcel, 1992; Alin, & Cohen, 2003), while Lake Victoria diatom records indicate low water levels between 2200 and 2000 yr. BP (Stager *et al.*, 1997, 2003). The central African region experienced a return to relatively moist environmental conditions after ca. 2000 yr. BP (Cohen *et al.*, 1997; Stager *et al.*, 1997, 2003; Laerdal *et al.*, 2002; Russell *et al.*, 2003).

Pollen records from the Interlacustrine highlands (Vincens, 1989; 1991; Taylor, 1990; 1993; Marchant *et al.*, 1997; Jolly *et al.*, 1994; 1997; Taylor *et al.*, 1999; Bonnefille & Chalie, 2000) indicate a marked change in vegetation composition and distribution during mid to late Holocene from ca. 4000 yr. BP to present. Tropical montane forest vegetation (Bonnefille & Riollet, 1988; Taylor, 1993; Bonnefille *et al.*, 1995; Jolly *et al.*, 1995) experienced a marked transition from moist montane forest vegetation to a drier type of forest vegetation, in which *Podocarpus* was a common component from about

3500 yr. BP. During this same period, areas around Lake Victoria (Kendall, 1969; Ssemmanda & Vincens, 2002) experienced a decrease in evergreen forest replaced by semi-deciduous forest. This was followed by a progressive decline of semi-deciduous forest replaced by grass dominated vegetation cover after ca. 2000 yr. BP to present.

All pollen records from the region indicate the presence of more open forest vegetation after ca. 2000 yr. BP, and this has been attributed to human-induced forest disturbance (Kendall, 1969; Ssemmanda & Vincens, 2002). Evidence for forest clearance is recorded for the Rukiga highlands at ca. 2200 and 800 yr. BP (Taylor, 1990; 1993). These phases of forest clearance were thought to relate to technological innovation among the developing communities in the region (Taylor, 1990). Clearances of forest in the Rukiga highlands appear, from the sediment records, to have been associated with fire (Taylor, 1990, 1993). Similarly, but subsequently, a phase of increased forest clearance was also associated with a marked increase in the amount of charcoal in sediments from Kabata swamp, dated ca. 400 yr. BP (cal 430 – 643 AD) (Taylor, 1999). Disturbances of forest in the Interlacustrine highlands, during the late Holocene, associated as they often are with indications of increased burning, presumably represent the impacts of early farmers in the region. The introduction of agriculture to the Interlacustrine region is commonly associated with Bantu-speaking people who are reported to have spread throughout much of central African after ca. 3000 yr. BP (Schoenbrun, 1998).

3.4 The rise and fall of pre-colonial states in the Interlacustrine highlands

Early archaeological research in the Interlacustrine highlands conducted during the 1960s (e.g., Lanning, 1953; 1955; 1960; Posnansky, 1969) was intended to assist in the interpretation of oral traditions (Posnansky, 1969). However, extensive investigations at several, major archaeological sites in the region since the early 1990s (e.g., Reid, 1990; 1993; Sutton, 1993; Robertshaw, 1994; 1997; Schmidt, 1997) has focused more on developing understanding of the origins and evaluation of pre-colonial states, and antecedent socio-economic conditions and settlement patterns. Archaeological and linguistic evidence suggest that the movement of early communities into the Interlacustrine highlands from around 3000 yr. BP marked the spread of iron technology and development of agriculture, and the onset of the Late Iron Age, about the beginning of the second millennium AD, marked the beginning of social, political and economic changes in the region (Schoenbrun, 1993a; Sutton, 1993; Robertshaw, 1997; Schmidt, 1997).

According to Schoenbrun (1993a) and Schmidt (1997), southern Cushitic pastoralists had settled the southern shores of Lake Victoria (northern Tanzania) from about 3000 yr. BP and by 2500 to 2000 yr. BP, mixed pastoralism is reported to have become established in the region (van Norton, 1979). Linguistic evidence suggests that the period dated to 3000 yr. BP marked the arrival of early Bantu-speaking communities from West Africa (Vansina, 1984), who are believed to have settled in Kivu Rift region in Rwanda and the eastern part of Kagera River in Buhaya, northern Tanzania (Vansina, 1984; Schoenbrun, 1993a; Schmidt, 1997). Unlike the Cushitic pastoralists, the early

Bantu–speaking communities were reported to have concentrated in the wetter areas of the region and to have practiced a mixed economy combining fishing, hunting, and iron working (Vansina, 1984; Schoenbrun, 1993a; Schmidt, 1997).

According to archaeological evidence (Schmidt, 1997), there was an expansion in iron and food production as Bantu-speaking populations increased towards the end of the first millennium BC. This resulted in diversification of the subsistence economy. During this period, the Bantu-speaking people were believed to have interacted with Cushitic-speakers living in the Karagwe region neighbouring central Buhaya (Schmidt, 1997), and such interactions would have diversified their subsistence economy considerably. Cereal crops, such as sorghum, gained popularity along with cattle to meet the demand of the growing population (Schoenbrun, 1993a; b; Schmidt, 1997). According to Schmidt (1997), by the beginning of the first millennium AD, Bantu-speaking populations experienced rapid socio-cultural changes, based on increased wealth and demand for natural resources for forest resources for both agriculture and iron smelting. This prompted some communities to move north and established settlements in the central plateau such as Bukaya, where competition for resources and agricultural land was less intense. Increased resource scarcity may also have eventually driven technological changes that are evidently in the archaeological record as the transition between the early and late Iron ages in the region (Taylor, 1990; 1993), ca. 1000 yr. BP.

Schmidt & Childs (1985) and Schmidt (1997) suggest that between 300 and 500 AD the iron producing groups in Buhaya as well as in Rwanda had increased the scale of iron production and exploited the forest resources along the once resource-rich Lake Victoria

shore-line in northern Tanzania. By 600 AD, the production of iron around the northern shore-line of Lake Victoria had declined, possibly forcing some communities to move further north to and settle in more open woodland and grassland environments, where they adopted pastoralism as their major economic activity (Schmidt, 1997). Increased reliance on pastoralism in those climatically more dry, grasslands and woodlands become the basis for the centralised polities focussed on settlements at for examples Ntusi and Bigo after 1000 AD (Reid, 1990; Schmidt, 1993; Schoenbrun, 1993a; b; Sutton, 1993; 1998; 2000). The subsistence basis of the inhabitants such as at Ntusi, comprised both pastoralism and agriculture, mainly cattle herding and the cultivation of cereals such as millet (Sutton, 1993, 2000; Schoenbrun, 1998).

The establishment and growth of permanent settlements in those areas between 1000 and 1200 AD (Reid, 1990; Sutton, 1993; 2000), which were also partly reliant on the production of cereals (Sutton, 1993, 2000; Schoenbrun, 1998), must have placed severe pressure on natural resources, including forest products and soils, in surrounding areas (Robertshaw & Taylor, 2000). During this same period, increased population densities in more forested areas (that eventually became part of the pre-colonial kingdom of Bunyoro), situated north of the Katonga River, also occurred (Robertshaw, 1997; Robertshaw & Taylor, 2000). The settlement at Munsa in Bunyoro was set within an extensive system of earthworks, constructed around 1300 to 1400 AD (Robertshaw, 1994; 1997). The site is centred on a hill (Bikegete) and includes evidence of iron-working, cattle-herding, cereal production and human burials (Lanning, 1955; Robertshaw, 1997).

According to archaeological evidence, the settlements located to the south of Katonga River such as that at Ntusi declined around 1300 AD (Reid, 1990). One possible reason for the decline is changes in environmental conditions including environmental degradation (Sutton, 1993; Robertshaw & Taylor, 2000; Taylor *et al.*, 2000). The decline of settlements such as Ntusi coincides with a phase of low River Nile water levels (Fig. 3.1), suggesting increased aridity in the region from around 1300 AD, which might have caused reduced grassland productivity for cultivation and grazing (Robertshaw & Taylor (2000). The decline of permanent settlements north of the Katonga River, such as that at Munsa (Robertshaw, 1997), around the end of the 1600 AD to the beginning of 1700 AD may have also been linked to environmental changes, as this decline appears to have occurred during a phase of relatively reduced precipitation, as evidenced by the River Nile records (see Figure 3.1) According to Robertshaw & Taylor (2000) and Taylor *et al.* (2000), however, abandonment of Munsa during this period may also have been part of major economic, political and social upheavals that brought about a shift in settlement patterns generally in the region from nucleated settlements to dispersed homesteads. This period is reported to mark the initial phase of the rise in pre-colonial states/kingdoms such as Bunyoro, Buganda, Toro and Ankole (Figure 3.5). However, one problem in attempts to link socio-economic and settlement changes in the Interlacustrine highlands with evidence of concurrent environmental changes, has been the great geographic and ecological differences that have existed between the two major sources of direct evidence: archaeological and palaeoenvironmental. The former is located in mid-altitude areas, whereas the latter has tended to be restricted to highland parts of the region or to lakes within huge catchment areas (and therefore, there is great

uncertainty in the specific geographic source of the evidence). Instead, the research presented in this thesis, in that it combines palaeoenvironmental and archaeological evidence from same site aims to address this problem.

By the 1800s AD, the pre-colonial states had become established in the Interlacustrine highlands, with well organised social, economic and political functions (Robertshaw, 1999; Doyle 2000). Agriculture was the major economic activity. Bananas were reported to be the staple food in the Buganda region, while in Bunyoro finger millet was the main staple, with few domestic animals (Schoenbrun, 1998; Robertshaw, 1999). The arrival of early European explorers in the region in the mid 1800s AD (Robertshaw & Taylor, 2000) marked the establishment of colonial rule in the region. This resulted in a political tension between the neighbouring states of Buganda and Bunyoro. The conquest of Bunyoro in the late 1890s by colonial-led forces led to the collapse of the kingdom and subsequent declines in population which had already experienced severe epidemics and other pressures during the 1800s AD (Doyle, 2000; Robertshaw, 2005).

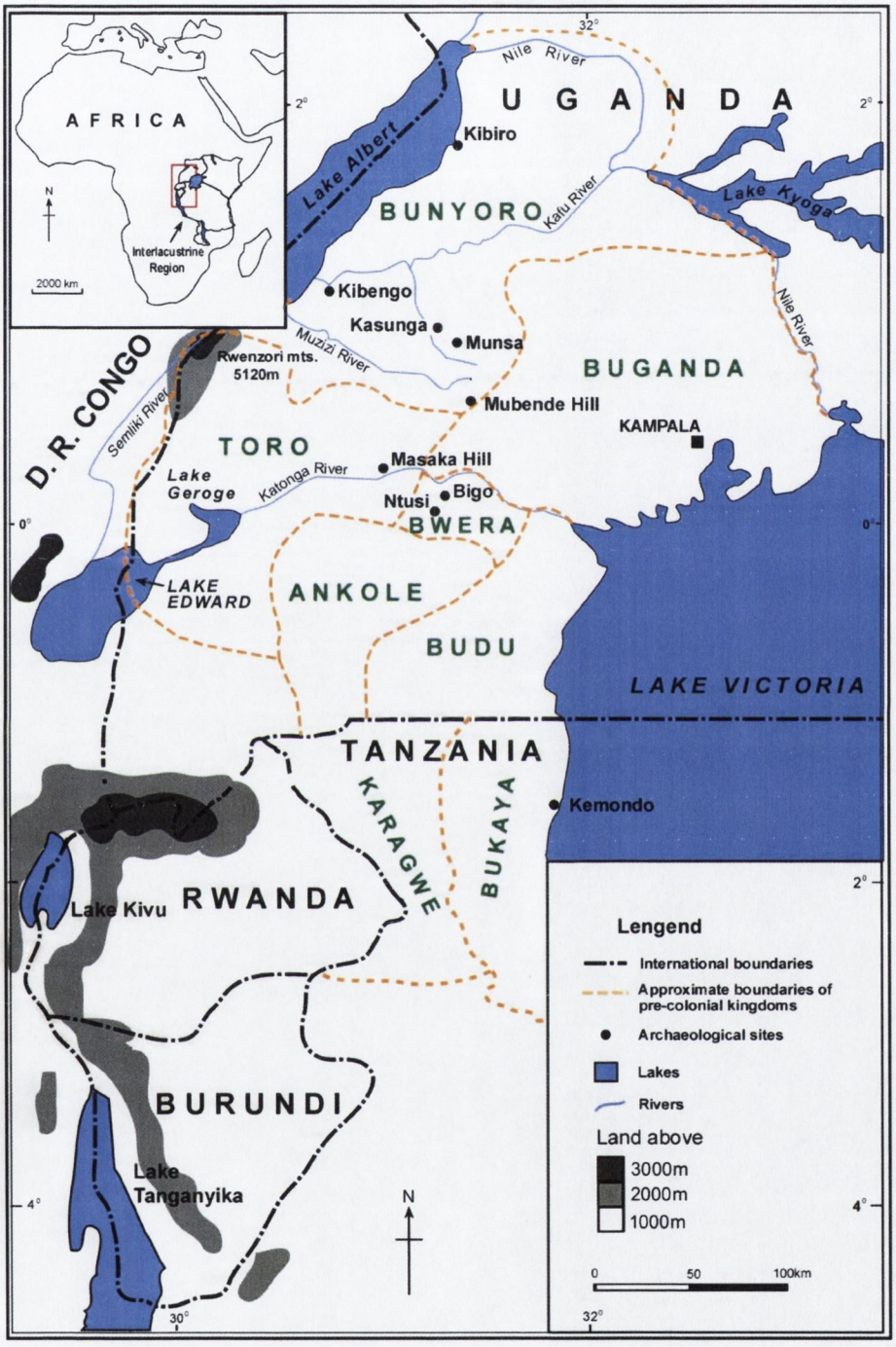

Figure 3.5 Map showing the location of major pre-colonial states in the Interlacustrine highlands of central Africa (Adapted from Sutton, 1993).

CHAPTER FOUR

MUNSA ARCHAEOLOGICAL SITE: DESCRIPTION AND FIELD-BASED SAMPLING

4.1 Introduction

This chapter describes the geographical location and present-day environment of the Munsa study site. The chapter also describes the cultural changes at Munsa evident in published archaeological records. Within this chapter, the methods used in the extraction of sediment cores from the field site are also described.

4.2 Munsa archaeological site

4.2.1 Geographical location

Munsa is located near Kakumiro Township, in the southeastern part of the pre-colonial kingdom of Bunyoro, now Kibaale District (Figure 4.1). The site occupies about 1km^2 of land and consists of an archaeological site located on a hill (known locally as Bikegete) (Plate 4.1) surrounded by concentric rings of earthworks and is situated at 0^0 49' 30" N and 31^0 18' 00" E (Lanning, 1955). The archaeological site at Munsa is boarded by three small papyrus-dominated swamps situated either entirely or partly within the earthwork.

4.2.2 Topography, geology and drainage

The study site at Munsa is situated on the plateau that lies between the western and eastern arms of the Great Rift Valley (Lanning, 1955). The site ranges in altitude from

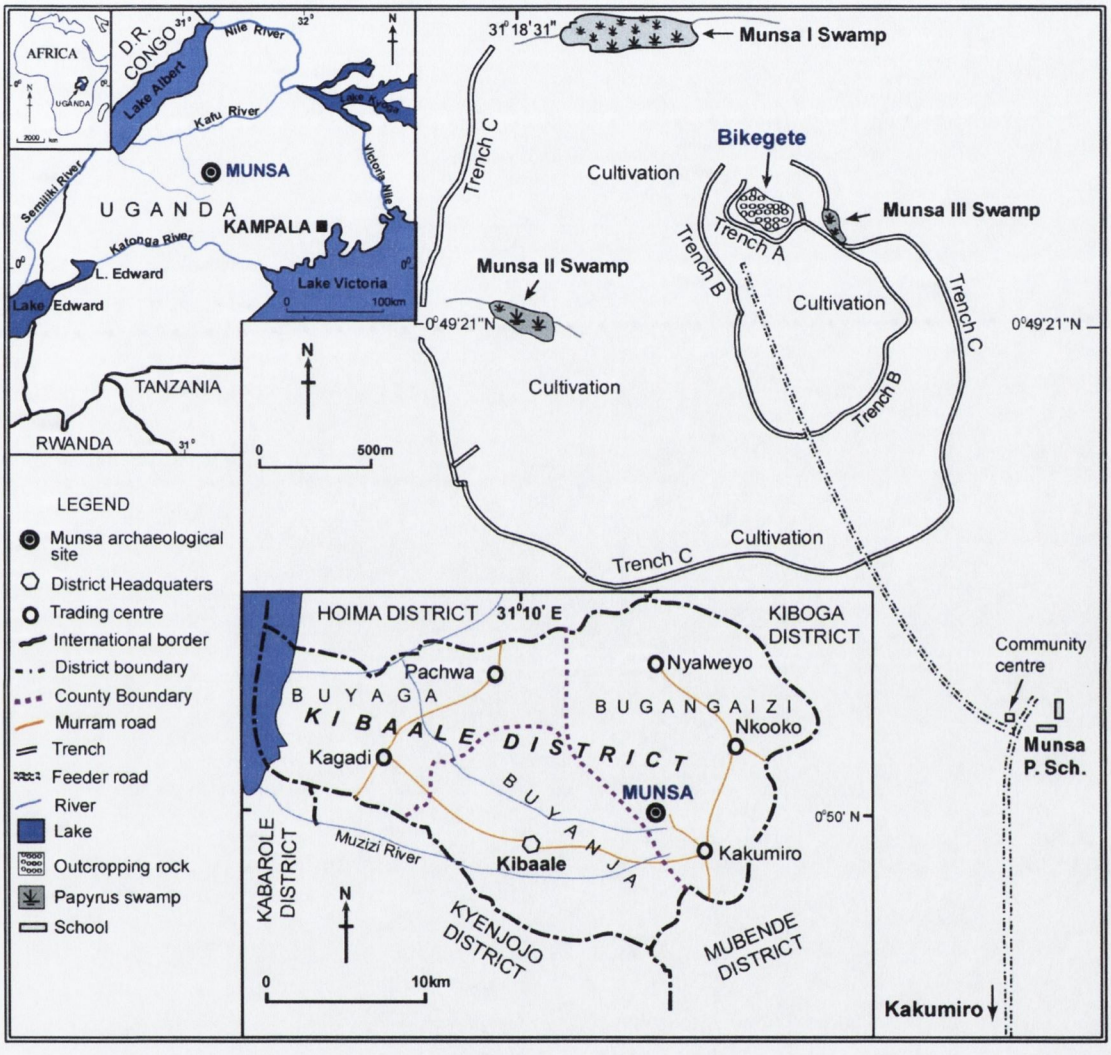

Figure 4.1 Location of Munsa study site and the earthwork systems (trenches) surrounding Bikegete.

1220 m to the highest point of 1340 m a.s.l at Bikegete, a granite outcrop (Lanning, 1955). The main basement rocks at Munsa are granite intrusions and argillites and quartzites of the Pre-Cambrian Bunyoro-Toro system (Harrop, 1960) that occasionally outcrop at the surface forming isolated, rocky hills (such as Bikegete). The site is surrounded by an undulating landscape within which there are many granite hill tops containing rocks shelters that provide evidence of past use by humans (Lanning, 1955). Bikegete itself (Plate 4.1) contains several rock shelters (Plate 4.2).

The earthworks at Munsa consist of an inner trench (A) dug close to Bikegete. Trench A is surrounded by trench B and an outer trench (C). Trench C, the outermost earthworks, describes about 1 km^2 of land that includes a small, papyrus-dominated swamp (Munsa II).

4.2.3 Local climatic conditions

The study area at Munsa lies within a climatic zone which experiences moderate to heavy precipitation (Figure 4.2). The annual rainfall is bimodal, and is mainly influenced by monsoonal circulations over the Indian Ocean (Henderson, 1949; Langdale-Brown, 1960; Hastenrath *et al.*, 1993; Nicholson, 1996a; Hastenrath, 2001; Conway, 2002; Mistry & Conway, 2003). Peak rainfall generally occurs from March to May, with a second wet season running from August to November (Figure 4.3). Two dry seasons also occur in the area, a pronounced one in June-July and a second, less intense, between December and February. The southeast monsoon, bearing moisture from the Indian Ocean, is responsible for the main wet season, while the northeast monsoon brings more

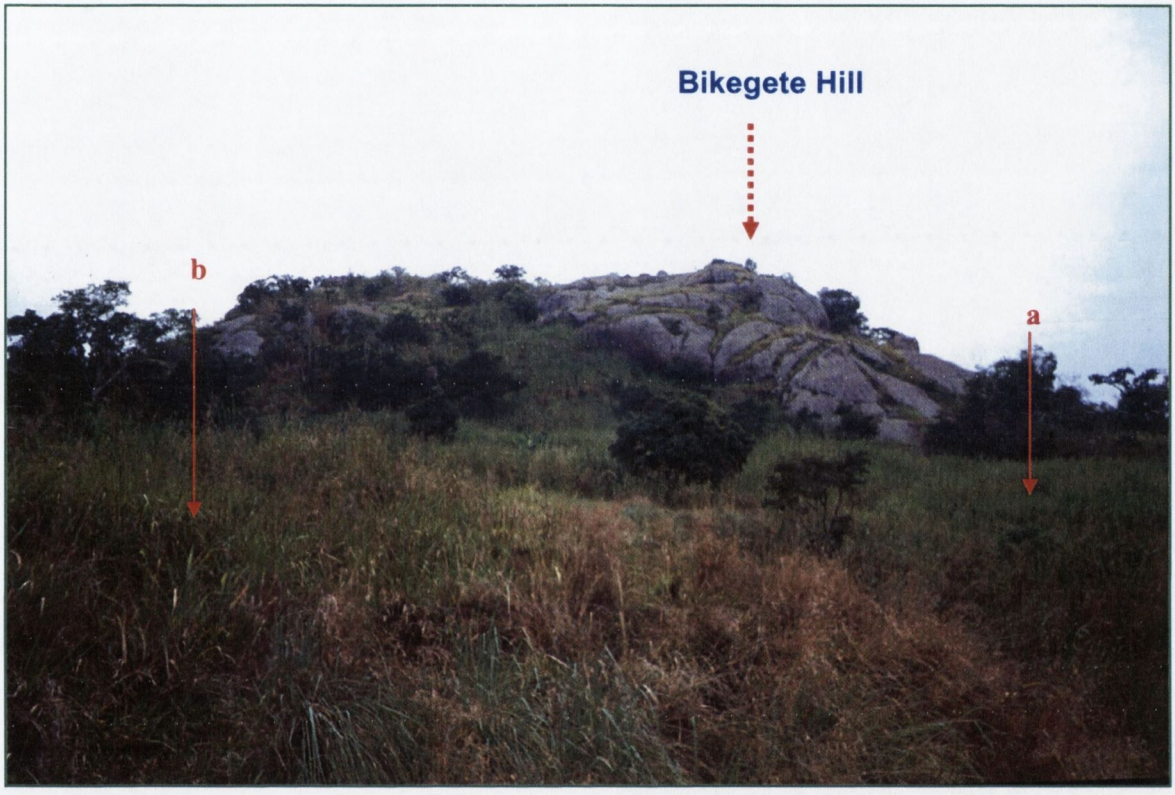

Plate 4.1 Bikegete surrounded by dense grass cover, mainly dominated by *Pennisetum purepurium* (a) and tussock grasses (*Cympopogon afronudus, Hypherrinia rufa* and *Aspera cylindrica*) (b). Scattered tress of *Albizia* spp, *Ficus* spp and *Sapium elipticum* occur in the background.

Plate 4.2 Rock shelters at Bikegete containing burial grounds. The area outside the rock-shelters has been cleared for agricultural purposes, and planted mainly with cassava, maize and bananas. The rocks contain a number of burial sites that have been excavated (see text for details).

limited amounts of rain later in the year (Langdale-Brown *et al.*, 1964; Lind & Morrison, 1974; Hastenrath, 2001). Occasional moist winds from the Atlantic Ocean (Langdale-Brown *et al.*, 1964; Nicholson, 1996a; Hastenrath, 2001) and irregularly occurring ENSO-related phenomena (Conway, 2002) also influence the rainfall in the region.

The closest reliable meteorological stations in the same climatic zone as Munsa, from which rainfall figures are available, are at Mubende and Masindi (Figure 4.2). According to the rainfall distribution shown in Figure 4.2 and 60 years (1910-70) rainfall data from Mubende meteorological site (Figure 4.3), the study area receives an average rainfall between 1000-1500 mm per year, with daily mean temperatures ranging between 19^0C and 22^0C.

4.2.4 Local vegetation

Local vegetation at and around Munsa study area has been described by Langdale-Brown (1960) and Langdale-Brown *et al.* (1964) as forest/savanna mosaic, consisting of remnants of regenerating forest and grasses dominated by *Cymbopogon afronadus*, *Imperata cylindrical* var. *africana*, *Hyperrhenia rufa* and *Pennisetum purpureum* (Elephant grass). Small patches of forest include species of *Albizia coriaria, A. grandibracteata*, *A. gummifera*, *Celtis spp*, *Markamia platycalyx* and *Sapium elipticum*. Mosaics of regenerating forest and herbaceous stages of succession represent post-cultivation vegetation communities associated with abandoned cultivation (Langdale-Brown *et al.* (1964).

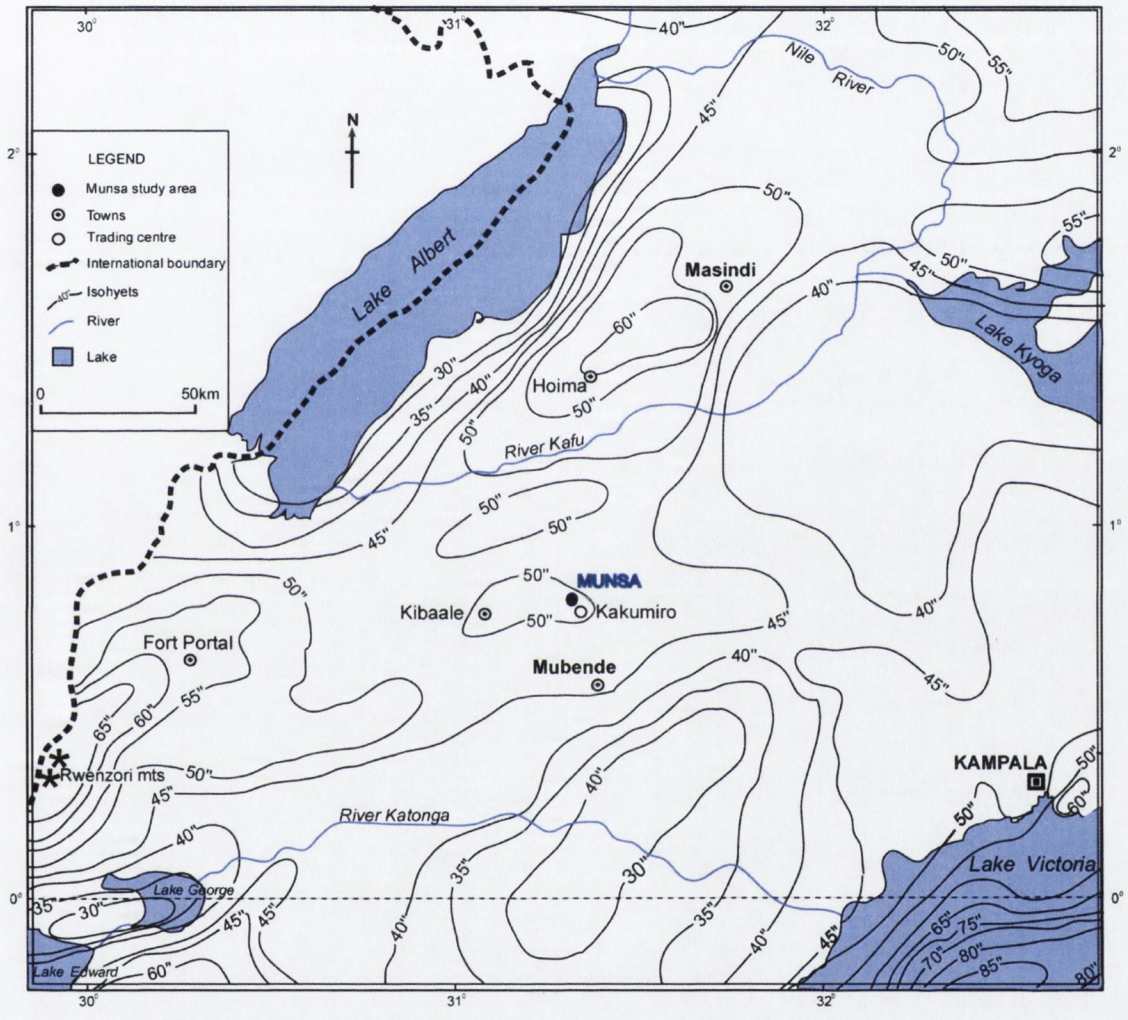

Figure 4.2 Mean annual rainfall distributions in the study area. Isohyets are in inches (Adapted from Landale-Brown *et al.* (1964) and Atlas of Uganda (1967).

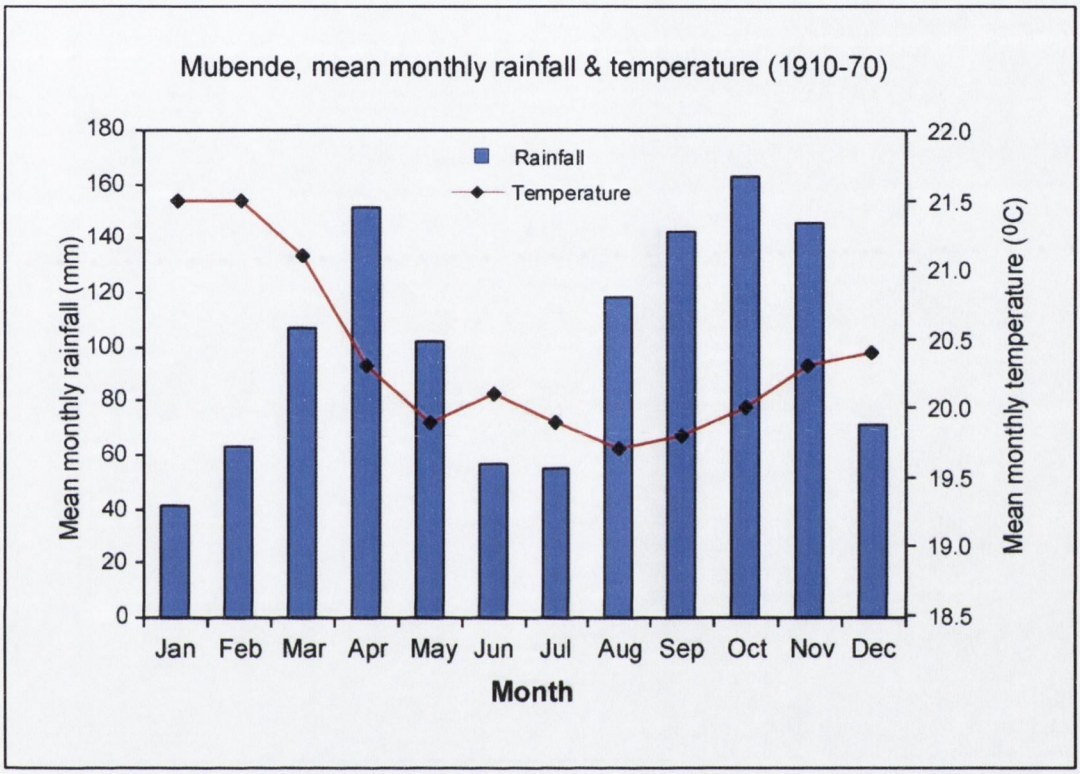

Figure 4.3 Mean monthly rainfall (mm) and temperature for Mubende District for the period 1910-1970 (Source of data: National Meteorological Department, Kampala).

The current vegetation is interspersed with small patches of cultivated and abandoned fields (Plate 4.3). Field work carried out as part of the current research revealed the following taxa to be prominent in the forest remnants around Munsa: *Albizia coriaria*, *A. zygia*, *Celtis africana*, *Ficus eriobotryoides*, and occasionally *Sapium ellipticum*, *Spathodea campanulata*. *Neoboutonia macrocalyx* and *Syzygium guineense* are confined to the riverine forest, while *Combretum molle* and *Terminalia brownie* are found in shallow rocky soils.

Pennisetum purpureum, which can reach several metres in height, occurs on abandoned farmland intermixed with *Panicum maximum* (Guinea grass) and *Imperata cylindrica* (Spear grass). These species are believed to represent the early stages of post-cultivation successions (Langdale-Brown, 1960; Langdale-Brown *et al.*, 1964), where *Panicum maximum* and *Imperata cylindrica* gradually give way to the establishment of *Pennisetum purpureum*. *Hypherrhenia rufa* occurs abundantly on shallow rocky soils and is intermixed with the tussock grass *Cymbopogon afronudus*, which is readily recognized by the absence *of Pennisetum purpureum.* Other common grass species growing locally in the area include *Setaria sphacelata* in association with *Brachiara brizantha* and *Paspalum commersonii*. Poorly-drained valley bottoms are dominated by sedges, mainly *Cyperus papyrus*, which is commonly found under waterlogged conditions in the area.

Plates 4.3 Distribution of local vegetation at Munsa, interspersed with patches of cultivated fields (i) and (iii). In the centre of the photograph (ii) is Munsa II swamp.

4.2.5 Agricultural activities

Subsistence agriculture is the major activity at Munsa, where a range of perennial crops, such as banana, cassava and coffee are grown. Annuals such as beans and cereals, mainly finger millet (*Eleusine coracana*), maize (*Zea mays*), and sorghum (*Sorghum bicolor*), are also cultivated. Cultivated varieties of bananas, including sweet banana, *Musa acuminate*, are used locally, mainly in the production of beer. Livestock, such as cattle and goats, are kept, but in relatively low numbers compared to other parts of the region where pastoralism is a more prominent, economic activity.

4.2.6 Occupation of Munsa archaeological site

The archaeological site at Munsa consists of settlement debris, burials, rock-shelters and evidence of iron working, grain storage and the consumption of cattle and cereals, centred upon Bikegete. According to the archaeological evidence (Robertshaw, 1997) the site at Munsa is believed to have been first occupied by a significant population towards the end of the first millennium AD, from about 900 AD. Initial occupation was followed by a period during which earthworks, in the form of concentric rings of trenches, were constructed between 1300 and 1650 AD, with the innermost trench constructed between 1300 and 1400 AD (Robertshaw, 1997). According to local traditions (Lanning, 1955), the exact reason for their construction is not known. However, according to evidence from recent archaeological excavations and historical linguistics (Robertshaw, 1997, 1999a, b; Robertshaw & Taylor, 2000), the construction of the earthworks is believed to relate to the emergence in the region of complex

chiefdoms, which were based upon agriculture, with some cattle, and may have served a defensive purpose.

Excavations at Munsa yielded animal bones dominated by those of cattle, together with numerous pits used for grain storage, as well as grindstones and pottery, all of which indicate cereal agriculture (Robertshaw, 1997). According to evidence from archaeological records, the early inhabitants appeared to have participated in iron working and long-distance exchange networks, trading in glass/ivory beads and copper bangles. The glass/ivory beads and iron/copper bangles recovered from burial sites are dated to the period between 1000 and 1200 AD, while iron working, is dated to the period between 1200 and 1400 AD (Robertshaw, 1997).

Available evidence indicates that permanent settlement at Munsa ceased around the end of the 1600 AD (Robertshaw, 1997). According to Robertshaw, (1997) and Taylor *et al.* (2000), abandonment of Munsa may have been part of major economic, political and social upheavals that brought about a shift in settlement patterns from nucleated settlements to dispersed homesteads (Robertshaw, 1994). The settlement foci of chiefdoms appear to have become more peripatetic as their rulers put more emphasis on the size and health of their herds (Robertshaw & Taylor, 2000). A move to a reliance on more temporary settlements may have marked the initial rise in pre-colonial states such as Bunyoro, Buganda and Ankole that were encountered by early Europeans explorers to central Africa in the mid nineteenth century (Robertshaw & Taylor, 2000), and in a class distinction between the noble cattle-keeper and the peasant farmer.

4.3 Sedimentary environments at Munsa

4.3.1 Location of Munsa swamps

The study site at Munsa is composed of three small papyrus-dominated swamps, namely; Munsa I, II and III (Figure 4.4). Munsa I swamp, through which flows River Katerere (Kiyiye), is the largest of the three swamps. It is situated to the north of Bikegete (00^0 49' 36.5" N and 31^0 18' 33.6" E, and at an elevation of 1220 m a.s.l). Munsa II Swamp, locally known as Lwentuka, is located within the outer most ring of earthworks. It is situated at the western edge of Bikegete at 00^0 49' 21.3" N and 31^0 18' 31.0" E, and at an elevation of 1265 m a.s.l. The swamp is approximately 26 m wide and is associated with a small seasonal stream which drains into a valley located close to trench C.

Munsa III is a narrow swamp measuring about 16 m wide, and is located on the eastern edge of the site (00^0 49' 29.1" N and 31^0 18' 54.3" E at 1280 m a.s.l) close to Bikegete Hill and is drained by a small stream known as Kyeju.

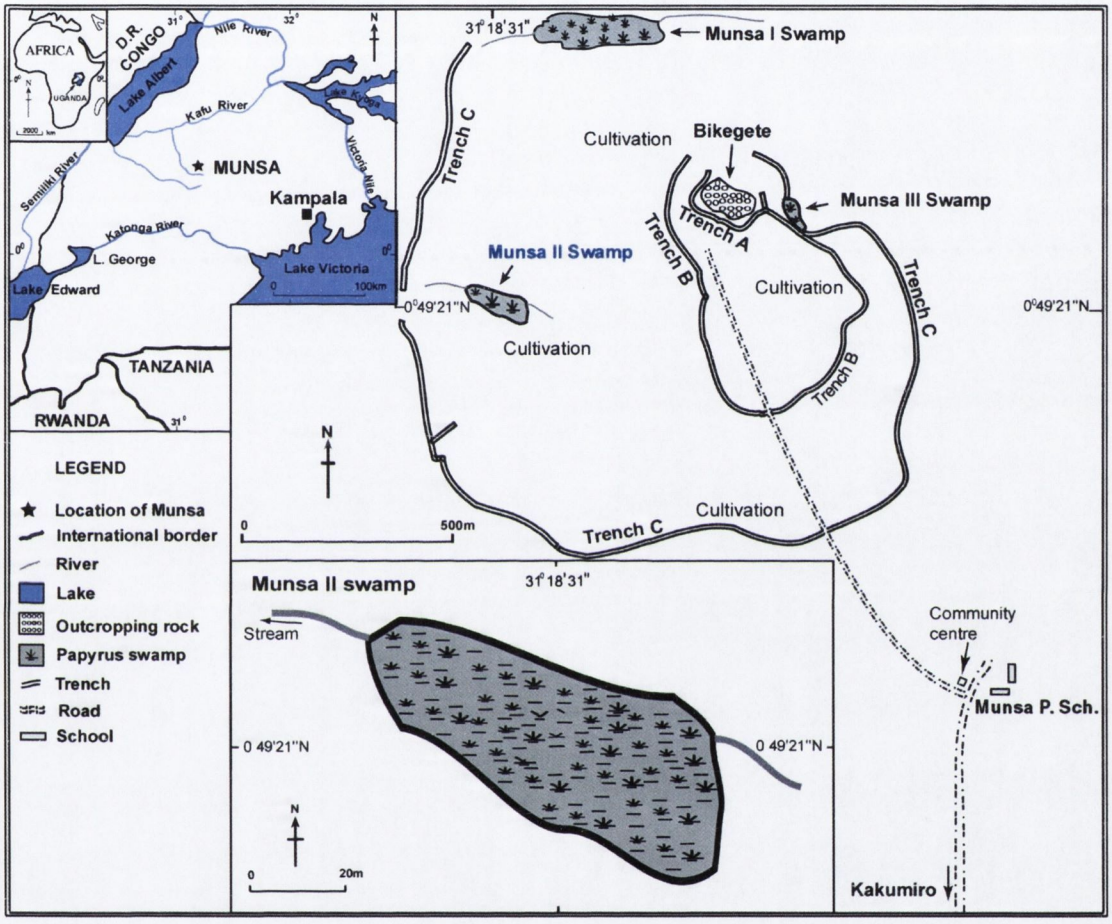

Figure 4.4 Location of Munsa swamps within the earthwork systems. Inset is Munsa II swamp.

4.3.2 Swamp vegetation

Vegetation of the Munsa swamps is dominated by papyrus (*Cyperus papyrus*) (Plate 4.4). Others species growing on the swamps include *Mimulopsis solmsii*, *Aframomum sanguineum*, *Polygonum pulchrum*, *Ipomoea* spp, *Setaria sphacelata* and *Commelina* spp. Species of fern (*Dryopteris striata*, *D. thelypteris*) also grow on the swamps. The vegetation adjacent to the Munsa I and II swamps margins is mainly composed of swamp forest trees, such as *Neoboutonia macrocalyx*, *N. melleri*, *Syzygium guineense* and *Ficus ovata*. Species of *Albizia zygia* and *Harisonia abysisnica* occur on the drier marginal parts of the swamp.

4.3.3 Munsa II swamp

The location of Munsa II swamp is presented in Figure 4.4. The swamp was the focus of the current research because of its location within the earthworks (Munsa I and Munsa III swamps were discountered because of evidence of sediment re-working). Munsa II swamp is situated in a valley that is currently surrounded by patches of cultivated fields (Plate 4.4). The catchment area for the swamp is relatively small; it is assumed that human activities and environmental changes in the catchment for the swamp will be registered in sediments that have accumulated in the swamp.

Plate 4.4 Munsa II swamp showing *Cyperus papyrus* (a) and agricultural land (b) planted with bananas, cassava and maize.

4.4 Sampling of sediments

Eight sediment cores including three overlap cores were collected from Munsa II swamp during fieldwork in July 2001 (Plate 4.5). The sediment cores were collected at regular intervals along a transect running from northeast to southwest, and perpendicular to the direction of the drainage (Figure 4.5). The cores were collected using a modified Livingstone piston corer of 7 cm in diameter (Plate 4.5). The coring intervals were positioned in such a way to incorporate sediments from marginal and more centrally located sedimentary environments. The overlap cores were collected to minimize the potential problems of loss of sediments and the sampling of disturbed and contaminated sediments.

The locations of the coring sites of the sediments at Munsa II are presented in Figure 4.5, including the stratigraphy of three major cores (M2C1, M2C2 and M2C3C) selected for analysis. M2C1 was collected at 0.5 m from the northern edge of the swamp and M2C2 was cored 5 m away from M2C1, while M2C3A, M2C3B and M2C3C were collected at the centre (13 m) of the swamp. M2C4 was collected 20 m from northern edge, whereas M2C5 and M2C6 were collected at the southern margin of the swamp. The overlap cores were collected adjacent to cores M2C2, M2C3C and M2C4.

Analysis of the core sediments was carried out in the field to select cores for further laboratory analysis. The cores were wrapped in polythene and aluminum foil for further analysis in the laboratory at Trinity College, University of Dublin where they were deep frozen to avoid material degradation. Full details of the stratigraphies of the cores from

Plate 4.5 Sediment coring at Munsa II site during July 2001 field work. The swamp is dominated by dense papyrus (*Cyperus papyrus*) vegetation cover.

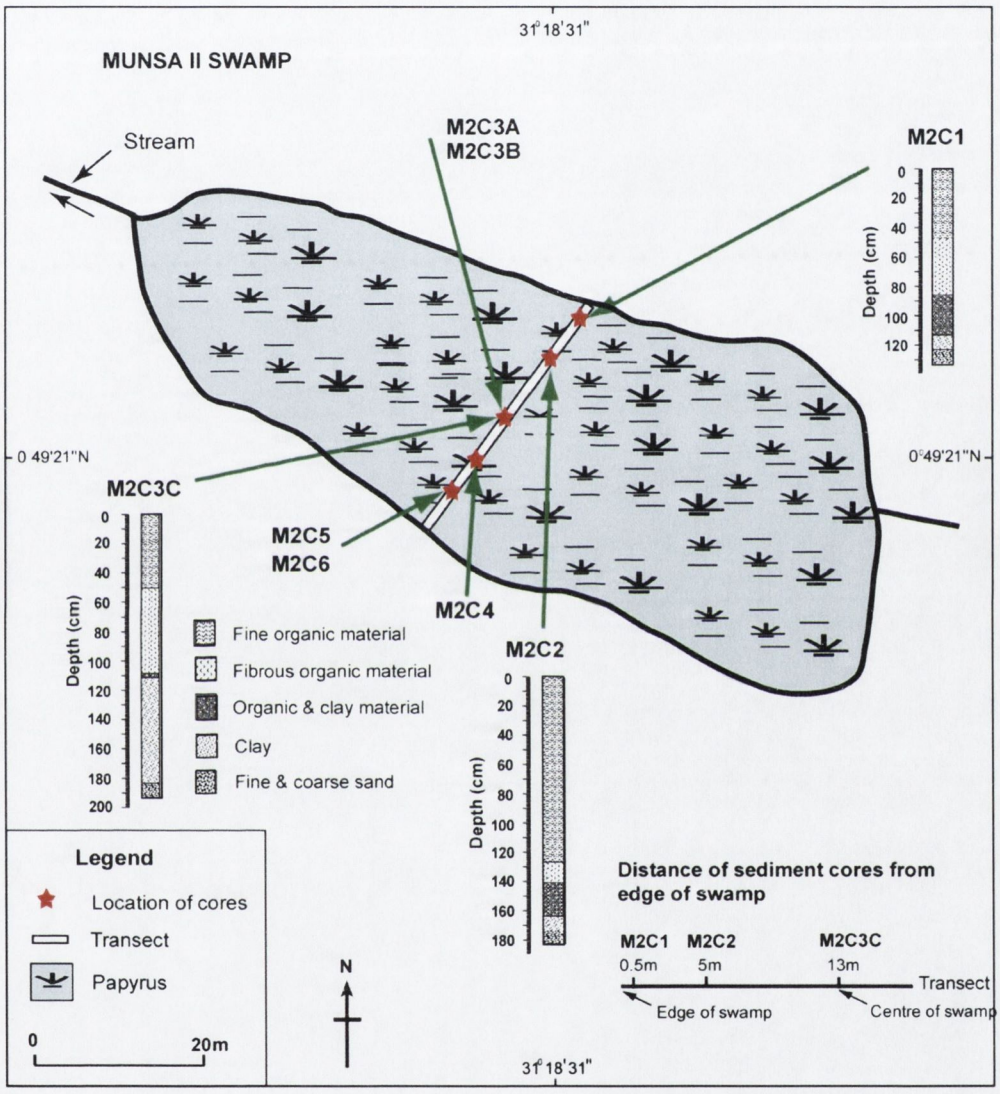

Figure 4.5 Location of Munsa II sediment cores along a transect cut across Munsa II swamp. The stratigraphies for M2C1, M2C2 and M2C3C are illustrated.

Munsa II selected for further analysis are provided in chapter five.

4.5 Collection and analysis of voucher specimens

Plant specimens for pollen and phytolith reference slides were collected in the study area during July-August 2002 field work, and transported to Trinity College, University of Dublin for analysis. Collection of voucher specimens focused on forest taxa, pasture grass and agricultural plants common locally (Table 4.1), particularly those that are of economic importance. Some of the plants collected are not usually recorded in pollen records. The latter is the case with cultivated members of the banana family (Musaceae). Musaceae is today mainly represented by two genera; *Musa* and *Ensete* (Simmonds, 1966; De Langhe, *et al.*, 1995; Rossel, 1994-5). *Musa* includes the cultivated, edible banana and plantains. Unlike *Eumusa* cultivars, which produce seeds (Simmonds, 1966; Denham *et al.*, 2003), varieties of *Musa acuminata*, as with other edible bananas in Africa, are seedless and therefore reproduce asexually via the production of suckers. The wild genus *Ensete* or false banana, however produce seeds, thus ensuring its propagation through seeds (Simmonds, 1966; Rossel, 1994-5).

Table 4.1 Voucher plant materials collected at Munsa study area.

Cultivated variety	**Non-cultivars / Tree/shrubs/ grasses**
Cajanus cajan (L.) Millsp.	*Aloe vera*
Dioscorea villosa L.	*Commelina bengalensis*
Eleusine coracana (L.) Gaertn.	*Cymbopogon afronadus*
Ensete ventricosum Maurelii (wild banana)	*Cyperus papyrus* L.
Ensete ventricosum (Welw.) E.E. Cheesman (wild banana)	*C. rotundus* L.
Ipomoea batatas (L.) Lam.	*Dombeya goetzenii* L. Schum
Musa paradisiana (cooking banana)	*Erythrina abysinica* Lam. Ex. DC
Musa sapientum (sweet [edible] banana)	*Ficus asperifolia*, Miq
Nicotiana tabacum L.	*F. ovata* Vahl
Phaseolus vulgaris L.	*Hyparrhenia rufa* (Nees) Stapf
Ricinus communis (LINN.)	*Imperata cylindrica* (L.) Palisot
Sorghum bicolor (L.) Moench	*Lantana trifolia* L.
Zea mays L (Maize)	*Miscanthus violaceus* K. Schum Pilg
	Ocimum suave Wild
	Panicum maximum Jacquin
	P. latifolium L.
	P. trichocladum K. Schum
	Paspalum scrobiculum, L.
	Pennisetum purpureum Schumach.
	Phoenix reclinata Jacq.
	*Sapium elipticum (*Hochst. Ex. Krauss) Pax
	Sesbania sesban (L.) Merrill
	Setaria sphacelata (Schumach.) Stapf
	Sorghum arundinaceum (Desv.) Stapf (wild sorghum)

PART TWO: METHODS AND RESULTS

CHAPTER FIVE

LABORATORY BASED ANALYSIS OF SEDIMENT CORES FOR MICROSCOPIC FOSSILS

5.1 Introduction

This chapter describes the laboratory based procedures used in the preparation of sediment samples and analyses of radiocarbon, stable isotope, and organic/inorganic matter, including plant microfossils (charcoal, pollen, spores and phytoliths) contents. Also included is a description of the criteria used in the identification of the main pollen, spore and phytolith types referred to in later chapters in this thesis. The procedures used in clarifying (i.e. clustering and zoning) of sediment based data are also discussed.

5.2 Sediment description

A sequence of sediment cores were sectioned at regular intervals for detailed analysis of microfossils. The intervals varied from 3 to 5 cm depending on stratigraphy, with some stratigraphic portions sectioned at 2 cm intervals to provide a higher resolution of analysis. The stratigraphic description of sediment cores was based on the standard system of Troel-Smith (1955). According to the Troel-Smith's system, sediments are described according to a range of possible physical properties. Three main properties of the sediments were used for the description in this study were; physical property (colour), humification (degree of decomposition identified by intensity of dark-brown colour), and elements contained in the sediment (clay, detritus, humus, sand, silt etc).

The relative abundance of each component was estimated based on a 6 point-scale, classified as absent (0), rare (+), trace (1), occasional (2), frequent (3) and abundant (4). The degree of decomposition (humification) of organic matter was determined by treating $1cm^3$ of sediment samples with hot dilute alkali (10% NaOH) and running the liquid (humic acid) through a filter paper. The intensity of colour was assessed through comparison with Munsell Soil Colours (2000), which are designated by a symbol HUE in relation to Red, Yellow, Green, Blue and Purple. The degree of humification for each lithological segment was rated on a five-point scale (0-4), where 0 refers to least humified and 4 is highly humified. The former is indicated by a light colour; the latter by very dark-brown colour. The results of sediment stratigraphy are presented in chapter six.

5.3 Estimation of organic matter by loss on ignition (LOI)

The ratio of organic-inorganic matter in sediments is important because it serves as an indicator of relative abundance of allochthonous sediment input. This ratio is determined by the loss of ignition (LOI) method (Gale & Hoare, 1991). The method involves drying weighed samples of approximately 1g in an oven at 105^0C for 24 hrs and igniting in a furnace at 550 ^{0}C for 24 hrs to obtain the LOI weight. Care was taken when transferring the samples from the furnace to a desiccator so that the contents were not exposed to ambient levels of humidity. The amount of organic content was calculated and expressed as a percentage of the dry weight of sediment as follows:

$$\% \text{ Organic matter } (LOI) \text{ (dry weight)} = \frac{(Dwt - Iwt)}{Dwt} X100$$

Where:

LOI = loss on ignition

Dwt = the dry weight of the sample after oven drying at 105^0C for 24hrs,

Iwt = the dry weight of the sample after ignition for 24hrs at 550^0C.

5.4 Sediment chronology and radiocarbon dating

In order to measure radiocarbon ages of organic material it is necessary to determine the amount of radiocarbon (^{14}C) in a sample. This measurement can be made either by measuring the radioactivity (the conventional *beta*-counting method) of the sample or by directly counting the radiocarbon (^{14}C) atoms using the Accelerator Mass Spectrometry (AMS) method (Stuiver *et al.*, 1998). The chronology of Munsa II sediments (cores M2C1, M2C2 and M2C3C) was provided by the AMS ^{14}C method and calibrated using the radiocarbon calibration program Calib Rev 4.4.2 (Stuiver *et al.*, 1998). The samples were dated at Beta Analytic Inc. Miami, USA. The chronology is based on a total of 15 AMS ^{14}C dated samples (11 samples of macrofossil plant materials and 4 samples of bulk sediments). The results of AMS ^{14}C dating are presented in chapter six. The AMS ^{14}C technique has advantages over the conventional *beta*-counting method in that it can date small sample sizes and gives more precise measurements.

The initial laboratory preparation of the samples for AMS ^{14}C dating involved carefully isolating plant macrofossils and the elimination of contaminants such as rootlets, which

could result in a radiocarbon date being too young or too old. The isolated plant macrofossils and bulk samples were triple wrapped in aluminium foil prior to dispatch. Details of the AMS radiocarbon dating procedure are described in the Beta Analytic website (http://www.radiocarbon.com/analytic.htm, access date: 04/11/2004). During the AMS dating process, the carbon is converted into carbon dioxide and reduced to graphite (pure C). The graphite is ionised into molecular ions ($12CH_2$-, 13CH- and ^{14}C-ions). The $12CH_2$- and 13CH- molecular ions are further broken-up. The ^{14}C-ions are filtered and enter a detector where their velocity is measured and the number of ions is counted. The ratio of $^{14}C/^{13}C$ is then calculated and compared with laboratory standard with known ratio. The difference in the ratios of $^{14}C/^{13}C$ generally expressed as δ value is then used to calculate the radiocarbon age. However, during the ionisation process not all of the radiocarbon atoms put in the ion source reaches the detector, so the stable isotopes ^{12}C and ^{13}C are also measured in order to monitor the detection efficiency. The $^{13}C/^{12}C$ ratio is then used to improve the accuracy of a radiocarbon date (website: http://www.radiocarbon.com/labmethods.htm, access date: 04/11/2004).

5.5 Construction of age-depth curves

Age-depth relationships for M2C1, M2C2 and M2C3C were constructed using the AMS ^{14}C radiocarbon dates. The curves provide a means of interpolating or extrapolating ages of sediment samples and of calculating sediment accumulation rates as illustrated in Figure 5.1. The age of a sample can be interpolated if its depth lies between the depths of two radiocarbon (^{14}C) dates, and where the depth of the sample lies beyond minimum and maximum depths then its age can only be extrapolated. The age-depth curves were

constructed by joining a line of best fit between the ^{14}C–dated depths. The results for age-depth curves for M2C1, M2C2 and M2C3C are presented in chapter six. Sediment accumulation rates for Munsa II cores were calculated from the age-depth curves as follows:

$$I = (d_2 - d_1)/T$$

Where:

I = sediment accumulation rate (influx)

$(d_2 - d_1)$ = depth range of sediment sample (cm)

T = sediment deposition time (yr. cm^{-1}), calculated from $(T_2\text{-}T_1)$

5.6 Methods for investigating charcoal content in Munsa II sediments

This study employed two standard methods to measure the charcoal content of swamp sediments; (1) the chemical assay method (Winkler, 1985), and (2) the point count method for estimation of charcoal area and particle size-class distribution by the standard point count method (e.g., Clark, 1982; Clark, 1988a; b, Rhodes, 1998).

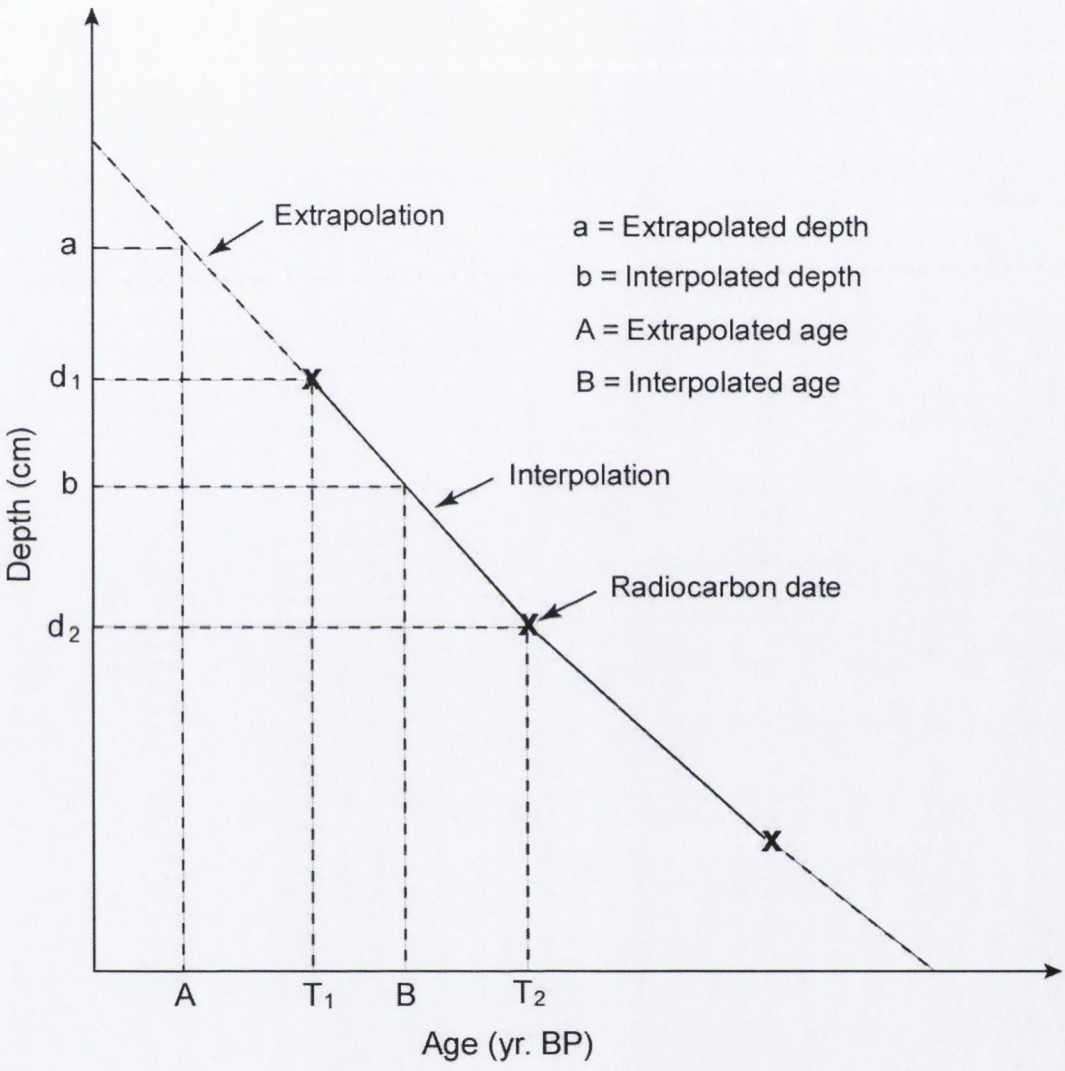

Figure 5.1 Construction of age-depth cures

5.6.1 Estimation of charcoal content by Chemical Assay method

Winkler (1985) described a relatively simple digestion and ignition method. In this method, charcoal in a sediment sample is considered as acid insoluble microcrystalline graphite (Winkler, 1985), or inert carbon. The weight of the charcoal relative to the dry weight of a sample of sediment is determined and expressed as a percentage. The data can be expressed as influx (accumulation rate) in grams per unit volume of sediment per year. The method is less time-consuming and avoids the problem of correct identification of charred fragments. However, the technique does not provide any information on charcoal particle size or morphology and hence does not permit the recording of characteristics that could be of palaeoecological significance.

In the chemical assay method and following Winkler (1985), approximately $2cm^3$ of sediment samples were dried in an oven at 105^0C for 24 hours, cooled to room temperature in a dessicator and weighed (Dwt). The samples were transferred into 10 ml plastic test tubes and approximately 3 ml of concentrated nitric acid was added to the sample in each test tube to digest the organic materials. The samples were placed in a hot water bath for 3 hours to ensure oxidation of the organic debris, carbonates and pyrites. The samples were then centrifuged at 3000 rpm for 5 minutes, decanted and washed twice in distilled water or until a clear solution was obtained. The samples were transferred to crucibles and dried in an oven at 105^0C overnight, cooled and reweighed (Nwt). The samples were then heated in a muffle furnace at 550^0C for 3 hours to remove the charcoal, cooled in a dessicator and reweighed to obtain the final (ignition)

weight (Iwt). The amount of inert carbon in a sample was then calculated and expressed as a percentage of the dry weight of sediment sample as follows:

% dry weight of inert carbon (charcoal) (dwt) =

$$\frac{(Nwt - Iwt)}{Dwt} X100$$

Where:

dwt = dry weight of inert carbon (charcoal)

Dwt = dry weight of the sample after oven drying at 105^0C for 24hrs

Nwt = dry weight of the sample after nitric acid treatment and dried in an oven at 105^0C for 12hrs

Iwt = dry weight of the sample after ignition

5.6.2 Estimation of charcoal surface area by point count method

The point-count method is described in Clark (1982) and involves classifying the area of charcoal particles in a sediment sample observed on a microscope slide. The abundance of charcoal is quantified by counting the number of points on an eyepiece reticule that fall on charcoal particles. In this method, charcoal abundance is assumed to be directly related to the surface area of the particles as seen under the microscope. The method allows for estimating the area of charcoal per unit weight or volume of sediment and calculating the influx of charcoal per unit area of sediment per volume per year in a given time period.

There are a number of limitations associated with the point count method. One of the major limitations in quantifying microscopic charcoal particles is that of identification (Waddington, 1969; Winkler, 1985; Patterson *et al.*, 1987; Clark, 1988b). In pollen prepared samples, there are often black and opaque, angular particles, which are clearly charcoal and brown structured particles that are vegetal matter (Patterson *et al.,* 1987). However, Waddington (1969) suggested a way to solve this problem by counting only uniformly opaque particles. The other limitation of the method is that it generally deals with only a limited size-range of particles; relatively small charcoal particles with long axis < 50 μm), which are often relatively insensitive to local fires (Patterson *et al.*, 1987; Clark, 1988a; Clark & Royall, 1995), may be over-estimated compared to larger-sized particles because of the technique used in sample preparation.

The point-count method involves smearing dried sediment samples previously prepared for pollen counts onto slides. These samples were spiked with exotic marker tablets containing 10,850 ± 200 (Batch number 201890) *Lycopodium* spores as described in pollen section 5.7. The prepared samples were mounted on microscope slides and viewed under x400 magnification using a Leitz Laborlux 12 microscope, with an eyepiece reticule, containing a row of 11 points (245 μm long). The number of points falling on charcoal particles in each field of view was noted. In addition, each field of view was tallied and the number of *Lycopodium* spores was recorded for calculation of absolute concentrations (charcoal influx). To standardize the method, charcoal particles less than 7.5 μm long were ignored to avoid recording other bodies, such as pyrites. Counting was also restricted to black, completely opaque and angular fragments

(Waddington, 1969; Clark, 1982; Patterson *et al.*, 1987; Clark, 1988a). For each sample, at least 500 fields of view were counted. The quantity of charcoal was calculated from the following formula:

$$P = C/N$$

Where:

P = the probability of a random point falling on a particle of charcoal:

C = total number of points falling on the charcoal fragments

N = total number of points applied

- Estimated area of charcoal (A) occurring in the fields of view

A = P (Nfw x Afw)

Where:

Nfw = total number of fields of view

Afw = area of field of view

- Estimated area of charcoal (Ac) per unit dry weight of sediment

Ac = (A x M) / (M x w)

Where:

A = estimated area of charcoal

M = number of exotic grains added

Mp = number of exotic grains counted

W = dry weight of material used

- Estimated mean annual influx (Ai) of charcoal (deposition rate per year),

$$Ai = Ac/T$$

Where:

Ac = estimated area of charcoal per unit dry weight of sediment.

T = number of years incorporated in original sediment sample. T is calculated from the age depth curves described earlier in this chapter.

In addition to tallying the number of points falling on charcoal particles, the size of charcoal particles was recorded, according to six different size-classes; 7.5 to < 25 μm, 25 to < 50 μm, 50 to < 75 μm, 75 to < 100 μm and 100 to ≤ 125 μm. The lower size-limit was set to exclude the very small particles (< 7.5 μm) that could not be distinguished from iron pyrites that often resemble charcoal particles and to incorporate the larger particles that passed through the sieve during sediment preparation. The abundance of charcoal particles was expressed in absolute terms as follows:

Number of charcoal particles per gram dry weight of sediment (C) = (charcoal particles countered (c) / dry weight of sample (dwt) x (marker grains added, N = 10,850) / marker grains counted (n).

$$C = (N / n)(c / dwt)$$

Where:

C = Estimated number of charcoal particles per gram dry weight of sediment

c = number of charcoal particles counted

N = Number of marker grains added

n = Number of marker grains counted

dwt = dry weight of sample analysed

5.7 Preparation and analysis of fossil pollen and spores

The preparation of sediments for microfossil pollen and spores was based on modified standard procedures published in Faegri & Iverson (1989) and Moore *et al.* (1991). The modification comprised an additional step of chemical treatment involving 10% sodium pyrophosphate, as employed by Bates *et al.* (1978). This step was included in order to disintegrate and remove clay particles, which can obscure pollen, making counting and identification difficult.

Approximately 2 cm^3 of sediments were sub-sampled from M2C1, M2C2 and M2C3C. The samples were dried, weighed and one *Lycopodium* marker tablet with known number of spores (10,850 ± 200), Batch no. 201890) was added to each sample in the test tubes for calculation of absolute pollen concentration and influx (Stockmarr, 1971).

5.7.1 Pollen identification and counting

The prepared samples were mounted on microscope slides and pollen and spores were countered under x400; detailed features were examined under x1000 magnifications. Identification was based on comparisons with a collection of prepared slides of East African modern pollen types at the Department of Geography, Trinity College,

University of Dublin, which was supplemented with reference to a range of publications (Hamilton, 1976; 1982; Taylor, 1988; Marchant, 1997) and digital photographs of pollen types obtained from the African pollen database website (website: http://www.geo.arizona.edu/palynology/apd.html., access date: 24/12/2002). Identification of pollen grains was made to the lowest possible taxonomic level, although some pollen types could only be identified to family level. The nomenclature used followed that of Benninghoff & Kapp (1962). The confidence in the identification of the microfossil is indicated by suffixes: "*sim*" when a fossil pollen type is similar, but not identical, to known types; "*comp.*" when the fossil pollen is comparable to known types, but there is a degree of uncertainty; and "id" when the identification of the genus is certain, but the species is not. At least 500 pollen grains were counted from each slide, except in a few samples where preservation was poor. According to other pollen investigations conducted in the region (Hamilton, 1972; Taylor, 1988; Marchant, 1997), a total of 500 pollen grains has been found to be appropriate for pollen analysis. Generally samples rich in clay and sand particle had very few or no pollen grains, resulting in gaps in the pollen record as in the case of M2C3C. The morphological descriptions of the common pollen types identified in the sediments are presented below.

5.7.2 Description of fossil pollen and spore types

The following are morphological descriptions of the main pollen types and spores (generally those with greatest Palaeoecological meaning) encountered in Munsa II sediments. The descriptions are based on Hamilton (1976), Taylor (1988), Marchant (1997), White (1999) and my own observations. The descriptions are only a brief profile

of fossil grains encountered during the count. The descriptions are arranged alphabetically according to family and the identifications are to the lowest taxonomic level possible. As stated in the previous section, the identification scheme used is based on a scale of increasing level of accuracy of identification ranging from comparative, similar to identical.

Family: Araliaceae

***Cussonia* comp.**

Description: A distinctive pollen type; trizonocolporate, reticulate, prolate in equatorial view and angular in polar view. The long axis measures about 20 μm and the short axis is 15 μm, being wider at the equator. In polar view, the pores are transversally elongated (Plate 5.1, 1 & 2). The exine is stratified with ectexine = endexine, 2 μm thick and stratified.

Family: Combretaceae

***Combretum* id.**

Description: A distinct pollen type, but can easily be confused with *Terminalia* pollen. The pollen type is psilate, elliptical in equatorial view and hexagonal in polar view (Plate 5.1, 3-6). It has six colpi and three pores. The long axis measures about 15 to 20 μm and the short axis is about 10 to 18 μm. The exine is approximately 1 μm thick. The potential sources of this pollen type are *Combretum bindaeranum, M. molle* and *C. volkensi*, which are often associated with savanna woodlands (Langdale-Brown *et al.*, 1964).

Family: Compositae

***Bidens* comp.**

Description: The pollen grain is characterised by the presence of spines, although these are sometimes absent (Plate 5.1, 7 & 8). The pollen is trizonocolporate, echinate with spines measuring approximately 3 to 5 μm long. It is spherical in polar view, with deeply intruding colpi. The pollen measures about 20 to 25 μm in diameter and the exine is stratified (ectexine > endexine). The pollen is derived from a varied group of herbs and shrubs that are often associated with cultivated land (Hamilton, 1972).

Family: Cyatheaceae

***Cyathea* id.**

Description: *Cyathea* is a distinctive trilete spore with furrows tapering to a fine point. The wall is about 1.5 μm thick and the long axis varies from 25 to 30 μm (Plate 5.1, 9-11). The spores are derived from the tree ferns (*Cyathea* spp), which commonly grow in valleys in moist forest types (Hamilton, 1991).

Family: Cyperaceae

Cyperaceae id.

Description: A distinct pollen type with lozenge shape. The pollen is inaperturate, and the long axis measures about 20 to 50 μm. A marked difference in size characteristics was observed among this pollen type (Plate 5.1, 12-14 and see Taylor, 1988). The origin of each particular type is not known, so no attempt was made to separate the pollen into distinct groups. The pollen is derived from a wide range of sedges, such as *Cyperus*

papyrus, which are common components of wetland vegetation in the region (Lind, 1956; see Chapters 2 and 4).

Family: Euphorbiaceae

***Acalypha* comp.**

Description: *Acalypha* pollen is described by Hamilton (1976) as 1 to 7 porate. According to Hamilton (1976), the pollen type is not easily distinguished from other small porate grains and can be confused with pollen from Urtricaceae, although there are differences in pore and wall structure. The pollen is usually tri- or tetrazonoporate, occasionally bizonoporate, psilate under x400 magnification. The size varies from 10 to 20 μm in diameter. The pollen type is produced by a wide range of herbs, shrubs and occasionally trees (Hamilton, 1976).

***Alchornea* comp.**

Description: A distinct pollen type, but can easily be confused with pollen from *Macaranga* in equatorial view. The pollen is trizonocolporate, operculate in polar view, tectate under x400. The shape of the pollen grain is spherical to oblate in equatorial view measuring 18 to 20 μm in diameter. It is circular to semi-angular in polar view with intruding colpi. The exine is ≈ 2 μm thick, being thicker around the colpi. The exetine = endexine. The pollen type is derived from species such as *Alchornea cordifolia*, *A. floribunda* and *A. laxiflora*. The pollen is reported to be moderately well dispersed (Hamilton, 1972).

***Croton* id.**

Description: A distinct pollen type, which resembles that of *Neoboutonia* pollen, but can be separated based on overall size and the organization of the main sculpturing elements. The pollen grain is very large, up to 50 μm in diameter, spherical, inaperturate, gemmate and intectate. The pollen type is derived from *Croton macrostachyus*, *C. sylvaticus* and *C. megalocarpus* (Livingstone, 1967). The pollen is poorly dispersed (Hamilton, 1972) and can therefore be under-represented in the pollen counts.

***Neoboutonia* id.**

Description: A distinct pollen type, inaperturate, intectate and morphologically similar to *Croton*, but smaller in size. The pollen measures up to 30 μm in diameter (Plate 5.1, 15 & 16). The pollen type is produced by *Neoboutonia macrocalyx* and *N. melleri*, which grow in wetter environments. *N. macrocalyx* is a common species in montane forests between 1400 to 2500 m a.s.l, while *N. melleri* occur in lower altitudes (Hamilton, 1982; 1991). The pollen has moderate to low export ability and may be under represented in pollen counts (Hamilton, 1972).

Family: Myrsinaceae

***Rapanea* id.**

Description: A distinct pollen type; trizonocolporate, occasionally tetrazonoporate. and subprolate in equatorial view (Plate 5.1, 17). The long axis measures about 17 μm and the short axis 15 μm. Circular in polar view with intruding colpi. The distinguishing

features are the colpi, which are truncated. The exine is 2 μm thick and stratified, ectexine = endexine. The pollen is derived from *Rapanea melanophloeos* and *R. rhododendroides*, which are common in montane forests, but also occur in swamp forests in lower altitudes (Lind & Morrison, 1974; Hamilton, 1991) The pollen is reported to be moderately well represented in the pollen counts (Hamilton, 1972).

Family: Myrtaceae

***Syzygium* id.**

Description: The pollen type is distinct, trizonocolporate, sometimes tetrazonocolporate, tectate and psilate. The exine is approximately 1 μm thick and clearly stratified. The ectexine = endexine. The pollen is derived from *Syzygium cordatum* and *S. guineense*, which are trees commonly growing in swamps, particularly near papyrus swamps and riverine forests (Hamilton, 1991). The pollen is moderately well dispersed (Hamilton, 1972).

Family: Oleaceae

***Olea* id.**

Description: The pollen type is very distinct, trizonoporate, occasionally tetrazonoporate, tectate, with heavy and dense reticulum (Plate 5.1, 18). The pollen grain is oblate in equatorial view, circular in polar view with intruding colpi running the full length of the pollen grain. The short axis measures about 16 μm and the long axis 20 μm. The exine is about 2 μm thick and stratified, the ectexine = endexine.

The pollen type is derived from *Olea capensis* spp *welwitschii*, *O. capensis* spp *hichstetteri* and *O. Africana* (Hamilton, 1991). *Olea* is reported to be an important colonising genus in forest edges, predominantly found between 1500 m to 2500 m and up to 3000 m a.s.l in drier mountain areas (Livingstone, 1967; Lind & Morrison, 1974; Hamilton, 1982, 1991). The pollen is reported to be poorly dispersed (Hamilton, 1972).

Family: Poaceae

Description: The Poaceae pollen type is distinct, large, spherical and monoporate, measuring up to 40 μm in diameter (Plate 5.1, 19-21). Considerable variations exist in the size of the pollen grains among the members of this family. However, it was not possible to distinguish between different genera. The pollen type is produced by a wide range of grasses and is generally well dispersed and can be over-represented within the pollen counts (Hamilton, 1972).

Family: Podocarpaceae

Podocarpus id.

Description: A distinct pollen type, saccate with considerable variation in size of the grain and the angle between the saccus and the saddle. The long axis varies from 35 to 60 μm. (Plate 5.1, 22). The pollen type is derived from *Podocarpus gracilior*, *P. milanjianus* and *P usambarensis* var. *dawei.* (Livingstone, 1967; Lind & Morrison, 1974). *Podocarpus gracilior* occurs in dry montane forest (Lind & Morrison, 1974; Hamilton, 1991), while *P. usambarensis* and *P. milanjianus* occur in a wide range of altitude from about 1200 m to 3500 m a.s.l (Hamilton, 1991) and common in lowland seasonal swamp forests (Kendall, 1969; Lind & Morrison, 1974; Hamilton, 1991).

According to Hamilton (1972), the pollen is well dispersed and may be over-represented in pollen counts.

Family: Rosaceae

***Alchemilla* id.**

Description: The pollen grain is very distinct, trizonocolpate, psilate, tectate and prolate in equatorial view with rounded ends. The grain measures approximately 20 μm long and 12 μm wide. It is circular to angular in polar view with intruding colpi. The exine is approximately 2 μm thick and stratified; exetine = endoxine. The pollen type is derived from species of *Alchemilla*, which are mainly composed of herbs or low shrubs. The genus is reported to be widely and often found in associations with swamp vegetation, but is common in montane vegetation (Lind & Tallantire, 1971). The pollen is reported to be poorly dispersed (Hamilton, 1972).

Family: Rutaceae

***Teclea* sim.**

Description: *Teclea* pollen is described by Bonnefille (1971). The pollen type is trizonocolporate, striate, and tectate. It is prolate in equatorial view, semi-angular in polar view with intruding colpi. The long and short axes measure about 20 μm and 15 μm respectively. The exine is 1.5 μm thick, stratified, ectexine = endexine. The pollen is produced by *Teclea nobilis* and *T. grandifolia*, which are common understorey trees in forests and can occur up-to 2500 m a.s.l (Lind & Morrison, 1974; Hamilton, 1991). The pollen is of low export ability (Hamilton, 1972) and can be under-represented in the pollen counts.

Family: Ulmaceae

East African Ulmaceae pollen is described by Hamilton (1976).

***Celtis* id.**

Description: *Celtis* pollen is described and illustrated by Bonnefille (1971). The pollen type is trizonoporate, scabrate, tectate, circular in polar view and spherical in equatorial view. The grain measures approximately 20 to 25 μm in diameter. Pores are round to elliptical, slightly annulate and operculate. This pollen type is reported in two other taxa, *Chaetacme* (Ulmaceae family) and *Hymenocardia* (Euphorbiaceae family) (Livingstone, 1967; Kendall, 1969; Hamilton, 1972; 1976). However, Hamilton (1976) noted that *Chaetacme* pollen has more protruding pores and a finer exine than *Celtis*.

Plate 5.1 Fossil pollen and spores extracted from Munsa II sediments

All photomicrographs were taken using TK-C1380E Camera under x400 magnification; the scale bar is 5 μm

1 - 2	*Cussonia* comp.	Equatorial view showing colpus and elongate pore
3 - 6	*Combretum* id.	3 & 4, polar view showing six colpi; 5 & 6, equatorial view showing colpi and porate (triporate)
7 -d 8	*Bidens* comp.	Polar view showing colpi (trizonocolporate) and spiny wall.
9 - 11	*Cyathea* id.	Polar view showing, trilete furrows (trilete spore)
12 – 14	Cyperaceae id.	Polar view, lonzenge shape, inaperturate
15 - 16	*Neoboutonia* id.	Polar view, inaperturate

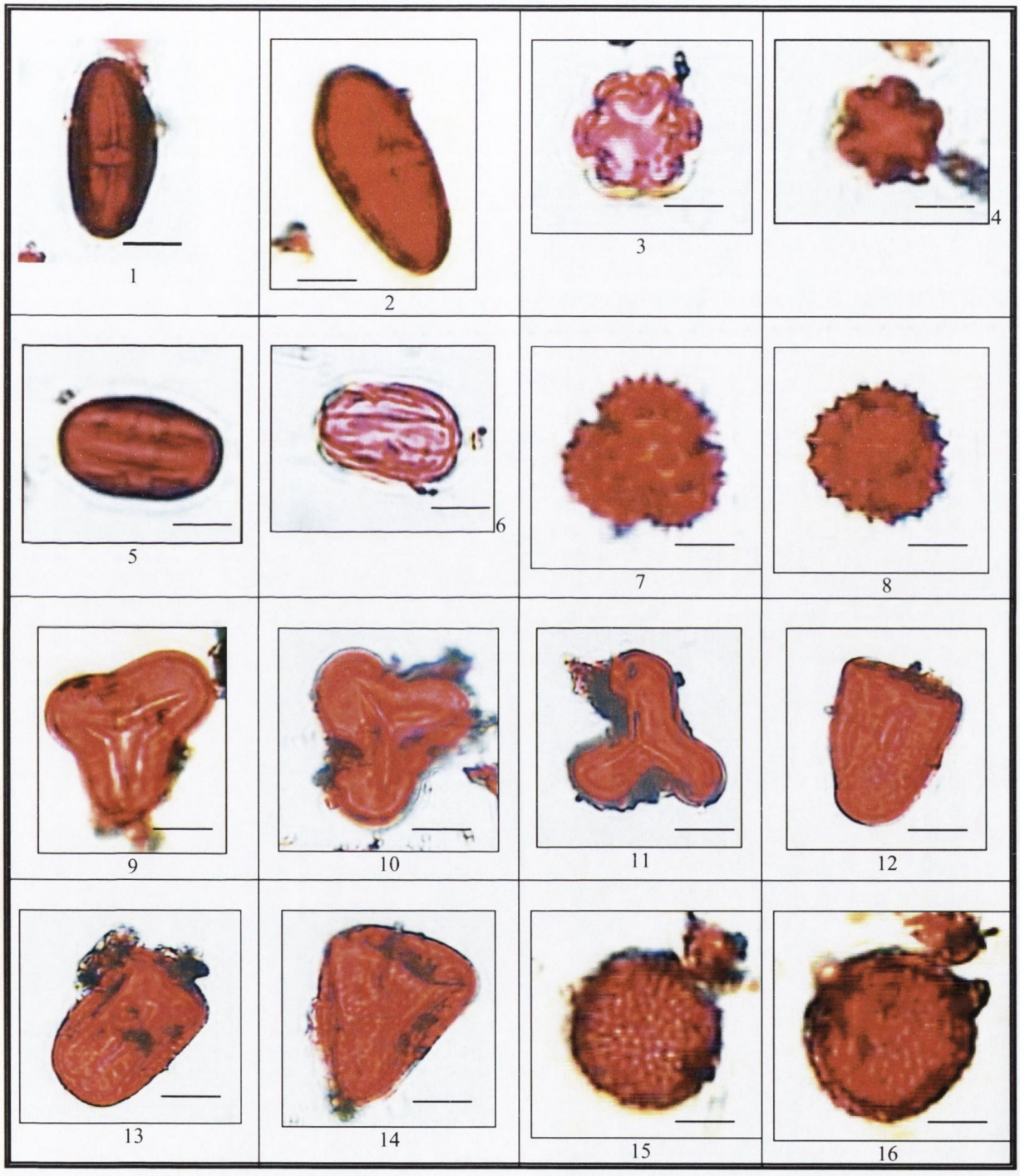
1
2
3
4
5
6
7
8
9
10
11
12
13
14
15
16

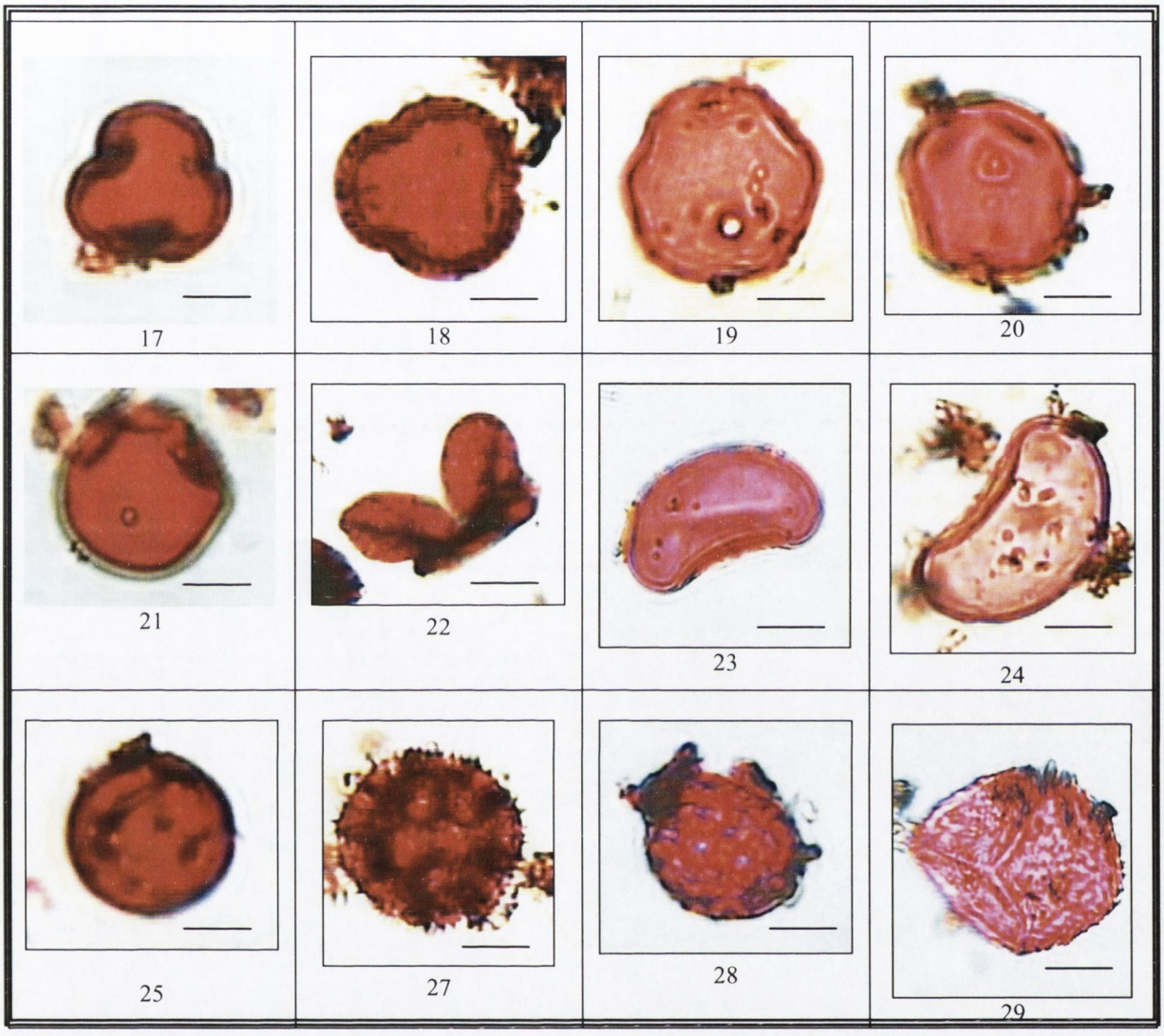

Plate 5.1 Fossil pollen and spores extracted from Munsa II sediments

17	*Rapanea* id.	Polar view showing trilete colpi (trizonocolporate)
18	*Olea* id.	Polar view showing trilete colpi (trizonoporate)
19 - 21	Poaceae id.	Polar view showing pore (monoporate)
22	*Podocarpus* id.	Equatorial view showing saddle and two saccus
23 - 24	Filicales id	Equatorial view, monolete spore with smooth walls

25	Chenopodiaceae	Showing pores
27	Caryophyllaceae	Showing pores
28	Amaranthaceae	Showing pores
29	Sphagnum comp.	Polar view, trilete spore

5.7.3 Relative and absolute abundance of pollen

The contribution of each pollen taxon in a sample is usually expressed as either relative to that of other taxa, in percentages or as an absolute figure, independent of other types. Pollen data for Munsa II sediments (cores M2C1, M2C2 M2C3C) are here presented as both percentage and absolute values.

In the present work, two pollen sums were established. The *non-local pollen* sum comprised pollen types thought to have originated from taxa growing in the catchment for Munsa II swamp. The *local-pollen and spores* sum was based on pollen and spore types from plants thought to have been growing on the swamp itself. Estimations of absolute pollen values used in this study are based on the method described by Maher (1981), Birks & Gordon (1985). As stated earlier in this chapter, marker tablets of *Lycopodium* spores were the source of the exotic grains and the quantity of *Lycopodium* spores in the marker tablets was 10,850 ± 200. Absolute pollen concentration was calculated using the standard formula as follows:

Pollen grains per gram dry sediment (P) = (marker grains added, N=10,850) / (marker grains counted, n) X (Pollen grains countered, p) / (dry weight of sample, dwt).

$$P = (N / n)(p / dwt)$$

Pollen Influx, I (pollen grains $cm^{-3}yr^{-1}$) was calculated from the above equation as follows:

$$I = \frac{(N / n)(p / v)}{T}$$

Where:

I = Pollen influx or accumulation rate (grains cm^{-3} yr^{-1})

N = total number of marker grains (*Lycopodium* spores) added

n = number of marker grains (*Lycopodium* spores) counted

p = number of pollen grains counted from the sample

dwt = dry weight of the sample analyzed (g)

v = volume of sediment sample analysed

T = sediment deposition time (yr cm^{-3})

The age of individual layers or sediment deposition time was calculated based on the age-depth curves described earlier in this chapter (see section 5.5). Ideally, pollen influx is a direct reflection of variations in plant productivity and preservation. However, fluctuations of pollen influx may also relate to variations in sedimentary environments.

5.8 Construction and zonation of pollen assemblage diagrams.

The percentage pollen data from M2C1, M2C2 and M2C3C are portrayed using histogram diagrams in chapter seven. In order to facilitate description, comparison and discussion of the pollen diagrams, the data from each core were divided into pollen zones. The pollen zones were delimited on the criteria of their pollen content, without referring to time scale or sediment stratigraphy; thus the pollen zones are the equivalent of biostratigraphic units (Moore *et al.*, 1991). In this thesis, the pollen diagrams were zoned numerically using Psimpoll program (Bennett, 1998), based on *non-local pollen* types with an abundance of > 2% in at least one sample. According to Gordon & Birks (1972), in numerical zonation schemes, pollen from local sources should be omitted as they can be subject to large fluctuations that may not be ecologically significant.

The results of the zonation of pollen data are discussed in chapter seven. To ease interpretation of the pollen diagrams in the three cores, the pollen zone boundaries were identified objectively by grouping similar samples together in a form of hierarchical dendrogram, in which each sample was linked to the adjacent sample with which it shares the greatest levels of similarity of content. The numbering of the zones adopted in this thesis is prefixed by the core notation (e.g. C1) followed by zone number (Z1). The numbering runs from the base to the top of the assemblage diagram, and each zone is separated from the other by a continuous line. In this thesis, the pollen zone boundaries were repositioned slightly to facilitate inter-core comparison between the three sediment cores.

Gordon (1982), Birks & Gordon (1985) and Birks (1986) recommend that an attempt should always be made to verify results obtained from one particular clustering technique. To verify the effectiveness of the results from the constrained zonation method, and to establish any relationships between non-contiguous samples and zones, the technique was checked by a stratigraphically unconstrained clustering technique. The unconstrained method applied in this study was Detrended Correspondence Analysis (DCA) and involved use of the computer program CANOCO (ter Braak & Smilauer, 1998). In the DCA, the 'arch' and 'compression' effects, which often arise from the dependence of a constrained second axis on the first axis during computation, are removed. The details of the 'arch' and 'compression' effects are explained in Gauch *et al.* (1977) and Kent & Coker (1992). DCA in CANOCO uses four axes to account for the main variations in a data matrix (Birks & Gordon, 1985). The relationships between individual data points are displayed graphically as a bi-plot. On the bi-plot display, samples close together have a similar composition, while those placed further apart are dissimilar in content (Kent & Coker, 1992).

5.9 Identification and enumeration fungal spores

Identification of fungal spores was based on the slides previously prepared for pollen counting. Between 200 and 300 fungal spores were enumerated per sample. The fungal spores were identified to the lowest possible taxonomic level using published illustrations and descriptions in van Geel (1978; 1986), van Geel *et al.* (1982-3) and Kalgutker & Jansonius (1999). The descriptions of the most ecologically and

numerically significant fungal spores, together with their probable source and the ecological range of the parent taxa (where known) are presented below.

5.9.1 Description of fossil fungal spores

The fungal spores presented below are described according to the morphological characteristics used by van Geel (1978; 1986).

***Alternaria*-type:**

Description: Ascospores have many transverse and longitudinal septa, which are flattened. The spores vary in size, measuring 25 to 45 μm long and 15 to 35 μm wide (Plates 5.2, 1-2).

***Arthrinium*:**

Description: A monoporate spore with varying size, measuring about 5 to 10 μm in diameter (Plate 5.2, 3-5).

***Cercophora*-type 112**

Description: Ascospores have a tapering apical end with a pore measuring approximately 0.5 μm in diameter. Each ascospore measures about 20 to 25 μm long, and 10 to 15 μm wide (Plates 5.2, 6). The ascospores are coprophilous, occurring on herbivore dung, decaying wood and herbaceous stems and leaves (van Geel, 1978; 1982-83; 2001).

Gaeumannomyces

Description: Spores have lobed hyphopodia, with varying shapes and sizes (Plates 5.2, 7). Gaeumannomyces fungi are commonly associated with sedges (Cyperaceae) and have been recorded in the epidermis of *Carex* species (van Geel, 1978; 2001; van Geel *et al.*, 1982-83).

***Sporomiella* - type**

Description: *Sporomiella* fungus is described by Ahmed & Cain (1972) and Davis (1987). The ascospores are distinct, with four to eight septa (Ahmed & Cain, 1972), and may occur as individual cells (Davis, 1987). Ascospores measure about 25 to 45 μm long and 5 to 25 μm wide. Each spore has a pronounced sigmoid germinal aperture measuring about 1μm wide. The fungus is common on the dung of herbivores (Davis, 1987), but they also occur on decaying wood (Ahmed & Cain, 1972).

Type 18

Description: Ascospores are one septate, measuring about 35 to 45 μm long and 10-15 μm wide (Plates 5B, 8). The ascospores often occur in fruiting bodies, which are ostiolate in shape with a wall measuring about 7-10 μm thick (van Geel, 1978).

Type 55

Description: Spores are ellipsoidal, one-celled with a smooth wall. Two forms of type 55 were identified in Munsa II sediments; Type 55A and Type 55B. Spores of type 55A (Plate 5.2, 9 & 10) measure about 15 to 20 μm long and 10 to 17μm wide, with one

protruding apical pore about 1.5μm wide. The wall is slightly thickened around the pore, and the other end of the pore is often flattened. The spores of type 55B (Plate 5.2, 11 & 12) measure about 25 to 40 μm long and 15 to 16 μm wide. The spores have two protruding apical pores measuring about 1-2 μm wide. Type 55A and B are reported to occur in eutrophic to mesotrophic environments (van Geel *et al.*, 1982-83).

Type 181

Description: The spores measure about 10 to 15 μm in diameter. Spores have broad hairs, approximately 0.5 μm long (Plate 5.2, 13 & 14). The spores may occur in groups of up to nine spores (van Geel *et al.*, 1982-83). The spores of type 181 are reported to be common in stagnant shallow open water, eutrophic conditions (van Geel *et al.*, 1982-83).

Ustulina

Description: This ascospore is asymmetric in shape, tapering at the apices into sharp ends. The ascospores measure about 20 to 35 μm long and 5 to 10 μm wide. Each ascospore has a longitudinal groove, measuring about 1.5μm wide (van Geel & Anderson, 1988). *Ustulina* is reported to be a mild parasite causing soft-rot of wood on several tree species and spores are well dispersed over long distances (van Geel & Anderson, 1988).

***Zygnemataceae* - Type 58**

Description: The spore is compressed, ellipsoidal, flattened, and the whole surface is covered with numerous deep dents about 2 to 3 μm and 2 μm wide. The spores measure about 50 to 45 μm wide (van Geel, 1978; 2001). *Zygnemataceae* fungi are reported to

inhabit shallow, stagnant oxygen-rich freshwater, lakes, ponds and wet soils (van Geel, 1978; 2001).

Unclassified fungal spores

Plate 5B, 15-32 illustrates a section of unclassified fungal spores encountered during the current research.

Plate 5.2 Fossil fungal spores extracted from Munsa II sediments

All photomicrographs were taken using TK-C1380E Camera under x400 magnification; the scale bar is 5 μm

1 - 2	*Alternaria*-type.	Equatorial view showing transverse and longitudinal septa
3 -5	*Arthrinium.*	Equatorial view (monoporate)
6	*Cercophora*-type	Equatorial view showing septa (monoporate)
7	*Gaeumannomyces*	Equatorial view showing, lobed hyphodia
8	Type 18	Equatorial view showing septa
9-10	Type-55A	Equatorial view showing apical pore
11-12	Type 55B	Equatorial view showing two apical pores
13-14	Type 181	Equatorial view showing broad hairs
15-16	Unclassified	Polar view (surface covered with dents)
17-18	Unclassified	Polar view showing apical pore (monoporate)
19-20	Unclassified	Equatorial view showing protruding apical pore
21-22	Unclassified	Equatorial view showing

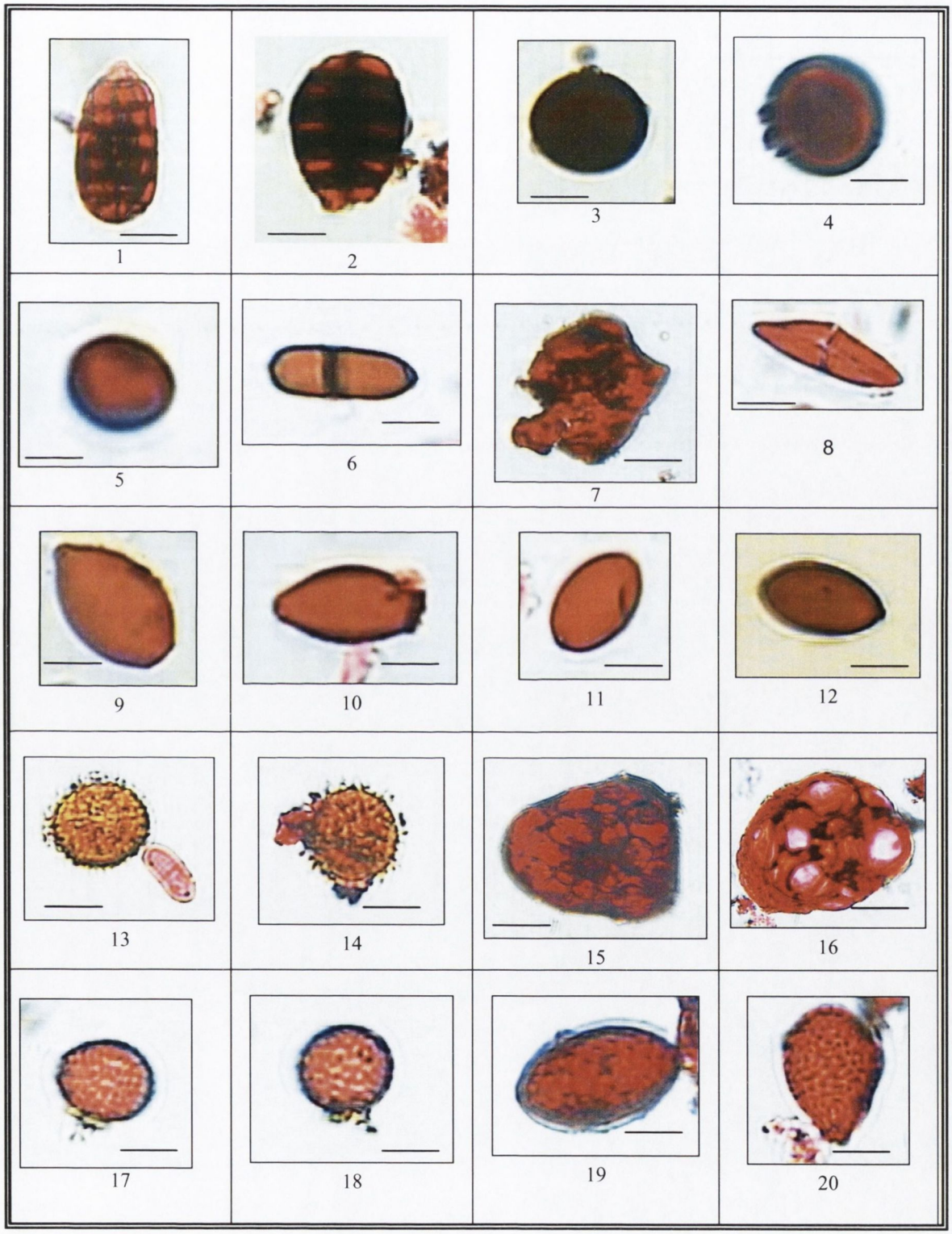

1 2 3 4 5 6 7 8 9 10 11 12 13 14 15 16 17 18 19 20

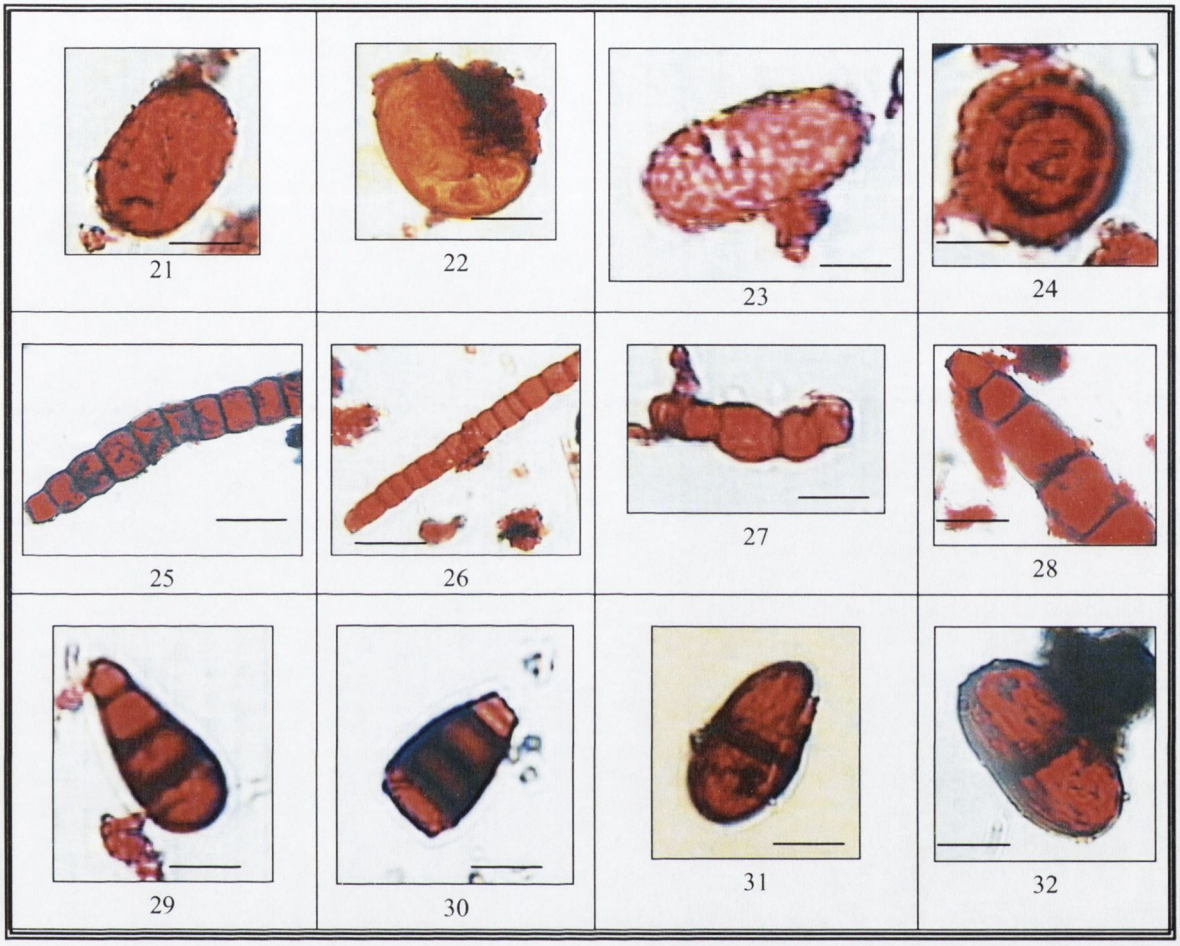

Plate 5B Fossil fungal spores extracted from Munsa II sediments

23	Unclassified	Equatorial view showing septa
24	Unclassified	Equatorial view showing septa
25-28	Unclassified	Equatorial view showing multi septa
29-30	Unclassified	Equatorial view (three septa)
31-32	Unclassified	Equatorial view (one-septa)

5.10 Analysis of phytoliths

Extraction of phytoliths for reference slides was based on the collection of voucher plant specimens collected in the study area (see section 4.5). The analysis of phytoliths was conducted at the Palynology Laboratory in the Department of Geography, Trinity College, University of Dublin.

5.10.1 Extraction of voucher specimens of phytoliths from plant materials

A number of studies have employed various methods for extracting phytoliths from plant materials (e.g., Rovner, 1971; Pearsall, 1978, 2000; Piperno, 1988; Bowdery, 1989; Runge, 1995; Parr *et al.*, 2001; Wallis, 2003). These methods are broadly divided into two; (1) dry ashing and (2) wet ashing (acid digestion). According to Rovner (1983), Piperno (1988) and Pearall (1989), the dry ashing technique tends to modify the resultant size and shape of phytolith morphotypes at temperatures greater than 600^0C. However, recent comparative studies conducted by Pearsall (2000) and Parr *et al.* (2001), have demonstrated that the dry ashing method produces reliable and comparable results at temperatures less than 600^0C. This study therefore employed the dry ashing method to extract phytoliths from voucher plant specimens. Sufficient morphological detail was retained by phytoliths concentrated through this technique to facilitate their identification.

The procedure involved drying approximately 1 g of freshly preserved plant material in an oven at 105^0C for 24 hours. The dried material was ignited in a muffle furnace at

500^0C for 1 hour to break down the organic plant material. The samples were transferred to 10 ml plastic test tubes and washed in 5 ml of 10% HCl, followed by concentrated Nitric acid (NHO_3), and benzene. The residues were transferred to crucibles and dried in an oven at 105^0C overnight. The phytolith bearing fractions were mounted on slides with Permount and observed under the microscope at x400 magnifications. The remaining (unused) phytolith fraction was transferred to storage vials for later use.

Micrograph images at x800 to x7000 magnifications were obtained using Scanning electron microscope (SEM) facilities (Hitachi S-3500N) at the Catholic University of Luven, Belgium and at the Centre for Microscopy and Analysis (CMA) (Hitachi S-4300, S.E.M, based at Trinity Collge, University of Dublin. Some SEM micrographs of *Ensete ventricosum* used in the present study were based on samples obtained from the Royal Museum of Central Africa in Belgium. Photomicrographs were obtained using Leitz Wetzlar Dialux 20 Microscope and TK-C1380E Camera.

5.10.2 Comparison of cross-shaped phytolith morphotypes extracted from maize (*Zea mays*) and wild grasses

Detailed analyses of morphology were conducted on selected voucher specimens (Table 5.1), which are of economic importance locally, with the aim of distinguishing cross-shaped phytoliths of cultivated plants from those that originate from wild grasses. Maize has distinct cross-shaped morphotypes that can be distinguished from non-cultivated (wild) grasses (Plate 5.3, 1 & 2). Cross-shaped short cell morphotypes were first used by

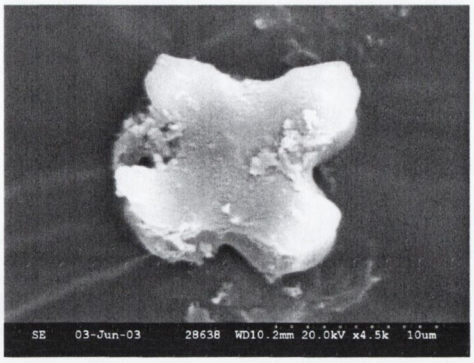

(a) Cross-shaped morphotype phytolith from *Zea mays*

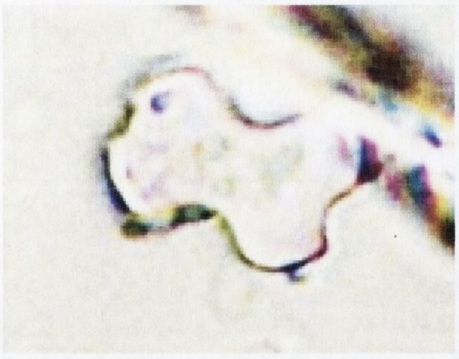

(b) Dumbbell-shaped morphotype phytolith from wild grass

Plate 5.3 Characteristic features of phytoliths used to distinguish maize cross-shaped morphotype (1) from a dumbbell-shaped morphotype (2).

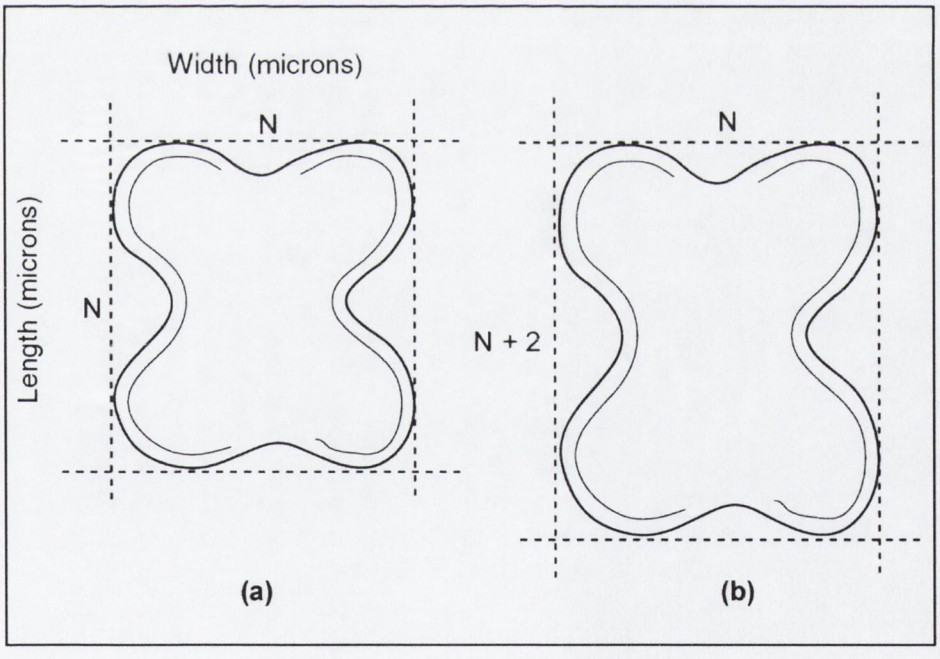

Figure 5.2 Dimensions of cross-shaped phytoliths used to distinguish the longer axis (length) from shorter axis (width), with measurements of N by N (**a**) or N by (N+2) (**b**), where N = 4.58μm (see 5.10.2).

Pearsall (1978) to distinguish cultivated maize from wild grasses. She noted that cross-shaped morphotypes from maize were significantly larger than those of the native Panicoid grasses. According to Pearsall's criteria, cross-shaped phytoliths are defined as those with at least three dimensions of N by N to N by (N + 2), where N represents 4.58 μm (Figure 5.2, a & b). The expression signifies that phytoliths more than 9.16 μm longer than the width are not classified as cross-shapes. This criterion helps to eliminate phytoliths that appear to be transitional between dumbbell-shaped and cross-shaped, thus defining the limits of cross-shaped type. Pearsall (1978; 2000) classified the cross-shaped phytoliths into four categories based on measurement of their shorter axis, namely: small (6.86 - 11.40 μm), medium (11.45 - 15.98 μm) large (16.03 - 20.56 μm) and extra-large (20.61 - 25.19 μm).

The technique of Pearsall (1978) was employed in this study as a means of distinguishing maize phytoliths from those produced by non-cultivated grasses. A comparison was first made on 11 voucher specimens (three cultivated varieties and eight non-cultivated grasses) (Table 5.1) to determine the size and frequency of cross-shaped morphotypes. A total of 100 cross-shaped morphotypes were randomly selected from each specimen to determine the dimensions of the short axis. A dimension limit of 15.19 μm was set to separate maize morphotypes from those of non-cultivated grasses. This limit ensures that cross-shaped phytoliths from non-cultivated grasses were not wrongly recorded as maize. Details of the results are presented in chapter eight.

Table 5.1 Voucher plant materials analysed for cross-shaped phytolith morphotypes.

Cultivated variety in the study area	**Non-cultivars / wild grasses in the study area**
Sorghum bicolor (L.) Moench (cultivated sorghum)	* *Sorghum arundinaceum* (Desv.) Stapf (Wild sorghum)
Eleusine coracana (L.) Gaertn. (finger Millet)	**Panicum maximum* Jacquin (Guinea grass)
Zea mays L (maize)	**Panicum latifolium* L.
Musa paradisiana (cooking banana)	**Pennisetum purpureum* Schumach. (elephant grass)
Musa sapientum (sweet banana)	+ *Cymbopogon afronardus* Stapf (tussock grass)
	+*Hyparrhenia rufa* (Nees) Stapf (yellow spike thatching grass)
	+*Imperata cylindrica* (L.) Palisot (spear grass)
	**Setaria sphacelata* (Schumach.) Stapf (Nandi grass)
	Ensete ventricosum Maurelii (wild banana)
	Ensete ventricosum (Welw.) E.E. Cheesman (wild banana)

* *Species used as pasture grass and* +*thatch grass / alternate source of pasture*

Piperno (1984) provides an alternative technique of distinguishing cross-shaped variants from maize in archaeological deposits from the humid tropics of Panama. The technique uses detailed morphological (three-dimensional) features to categorize cross-shaped morphotypes into eight variants (Figure 5.3). Piperno (1984) noted that variant I cross-shape is dominant in maize, but less frequent in non-cultivated grasses. Low ratios of variants II and VI are found in some races of maize, although these variants are dominant in non-cultivated grasses. Variants III, IV, VII and VIII are found in non-cultivated grasses.

According to the technique of Piperno (1984), both sides of variant I cross-shaped morphotypes have the same shape, and form mirror images of each other (Figure 5.3, a-c). Variant II has only one cross-shaped side, and the other side is arched into a tent-like shape (Figure 5.3, d-f). Variant III cross-shaped morphotype has four large nodules projecting from each corner of the morphotype (Figure 5.3, g). Variant IV cross-shaped morphotype has a thin, elongated plate of silica on the back of the cross-shaped side, and appears as a narrow rectangle lying along the long axis (Figure 5.3, h). Variant V cross-shaped morphotype has two elevated pieces of silica along the long axis, forming an outline of a near dumbbell (Figure 5.3, i). Variant VI is complex in shape and has roughly a trapezoidal to rectangular structure on the back of the cross-shaped side of the morphotype (Figure 5.3, j). Variant VII cross-shaped morphotypes have dumbbell shapes on the non-cross-shaped side of the morphotypes (Figure 5.3, k), while in variant VIII, the cross-shaped side exhibits a conical-shaped projection at each corner of the non-cross shaped side of the phytolith (Figure 5.3, l).

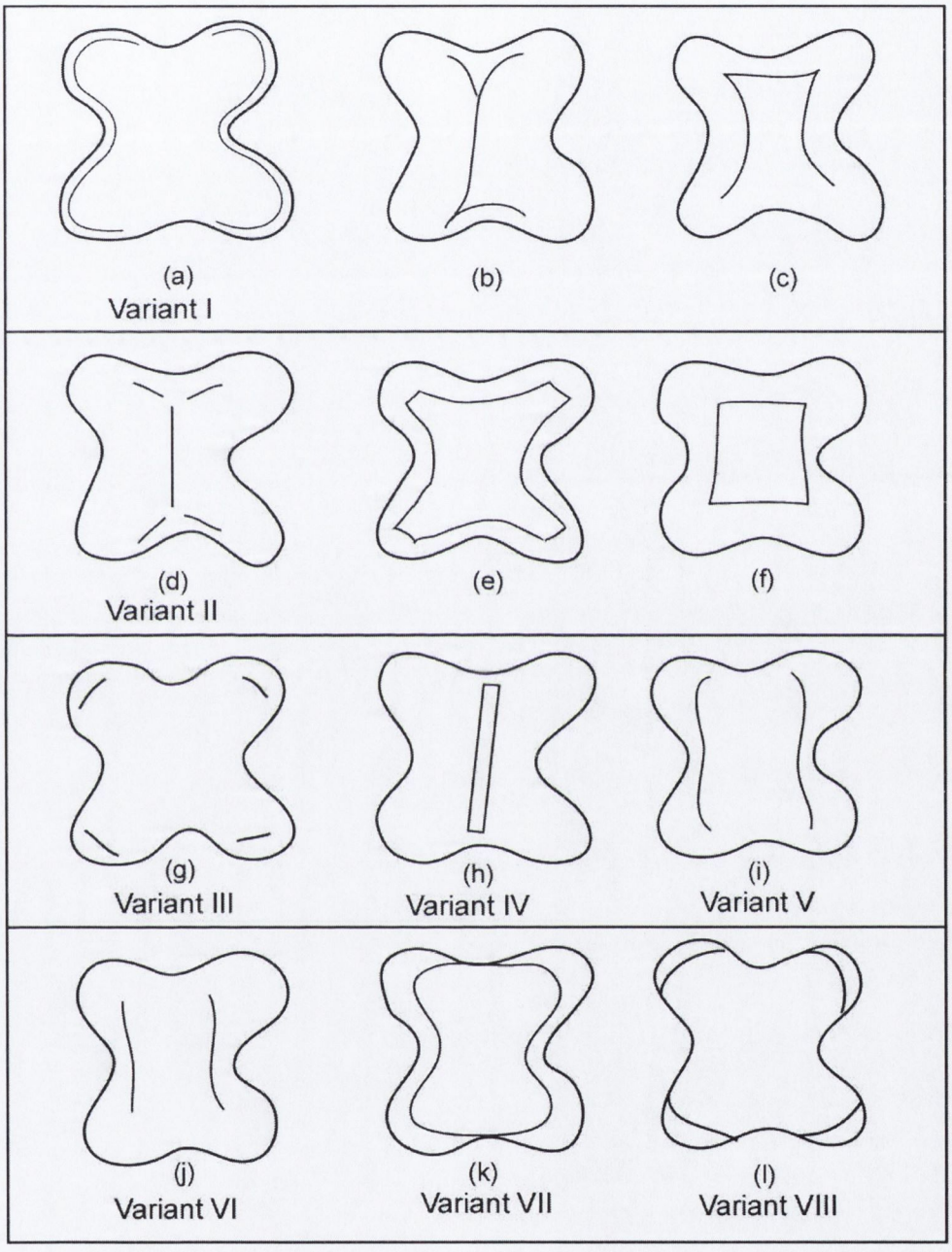

Figure 5.3 Cross-shaped variants of maize and wild grasses (Adapted from Piperno (1984) and Pearsall (1978; 2000).

5.10.3 Morphological characteristics of Musaceae phytoliths

In order to discriminate between *Musa* and *Ensete* phytoliths in Munsa II sediments, it was necessary to analyse voucher specimens of both the cultivated / edible *Musa* and wild *Ensete* type obtained from the study area. Four specimens (two *Musa* and two *Ensete*) were analysed for their phytolith morphotypes (Table 5.1) using dry ash method (see section 5.10.1). Details of morphological characteristics are presented in chapter eight

5.10.4 Extraction of phytoliths from soil sediment

Fossil phytoliths were extracted from samples of sediment from cores M2C1, M2C2 and M2C3C using standard procedures described in Piperno (1988) and Pearsall (2000). The procedure involves drying approximately 2-3 cm^3 of sediment samples in an oven at 105^0C overnight. The dried sediments were sieved through a 1 mm sieve to remove any large-sized material prior to phytolith extraction. The samples were treated with 10 ml of 10% HCl to remove carbonates, centrifuged and decanted. Approximately 3 to 5 ml of concentrated nitric acid (NHO_3) was added to each sample and placed in a hot water bath for about 3 hours to digest the organic material. Care was taken to ensure that the reaction had subsided and all the material had settled at the bottom. The samples were then transferred to 50 ml beakers and deflocculated in 10 ml of 5% Calgon solution (sodium hexametaphosphate) by repeated stirring and shaking overnight using an automatic shaker to separate the phytoliths from the sediment sample. The samples were wet sieved through a 250 μm mesh sieve, to separate sand from the remains of the

sediment, and placed in 50 ml beakers for sedimentation. About 3-5 ml of distilled water was added to each sample, stirred and the suspension was allowed to settle for about 5 minutes. The supernatant (fine silt) was decanted and the procedure was repeated several times until the supernatant was clear.

The samples were transferred into 10 ml test tubes. The phytoliths were floated in 5 ml portion of heavy liquid of $ZnBr_2$ /HCl at a density of 2.3 and centrifuged at 3000 rpm for 5 minutes. The floating phytolith material was carefully removed at the top of the test tube with a Pasteur pipette and transferred to another clean test tube. This procedure was repeated until no floating phytoliths were visible. Distilled water was added to each test tube containing the phytolith extracts in a ratio of 3:1 and stirred vigorously to mix the heavy liquid and water. This lowered the specific gravity to less than 2.3, allowing phytoliths to settle at the bottom of the test tube. The samples were centrifuged at 3000 rpm for 5 minutes and the supernatant decanted. The procedure was repeated twice to remove all the heavy liquid from the phytoliths. The phytolith fraction was washed twice with distilled water and dried in an oven at 105^0C overnight. The phytolith fraction was then mounted on microscopic slides with Permount.

5.10.5 Phytolith classification and counting

Enumeration of phytolith morphotypes was made on material mounted on microscopic slides and observed under 400x magnification using Leitz Laborlux 12 Microscope. The number of phytoliths counted per sample ranged from 500 to over 1000, with at least 200 short-cells in each count. According to Pearsall (2000), a minimum count of 200

short-cell phytoliths is appropriate for vegetation reconstruction. Poaceae phytoliths were identified according to the standard taxonomic classification of Twiss *et al.* (1969) and Mulholland (1992), while the non-Poaceae phytoliths were classified according to Piperno (1988), Rungi (1999), and voucher materials collected during the present research and described earlier in this chapter.

Phytoliths with distinguishing taxonomic characteristics were classified into eight morphotypes as follows: (i) cross-shaped, (ii) dumbbell-bilobate and -polylobate (iii) rectangular/rondel-shaped, (iv) saddle-shaped, (v) spherical-rugose (trees./shrubs), (vi) spherical-crenate, (vii) cone/hat-shaped (Cyperaceae), and (viii) cone with trough (Musaceae). Phytoliths that occur in all members of the Poaceae family or in both Poaceae and non-Poaceae families were classified as follows: elongate (smooth & sinuous), point-shaped, fan-shaped, and cork-cell morphotypes (produced by epidermal cells of all the Poaceae and non-Poaceae (Alexandre *et al.*, 1997; Barboni, *et al.*, 1999).

According to the classification of Twiss *et al.* (1969) and Mulholland (1992), the Poaceae family can be separated according to phytolith morphotypes into cross-shaped, dumbbell-shaped (bilobate/polylobate) and saddle-shaped phytolith morphotypes. The cross- and dumbbell-shaped phytolith morphotypes are produced in abundance by mixed C_3/C_4 tall Poaceae belonging to the subfamily Panicoideae. According to Twiss *et al.* (1969) and Piperno (1988), the saddle-shaped morphotype is produced by C_4 short Poaceae belonging to the subfamily Chloridoideae. The rectangular/rondel-shaped morphotypes are produced by C_3 Poaceae of the subfamily Festucoideae, while the spherical rugose morphotype is produced by ligneous dicotyledons characteristic of trees

& shrubs. The spherical-crenate morphotype is a characteristic of the Palmae, while the cone/hat-shaped morphotype is produced by the Cyperaceae family (Piperno, 1988; Hart, 1990; Willis, 2003). Morphotypes belonging to the Musaceae family have a raised cone with a trough (Piperno, 1988). Elongate (smooth and rough), point-shaped, and fan-shaped, morphotypes are produced by epidermal cells of whole Poaceae family, while cork-cell morphotype occurs in all members of Poaceae and non-Poaceae (Twiss *et al.*, 1969; Alexandre *et al.*, 1997; Barboni *et al.*, 1999).

5.10.6 Descriptions of phytolith morphotypes

Phytolith morphotypes described below include fossil morphotypes encountered during the count and those obtained from voucher specimens. The criteria for description are based on the standard classification of Twiss *et al.* (1969), Mulholland (1992), Piperno, 1988, Alexandre *et al.* (1997), the standard International Code for Phytolith Nomenclature (ICPN, 2003) as well as my own observations. The classification is based on morphological features that include shape, size and surface texture and the identification is to the lowest taxonomic level possible.

Dumbbell-shaped phytoliths

Description: Two distinct dumbbell-shaped phytoliths were observed in Munsa II sediments, bilobate and polylobate morphotypes. The bilobate morphotype has two lobes of unequal diameter, with the long axis varying from 5 to 25 μm. According to the classification of Fredlund & Tieszen (1994), the bilobate morphotype is further

subdivided into simple lobate, panicoid-type, and stipa-type. The simple lobate type has a more pronounced shank separating the lobes and lateral plane of symmetry and has rounded ends (Plate 5.4, 1 & 2), while the panicoid-type differs by having a well developed lateral plane of symmetry and indented or sculptured ends (Plate 5.4, 3-4). The stipa-type has distinctly asymmetrical (trapezoidal) cross-section with much smaller plateau of varying outline and a typically flat or unsculptured surface (Fredlund & Tieszen. 1994) (Plate 5.4, 5).

The polylobate morphotypes have symmetrical and asymmetrical shapes, having a maximum number of three lobes on each side. The symmetrical forms have equal number of lobes on each side and well-developed vertical and lateral plane of symmetry, with the base slightly wider than the plateau (Plate 5.4, 6). The asymmetrical forms have unequal number of lobes on each side. They have a poorly developed lateral plane of symmetry, with a base much wider than the plateau (Plate 5.4, 7).

Potential sources: According to Fredlund & Tieszen (1994), the bilobates (simple lobates & panicoid-types) are produced abundantly by C_4 tall Poaceae subfamily Panicoideae, however occurrences of this morphotype has been observed in members of subfamily Andropogoneae, Arundinoideae and Bumbusoideae (Brown, 1984; Mulholland, 1989; Alexandre *et al.*, 1997).

Cross-shaped phytoliths

Description: Cross-shaped phytoliths have four lobes, with shapes varying from symmetrical to asymmetrical forms (Plate 5.4, 8-10). The details of cross-shaped

variants have been described earlier in this chapter (see 5.10.2) and are illustrated in Figure 5.3.

Potential sources: The cross-shaped morphotype occurs in Panicoideae subfamily (Pearsall, 1978; 2000; Piperno, 1984).

Saddle-shaped phytoliths

Description: Two saddle-shaped morphotypes exhibiting narrow to wide bases were observed in Munsa II sediments (Plate 5.4, 11-12). The saddle-shaped forms have two opposite convex edges and two straight or concave edges. The first form is characterised by an ovoid to saddle-shaped base narrowing to a ridge plateau (Plate 5.4, 11). The second form has a wider base than the plateau (Plate 5.4, 12).

Potential sources: Saddle-shaped phytolith morphotypes are produced abundantly by most genera in Chloridoid grasses (C_4 short Poaceae) (Metcalfe, 1960; Twiss *et al.*, 1969; Mulholland, 1989, Alexandre *et al.*, 1997). However, saddle-shaped morphotypes have also been reported in Phragmaites (a C_3-Arundinoideae) (Barboni *et al.* (1999). Saddle-shaped morphotypes also occur in other grass genera e.g. *Aristida* and *Sparta* (Fredlund & Tieszen, 1994).

Elongate (long cell) phytoliths

Description: Two distinct types of elongate phytolith morphotypes were observed in Munsa II sediments, namely smooth and crenate. The elongate smooth morphotypes

occur as cylindrical rods (Plate 5.4, 13) or elongate-angular forms with four or more edges along the surface (Plate 5.4, 14-16). The latter may also have facets across the surface (Plate 5.4, 16), which are typical of lignified plants (Piperno, 1988). The elongate sinuous morphotypes have irregular (crenate) surfaces with annular/spiral surfaces (Plate 5.4, 17) or echinate surfaces (Plate 5.4, 18). The lengths of the elongate phytolith morphotypes vary from 5 to >100 μm.

Potential sources: Elongate morphotypes occur abundantly in all members of the Poaceae family, however, some morphotypes, particularly those with annular/spiral and echinate surfaces have been reported in vascular tissues of dicotyledons (Rovner, 1971; Piperno, 1988; Rungi, 1999; Thorn, 2004).

Cone/hat phytoliths

Description: Each individual cell consists of a squat/short cone (Plate 5.4, 19 & 20) arranged in the centre of a square plate with satellite tuberculate nodes around the base (Wallis, 2003; Thorn, 2004). The cone/hat-shaped phytoliths are commonly arranged in a thin and translucent linear silica skeleton, with up to five others (Thorn, 2004).

Potential sources: Cone/hat-shaped phytoliths are produced in abundance by members of Cyperaceae family (Piperno, 1988; Pearsall, 2000; Wallis, 2003). However, comparable cone/hat-shaped phytolith morphotypes have been reported in non-Cyperaceae, mainly members of the family Mimosaceae (e.g. *Acacia* spp, *Bankisa oblongiflia* and *Cusuarina distyla*) (Hart, 1990)

Fan-and point shaped phytoliths

Description: Fan-shaped (bulliform) and point-shaped morphotypes vary in size and shape. The former have oval to rectangular shapes (Plate 5.4, 21-24), while the later have point shapes at the ends, with length ranging from 10 μm to >100 μm (Plate 5.4, 25-28).

Potential sources: Fan-and point-shaped (bulliform) morphotypes are produced by all members of the Poaceae family (Piperno, 1988; Alexandre *et al.*, 1997; Barboni *et al.*, 1999).

Trichomes

Description: Trichomes are hair-cell phytolith morphotypes, with prickles. Trichomes vary from segmented to non-segmented forms (Plate 5.4. 29).

Potential sources: Hair-cell and base phytoliths occur in the epidermis of all members of monocotyledons and dicotyledons (Piperno, 1988).

Cork cell-like

Description: Circular in shape with flattened and slightly rough surface (Figure 5C, 30), The diameter ranges from 5 to 15 μm.

Potential sources: Cork cell-like morphotyes are reported to occur in both Poaceae and non-Poaceae (Alexandre *et al.*, 1997).

Spherical phytoliths

Description: Spherical phytolith morphotypes occur in two forms; spherical-rugose and spherical-crenate. The spherical-rugose have a smooth to slightly rough surface, with the diameter ranging from 3 to 25 μm (Plate 5.4, 31-35). Spherical crenates morphotypes have a spinulose (irregular) surface with spines up to 2 μm in length, and a diameter of 5 to 25 μm. (Plate 5.4, 36 & 37).

Potential sources: Spherical-rugose morphotypes are predominantly produced by deciduous angiosperms, though some occurrences of smooth spherical morphotypes have been reported to occur in some monocotyledons such as Marantaceae, Cannaceae and Zingiberaceae (Piperno, 1988; Runge, 1999). Spherical-crenate morphotypes occur abundantly in Palmae (Piperno, 1988; Alexandre *et al.*, 1997; Runge, 1999).

Musaceae phytoliths

Description: The morphological features of Musaceae phytoliths are described in chapter eight. Some of the fossil and type material phytolith morphotypes are illustrated in Plate 5.4, 38-47. Some morphological variations were apparent in fossil and type Musaceae morphotypes (Plate 5.4, 44-47), probably due to variation in the level of silica deposited during developmental stages (Alexandre *et al.*, 1997). Plates 5.4, 44-47 are some examples of these variations. The shapes are oval to rectangular and the sizes vary from 6 to 10 μm. Morphotypes illustrated in Plate 5.4, 44-46 were the most common type recorded in Munsa II sediments. Morphotypes 38, 43, 45 and 46 were extracted

from domesticated genus *Musa*, while morphotypes 40-41 were obtained from the wild type (*Ensete*).

Some of the phytolith morphotypes extracted from voucher plant materials and fossil records are presented in Plate 5.4. All photomicrographs were taken using TK-C1380E Camera under x400 magnification, The scale bar is 5 μm. The SEM micrographs were taken using Hitachi S-4300 SEM.

1 - 2	Dumbbell	Bilobte type with rounded ends (SEM, x5000)
3 - 4	Dumbbell	Bilobate type with sculptured ends (x400)
5	Dumbbell	Tripezoidal (SEM, x4500)
6	Dumbbell	Polylobate, symmetrical form (SEM, x4000)
7	Dumbbell	Polylobate, asymmetrical form (SEM, x2500)
8-10	Cross	Symmetrical forms (SEM, x1800-4500)
11 – 12	Saddle	Concave edges (x400)
13 – 14	Elongate	smooth (SEM, x500-2000)
15-16	Elongate	angular (SEM, x600-1000)
17-18	Elongate	annular/spiral (SEM, x700-1200)
19-20	Cone/hat-shape	(x400)
21-24	Fan-shaped	(SEM, x800-1200)
25-28	Point-shaped	(SEM, x1500-3000)
29	Trichome	(SEM, x1200)

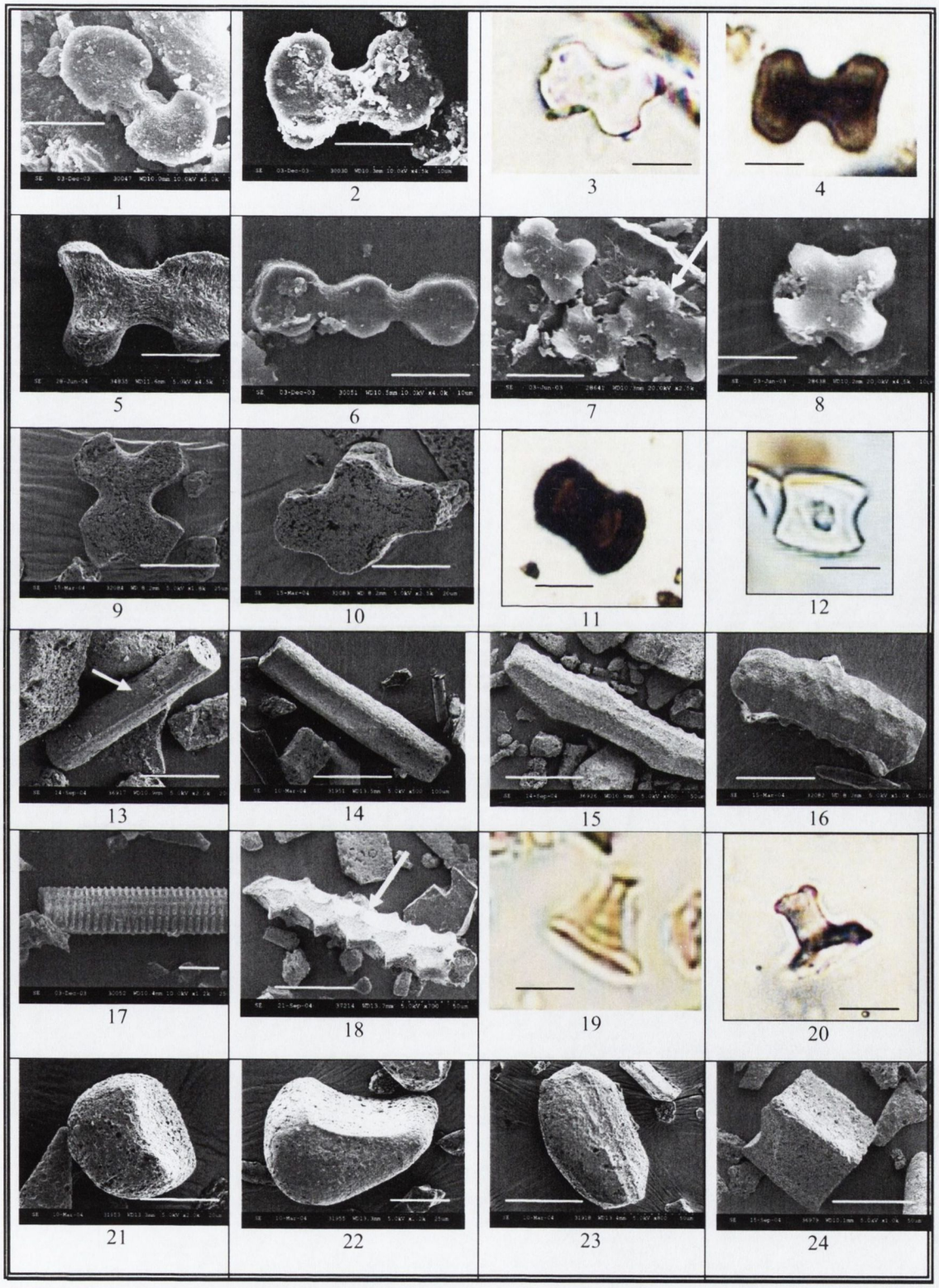
1
2
3
4
5
6
7
8
9
10
11
12
13
14
15
16
17
18
19
20
21
22
23
24

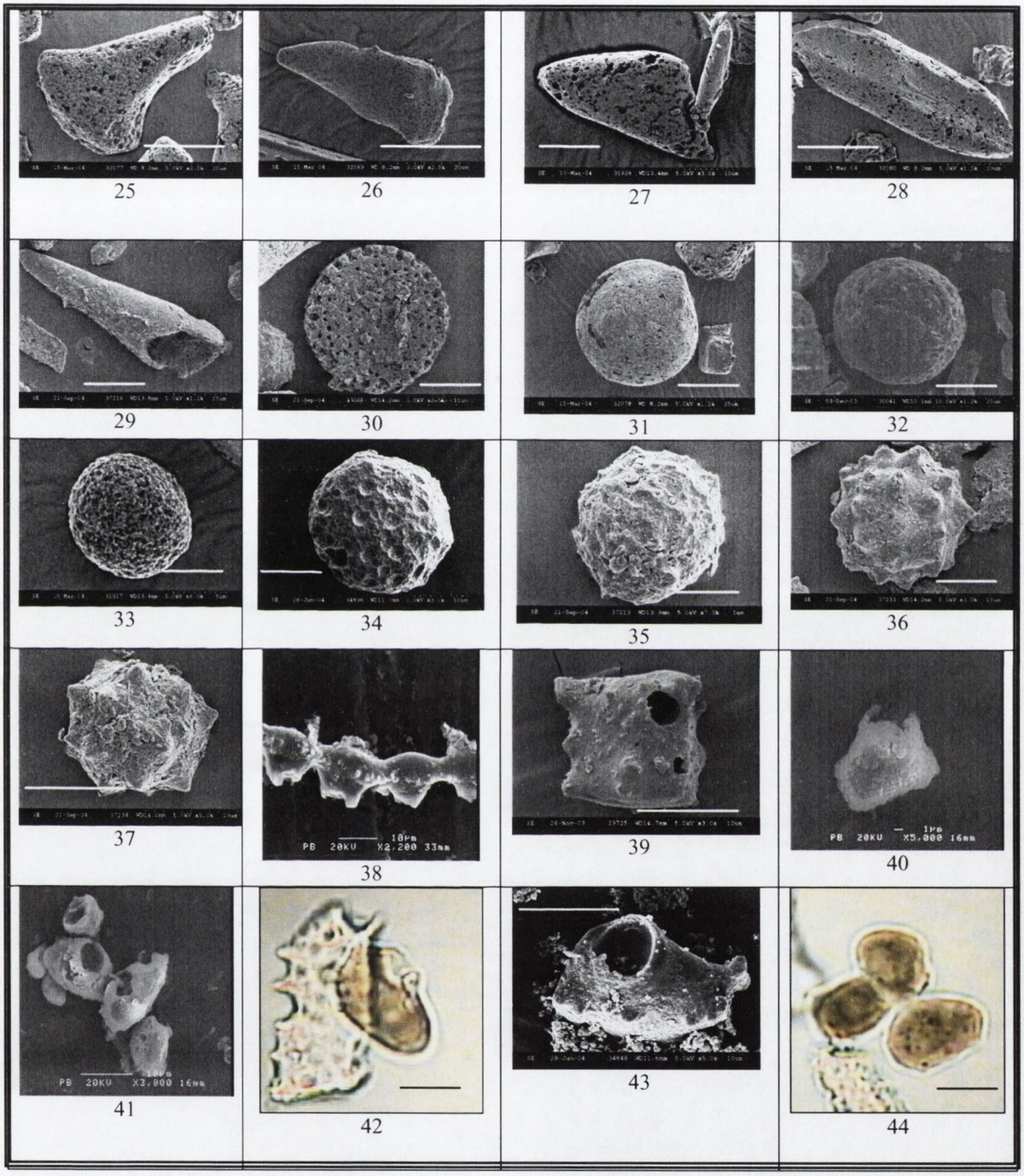
25
26
27
28
29
30
31
32
33
34
35
36
37
PB 20KU X2,200 33mm
38
39
PB 20KU X5,000 16mm
40
PB 20KU X3,000 16mm
41
42
43
44

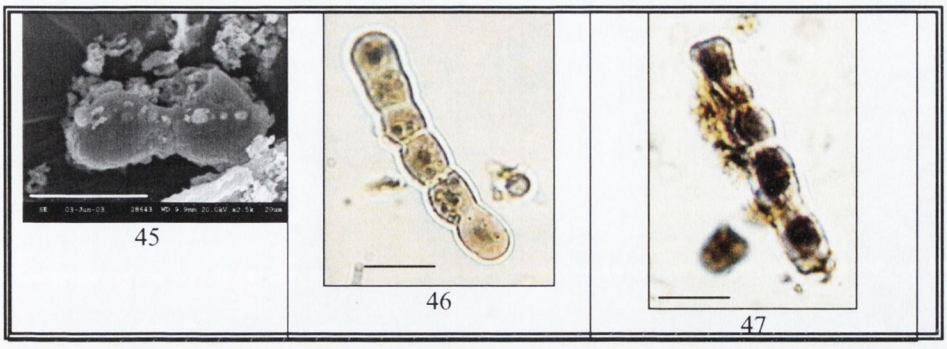

Plate 5.4 Phytolith morphotypes extracted from plant materials and fossil records.

30	Cork cell	(SEM, x3500)
31-33	Spherical rugose	smooth surface (SEM, x1200-6000)
34-35	Spherical rugose	rough surface (SEM x3000-7000)
36-37	Spherical crenate	spiny surface (SEM, x3000-5000)
38, 43, 45, 46	Musa phytolith (type material)	(SEM, x2200-5000)
46	Musa phytolith (type material)	(x400)
39,	Fossil phytoliths (Musa?)	(SEM, x3000)
42, 44, 47	Fossil phytoliths (Musa?)	(x400)
40-41	Ensete phytolith (type material)	(SEM, x 3000-5000)

5.10.7 Vegetation indices

In the present study two indices based on phytoliths, *D/P* and I_{ph} were used to provide additional palaeoecological information. These indices were derived from the comparison of ligneous dicotyledonous and Poaceae phytolith morphotypes. The index *D/P* is used as a proxy of tree vegetation cover, where *D* is the proportion of wooden

(tree) elements and *P* is the proportion of Poaceae. The *D/P* index is defined as the ratio of ligneous dicotyledon morphotypes (consisting of spherical-rugose and -crenate) versus the Poaceae morphotypes (Panicoid, Chloridoid & Pooid). Alexandre *et al.* (1997) and Barboni *et al.* (1999) used the *D/P* to estimate the proportion of trees and shrubs in Sahelian shrub and grass savanna in West Africa and the riparian forest in Awash Valley in Ethiopia, respectively. A *D/P* value of less than 1 was found to characterise abundant grass cover, while a value greater than 1 is said to reflect a high proportion of ligneous dicotyledon (tree and shrub) morphotypes, and therefore forest vegetation cover (Alexandre *et al.*, 1997; Barboni *et al.*, 1999).

Alexandre *et al.* (1997) and Barboni *et al.* (1999) applied I_{ph} to the characterisation of grass communities inhabiting different climatic conditions. This index is derived from the ratio of C_4 short Poaceae belonging to the sub-family Chloridoideae, and tall C_3/C_4 Poaceae belonging to the sub-family Panicoideae. The I_{ph} index is expressed as the ratio of Chloridoid versus the sum of Chloridoid and Panicoid morphotypes {Chloridoid / (Chloridoid +Panicoid)}. According to Alexandre *et al.* (1997), high I_{ph} values suggest grasslands in which short C_4 Poaceae adapted to warm and dry climatic conditions are abundant; low I_{ph} values indicate the common occurrence of tall C_3/C_4 Poaceae, suggesting humid climatic conditions with high moisture availability in the soil. An I_{ph} value of 30% has been used as a boundary limit to distinguish tall-grass savannas of the humid Sudanian zone from the short-grass savannas of the arid Sahalian region in Senegal (I_{ph} > 30%) (Alexandre *et al.*, 1997). In this study, the results of *D/P* and I_{ph} values for Munsa II sediments are presented in chapter eight.

In addition to the two indices described above, the proportion of C_4 and C_3 plants (referred to here as dilution factor) in the phytolith assemblage was calculated. The dilution factor corresponds to the proportion of C_4 plants in the phytolith sum {C_4 plants / (C_3 plants + C_4 plants)}. According to Hillaire-Marcel *et al.* (1989), C_4 and C_3 plants constitute the bulk of organic matter and thus produce the carbon signal. Since phytliths are formed from the decay of C_4 and C_3 plant parts, calculating dilution factor provides an interpretation of the vegetation changes in the catchment area. In this thesis the dilution factor was calculated from the phytoliths contributed by C_3 plants (trees/shrubs) and C_4 plants that comprise Cyperaceae and Poacaeae plants. To establish the effectiveness of the dilution factor it was compared with the $\delta^{13}C$ values (see chapter six) to establish any correlation between the two. Details of the results are presented in chapter six.

5.10.8 Principle Component Analysis (PCA)

In order to examine the inter-sample variability and the degree of correspondence between phytolith morphotypes, the assemblage data was subjected to statistical analysis using Principle Component Analysis (PCA). PCA is a multivariate ordination technique within the program CANOCO (ter Braak & Smilauer, 1998). The details of PCA are described in Kent & Coker (1992). In this thesis, the percentage composition of the morphotypes was square root transformed, rare morphotypes were down weighted and the scores were scaled to weighted averages of the down-core samples (ter Braak, 1990), yielding two principal axes; Axis 1 and Axis 2. Details of the results are described in chapter eight.

RESULTS

CHAPTER SIX

RESULTS OF SEDIMENT STRATIGRAPHY AND CHRONOLOGY ANALYSES

6.1 Introduction

This chapter presents the results of the analyses of sediment stratigraphy and chronology of the three sediment cores for Munsa II. The chapter also contains results of laboratory techniques aimed at assisting the determination of autochthonous and allochthonous sediments.

6.2 Sediment stratigraphy for Munsa II cores

Figure 6.1 illustrates sediment stratigraphy for M2C1, M2C2 and M2C3C and their relative coring locations along the transect (26 m) running across Munsa II swamp. The three cores consist of a similar depositional sequence of peat, clay and fine/coarse sand. To ease interpretation, the sediments have been divided into four stratigraphic zones, labelled A, B, C and D from the base of the cores towards the top. Stratighraphic zone A forms the base of the three cores and is composed of fine and coarse sand particles. It extends from 126 cm to 115 cm in M2C1, 175 cm to 165 cm in M2C2 and 185 cm to 176 cm in M2C3C. A clay-rich layer, stratigraphic zone B, overlays zone A, varying considerably in depth and composition, attaining its greatest depth of 69 cm in M2C3C. Zone C extends over the clay with its greatest depth of 22 cm attained in M2C1. This

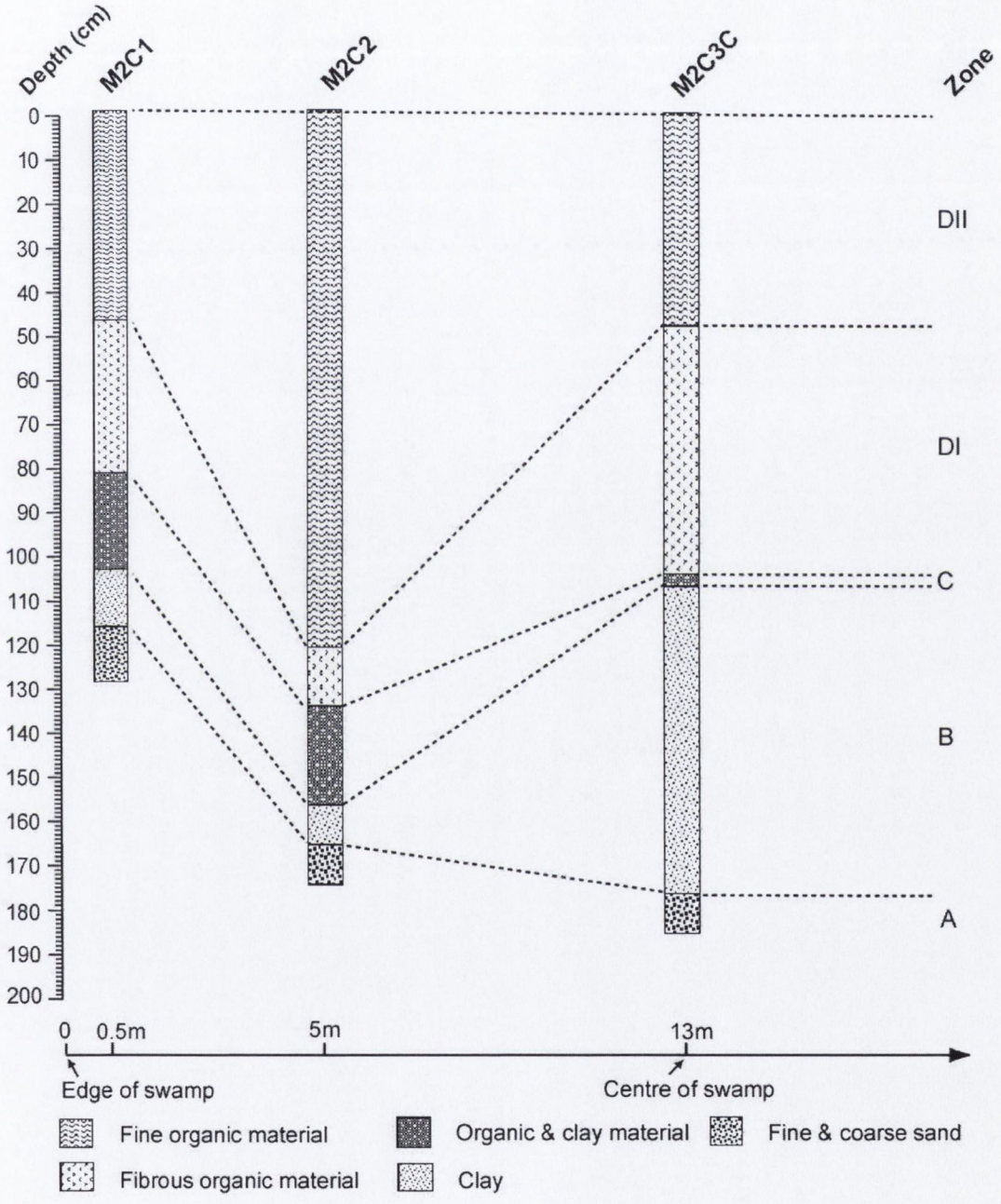

Figure 6.1 Sediment stratigraphy for cores M2C1, M2C2 and M2C3C

stratigraphic zone is composed of clay and organic remains, which are present in approximately equal proportions.

The three cores contain an uppermost deposit, zone D, of herbaceous peat, forming the deepest stratigraphic zone in all the three cores and ranging from 81 cm to 121 cm deep in M2C1 and M2C2 respectively. In the three cores, zone D varied considerably in composition and thus has been subdivided into two sub-zones (DI and DII) based on the degree of decomposition of the herbaceous peat. Sub- zone DI is composed of more fibrous (less decomposed) herbaceous plant materials, possibly caused by more permanent water logging, retarding the decomposition rate. This sub-zone is 35cm deep in M2C1, 14 cm in M2C2 and 56 cm in M2C3C. Sub-zone DII is composed of more decomposed herbaceous peat, with thin layers of inorganic particles, and may reflect the depth of seasonal fluctuations in the water table. This sub-zone is deepest (120 cm) in M2C2 and least deep (46 cm) in M2C1.

6.3 Results of sediment chronology and age-depth curves for Munsa II core

The results of the AMS ^{14}C dating of samples from M2C1, M2C2 and M2C3C are presented in Table 6.1. The calibrated dates are presented as 2-sigma calibrated age (BC/AD) at 95% probability. All AMS ^{14}C ages are stratigraphically consistent, and range from: 1590 ± 40 (106–107 cm) to 180 ± 40 yr. BP (30–31 cm) for M2C1; 940 ± 40 (134–135 cm) to 240 ± 40 yr. BP (26–27 cm) for M2C2; and 4560 ± 40 (162–167 cm) to 540 ± 40 yr. BP (31–32 cm) for M2C3C. The age-depth curves for three M2C1, M2C2 and M2C3C are presented below.

Table 6.1 AMS radiocarbon dates and $^{13}C/^{12}C$ ratios ($\delta^{13}C$ ‰) values for M2C1, M2C2 and M2C3C. The AMS dates were calibrated using Calib 4.4 and calibration curve INTCAL 98 Radiocarbon Age Calibration and presented as 2-sigma calibrated age (BC/AD) at 95% probability.

Sediment core	Laboratory number	Depth (cm)	Conventional ^{14}C age (yr. BP) ± 1δ	Calibrated ^{14}C age (cal BC/AD) ± 2δ	Median cal. ^{14}C age	$^{13}C/^{12}C$ $\delta^{13}C$(‰) values	Material dated
M2C1	Beta-185992	30 - 31	180 ± 30	1654 – 1949 AD	1770 AD	-14.3‰	Plant macrofossils (leaves, stems, seeds)
M2C1	Beta-185993	50 – 51	750 ± 40	1212 – 1378 AD	1265 AD	-13.2‰	Plant macrofossils (leaves, stems, seeds)
M2C1	Beta-185994	74 - 75	900 ± 40	1032 – 1217 AD	1123 AD	-26.0‰	Plant macrofossils (leaves, stems)
M2C1	Beta-185995	106 - 107	1590 ± 50	356 – 599 AD	476 AD	-26.8‰	Bulk sediment (organic/clay sediment)
M2C2	Beta-185996	26 - 27	240 ± 30	1527 – 1947 AD	1660 AD	-22.4‰	Plant macrofossils (leaves, stems, seeds)
M2C2	Beta-175374	50 - 51	430 ± 40	1412 – 1625 AD	1461 AD	-13.4‰	Plant macrofossils (leaves, stems)
M2C2	Beta-175375	105 -106	700 ± 40	1244 – 1393 AD	1294 AD	-10.9‰	Plant macrofossils (leaves, stems, seeds)
M2C2	Beta-175376	134 -135	940 ± 40	1019 – 1206 AD	1098 AD	-28.8‰	Plant macrofossils (leaves, stems, seeds)
M2C3C	Beta-175370	31- 32	540 ± 40	1307 – 1440 AD	1400 AD	-11.9‰	Plant macrofossils (leaves, stems)
M2C3C	Beta-168965	45 - 46	560 ± 40	1303 – 1433 AD	1365 AD	-15.6‰	Bulk sediment (organic sediment)
M2C3C	Beta-175371	74 - 75	670 ± 40	1277 - 1396 AD	1337 AD	-24.4‰	Plant macrofossils (leaves, stems, seeds)
M2C3C	Beta-168966	102 -103	850 ± 40	1042 - 1276 AD	1192 AD	-27.8‰	Bulk sediment (organic/clay sediment)
M2C3C	Beta-175372	117 - 118	910 ± 40	1030 – 1211AD	1114 AD	-23.9‰	Plant macrofossils (leaves, stems)
M2C3C	Beta-185997	137 - 138	3640 ± 40	2136 – 1891 BC	2003 BC	-23.5‰	Bulk sediment (organic/clay sediment)
M2C3C	Beta-175373	162 - 163	4560 ± 40	3492 - 3100 BC	3219 BC	-23.8‰	Bulk sediment (organic/clay sediment)

6.3.1 Age-depth curve for M2C1

The AMS ^{14}C data and the age-depth relationship for M2C1 (Figure 6.2) indicates that the core contains a record of past environmental conditions at this site for the last ca. 2000 yr. BP (cal 84–118 AD). The oldest AMS ^{14}C date, 1590 ± 50 yr. BP (cal 356–599 AD) was from close to the base at 134–135 cm depth. The age-depth curve for the core was based on four AMS ^{14}C dates; 1590 ± 40 yr. BP (cal 356 – 599 AD), 900 ± 40 yr. BP (cal 1032–1217 AD), 750 ± 40 yr. BP (1212–1378 AD), and 180 ± 40 yr. BP (cal 1654–1949 AD). A linear regression analysis yields a high coefficient value ($R^2 = 0.96$), suggesting a close relationship between depth and age and an overall sedimentation rate for the core of 0.05 cm yr^{-1}.

Assuming that the rate of sedimentation between AMS ^{14}C-dated sediment samples remained constant, the sedimentation rate for the lower part of the core is 0.05 cm yr^{-1} between the AMS ^{14}C dates, 1590 ± 50 yr. BP (106–107 cm), and 900 ± 40 yr. BP (74–75 cm). The sedimentation rate increases to 0.16 cm yr^{-1} between the AMS ^{14}C dates 900 ± 40 yr. BP (74–75 cm), and 750 ± 40 yr. BP (50–51 cm). However, the rate drops to 0.04 cm yr^{-1} between the AMS ^{14}C dates 750 ± 40 yr. BP (50–51 cm), and 180 ± 40 yr. BP (30–31 cm).

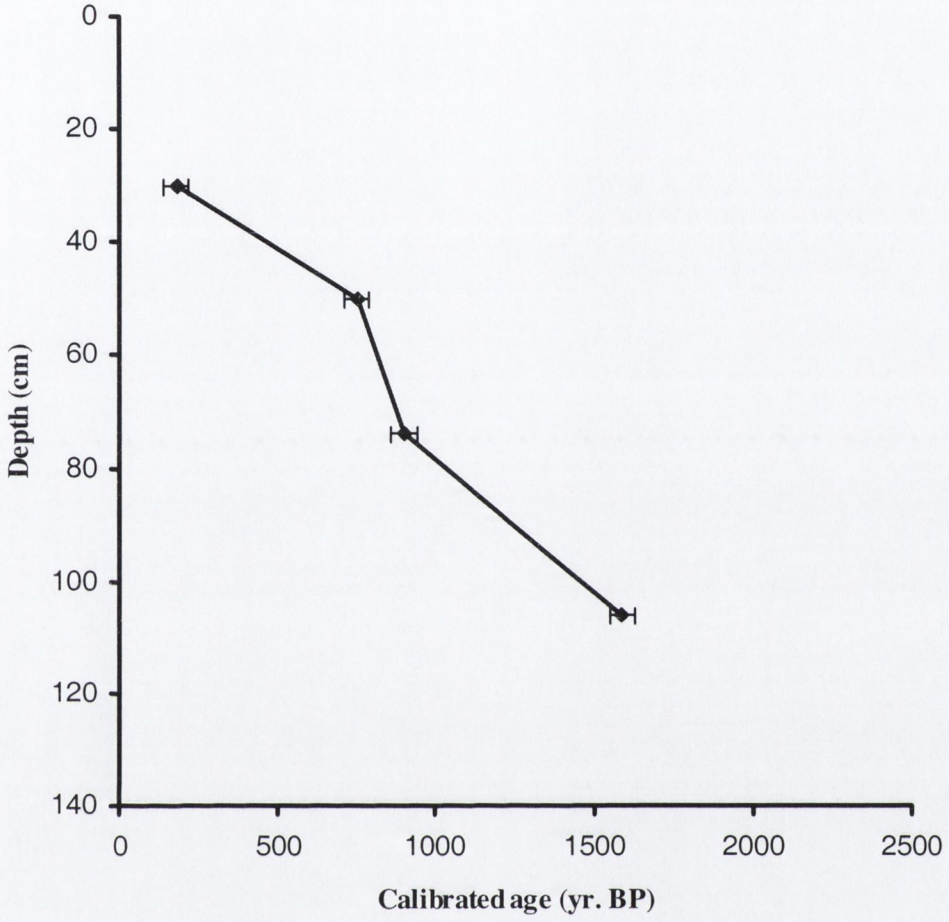

Figure 6.2 M2C1, Age-depth curve. A linear relationship between age and depth is assumed between AMS ^{14}C dates.

6.3.2 Age-depth curve for M2C2

Figure 6.3 presents the age-depth curve for M2C2. The oldest AMS ^{14}C date, 940 ± 40 yr. BP (cal 1019-1206 AD) for the core was obtained for a sample of sediment at 134-135 cm depth. The extrapolated age for the base of the core is ca. 1250 yr. BP (cal 683-884 AD). Four AMS ^{14}C dates were used to estimate the overall rate of sedimentation: 940 ± 40 yr. BP (134-135 cm); 700 ± 40 yr. BP (105-106 cm); 430 ± 40 yr. BP (50-51 cm); and 240 ± 40 yr. BP (26-27 cm). Using linear regression analysis, a high coefficient value ($R^2 = 0.99$) was obtained for this part of the core with a sedimentation rate of 0.15 cm yr^{-1}. Assuming a constant rate of sediment accumulation between AMS ^{14}C dates, the sedimentation rate is lowest (0.12 cm yr^{-1}) at the base of the core between the AMS ^{14}C date, 940 ± 40 yr. BP (134-135 cm) and 700 ± 40 yr. BP (105-106 cm) and highest (0.23 cm yr^{-1}) between the AMS ^{14}C dates, 700 ± 40 yr. BP (105-106 cm) and 430 ± 40 yr. BP (50-51 cm).

6.3.3 Age-depth curve for M2C3C

This core covers the longest time period and is dated with the most (seven) AMS ^{14}C dates. The age-depth curve for this core is presented in Figure 6.4. The oldest AMS ^{14}C date, 4560 ± 40 yr. BP (cal 3492-3100 BC) is for a sample from close to the base of the core at 162-163 cm depth. The age-depth curve indicates a phase with very low sedimentation rate (0.01 cm yr^{-1}) between the AMS ^{14}C dates of 3640 ± 40 yr. BP (137-138 cm), and 910 ± 40 yr. BP (117-118 cm), suggesting presence of a major hiatus, or hiatuses in sedimentation. Above the estimated part of the hiatus, five AMS ^{14}C dates

(910 ± 40 yr. BP, 850 ± 40 yr. BP, 670 ± 40 yr. BP, 560 ± 40 yr. BP and 540 ± 40 yr. BP) were obtained. Applying a linear regression analysis, a high coefficient value (R^2 = 0.98) is obtained, and an overall sedimentation rate of 0.23cm yr^{-1} suggesting a line of best-fit. A second hiatus may have interrupted sedimentation above 31cm in the core. If this was not the case, then the rate of sediment accumulation was much reduced (0.06 cm yr^{-1}) in the upper most part of the core (i.e. above 31 cm). In the absence of any stratigraphic evidence for a hiatus, in the form of an erosion layer or abrupt change in sediment type in the upper part of the core, other than a change in the rate of sediment accumulation, a reduced sedimentation rate has been assumed and the ages of sediment sample from above 31 cm have been extrapolated according. Their ages should, however, be viewed with some caution.

6.3.4 Extrapolating and interpolating the ages of depths

Estimated rates of sediment accumulation were used as the basis for extrapolating and interpolating the ages of depths with the three sediment cores (Figure 6.5).

6.4 Loss on ignition (LOI) results for Munsa II cores

The relative abundances of organic and inorganic matter in sediment samples from M2C1, M2C2 and M2C3C determined thermogravimetrically through the LOI technique are illustrated in Figures 6.6, 6.7 and 6.8 respectively.

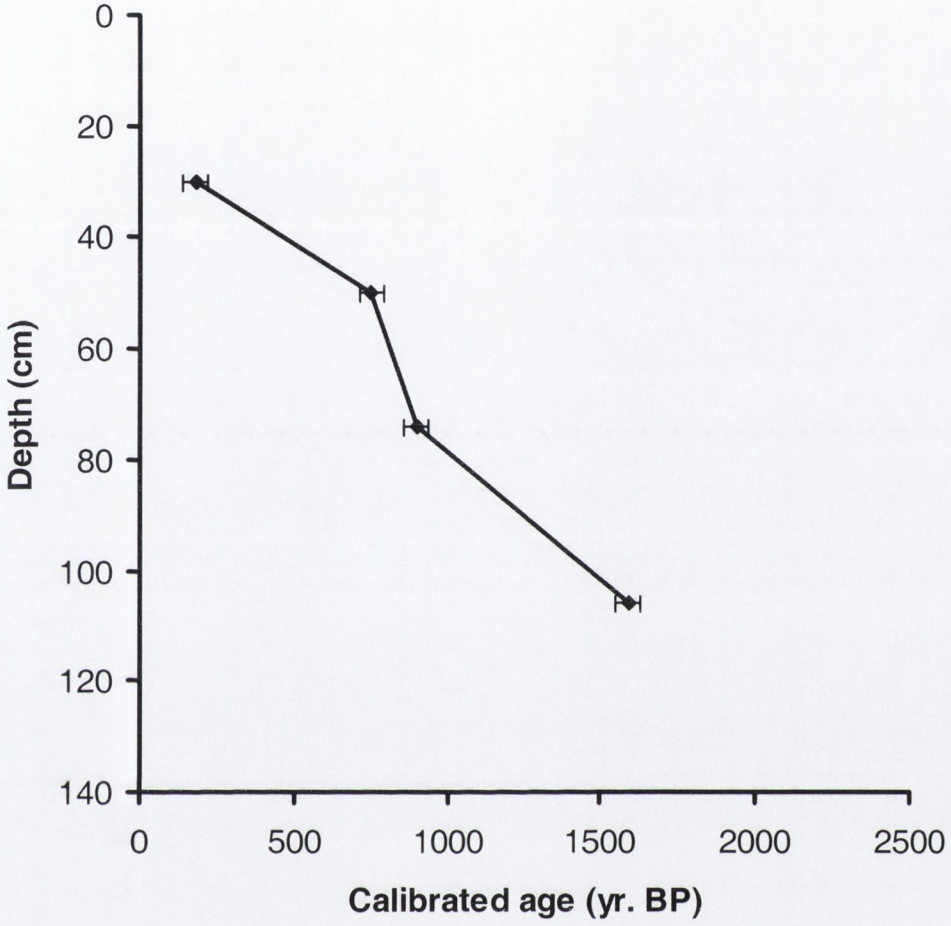

Figure 6.3 M2C2, Age-depth curve. A linear relationship between age and depth is assumed between AMS ^{14}C dates.

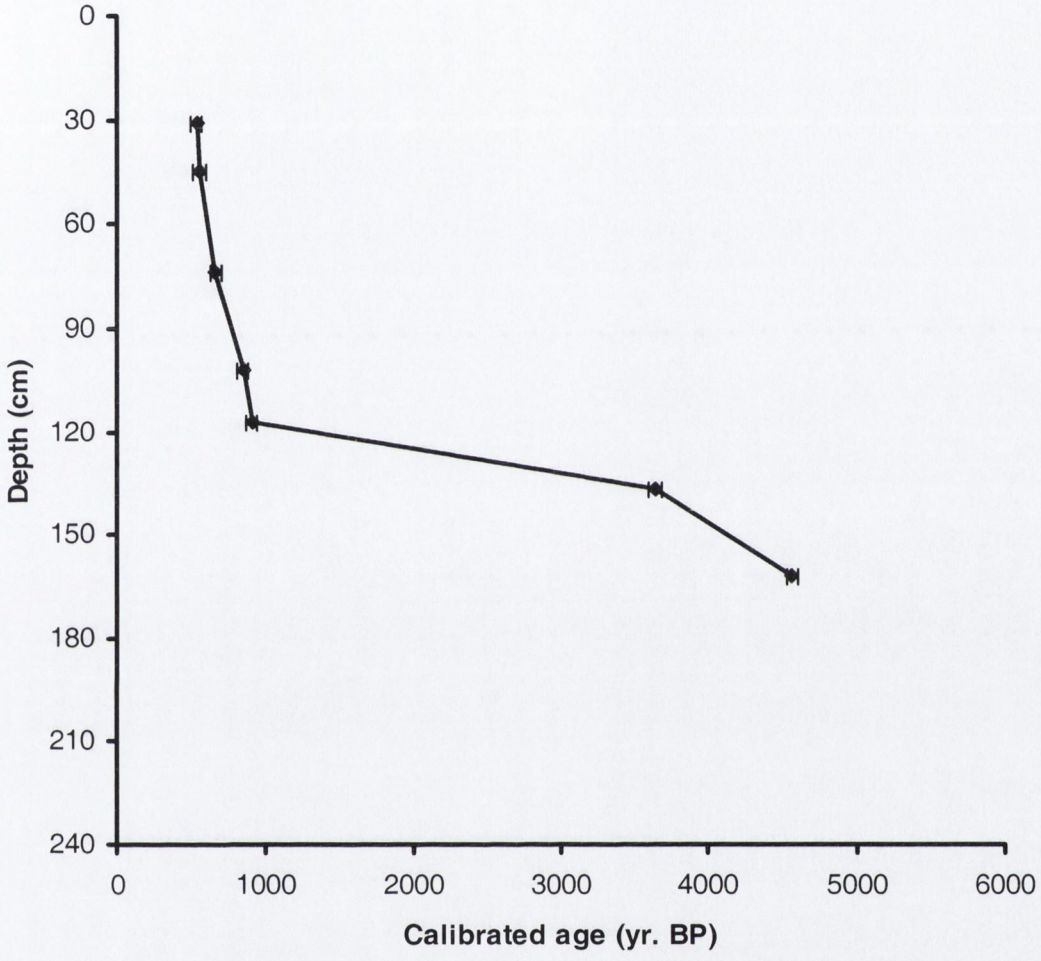

Figure 6.4 M2C3C, Age-depth curve. A linear relationship between age and depth is assumed between AMS ^{14}C dates.

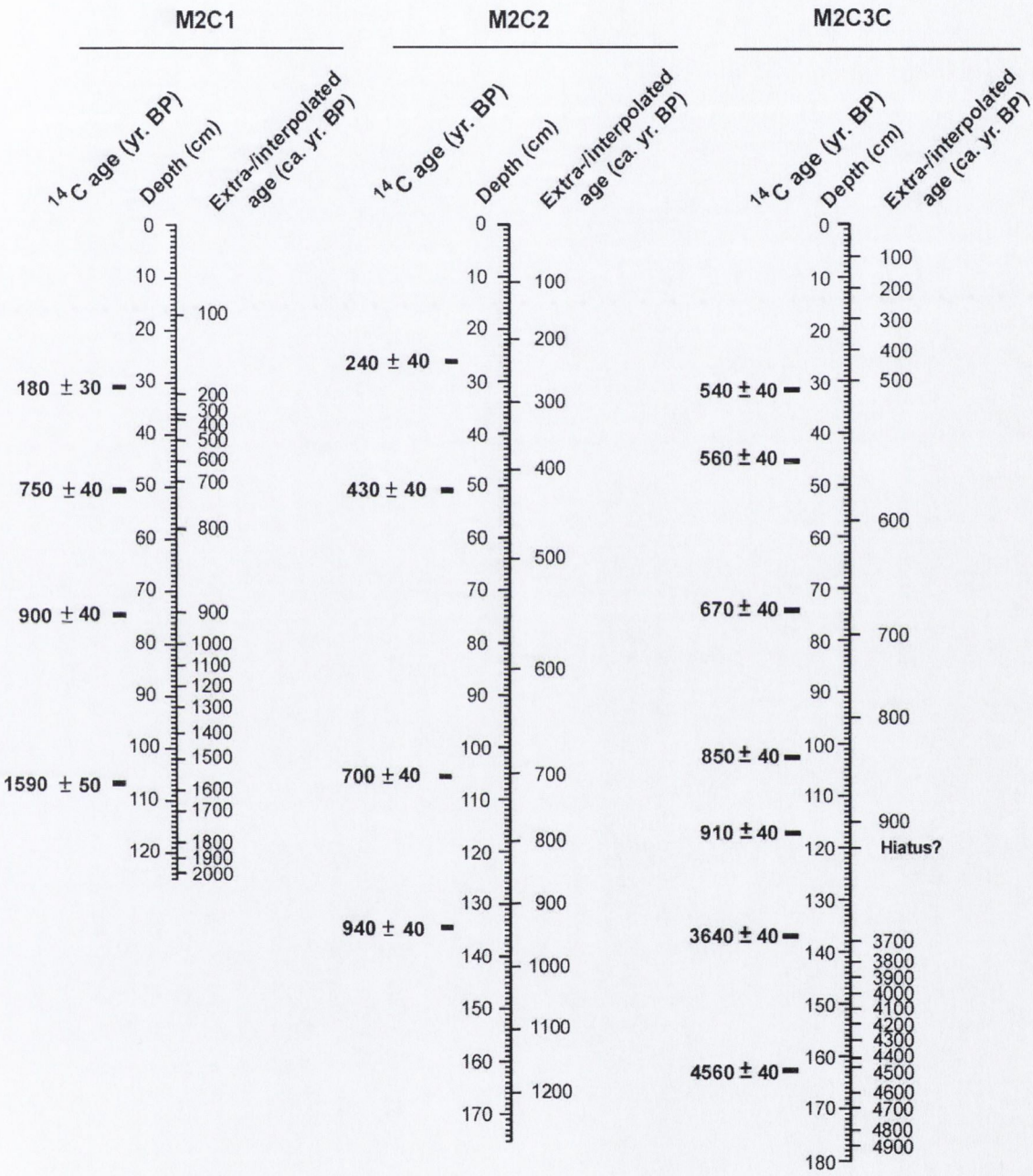

Figure 6.5 Interpolated ^{14}C age (ca. yr. BP) for cores M2C1, M2C2 and M2C3C.

6.4.1 Core M2C1

Figure 6.6 illustrates down-core variation in organic/inorganic matter for M2C1. Stratigraphic zones A and B towards the base of this core are characterised by very low levels of organic matter (< 15%) and the abundant presence of fine/coarse sand and clay particles in zones A and B, respectively. The amount of organic matter rises to higher levels (> 20%) towards the upper boundary of stratigraphic zone C (112-81 cm).

The amount of organic matter attains a maximum level of 85% at 70 cm in sub-zone DI (82–46 cm) before declining (< 60%) towards the upper boundary of the stratigraphic zone. Sub-zone DII is marked by a general decline (< 40%) in the amount of organic matter. This sub-zone is, however interrupted by a sharp rise in the level of organic matter to 81% at 30-31 cm depth, (AMS ^{14}C date 180 ± 40 yr. BP, cal 1654-1949 AD). The level of organic matter drops back to less than 40% at 25 cm, and remains relatively constant (30-32%) thereafter.

6.4.2 Core M2C2

For M2C2 (Figure 6.7), the lowermost stratigraphic zones A, B and C (175 – 135 cm) are characterised by low levels (< 10%) of organic matter, and abundant inorganic materials (fine/coarse sand and clay particles). This corresponds to the time period ca. 1250 yr. BP (cal 791-413 BC) to 948 yr. BP (cal 1005-1205 AD). This period is followed by increased organic matter (15-50%) in sub-zone DI (135-122 cm), corresponding to the time period ca. 948 yr. BP (cal 1005-1205 AD) to 840 yr. BP (cal 1045-1278 AD). Sub-zone DII is marked by further increases in the level of organic

matter (> 50%). However, the level of organic matter drops to 20% at 69 cm, ca. 475 ± 40 yr. BP (cal 1333-1484 AD), before rising to a maximum of 83% at 46 cm, ca. 380 yr. BP (cal 1440-1634 AD). A relatively high level of organic matter (48-82%) is maintained thereafter.

6.4.3 Core M2C3C

The lowermost stratigraphic zones in this core contain low levels of organic matter (< 10%) between 180 cm and 120 cm, attributed to the presence of high amounts of inorganic materials of fine/coarse sand and clay particles in stratigraphic zones A and B, respectively (Figure 6.8). Zone B is characterised by an abrupt change in the apparent age of the sediments, between the AMS ^{14}C dates 3640 ± 40 (cal 2136-1891 BC) at 137-138 cm and 910 ± 40 yr. BP (cal 1030-1211 BC) at 117-118 cm, suggesting the presence of a sedimentary hiatus, or hiatuses, between these dates. The level of organic matter increases to > 30% in the upper part of zone B, attaining a level of 75 % at the upper boundary (106 cm). The level of organic matter attains a maximum level of 87% at 102 cm, ca 850 yr. BP (cal 1042-1276 AD) and maintains a high level, between 35% and 87%, in zone DI (103-48 cm). Zone DII is marked by a drop in the level of organic matter to less than 60% at 43 cm, ca. 550 yr. BP (cal 1304-1437 AD), and remains relatively constant (53-60%) thereafter.

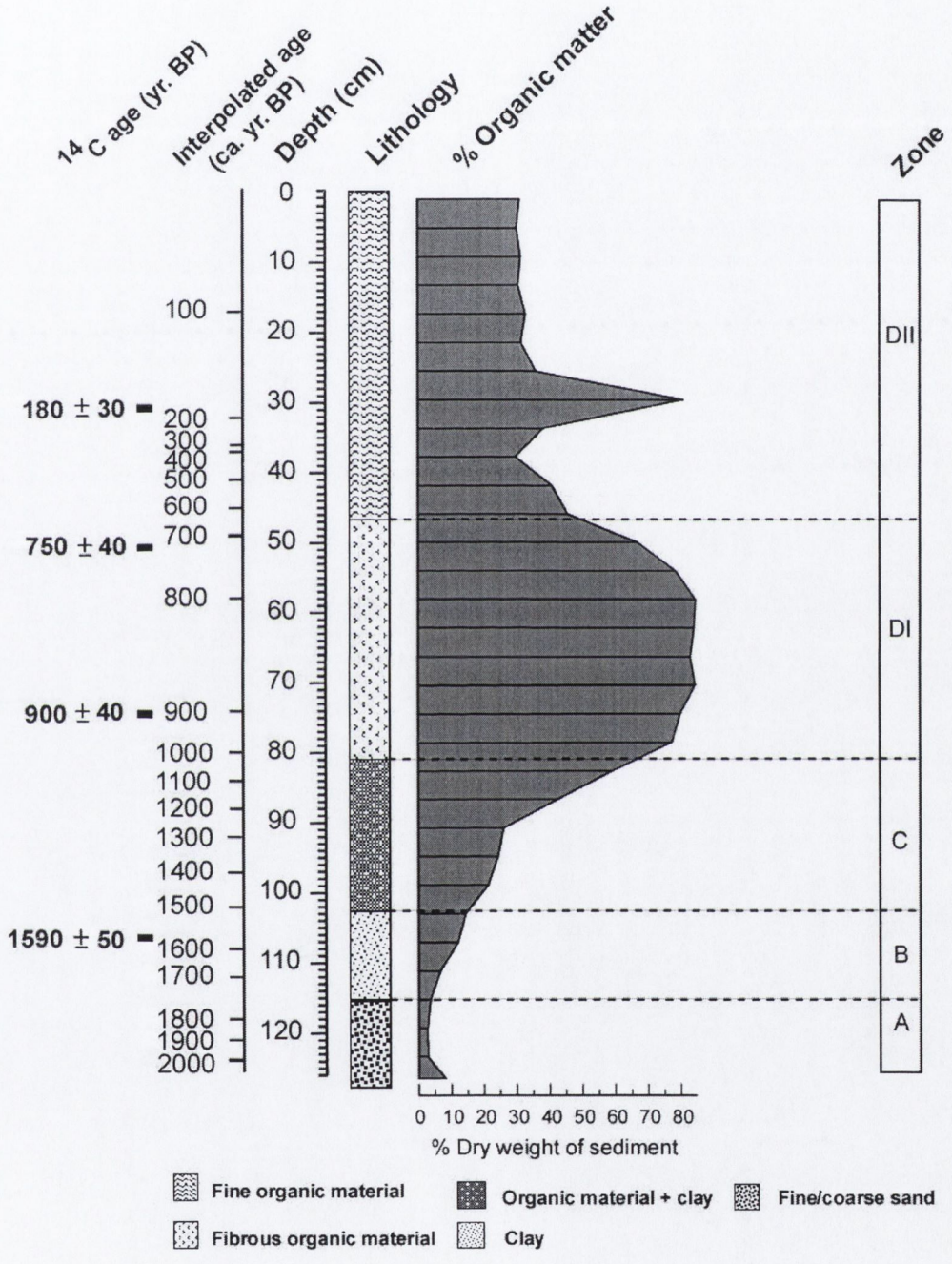

Figure 6.6 M2C1, Percentage organic matter calculated from LOI

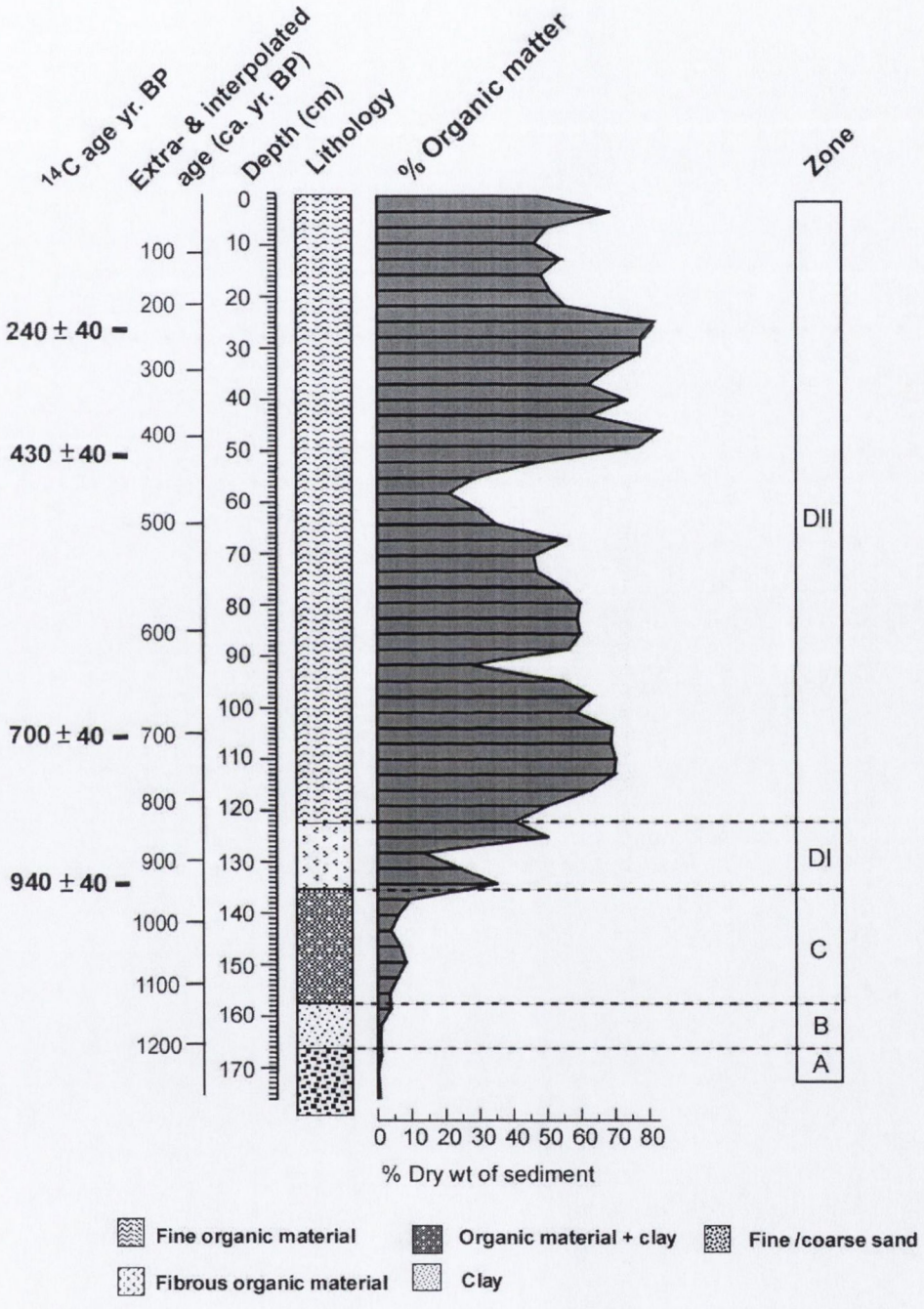

Figure 6.7 M2C2, Percentage organic matter calculated from LOI

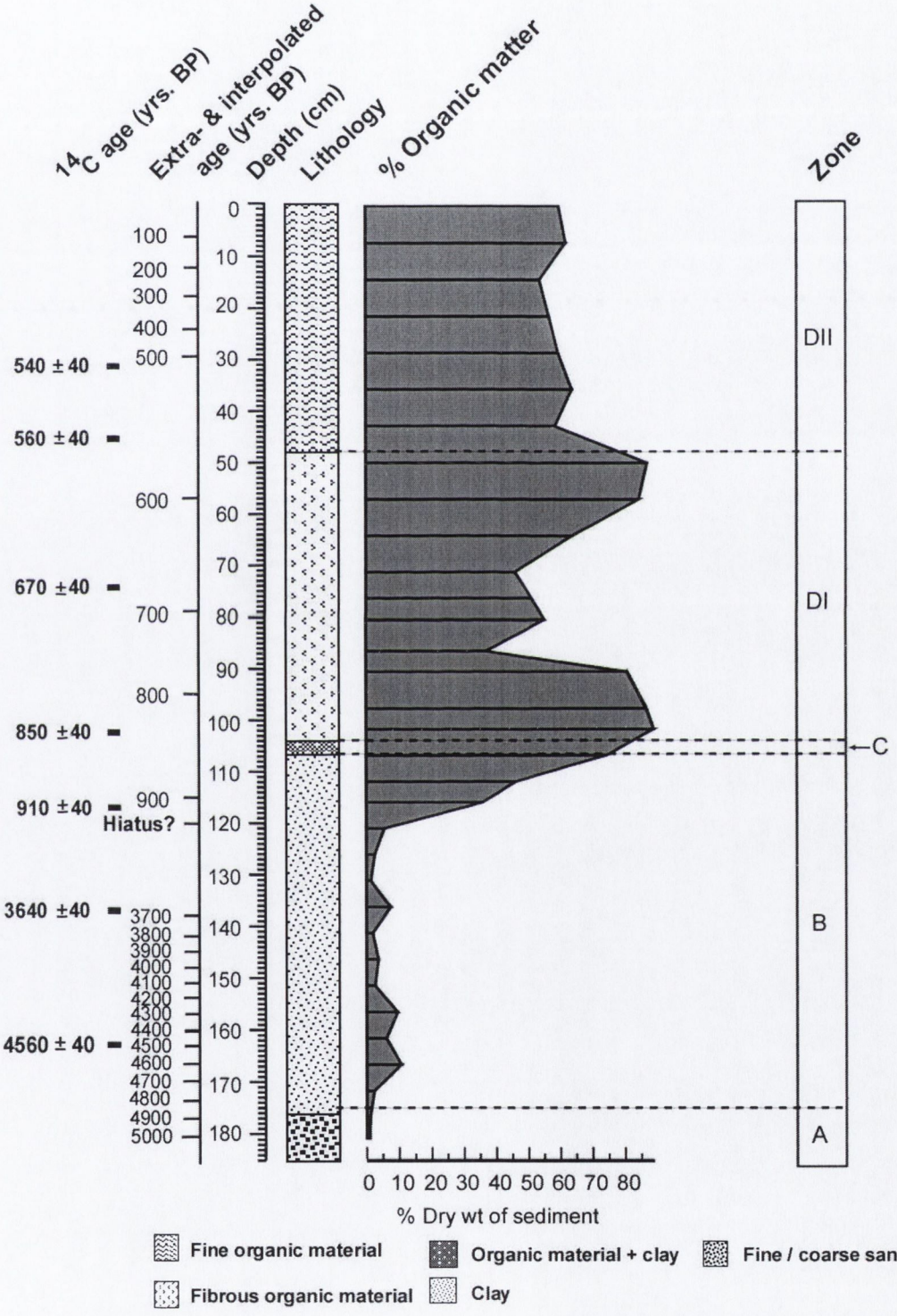

Figure 6.8 M2C3C, Percentage organic matter calculated from LOI

6.5 Results of $\delta^{13}C$ isotope analysis

$\delta^{13}C$ values for samples from M2C1, M2C2 and M2C3C are presented in Table 6.1. All $\delta^{13}C$ values for the three cores are within the range expected for C_3 and C_4 sources for organic carbon (Cerling, 1999). According to Bird & Grocke (1997), Cerling (1999), Pack *et al.* (2003) and Thorn (2004), $\delta^{13}C$ values ranging between -21‰ to -35‰ (averaging about -26‰ to -27‰) are for C_3 plants and between -10‰ to -21‰ (averaging about -12‰) are for C_4 plants. The $\delta^{13}C$ values are generally more negative in the lowermost samples analysed for the three cores, and are less negative towards the upper parts of the cores. There is one obvious exception to this: the uppermost sample analysed from core M2C2, 26-27 cm, yielded a $\delta^{13}C$ value of -22.4‰, whereas samples from 50-51 cm and 105-106 cm in the same core yielded values of, respectively, 13.4‰ and -10.9‰.

Since the samples dated contained macrofossils (leaves, stems and seeds) that are representative of the vegetation, a comparison of $\delta^{13}C$ values with C_4 ratios (dilution factor) for M2C1, M2C2 and M2C3C was carried out. The results are presented in Figures 6.9 to 6.11. The dilution factor indicates the proportion of C_4 plants comprising Cyperaceae and Poacaeae in the phytolith sum {C_4 plants / (C_3 plants + C_4 plants)} as described in chapter five (also see results in chapter eight). The down-core variations in C_4 ratios for M2C1, M2C2 and M2C3C) (Figures 6.9 - 6.11) show similar trends, with very low values (< 0.3) at the base of the three cores between 126-75 cm for M2C1, 170-120 cm for M2C2, and 180-100 cm for M2C3C. This suggests that the organic material originates from a predominantly C_3 plant source, presumably from forest taxa utilising

the C_3 photosynthetic pathway. A marked change in C_4 ratios to higher levels (0.5 - 0.9) occurs towards the upper parts of the three cores, suggesting an increase in the proportion of C_4 sources of organic material. This correlates with the change in $\delta^{13}C$ signal to less negative values (> -21‰) in the three cores. The C_4 values remain generally high (0.3 – 0.8) in the top part of three core zones, corresponding to relatively less negative $\delta^{13}C$ values ranging from -14.3‰ for M2C1 to -11.9‰ for M2C3C. However, for M2C2, a sharp drop in C_4 ratios from 0.8 to less than 0.4 occurs between 38 cm and 15 cm, corresponding to a change to a more negative $\delta^{13}C$ value (-22.4‰) at 26-27 cm depth, suggesting C_3 plant taxa were a major carbon source.

6.6 Summary of sediment stratigraphy and chronology for Munsa II

Generally down-core variations in sediment stratigraphies for Munsa II cores indicate dominance of inorganic materials in the basal zones A and B comprising sand and clay, suggesting fluvial deposit from the catchments area. These two zones pre-date ca. 1500 yr. BP in M2C1, but extend to ca. 940 yr. BP and 860 yr. BP in M2C2 and M2C3C respectively. The clay-rich stratigraphic zone B is longest in M2C3C, probably due to its location at the centre of the swamp compared to M2C1 and M2C2. The more organic stratigraphic zone C is shortest in the M2C3C, while the organic-rich sediment zone is longest in M2C2. Sedimentary rate is lowest in M2C3C between ca. 3000 and 1000 yr. BP, suggesting a period of sedimentation break (hiatus), which may be attributed to erosion process.

Generally the down-core variations in $\delta^{13}C$ values for M2C1, M2C2 and M2C3C correlate with the calculated proportion for C_4 plants, suggesting abundant contribution of C_3 plants to the sediment records pre-dating ca. 900 yr. BP in M2C1, but continued till ca. 850 yr. BP in M2C3C and ca. 800 yr BP later in M2C2. The $\delta^{13}C$ values generally become are less negative towards the upper parts of the cores, suggesting increasing dominance of C_4 plants. This evidence is also apparent in the trend of dilution factor, which are relatively high between ca. 900 and 150 yr. BP for M2C1 and M2C2, but continued to the upper part of the core in M2C3C.

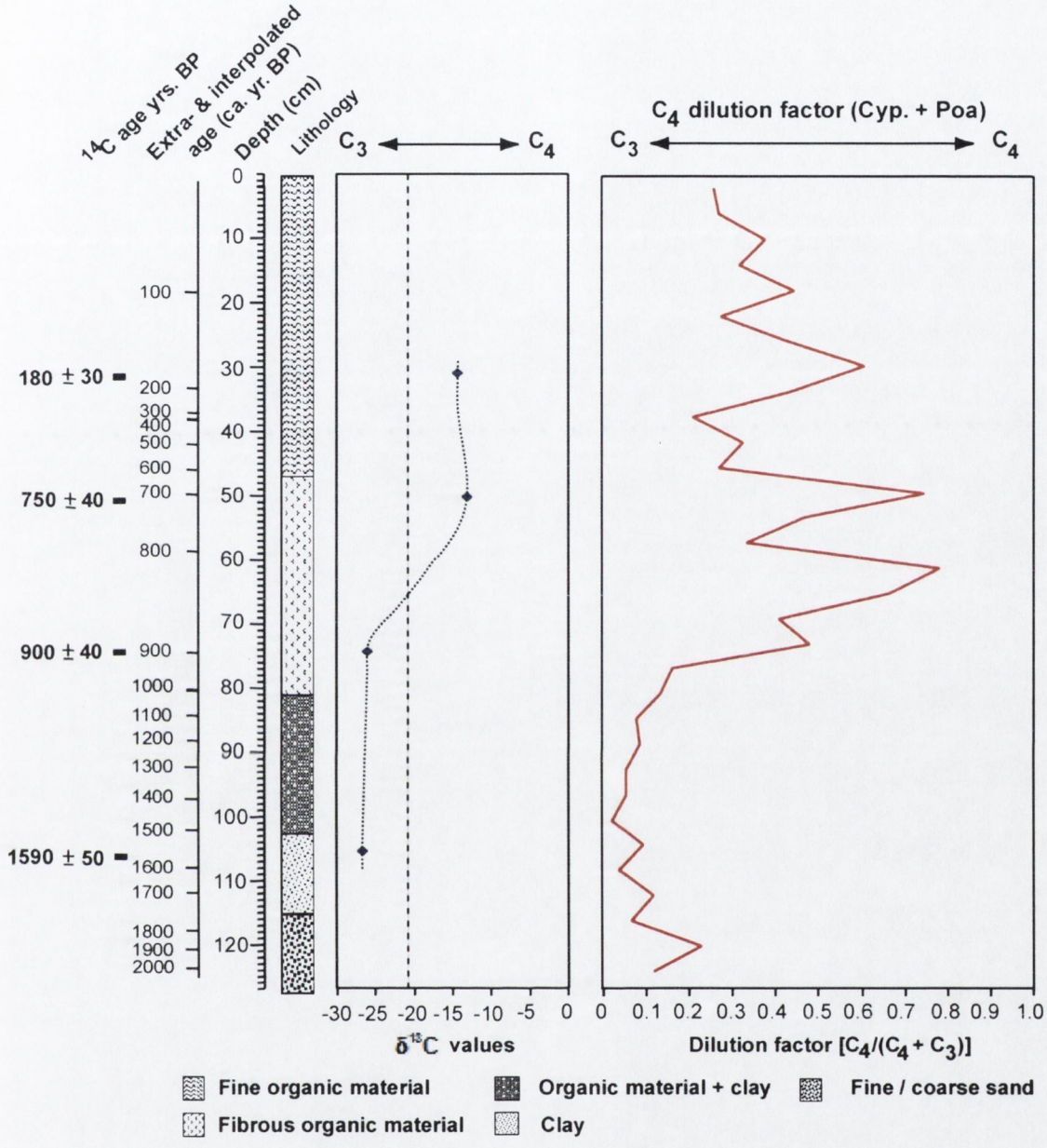

Figure 6.9 M2C1, dilution factor calculated from phytoliths of C_4 (Cyperaceae + Poaceae) versus sum of C_4 and C_3 (trees/shrubs).

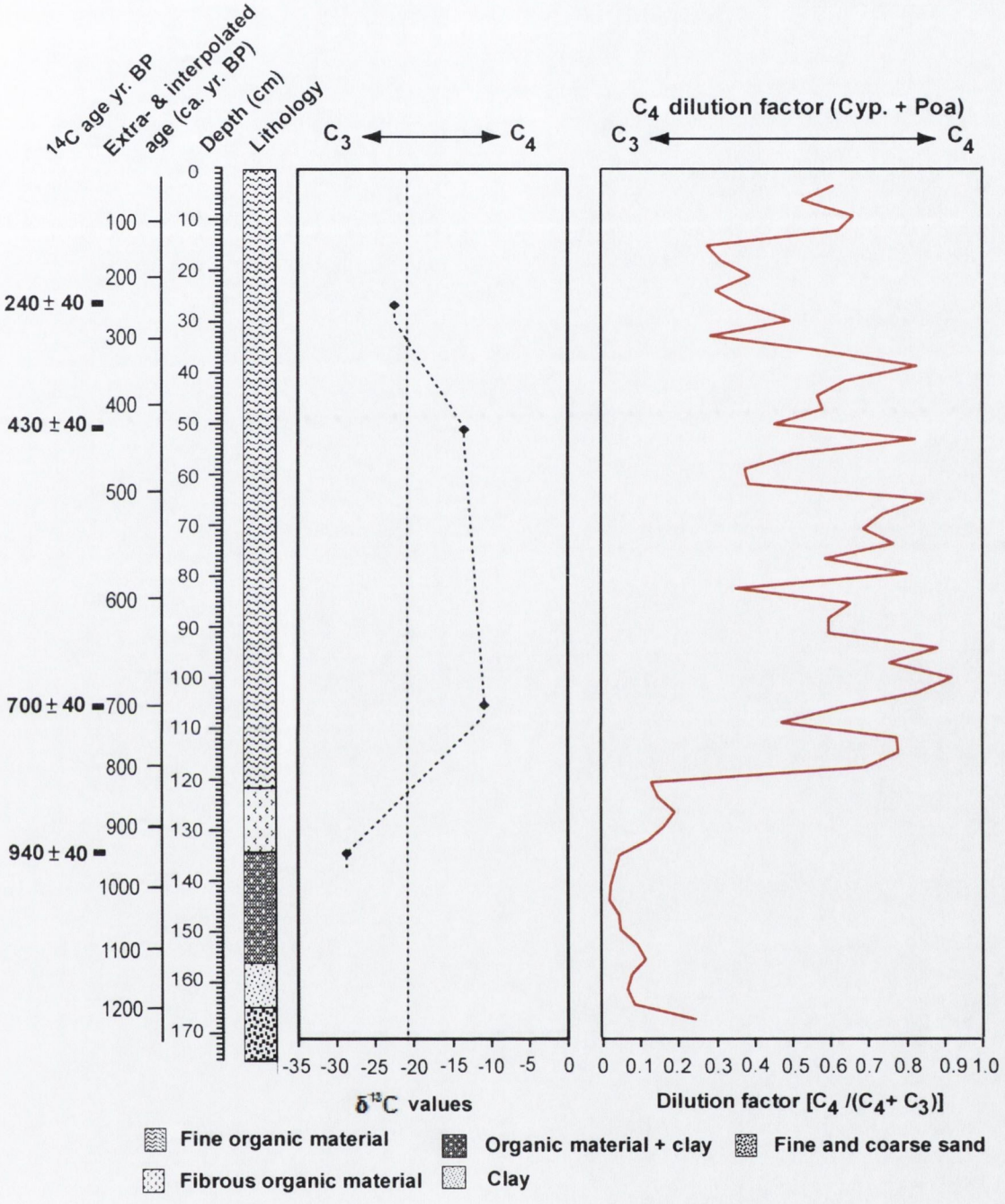

Figure 6.10 M2C2, dilution factor calculated from phytoliths of C_4 (Cyperaceae + Poaceae) versus sum of C_4 and C_3 (trees).

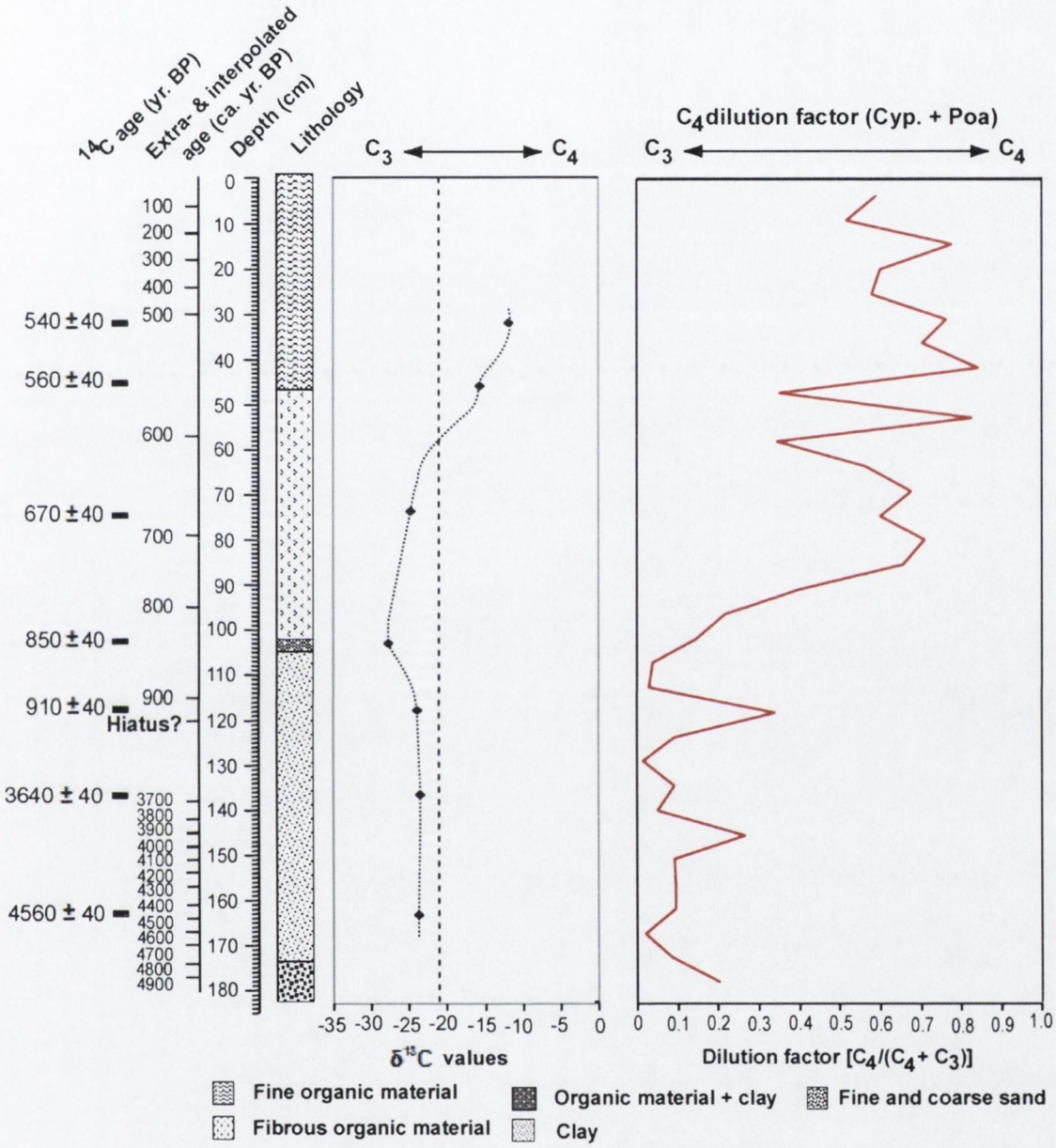

Figure 6.11 M2C3C, dilution factor calculated from phytoliths of C_4 (Cyperaceae + Poaceae) versus sum of C_4 and C_3 (trees).

CHAPTER SEVEN

RESULTS OF POLLEN AND FUNGAL SPORES ANALYSIS

7.1 Introduction

This chapter presents the results of microfossil pollen and fungal spore analyses for Munsa II sediment cores. It describes the down-core variations in fossil pollen and fungal assemblages for M2C1, M2C2 and M2C3 and, where possible interprets these results.

7.2 Results of pollen analysis

The results of down–core variations in and the zonation of pollen assemblages for M2C1, M2C2 and M2C3C are presented in Figures 7.1 to 7.4. Three pollen zones identified in each core are labelled Z1, Z2 and Z3 following the prefix notation of each core by a combination of numerical techniques and in ascending order from the base of the core to the top (e.g. C1Z1, C1Z2, C1Z3 etc.).

7.2.1 Pollen stratigraphy for M2C1 sediment core

The three pollen zones identified within the pollen assemblages of M2C1 (Figure 7.1) are labelled C1Z1, C1Z2 and C1Z3. Figure 7.1 presents the grouping pattern of the pollen zones for M2C1 on the DCA axes 1 and 2. In general the same clusters of sample as defined by the stratigraphically constrained zonation technique are discernible from the DCA ordination plot. On the DCA axis 1, the positive scores represent zone C1Z1,

in the lowermost part of the core, while the negative scores represent zones C1Z2 and C1Z3.

Figure 7.2 presents the DCA biplot distribution pattern of non-local pollen types. DCA axis 1 appears to represent a gradient of vegetation, with arboreal (forest) taxa generally receiving positive scores, while pollen types from taxa associated with secondary or degraded forest habitat have negative scores. Thus the ordering of pollen samples along DCA axis 1 in Figure 7.1 is, in part, in accordance with their relative abundances of pollen from forest taxa. By comparison, DCA axis 2 may partially relate to disturbance, with pollen taxa and spores associated with forest-edge and disturbed habitats (e.g., *Alchornea*, Amaranthaceae, Caryophyllaceae, *Cyathea* and Poaceae being allocated negative scores.

Figure 7.3 illustrates the down-core variation in M2C1 in the non-local pollen assemblages and accumulation rates. Down-core variation in local pollen assemblages are shown in Figure 7.4. Descriptions of each pollen zone follow below.

Zone C1Z1 (126 – 76 cm, ca. > 2000 – 945 yr. BP).

Pollen zone C1Z1 extends from the base of the core at 126cm, > ca. 2000 yr. BP (cal 84-118 AD) to 76 cm, ca. 945 yr. BP (cal 1018-1206 AD) and accommodates stratigraphic zones A-lower part of DI (see Figure 6.6). This pollen zone is dominated by arboreal taxa (ranging from 60% to 90% of the pollen sum). Among the mid altitude forest taxa, *Alchornia* pollen dominates zone C1Z1, with a contribution of up to 61%, while *Teclea*

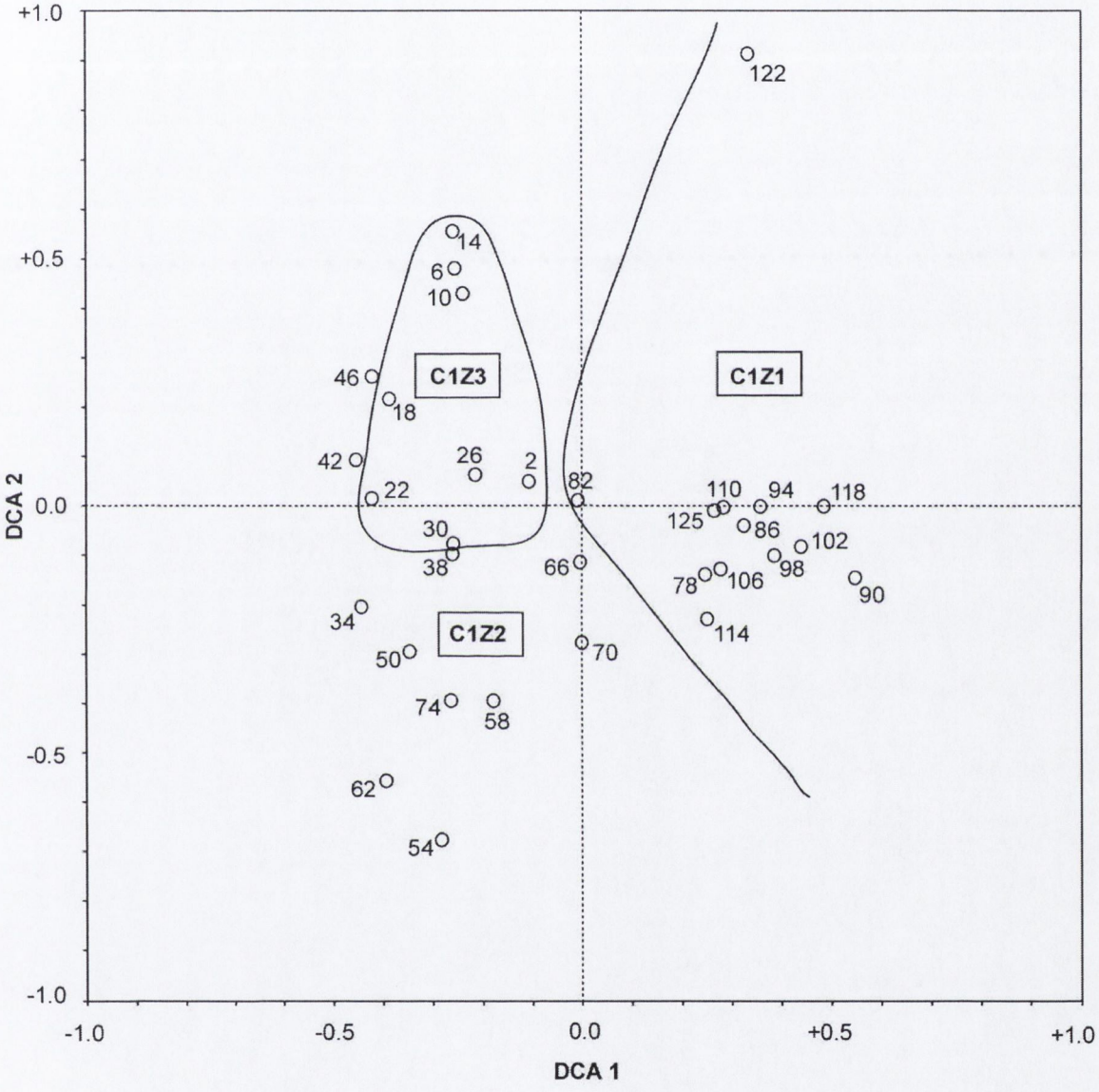

Figure 7.1 M2C1, Distribution of pollen samples for core M2C1 according to DCA axes 1 and 2. The grouping of pollen samples according to the three pollen zones discussed in the text are shown and labelled.

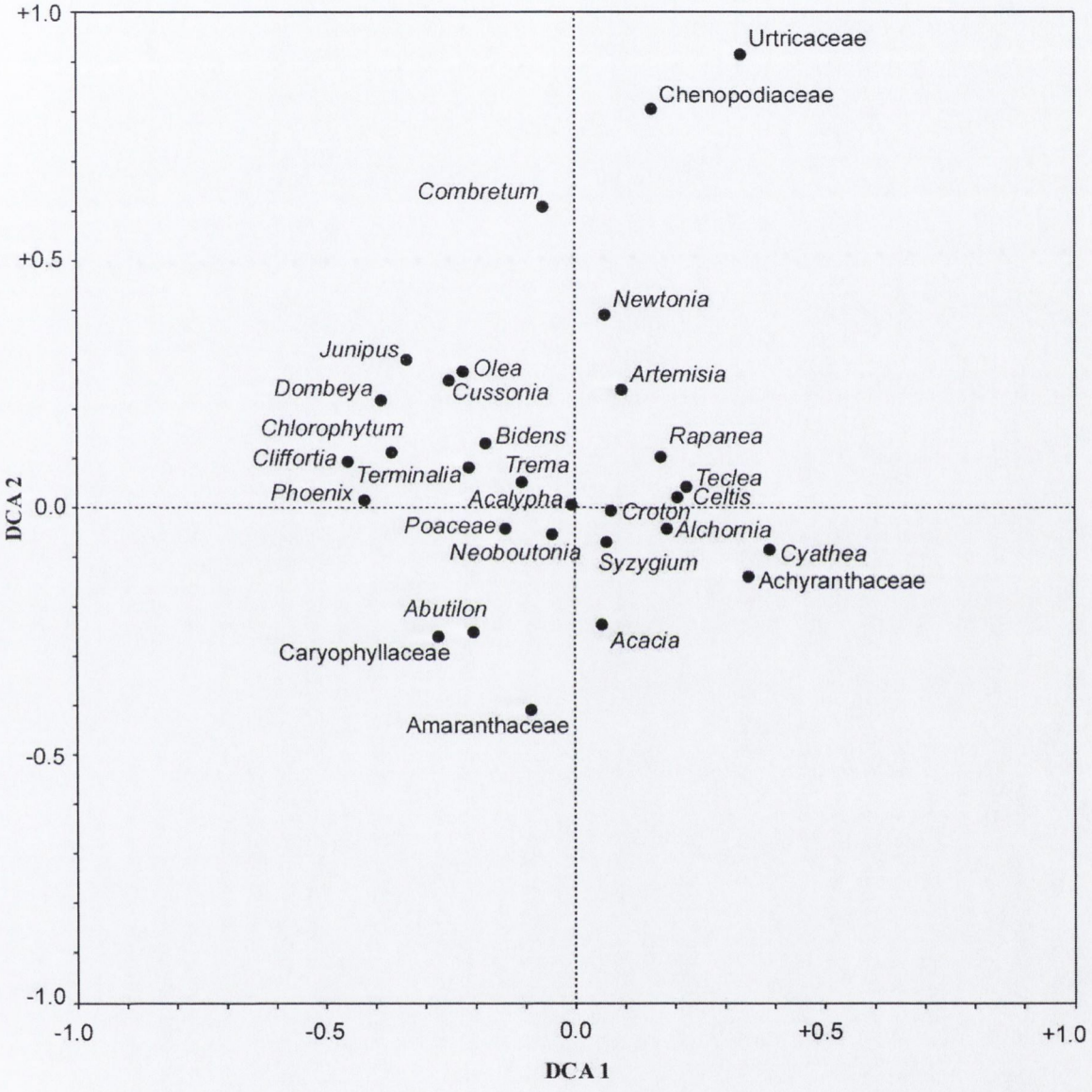

Figure 7.2 M2C1, Distribution of non-local pollen types used in numerical zonation of M2C1 according to DCA axes 1 and 2.

and *Celtis* each represents up to 15%. The presence of edaphically wet conditions is indicated by pollen from *Rapanea* and *Cyathea*, while the degraded forest category has relatively low proportions, with most taxa accounting for less than 10% of the pollen sum. *Acalypha* pollen contributes up to 27%, while Poaceae represents 4% to 27%. *Bidens* (a member of Asteraceae family), which is often associated with human activities (Lind & Tallantire, 1971), is rare in this zone. Pollen concentration and influx are generally low at the base of this zone, but increase to 125,000 grains g^{-1} and 700 grains cm^{-3} yr^{-1} at 86cm, ca. 1155 yr. BP (cal 780- 978 AD) respectively, before dropping to lower levels towards the boundary with zone C1Z2.

Among the local pollen and spores (Figure 8.4), Cyperaceae dominates zone C1Z1, with proportions of up to 69%, suggesting a period of sedge-dominated vegetation close to coring site. According to the $\delta^{13}C$ value for bulk sample of peat from this zone outlined in chapter six, however, which is more negative than would be expected for a C_4 carbon source, it would seem likely that the sedge papyrus, which is a C_4 plant, was not abundant at the time. *Alchemila* contributes a low proportion of about 5% to the sum. The spores are dominated by Filicales, with proportions ranging from 5% to 80%, possibly indicating a fluvial source for some of the deposit (Taylor, 1988). The proportion of *Sphagnum* spores decreases (< 5%), while that of *Polypodium* increases (> 5%), towards the upper boundary of the zone. *Anthoceros* and *Nymphaea* have low proportions of less than 10% and 5%, respectively.

The local pollen and spore concentration and influx are generally low (< 300,000 grains g^{-1} and 1250 grains cm^{-3} yr^{-1}, respectively) at the base of the zone, rising towards the upper boundary.

Zone C1Z2 (76 – 32 cm, ca. 945 – 190 yr. BP)

Pollen zone C1Z2 lies between 76cm (ca. 945 yr. BP) and 32 cm, ca. 190 yr. BP (cal 1649-1949 AD) and accommodates the majority of strategraphic zone DI and the lower part of DII (Figure 6.6). This zone represents a period of decline in arboreal taxa at the expense of non-arboreal taxa. The later is mainly represented by Poaceae. The proportions of medium altitude forest taxa drop to low levels, with most taxa becoming rare. The proportion of *Acalypha* pollen remains relatively constant (<30%) to that in zone C1Z1, while *Bidens* reappears at the upper boundary, reaching a proportion of 5% at 40 cm, ca. 410 yr. BP (cal 1426-1629 AD).

Local pollen and spores (Figure 7.4) are dominated by Filicales, contributing up to 88% of the local pollen and spore sum, followed by Cyperaceae pollen (12-67%). The proportion of *Sphagnum* spores increases towards the upper part of the boundary, reaching 15% at 38cm. Other spores have low proportions, contributing less than 15% of the local pollen sum.

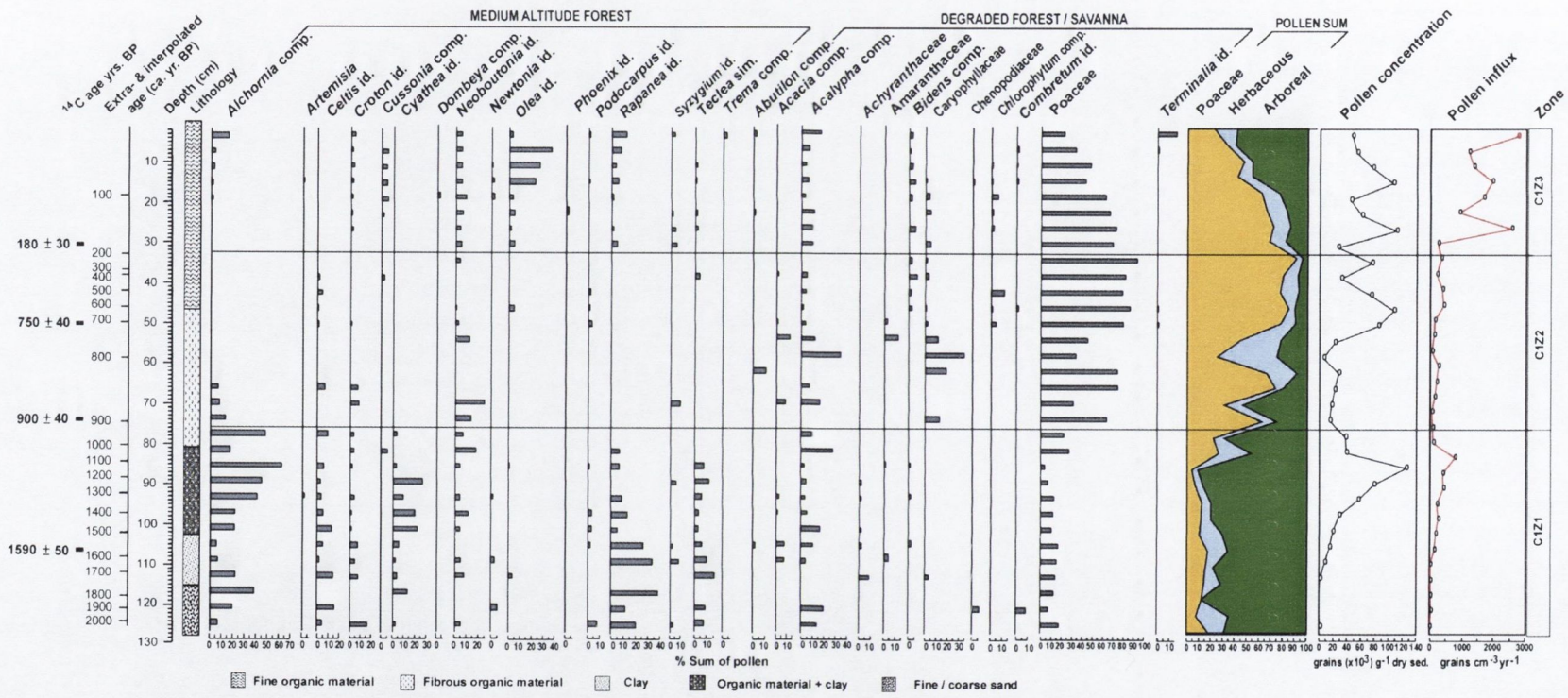

Figure 7.3 M2C1, down-core variations in abundances of non-local subfossil pollen taxa. A total of 32 samples were analysed, with total pollen counts ranging from 503 to 746 (mean = 544).

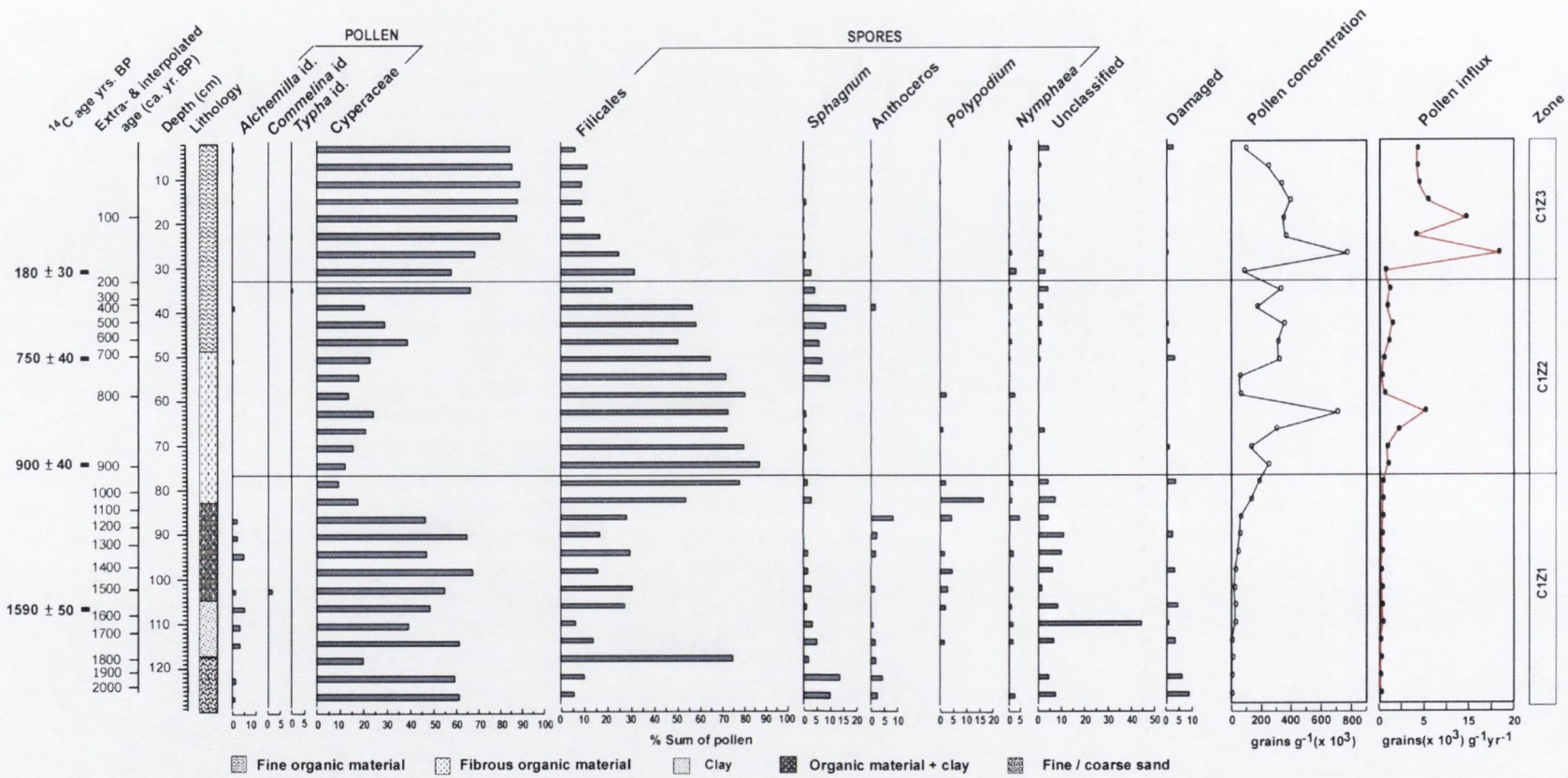

Figure 7.4 M2C1, down-core variations in abundances of local subfossil pollen and spores.

The local pollen and spores in zone C1Z2, when viewed in the context of the stratigraphy and $\delta^{13}C$ data outlined in chapter six, would appear to represent the development of peat-forming, herbaceous-dominated swamp condition at the coring site. C_4 plants, such as *Cyperus Papyrus*, may have been prominent, and the site could have remained fluvially-influenced, hence the high levels of Filicales spores, which are known to be particularly resistant to physical damage and hence are often common among fluvially-transported material (Taylor, 1988). The high levels of organic matter present in samples from below 46 cm (ca. 650 yr. BP). This zone (> 80% in some cares) would tend to suggest that any fluvial influence is minimal and therefore that the high levels of Filicales spores had a very local source.

Zone C1Z3 (32 – 0cm, ca. 190 yr. BP to present)

Pollen zone C1Z3 extends from 32 cm to the top of the core, ca. 190 yr. BP (cal 1649-1949 AD) to the present and corresponds to the upper part of stratigraphic zone DII (Figure 6.6). This pollen zone represents a period of increased proportion of some arboreal taxa. *Olea* pollen increases towards the top of the core, reaching a peak of 35%, while *Alchornea* and *Rapanea* attain a proportion of 15% and 12% respectively. The abundance of *Combretum* and *Terminalia,* which are characteristic of degraded forest or savanna habitats, are low in this zone, with the later attaining a maximum value of 14% in the upper part of the core. The abundance of Poaceae pollen declines across the C1Z2 –C1Z3 pollen boundary, and continue to decline through zone C1Z3. The proportion of *Bidens* remains relatively constant between 2% and 5%, while that of *Acalypha* ranges from 3% to 16%.

Local pollen and spores (Figure 8.5) are dominated by high proportions (65-90%) of Cyperaceae pollen, while Fillicale and *Sphagnum* spores decline towards the top of the core. *Polypodium* spores disappear from the record. The concentration and influx of local pollen and spores peak at about 768,000 grains g^{-1} and 6700 grains cm^{-3} yr^{-1} respectively at 26cm, before declining towards the top part of the core.

Pollen zone C1Z3 would thus appear to represent, when viewed within the context of results presented in chapter six, some recovery of mid altitude forest in the catchment area at Munsa. At the site itself, the data indicate the presence of a productive sedge-dominated swamp of which C_4-plants, such as Cyperus papyrus, are likely to have been important component. The reduced levels of organic matter throughout most of this zone (which equates to the upper part of stratigraphic zone DII) and sediment stratigraphy would also appear to indicate increased decomposition, possibly as a result of less frequent inundation and therefore a drying-out of the swamp surface for longer periods of time.

7.2.2 Pollen stratigraphy for M2C2 sediment core

The pollen sequence for M2C2 is divided into three zones, based on the zonation process outlined in chapter five, labeled C2Z1, C2Z2 and C2Z3 from the base to the top of the core (see below). The grouping of pollen samples according to DCA axes 1 and 2 is presented in Figures 7.5. The three strategraphically constrained groupings of samples into pollen zones is not an evident in the DCA ordination plot (Figure 7.5) as it was for

core M2C1, and suggests less of a distinction in composition between pollen zones C2Z2 and C2Z3. Samples from the lower part of the core (C2Z1) have positive scores on DCA axis 1, while samples comprising zones C2Z2 and C2Z3 largely receive negative scores. The distribution on DCA axes 1 and 2 of pollen taxa used for zonation is presented in Figure 7.6. Again, the distinctions are less clear than for core M2C1. However, as with M2C1, positive scores on DCA axis 1 appear to represent pollen from arboreal taxa, while pollen from taxa associated with degraded forest and grassland habitats generally receive more negative scores. Accordingly, samples comprising pollen zone C2Z1 are more strongly influenced by pollen from arboreal taxa than samples from C2Z2 and C2Z3.

Descriptions of pollen assemblages and accumulation rates for each pollen zones of core M2C1 are presented below and illustrated in Figures 7.7 and 7.8.

Zone C2Z1 (176 – 122cm, > ca. 1200 - 840 yr. BP)

Pollen zone C2Z1 extends from the base of the core at 176cm, ca. > 1200 yr. BP (cal 692-959 AD), to 122 cm, ca. 840 yr. BP (cal 1045-1278 AD) (Figure 7.7) and corresponds to stratigraphic zones A, B, C and DI (Figure 6.7). This pollen zone is dominated by arboreal taxa, contributing 50% to 96% of the pollen sum. *Alchornia* pollen is abundant, contributing up to 72% of the non-local pollen sum. *Cyathea* spores are also common initially, but decline towards the upper boundary of the zone. *Rapanea* contributes up to 42%, and pollen from *Macaranga*, *Neoboutonia* and *Olea* are present, although not abundantly so. Among the degraded forest taxa, *Acalypha* and Poaceae

pollen are common. *Bidens* pollen increases to about 30% at the upper boundary of the zone corresponding to the decline of arboreal taxa. Generally pollen concentrations are low in this zone (< 50,000 grains g^{-1}), as are rates of influx (<500 grains cm^{-3} yr^{-1}).

The local pollen and spores assemblage (Figure 7.8) is dominated by Cyperaceae pollen (up to 76% of the pollen sum), while *Alchemilla* pollen is rare in zone C2Z1. Filicales spores are well represented, whereas other spores such as *Anthoceros* are rare in this zone. The concentration and influx of local pollen and spores are very low at the base of the zone, representing less than 100,000 grains/g and 10,000 grains cm^{-3} yr^{-1} respectively.

Taken together, the data indicates generally forested conditions. Given the nature of the catchement, and the occurrence of relatively poorly dispersed pollen from forest taxa, it is likely that this forest was growing relatively close to the coring site, within the Munsa II swamp catchment. On the swamp itself the local pollen and spore vegetation within which sedge ferns were common. Variations in local pollen and spore on this zone appear to be relatively complacent, however, when compared to the sediment stratigraphy, presumably because of their low taxonomic revolution. Data presented in Figure 6.10 indicate a predominance of C_3 plants and a C_3-carbon source for the core AMS ^{14}C date for this zone.

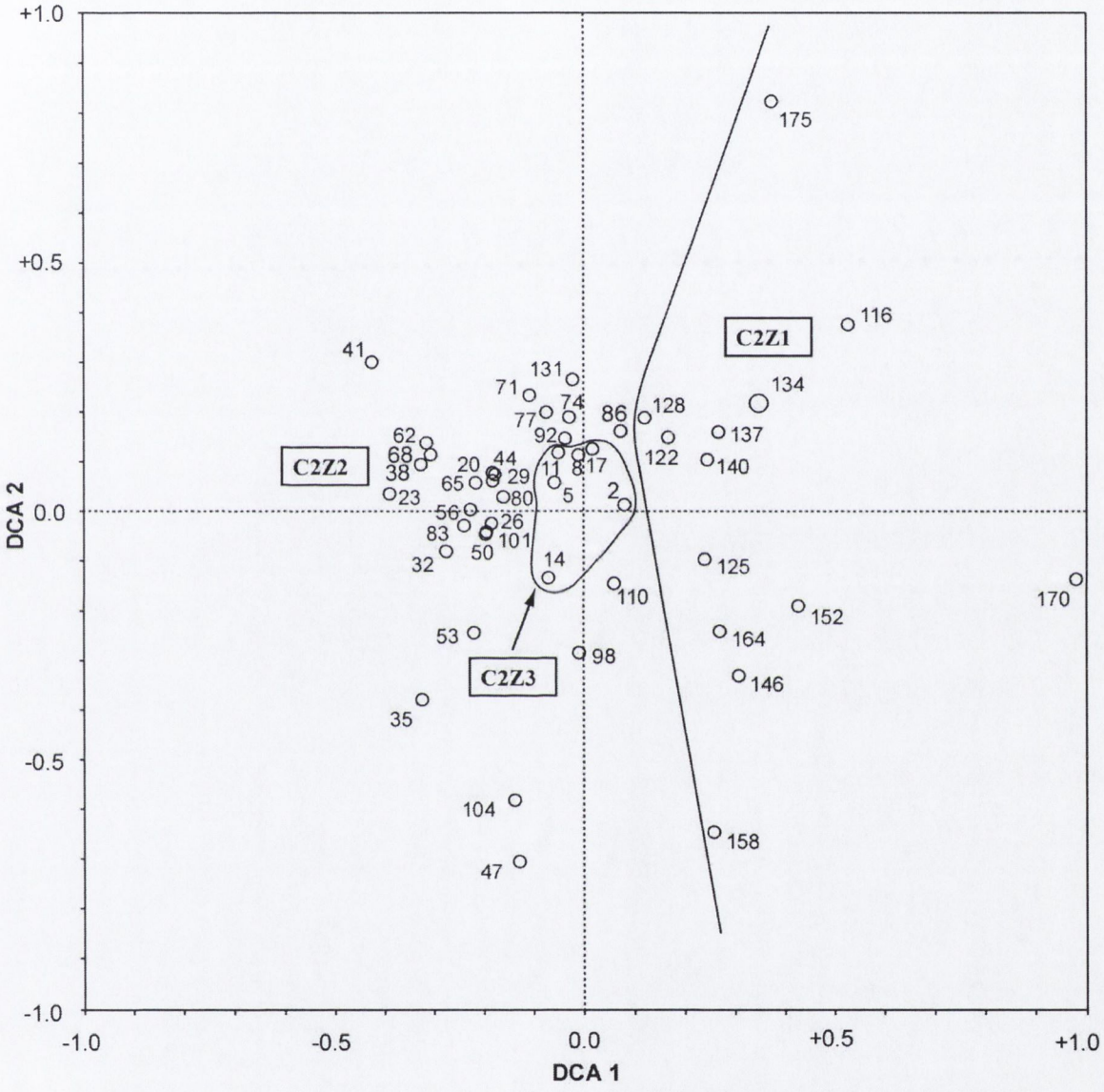

Figure 7.5 Distribution of pollen samples for core M2C2 according to DCA axes 1 and 2. The groupings of pollen samples according to the three pollen zones discussed in the text are shown and labelled.

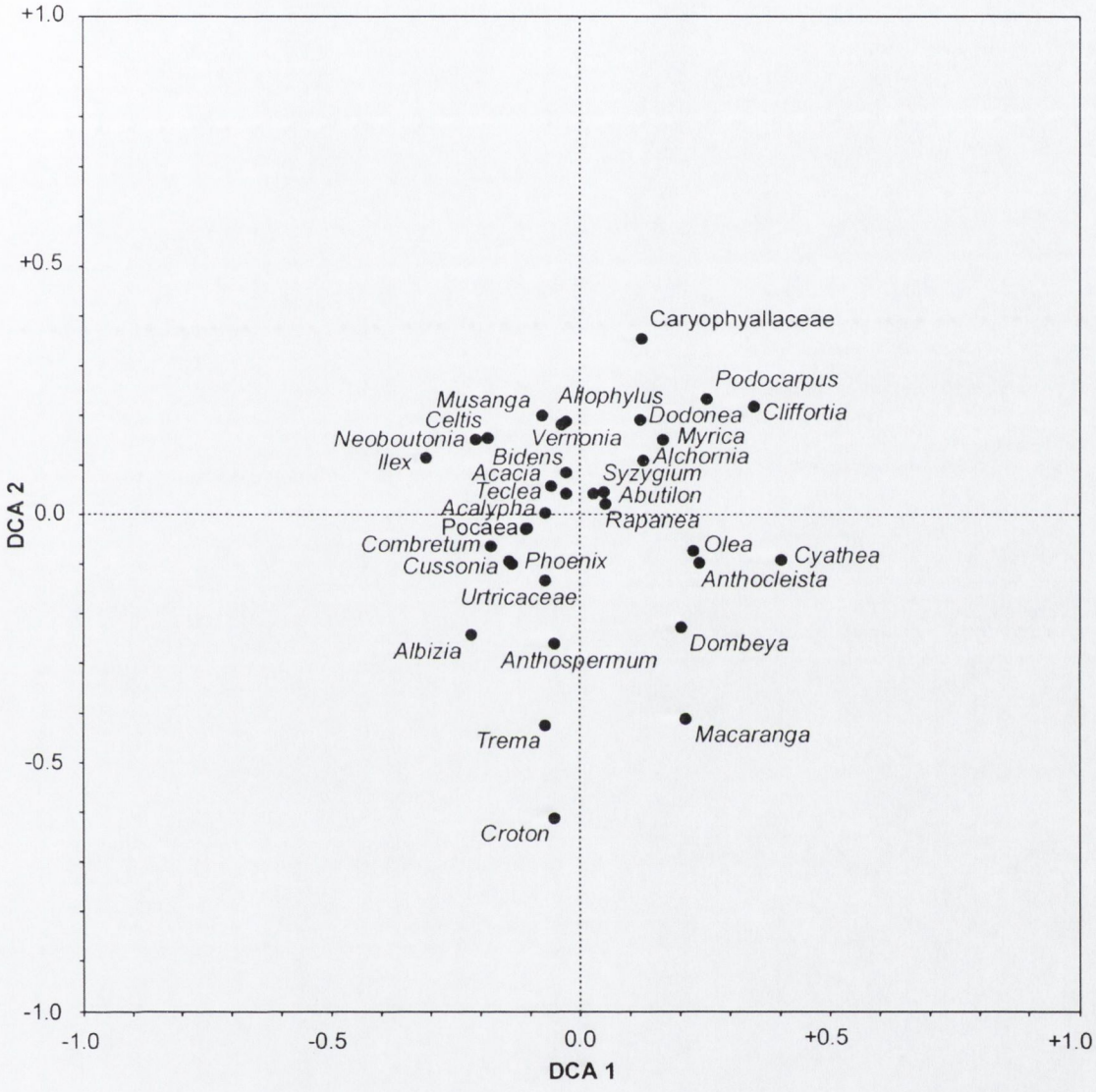

Figure 7.6 M2C2, distribution of non-local pollen types used in numerical zonation M2C2 according to DCA axes 1 and 2.

Zone C2Z2 (122 – 20 cm, ca. 840 - 190 yr. BP)

Pollen zone C2Z2 lies between 122 cm, ca. 840 yr. BP (cal 1045-1278 AD), and 20 cm, ca. 190 yr. BP (cal 1649-1949 AD) and accommodates the majority of stratigraphic zone DII (Figure 6.7). This pollen zone represents a decline in arboreal taxa and presumably, therefore reduction in forest cover in the Munsa II catchment. Most pollen and spores from medium altitude forest taxa drop to low levels (<10%) in this zone. However, pollen from *Celtis*, *Neoboutonia* and *Phoenix* are occasionally relatively abundant. *Celtis* pollen is relatively widely dispersed (Hamilton, 1972), and could therefore have transported some distance to the coring site. *Neoboutonia* and *Phoenix* have been recorded in forest on swamp (i.e. edaphically wet) soils in the region, and may thus represent the presence locally patches of swamp forest. Pollen from the degraded forest category dominates the non-local sum in zone C2Z2, particularly pollen from Poaceae and *Acalypha*. *Bidens* contributes up to 25% to the pollen sum. The concentration and influx of pollen range from 10,000 to 470,000 grains g^{-1} and 100 to 4600 grains cm^{-3} yr^{-1} respectively.

The local pollen and spore sum is dominated by Cyperaceae pollen and Filicales spores (up to 85% at the lower boundary). *Sphagnum* spores increase from the lower boundary, reaching about 16% of the local sum at 80 cm, but decline in the upper part of the zone. The concentration and influx of pollen and spores are generally high in this zone, ranging from 100,000 to 1,200,000 grains g^{-1} and 500 to 10,000 grains cm^{-3} yr^{-1} respectively.

Pollen zone C2Z2 would thus appear to represent a replacement of forest in Munsa II catchment by more open, disturbed vegetation types. Locally the vegetation at the coring site was dominated by sedge and ferns, including on the basis of the data presented in Figure 6.10, a significant proportion of C_4 plant taxa, such as *Cyperus papyrus*.

Zone C2Z3 (20 – 0 cm, ca. 190yr. BP to present)

Pollen zone C2Z3 extends from 20 cm to 0 cm, ca. 190 yr. BP to the present. This zone represents an increase in *Alchornea* (>20%) and *Rapanea* (>15%) towards the top part of the core. Pollen from other taxa remains low in this zone. Poaceae pollen dominates the degraded/savanna forest category, accounting for up to 73% of the pollen sum, while *Acalypha* accounts for up to 26%. *Bidens* is relatively low, representing less than 5% of the pollen sum. Pollen concentration and influx increase from 50,000 to 120,000 grains g^{-1} and 500 to 700 grains cm^{-3} yr^{-1}, respectively.

Local pollen is dominated by Cyperaceae (66-84%) (Figure 8.8). The proportion of Filicales declines towards the top part of the core, while the concentration and influx of pollen and spore are generally high, ranging from 300, 000 to 700,000 grains g^{-1} and 3000 to 7000 grains cm^{-3} yr^{-1}.

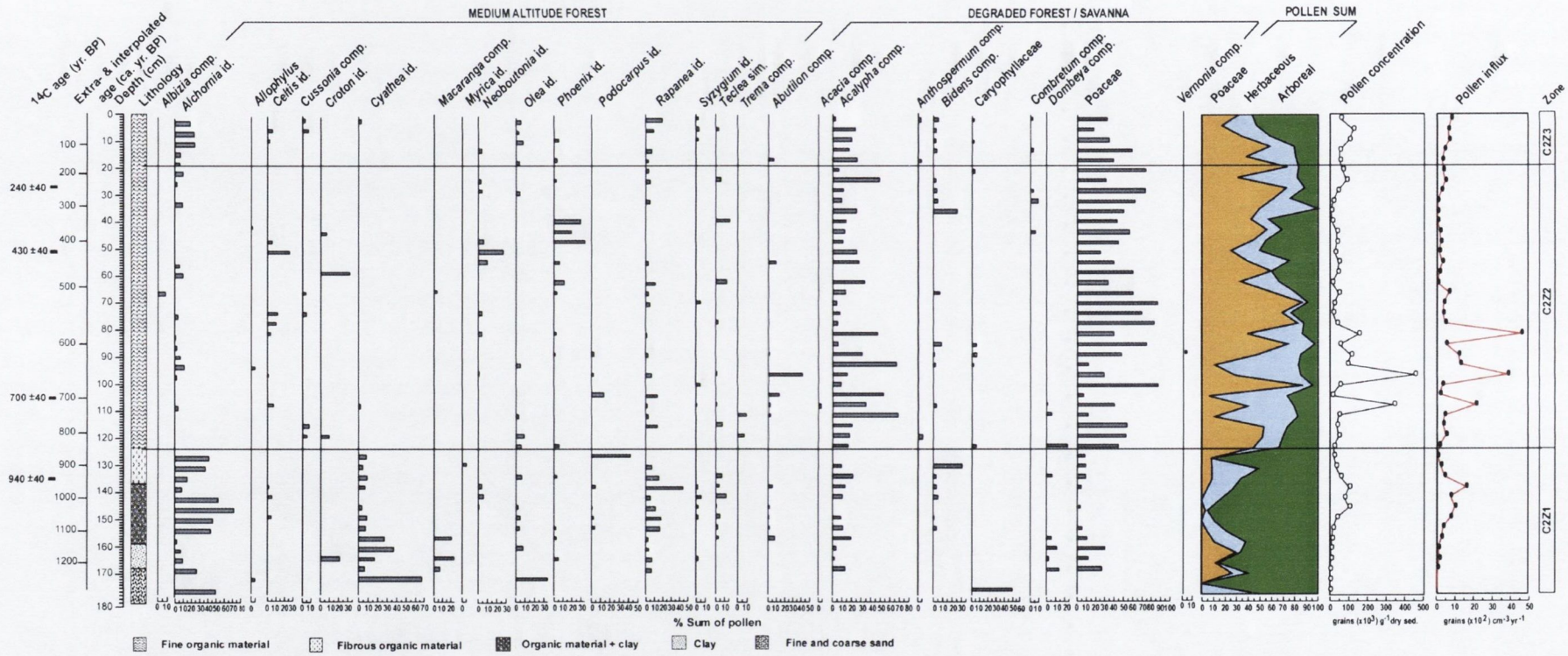

Figure 7.7 M2C2, down-core variations in abundances of non-local subfossil pollen taxa. A total of 49 samples were analysed, with local pollen counts ranging from 495 to 525 (mean = 510).

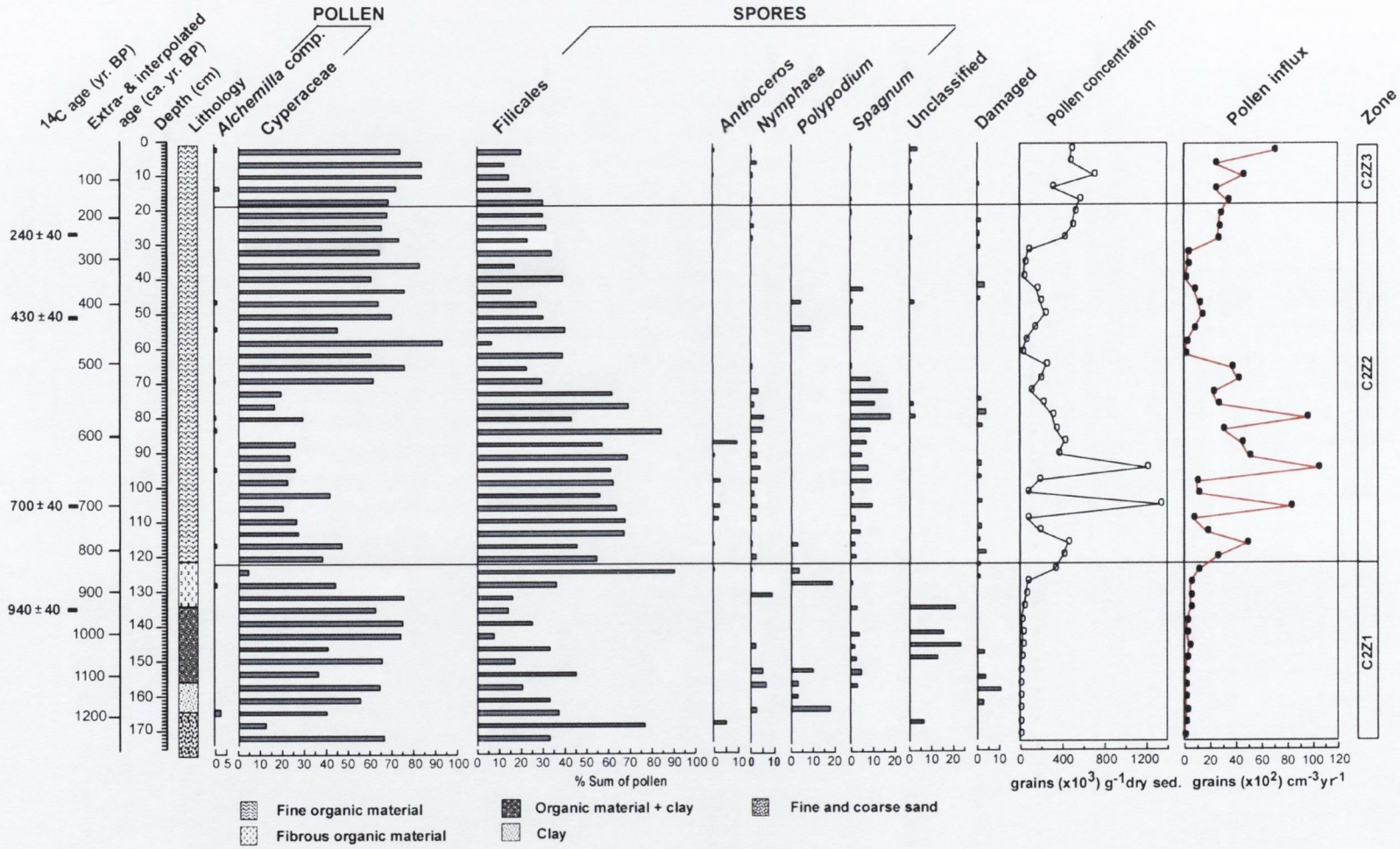

Figure 7.8 M2C2, down-core variations in abundances of local subfossil pollen and spores.

7.2.3 Pollen stratigraphy for M2C3C sediment core

The results of the DCA ordination of pollen samples from M2C3C are presented in Figure 7.9. The three pollen zones described below are labeled C3Z1, C3Z2 and C3Z3. Samples constituting zones C3Z2 and C3Z3 are closely located according to DCA axes 1 and 2, suggesting strong similarity in pollen composition of these zones as was the case for M2C2 (Figure 7.5). Samples forming pollen zone C3Z1 are, by comparison, more widely dispersed over the plot, suggesting some intra-zone variability and a degree of overlap within the zones above. Figure 7.10 illustrates the results of ordination the non-local pollen taxa. The vegetation gradient on the DCA axis 1 is less distinct than for M2C1 and M2C2, although pollen from taxa associated with degraded forest and savanna habitats mainly receive low positive scores, which accounts for the less distinct grouping of pollen samples according to these data.

The pollen assemblages and accumulation rates occurring in each pollen zone of core M2C3C are presented in Figures 7.11 and 7.12.

Zone C3Z1, 185 – 94 cm (ca. 5000 - 800 yr. BP)

Pollen zone C3Z1 extends from the base of the core at 185 cm, ca. 5000 yr. BP (cal 3941-3667 BC), to 94 cm, ca. 800 yr. BP (cal 1163-1285 AD). As suggested in chapter six, this zone may include the presence of at least one sedimentation break (hiatus) between the AMS (^{14}C) dates 3640 ± 40 yr. BP (cal 2136-1891 BC) and 910 ± 40 yr. BP (cal 1030-1211 AD). The zone corresponds to stratigraphic zones A-C and lower part of

DI (Figure 6.8). The lower part of this zone, from 185 cm (ca. 5000 yr. BP) to 166 cm (4680 yr. BP, cal 3626-3365 BC), is characterised by a relatively diverse pollen and spore flora. The medium altitude forest category is mainly represented by pollen from *Teclea*, which accounts for about 15% of the pollen sum. The degraded forest/savanna category is dominated by *Acalypha* pollen, contributing up to 46% to the pollen sum, while other taxa are relatively poorly represented. The pollen and spore flora is less diverse in the middle of this zone, but increases in diversity towards the upper boundary. The concentration and influx of pollen are very low, ranging from 1000 to 40,000 grains g^{-1} and 100 to 8000 grains cm^{-3} yr^{-1}, respectively.

Cyperaceae and Filicales are the most abundant local pollen and spore types. The concentration and influx of pollen and spores are very low in this zone (<200,000 grains g^{-1} and <1500 grains cm^{-3} yr^{-1}, respectively).

Pollen zone C3Z1, thus provides albeit apparent broken, record of broad expanse of time. Generally forested conditions are represented by the pollen zone, with sedges and term characterising the local wetland vegetation. However, this is a degree of intra-zone variation that is supported by the results of DCA ordination analysis refered to above (Figure 7.9), which presumably reflects changes in forest composition as well as varying impacts of taphonomic process, including decomposition, during the ca. 4000 yrs represented by the pollen zone.

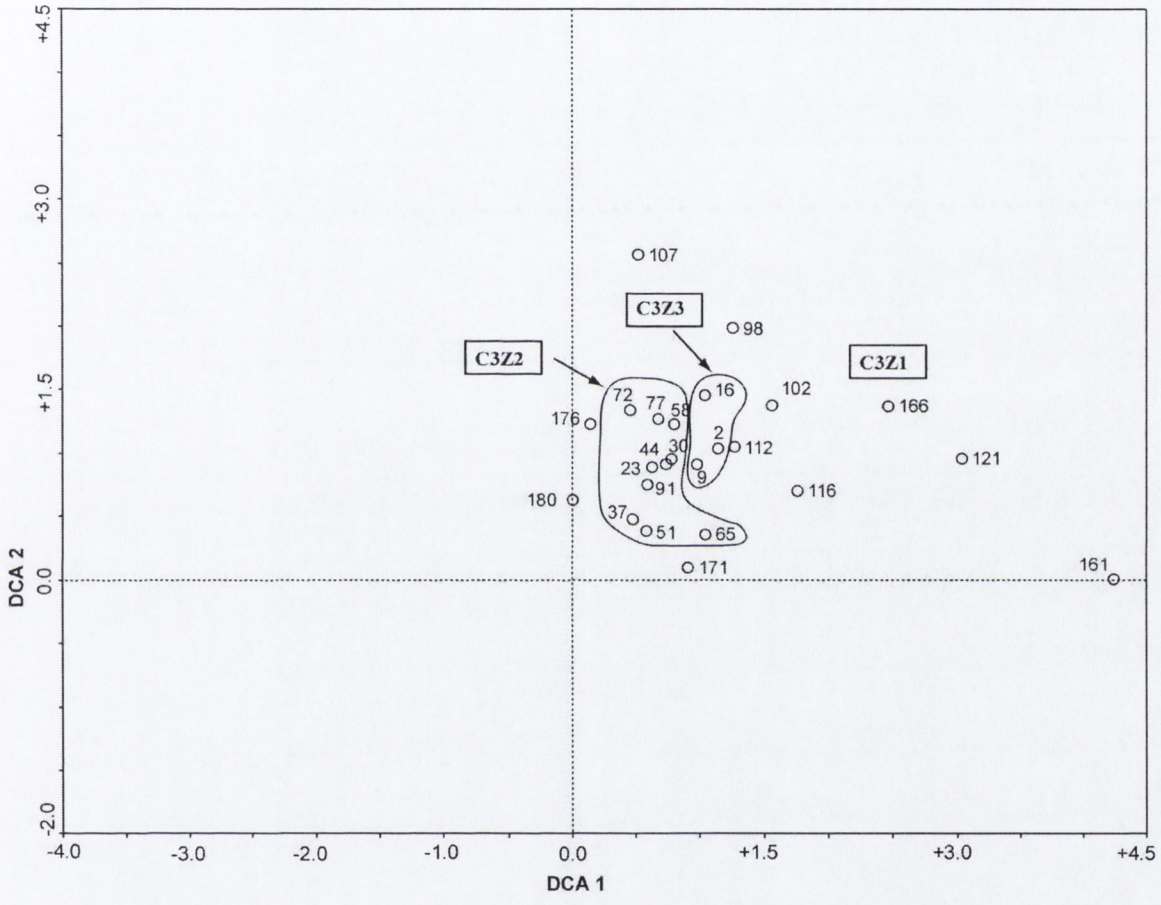

Figure 7.9 Distribution of pollen samples for core M2C3C according to DCA axes 1 and 2. The grouping of pollen samples according to the three pollen zones discussed in the text are shown and labelled.

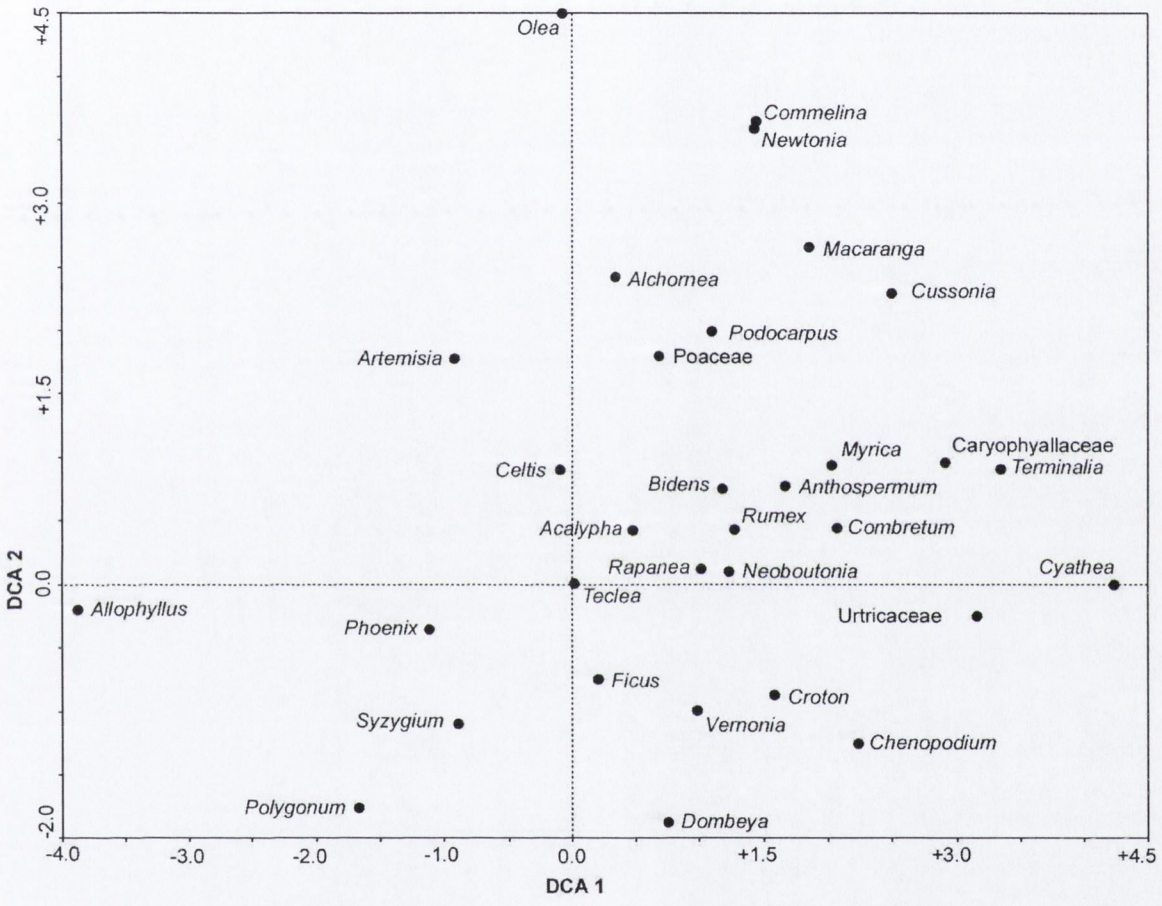

Figure 7.10 Distribution of non-local pollen types used in numerical zonation of M2C3C according to DCA axes 1 and 2.

Zone C3Z2 (94 – 28 cm, ca. 850 - post 540 ± 40 yr. BP, possibly post ca 480 yr. BP)

As mentioned in chapter six, the upper part of core M2C3C may contain at least one hiatus. Either that or there is an abrupt reduction in the rate of sediment accumulation. In the absence of any stratigraphic evidence for an hiatus, other than the change in sedimentation rate and such as a clear erosion layer or other substantive change in stratigraphy, a reduced sedimentation rate has been assumed when extrapolating the age of sediment in the upper part of this core. However, having said this, the extrapolated ages should be viewed with some caution. Thus this pollen zone, which equates to the majority of stratigraphic zone DI and the lower part of DII, has tentatively been dated at AMS ^{14}C date 850 ± 40 yr. BP (102-103 cm) to post 540 ± 40 yr. BP, and possibly ca 480 yr BP. This zone is characterised by a lower abundance of pollen and spores from forest taxa when compared to C3Z1 and greatly increased abundance of pollen from degraded forest plants (mainly *Acalypha* and Poaceae). The proportion of *Acalypha* increases to 44% at the upper boundary, while Poaceae contributes up to 94% of the non-local pollen sum. The proportion of *Bidens* is relatively high in this zone, representing up to 14% of the non-local pollen sum. Pollen concentration and influx attain high peaks in the zone, ranging from 10,000 to 370,000 grains g^{-1} and 100 to 4000 grains cm^{-3} yr^{-1}, respectively.

Cyperaceae pollen and Filicale spores dominate non-local spectra. The proportions of other spores remain low. The concentration and influx of local pollen are generally high in this zone, ranging from 500,000 to 1,800,000 grains g^{-1} and 1000 to 11,000 grains cm^{-3} yr^{-1}, respectively.

Pollen zone C3Z2 would thus appear to record some disturbance of medium altitude forest in the catchment for Munsa II, from around ca 850 yr. BP. This period of forest disturbance and a concomitant spread of taxa associated with after 540 ± 40 yr. BP, and, depending on the rate of sediment accumulation in the upper part of the core, possibly ca 480 yr. BP. Vegetation at the coring site continued to be characterised by sedge and ferns. According to the data presented in Figure 6.11, the composition of local rejection may have changed during this zone, form a predominantly C_3 flora to a C_4 flora.

Zone C3Z3 (28 – 0 cm, ca. post 540 ± 40 yr. BP **to present)**

Pollen zone C3Z3 extends from 28cm (post 540 ± 40 yr. BP), and possibly ca 480 yr. BP to the top of the core, and accommodates the middle and upper parts of stratigraphic zone DII. As has already been discussed, this zone may include a sediment hiatus. The percentage proportions of most medium altitude forest taxa remain relatively low (<10%) in this zone, while pollen from forest taxa associated with edaphically wet conditions (*Myrica*, *Neoboutonia and Phoenix*) increases towards the top part of the core. *Syzygium* becomes rare in this zone, while *Cyathea* spores disappear from the record. Among the degraded forest/savanna category, *Acalypha* pollen becomes less abundant towards the top of the core, while the abundance of Poaceae pollen fluctuates, falling from 48% to 13%, before increasing towards the top of the core and reaching a peak of 40%. *Bidens* increases to higher levels (14%) at the upper part of the core. The concentration and influx of pollen remain relatively low in this zone.

The abundance of Cyperaceae pollen and Filicale spores remain relatively constant at 49% and 41%, respectively in this zone (Figure 8.12), while *Sphagnum* spores contribute up to 7% to the sum. Pollen and spore concentration of local spectra fluctuates between 250,000 and 1,250,000 grains g^{-1}, while the influx is relatively low (500 to 3000 grains cm^{-3} yr^{-1}.) compared to that in zone C3Z2.

Overall, C3Z3 indicates some degree of forest recovery, although not as marked as in C3Z2 (M2C1). Relatively little difference between C3Z3 and C3Z2 is also evident in the DCA ordination results (Figure 7.9). The DCA ordination results also indicate a degree of similarity between the composition of samples zoned in C3Z3 and those in the upper part of C3Z1.

The data presented here in Figure 7.12, suggest a continuation of a C4-dominated, sedge and fern community at coring site.

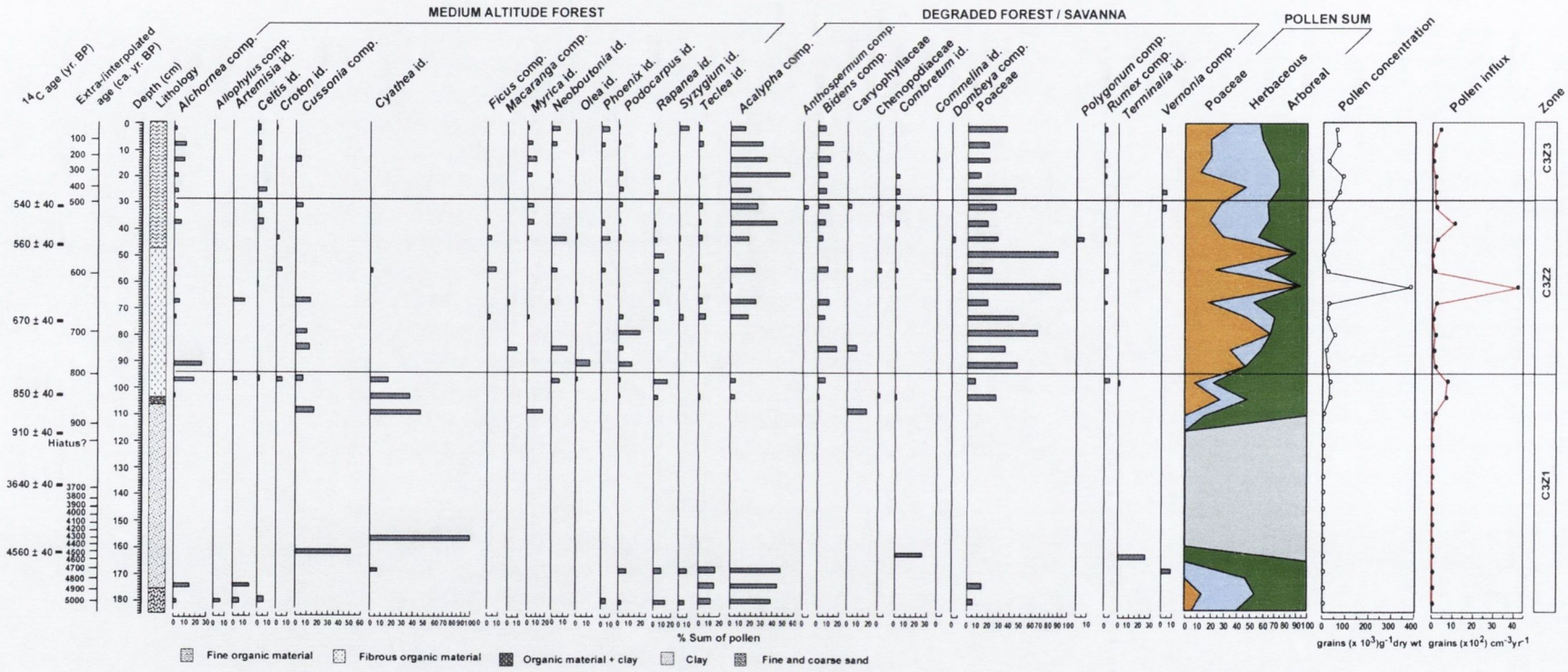

Figure 7.11 M2C3C, down-core variations in abundances of non-local subfossil pollen taxa. A total of 32 samples were analysed for their contents, with counts ranging from 496 to 1849 (mean = 585).

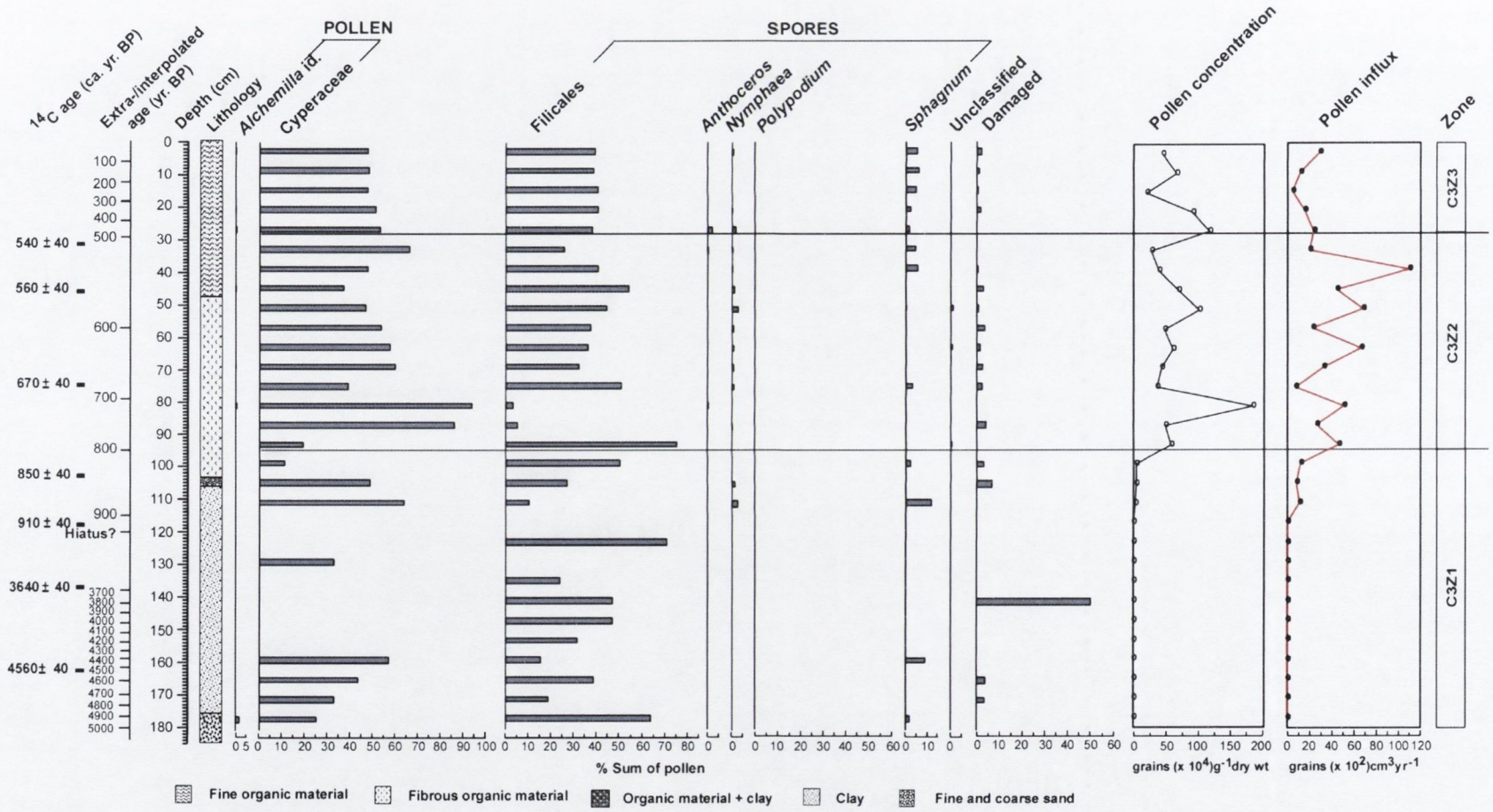

Figure 7.12 M2C3C, down-core variations in abundances of local subfossil pollen and spores.

7.3 Inter-core comparison of pollen data for Munsa II sediments

The results clearly indicate that the non-local pollen and spore data vary much more down core in M2C1 than in cores M2C2 and M2C3C. The pollen zones are more marked in M2C1, for example, possibly because the more marginal location of M2C1 means that it is more sensitive to variations in the input of non-local pollen and spores than, for example, core M2C3C. This evidence is apparent in the phytolith records presented in chapter eight. The DCA ordination results of pollen samples from the three cores indicate similar distribution pattern of forest taxa in the local zones.

Generally the three cores indicate a period of forest vegetation in Munsa II sediment pre-dating ca 900 yr. BP The local pollen zone is dominated by medium altitude evergreen and semi-deciduous forest within Munsa II catchment area. The details of the potential sources of pollen and possible environmental impacts are discussed in chapter ten.

7.4 Results of fungal spore analysis

This section presents results of the analyses of fungal spores in sediment samples from M2C1, M2C2 and M2C3C. To ease interpretation and comparison of the fungal assemblage data, the boundaries used in the zonation of pollen diagrams are also used here to classify the fungal data.

7.4.1 Fungal spore stratigraphy for core M2C1 sediment core

Figure 7.13 presents down-core variations in fungal spore assemblages for M2C2.

Zone C1Z1 (126 – 76 cm, ca. 2000 - 945 yr. BP). The lower parts of this zone are dominated by the spores of Gaeumannomycetes (40-55%). Type 181 fungi contribute up to 50% of fungal spore counts in this zone, while *Sordaria*-type 55 accounts for up to 55% of the total sum. *Ustulina* contributes up to 80%. Percentages of *Arthrinium* fungi are low at the base of the zone, but increase to 30% towards the upper boundary of the zone. *Alternaria*-type, *Pseudoschizae* and the dung fungus *Cercophora* are rare in zone C1Z1.

Zone C1Z1 is generally dominated by fungal spore that are associated with forested conditions (*Ustulina*) and edaphically-wet habitats (*Sordaria*-type 55, Type 181). Gaeumannomtces which is associated with sedge vegetation (van Geel, 2001) is relatively abundant at the base of the zone.

Zone C1Z2 (76 – 32 cm, ca. 945 – 190 yr. BP). This zone is dominated by the spores of *Arthrinium* (10-40%), Type 181 fungi (10-40%) and *Sordaria*-type (30-70%). Most other fungal spores are less abundant compared to zone C1Z2. *Alternaria*-type disappears in the record, while *Ascospore-type*18 and *Ustulina* become rare. The dung fungus *Cercophora*-type remains rare in this zone, while spores of *Pseudosschizae* rise to 25% of the total sum towards the upper boundary.

Zone C1Z2 appears to indicate the sensitivity of *Ustulina* to habitat change from forested to more open vegetation in the catchment of Munsa II as suggested by pollen and phytolith data (see section 8.2.1, also chapter eight). The rise in abundance of *Arthrinuim* spores appears to correlate with increased abundance of charcoal in sediment record (see chapter nine) and also corresponds to stratigraphic zone D, which dominated organic materials.

Zone C1Z3 (32 – 0 cm, ca. 190 yr. BP to present). The spores of *Sordaria*-type 55 peak at 10cm, ca. 60 yr. BP (cal 1693-1955 AD), before declining towards the top of the core. *Arthrinium* and Ascospore-type 18 decline towards the top of the core, while *Alternaria*-type reappears in the zone. The dung fungus, *Cercophora*-type, increases to relatively high levels (10%), before declining in the uppermost parts of the core. *Ustulina* fungus remains rare in this zone on the whole, although it does reach a maximum of 11% at the top part of the core.

In Zone C1Z3 the increase in the number of spores of the dung fungus *Cercophora* appears to suggest an increase in the number of herbivores at Munsa.

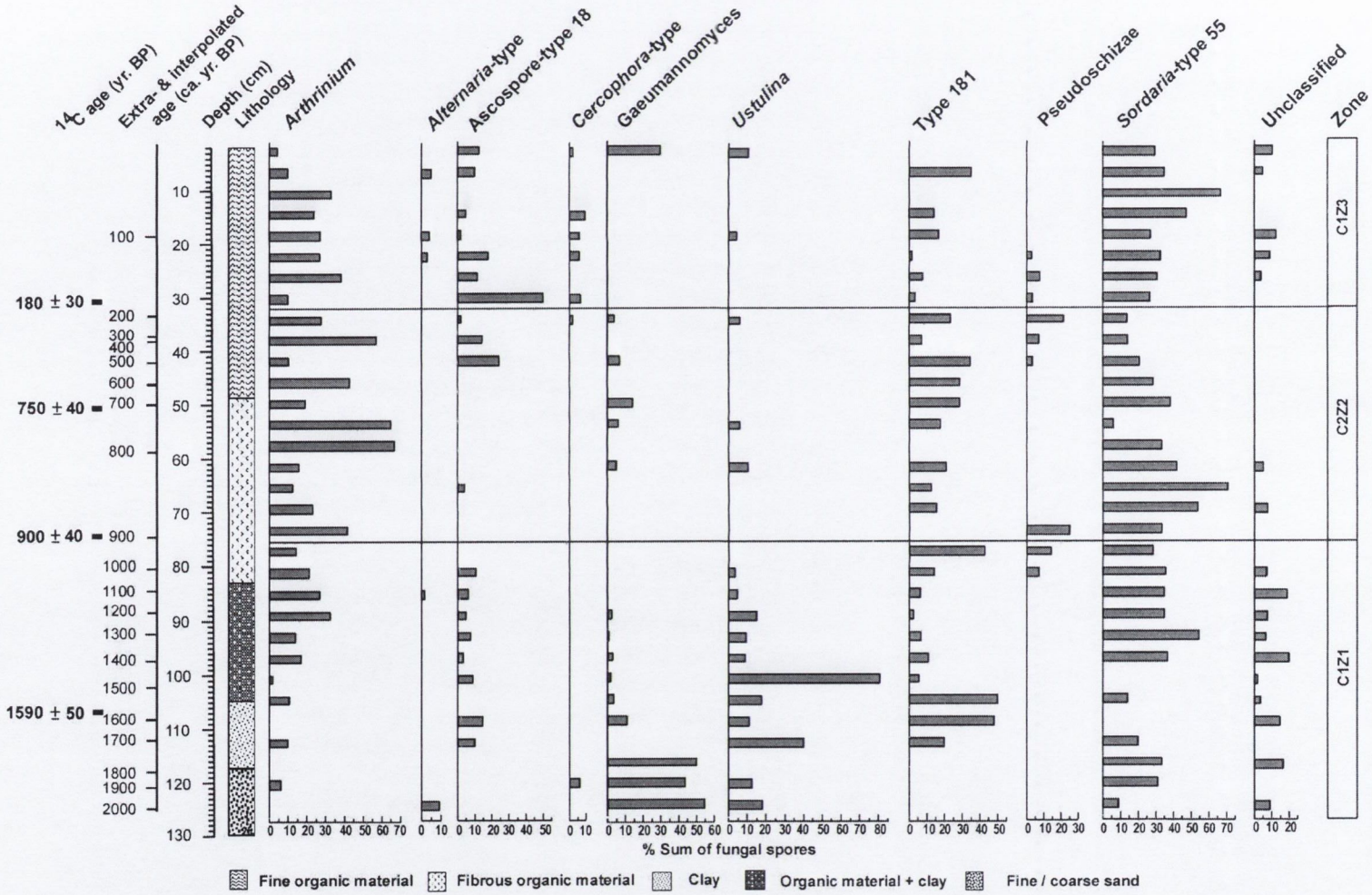

Figure 7.13 M2C1, down-core variations in abundances of subfossil fungal spores. A total of 32 samples were analyzed for their fungal spore content, with counts ranging from 205 to 211 (mean = 209).

7.4.2 Fungal assemblages for M2C2 sediment core

Down-core variations for fungal spore assemblages in M2C2 are presented in Figure 7.14. Three zones labelled C2Z1, C2Z2 and C2Z3 are distinguished.

Zone C2Z1 (176–122 cm, > ca. 1200 - 840 yr. BP). The diversity of fungal spores is relatively rare in this zone. However, the zone contains abundant spores of *Sordaria*-type 55 (20-100%), and *Arthrinium* is relatively abundant (5-65%) in the lower part of the zone. Spores of the dung fungus *Sporomiella* are rare, with only two records of 5% and 15%, while *Cercophora*-type spores comprise contributes from 3% to 15% of the total sum. The spores of *Ustulina* account for 5% to 20% of the total sum.

Zone C2Z1 appears to represents a period of edaphically-wet environment as suggested by dominance of *Sordaria*-type 55 spores. The low abundance of *Ustulina* correlates with reduced forest vegetation in the catchment of Munsa II.

Zone C2Z2 (122 – 20 cm, ca. 840 - 190 yr. BP). This zone is dominated by *Sordaria*-type 55 spores, which contribute 5% to 70% of the total counts, while the spores of Gaeumannomycetes account for 5% to 45%. The dung fungus *Cercophora*-type contributes 3% to 15%, and Type 181 represents 5% to 90%, while *Arthrinium* contributes 5% to 53%. The spores of *Sporomiella*-type were not recorded in this zone.

A significant increase in the abundance of Type 181 spores in zone C2Z2, suggests an edaphically-wet conditions in Munsa II swamp.

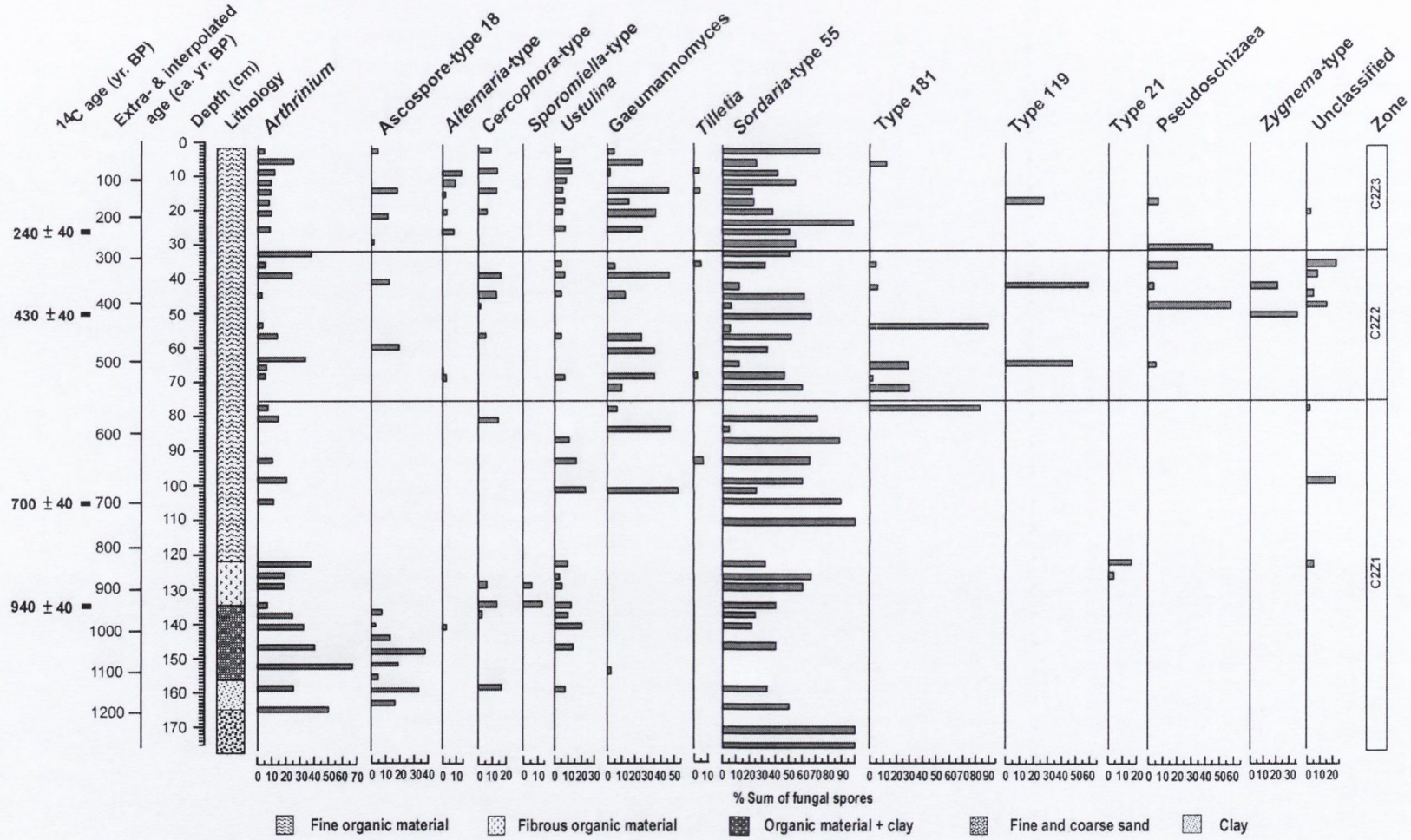

Figure 7.14 M2C2, down-core variations in abundances of subfossil fungal spores. A total of 49 samples were analyzed for their fungal spore content, with counts ranging from 210 to 223 (mean = 205)

Zone C2Z3 (20 – 0cm, ca. 190 yr. BP to present). *Sordaria*-type 55 is the most abundant fungal spore type in this zone. The spores of Gaeumannomycetes are also abundant, ranging form 5% to 45%. This zone is marked by relatively low and constant proportions of *Arthrinium* (<25%) and *Ustulina* (<15%) spores. *Cercophora*-type spores account for up to 14% of the total count, while Type 119, 181, and *Zygnema*-type spores are rare.

Generally this zone appears to indicate an edaphically-wet environment as suggested by dominance of *Sordaria*-type 55 spores.

7.4.3 Fungal stratigraphy for M2C3C sediment core

Fungal assemblage data for M2C3C are presented in Figure 7.15.

Zone C3Z1, (185 – 94 cm, ca. 5000 - 800 yr. BP). This zone is interrupted by a gap in the record, between 171 cm to 121 cm depth. Samples from this depth range were devoid of fungal spores as was the case for microfossils from higher plants, probably because of poor preservation. The gap in the record includes the hiatus between 137 cm and 117 cm, suggested in chapter six and appears to represent a period of relatively high energy environments at Munsa II compared to present. The lower part of zone C3Z1 is mainly dominated by spores from *Sordaria*-type 55 and unclassified fungal spores, which account for up to 100% of the overall count. *Usutulina* spores are also common (up to 57%), while *Sporomiella*–type spores are rare at the base of this zone. The spores of *Cercophora*-type account for up to 29%. The abundance of *Arthrinium* spores vary widely.

Zone C3Z1 is generally dominated by *Sordaria*-type 55, suggesting an edaphically-wet environment in Munsa II swamp. Evidence for forested environments is suggested by presence of *Ustulina* spores at the base of the core.

Zone C3Z2 (94 – 28 cm, ca. 800 - 480 yr. BP). This zone is characterised by the abundance of *Sordaria*-type 55 spores. The proportions of *Arthrinium* spores vary, though the spore type is common throughout the zone. Spores from the fungus *Sporomiella*–type remain rare, while the abundance of *Cercophora*-type spores decline from 17% to less than 5% at the upper boundary of the zone. The proportions of *Ustulina* remain relatively constant throughout the zone.

Zone C3Z1 is generally dominated by *Sordaria*-type 55 and *Ustulina* spores is also apparent at the base suggesting an edaphically-wet environment and forested environments respectively.

Zone C3Z3 (28 – 0 cm, ca. 480 yr. BP to present). Type 181 and *Sordaria*-type 55 spores are relatively abundant in this zone, with the former increasing towards the top part of the core. Spores of *Sporomiella*-type and *Cercophora*-type disappear from the record, while spores of *Ustulina* remain at relatively low levels through the zone.

The relative dominance in this Type 181 and *Sordaria*-type 55 spores suggest an edaphically-wet environment in Munsa II swamp.

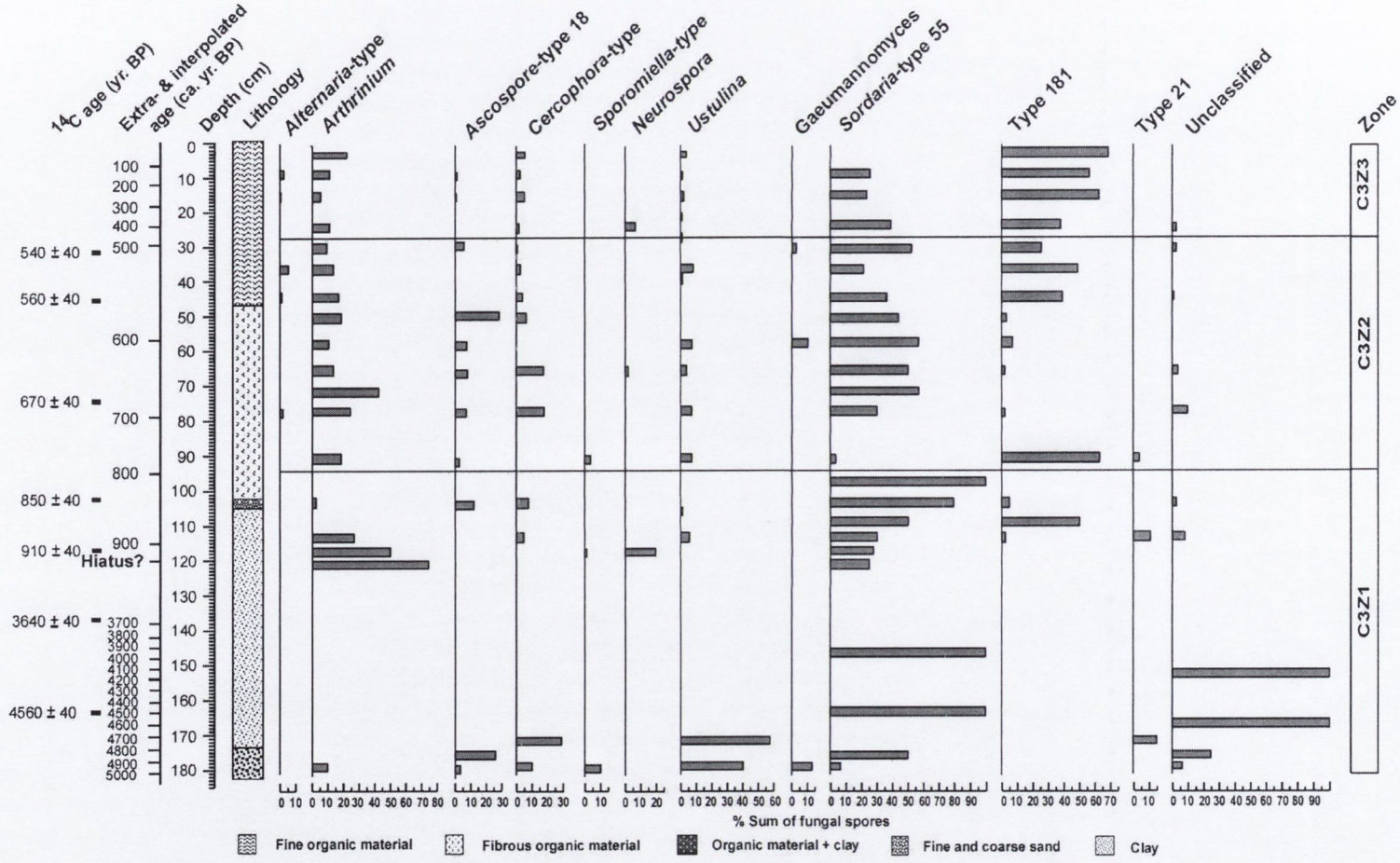

Figure 7.15 M2C3C, down-core variations in abundances of subfossil fungal spores. A total of 32 samples were analyzed for their fungal spore content, with counts ranging from 200 to 340 (mean = 271).

CHAPTER EIGHT

RESULTS OF PHYTOLITHS ANALYSIS

8.1 Introduction

This chapter presents the results of phytolith analysis for Munsa II sediment cores. It describes and accounts for the down-core variations in phytolith assemblages for M2C1, M2C2 and M2C3.

8.2 Distribution of modern phytolith morphotypes

In order to provide a means of discriminating phytoliths from cultivated plants in the phytolith record, an analysis of phytoliths produced by modern specimens of commercially important plant families (Musaceae and Poaceae) was carried out. The following is a summary of the results. Table 8.1 presents the percentage size-class distribution of cross-shaped morphotypes identified in examples from the study area of cultivated and non-cultivated members of Poaceae. Among the eleven plant specimens analyzed, three species (*Eleusine coracana*, *Panicum maximum* and *Setaria sphacelata*) did not possess cross-shaped morphotypes. In the eight species with cross-shaped morphotypes, category I, which constitutes the smallest size-class, has the highest frequency of occurrence (55-100%), with a cultivated variety of sorghum (*Sorghum* bicolor) contributing the highest frequency (100%) of cross-shape morphotype. Category II (medium size-class) account for up to 45% of the total. The categories of large and extra large size-classes have the least frequency of occurrence, with no cross-shaped morphotypes recorded among the non-cultivated species. *Zea mays* produced the

Table 8.1 The percentage distribution of cross-shaped phytoliths in each size-class category for the eleven species analysed.

	% size-class distribution of cross-shaped morphotypes				
	Category I (Small) (4.90 – 11.03µm)	Category II (Medium) (11.27 – 14.95µm)	Category III (Large) (15.19 - 18.87µm)	Category IV (Extra-large) (19.35 – 24.50µm)	Total
Cultivated species					
Zea mays L.	97	1	1	1	100
Sorghum bicolor (L.) Moench	100	0	0	0	100
Eleusine coracana (L.) Gaertn.	-	-	-	-	-
Non-cultivated (wild) species					
Sorghum arundinaceum (Desv.) Stapf	95	5	0	0	100
Panicum maximum Jacq.	-	-	-	-	-
Panicum latifolium L.	77	23	0	0	100
Pennisetum purpureum Schumach	82	19	0	0	100
Cymbopogon afronadus Stapf.	55	45	0	0	100
Hyparrhenia rufa (Nees) Stapf	88	12	0	0	100
Imperata cylindrica (L.) Beauv.	81	19	0	0	100
Setaria sphacelata (Schum.) Moss	-	-	-	-	-

only cross-shaped morphotypes in the large and extra-large size-classes, yielding overall categories that distinguish *Zea mays* from other cross-shaped morphotypes originating from cultivated and wild grasses in the study area.

8.3 Morphological characteristics used for distinguishing *Musa* from *Ensete* phytoliths

The following are the morphological characteristics used to distinguish between *Musa* and *Ensete* phytoliths in Munsa II sediments. The characteristic features are based on descriptions in Mbida *et al.* (2001), Denham *et al.* (2003), Vrydaghs & De Langhe (2003) and my own observations.

Both *Musa* and *Ensete* produce chains of cone-shaped phytoliths that easily fragment into individual bodies comprising a base and a raised cone with a crater at the summit (Plate 8.1, a & b). In *Musa* the cone has concave slopes in equatorial view and a saddle-shaped crater at the summit containing up to one indentation. Under SEM the surface of the cone appears verrucate with wart-like sculpturing, although it appears smooth under an optical microscope, while the rim of the crater appears smooth to crenate with round teeth. The form of the base in polar view also provides a means of distinguishing *Musa*. The base usually supports distinct protuberances along all sides and SEM reveals the base to have verrucate sculpturing. By comparison, *Ensete* phyoliths have a truncated cone with convex slopes in longitudinal view and is flat (not saddle-shaped) without crenations but with two to three indentations. The base is without protuberances. According to Mbida *et al.* (2001), no obvious differences in morphology were apparent

among phytoliths from eight different varieties of cultivated bananas and two different species of *Ensete* analysed.

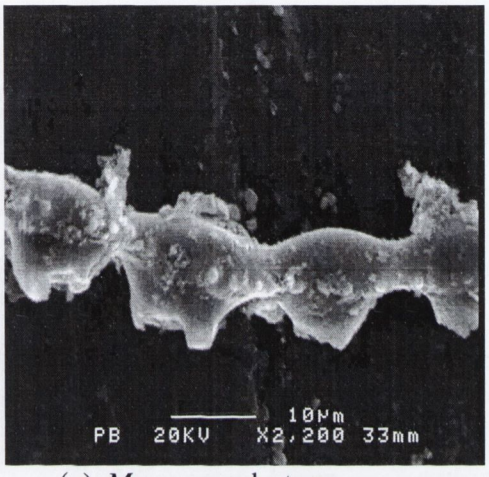

(a) *Musa* morphotype

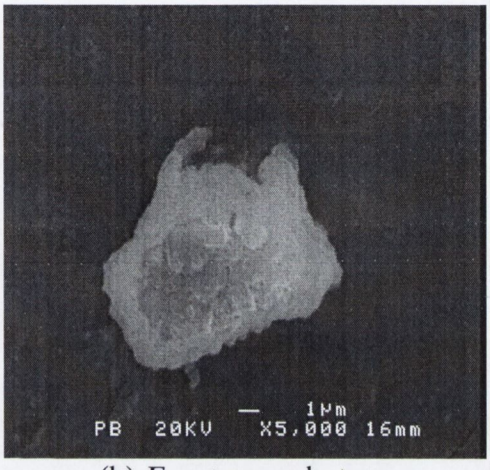

(b) *Ensete* morphotype

Plate 8.1 Characteristic features of Musaceae phytoliths used to distinguish *Musa* (1) from *Ensete* (2).

8.4 Fossil phytolith assemblages

To ease comparisons and interpretations of the down-core variations in phytolith assemblage diagrams for M2C1, M2C2 and M2C3C, the location of phytoliths zone boundaries has been adopted from the pollen zones described earlier in this thesis Ligneous dicotyledon (spherical-rugose and -crenate) morphotypes that include trees/shrubs and Palmae are produced by forest (arboreal) taxa. Non-arboreal (herbaceous) taxa, which are indicative of open vegetation habitats, are represented by

Poaceae (dumbbell, saddle and cross shape morphotypes), while Cyperaceae (cone/hat-shaped morphotypes) represent edaphically wet (including swamp) habitats.

As described in chapter five (see 5.10.8), the results of phytolith assemblages for M2C1, M2C2 and M2C3C were subjected to PCA analysis to examine the variability in vegetation composition between the phytolith assemblages. Interpretation of the vegetation composition is based on PCA scores, which are represented on a biplot diagram, comprising of two PCA axes (PCA 1 and PCA 2). The importance of each morphotype on the two PCA axes is represented by an arrow drawn from the joint ordination centre (0.0) of the two axes. The length and direction of the arrow shows the score or the rate of change in abundance of each morphotype in that direction. Thus a long arrow indicates high scores or gradual rate of change in abundance, while a short arrow represents low scores or very rapid change (Kent & Coker, 1992). PCA axis 1 appears to represent a vegetation gradient along which the negative scores correspond to forest vegetation (C_3 plants), while the positive scores correspond to grassland vegetation cover (C_4 plants). PCA axis 2 partly appears to separate Poaceae from Cyperaceae morphotypes, with the later possessing high positive scores.

8.4.1 Fossil phytolith stratigraphy for M2C1

The PCA biplot ordination results of phytolith morphotypes for M2C1 are presented in Figures 8.1 and 8.2. Figure 8.1 illustrates the scores of phytolith morphotypes corresponding to C_3 and C_4 plants. The PCA axes 1 and 2 account for 94% of the

variability in the phytolith assemblage data in which 51% is contributed by PCA axis 1 and 43% by PCA axis 2.

The spherical-rugose and -crenate morphotypes have negative scores on PCA 1 axis, and represent the presence of C_3 plants and a forest vegetation cover. Spherical rugose morphotype receive scores of -0.9561, while the Palmae (spherical-crenate) morphotype has a score of -0.7331. Grassland vegetation cover is represented by C_4 phytolith morphotypes which receive positive scores. Dumbbell bilobate morphotype (+0.8462), represent a predominantly C_3/C_4 tall Poaceae. The C_4 short Poaceae (saddle-shaped morphotype) is also well represented in the assemblages with a score of +0.7259. On the PCA 2 axis the C_4 non-Poaceae (Cyperaceae) morphotype has the highest positive component with a positive score of +0.4822 (Figure 8.1). Among the C3 plants the spherical crenate (Palmae) a morphotype has a score of +0 .2851.

The separation of phytolith assemblages on the PCA biplot suggest that forest vegetation (represented by C_3 plants) increases with increased negative scores on PCA axis 1 (Figure 8.1), and are abundant in zone C1Z1 (Figure 8.2). Dominance of Poaceae (C_4 plants) increases with increased positive scores on PCA axis 1 and their abundance in the assemblage are apparent zone C1Z2.

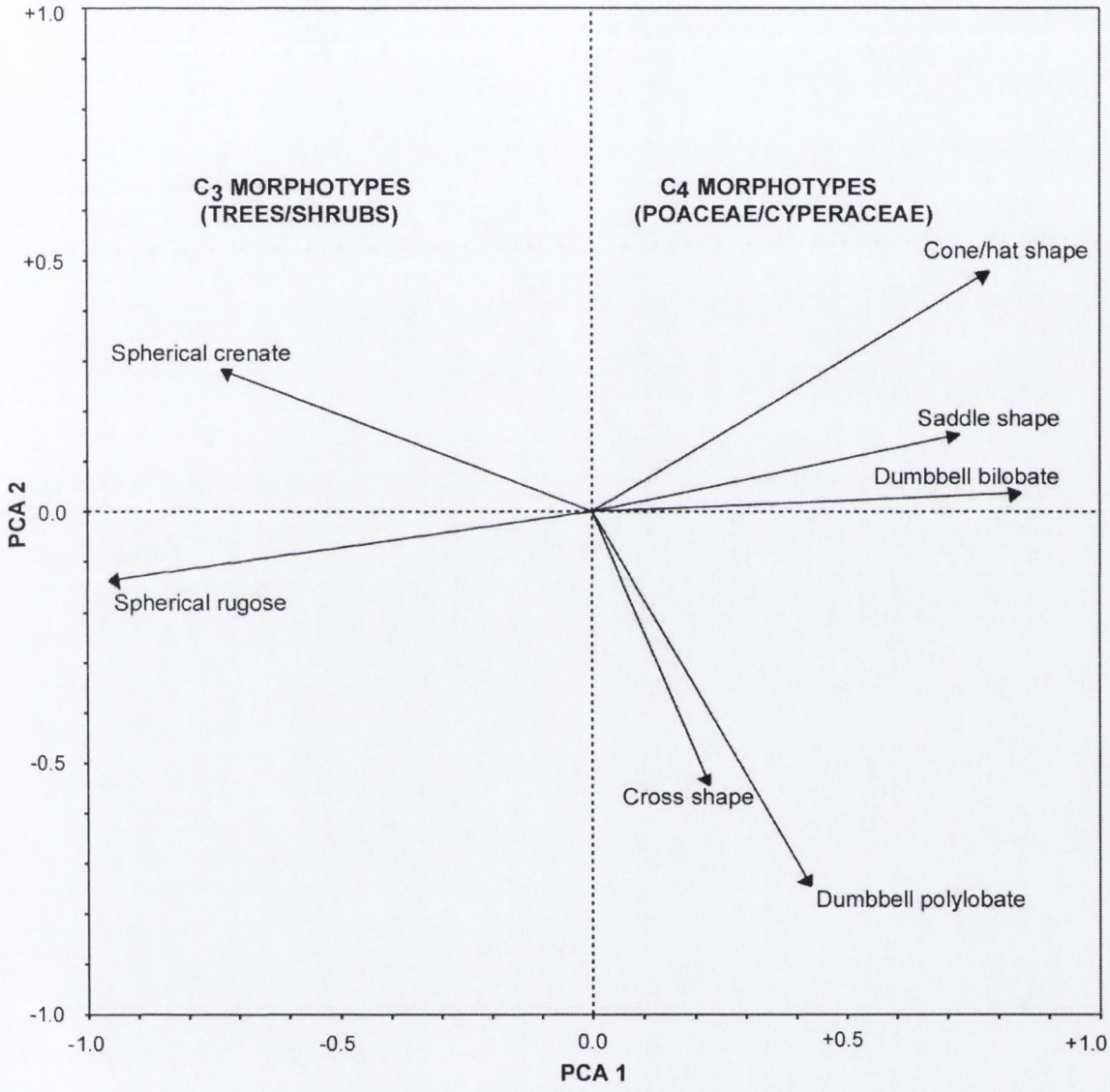

Figure 8.1 M2C1, Biplot distribution of principle component analysis (PCA) scores of fossil phytolith morphotypes showing the separation of C_3 plants from C_4 tall and short Poaceae.

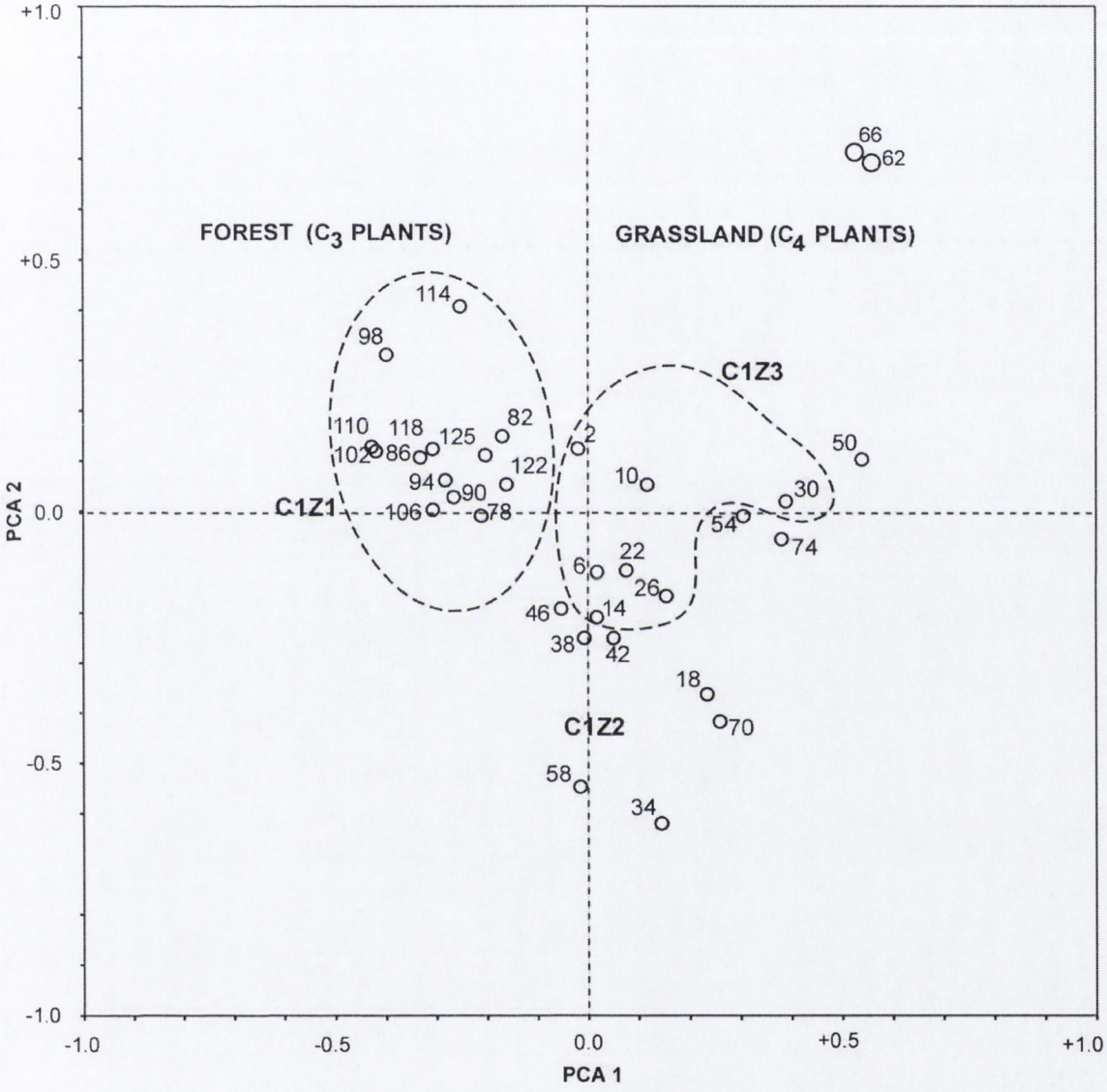

Figure 8.2 M2C1, Biplot distribution of principle component analysis (PCA) of fossil phytolith assemblages showing the relative distribution of forest (C_3 plants) and grassland (C_4 Poaceae) morphotypes in the three zones.

Zone C1Z1 (126 – 76 cm, ca. >2000 - 950 yr. BP). This zone is characterised by high percentages of spherical rugose (ligneous dicotyledon) morphotypes, which contribute about 74% to 96% to the phytolith sum (Figure 8.3). The Palmae (spherical crenate) morphotype represents less than 5% of the phytolith sum. Similarly, the percentage proportion of cone/hat-shaped (Cyperaceae) morphotype is relatively low (<5%) in this zone. The percentages of dumbbell bilobate and polylobate morphotypes (C_3/C_4 tall Poaceae) are relatively low, and are mainly dominated by the former. The cross-shaped morphotype is rare in this zone. Abundance of the saddle-shaped morphotype (C_4 short Poaceae) are also low (<5%). Musaceae phytoliths (*Musa* and *Ensete*) were recorded in this zone.

The percentages of burnt phytoliths are very low at the base of zone C1Z1, rising towards the upper part of the zone, reaching a value of 10% at 90 cm, ca. 1255 yr. BP (cal 678- 881 AD). Burnt phytoliths from non-Poaceae (trees/shrubs) sources are absent from zone C1Z1.

Zone C1Z1 represents a period dominated by forest vegetation in the catchment of Munsa II as supported by generally high *D/P* values (Figure 8.4), which range between 4 and 43. The phytoliths from the trees/shrubs which dominate this zone may have been derived from local catchment areas at Munsa as they are often derived from plants within the local area. However, it is also possible that phytoliths from upland areas could have been deposited at the site through erosion as based on the stratigraphic zones A-C, which are fluvialy deposited (see chapter six). Among the Poaceae, the I_{ph} values

indicate an association in which Panicoideae (C_3/C_4 tall Poaceae) dominates the grass vegetation cover as suggested by generally low values (< 30%).

Zone C1Z2 (76 – 32 cm, ca. 945 – 190 yr. BP). This zone is marked by a sharp decline in spherical rugose morphotypes to about 21% at 62 cm, ca. 825 yr. BP (cal 1066-1282 AD), presumably due to a reduced forest cover in the catchment area. The Palmae morphotype becomes rare in this zone, while the abundances of the Cyperaceae morphotype increase to a maximum of 21% at 62 cm (ca. 825 yr. BP, cal 1066-1282 AD), indicating the establishment of sedge-dominated swamp and thus providing support for the pollen and stratigraphy based interpretation outlined in chapter seven. The proportion of Cyperaceae, however, declines towards the upper boundary of the zone. Zone C1Z2 is also marked by an increase in C_3/C_4 tall and C_4 short Poaceae morphotypes, suggesting a shift to grassland dominated vegetation cover. The dumbbell bilobate morphotype increases to higher levels of 50% between 62 cm and 50 cm. The proportion of dumbbell polylobate morphotype increases from the lower boundary of the zone to a maximum of 22% at 58 cm (ca. 470 yr. BP, cal 1330-1488 AD), before dropping to 12% at 54 cm (ca 445 yr. BP, cal 1408-1616 AD). The proportion of cross shape morphotype is low, ranging from 3% to 6%. The C_4 short Poaceae morphotype increases to 20% at 66 cm (ca. 850 yr. BP, cal 1042-1276 AD). Abundances of short Poaceae morphotype, however, decline towards the upper boundary of the zone.

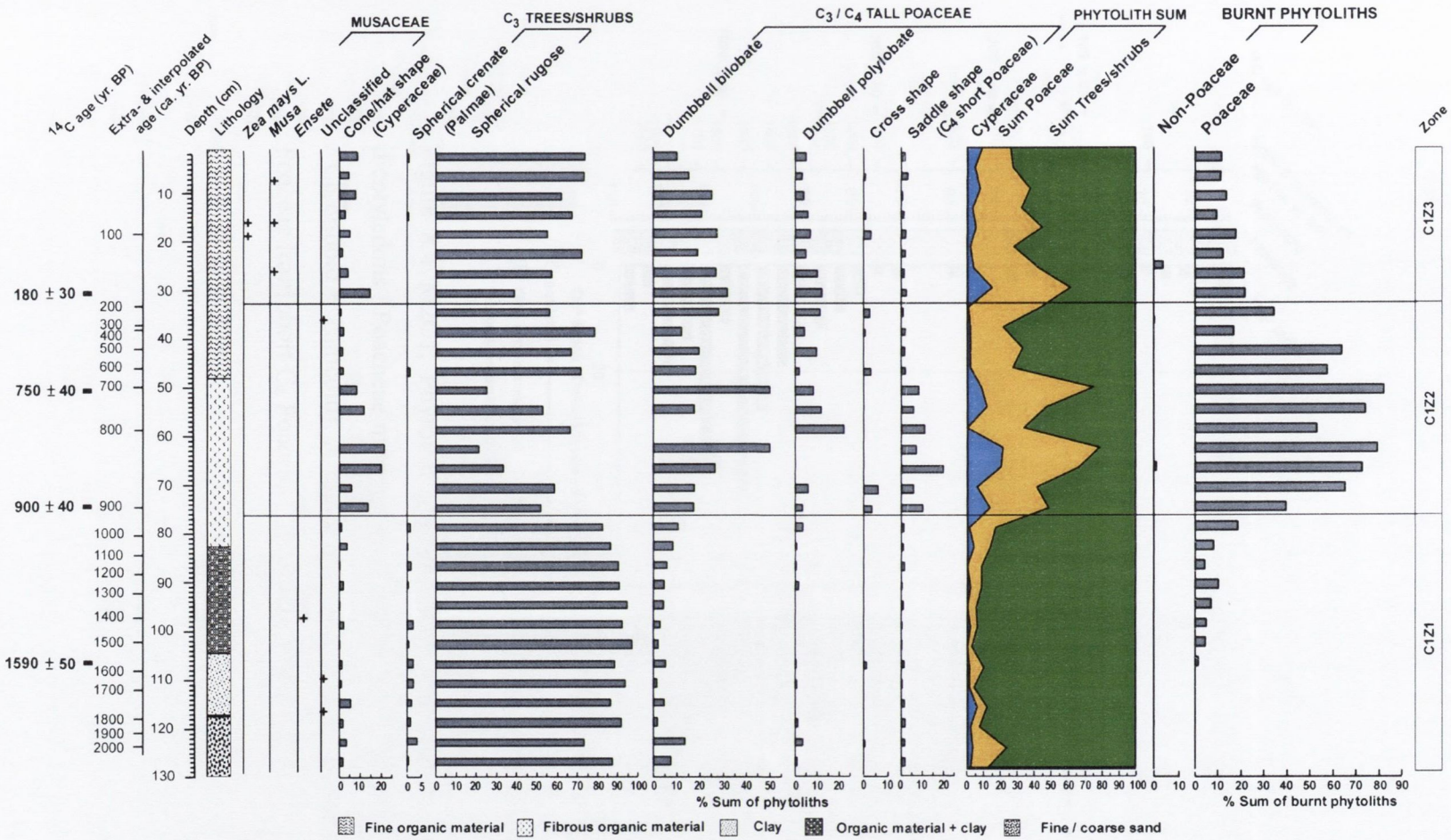

Figure 8.3 M2C1, down-core variations in abundances of subfossil phytoliths. 32 samples were analysed for their phytolith contents and counts ranged from 503 to 582 (mean = 544).

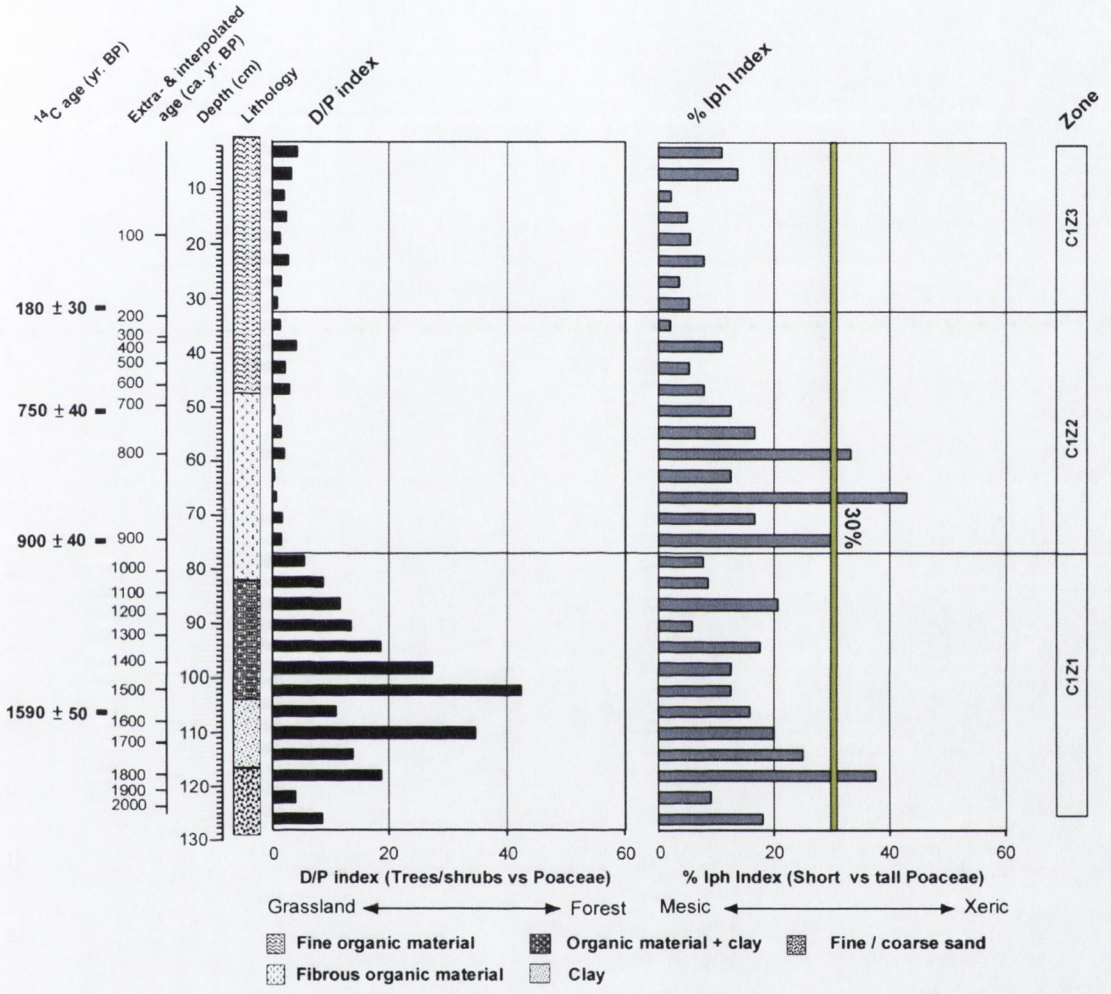

Figure 8.4 M2C1, Phytolith indices, D/P = tree cover density (ligneous dicotyledons / Poacaeae morphotypes) and % Iph = aridity index (Chloridoid / Chloridoid + Panicoid). A minimum value of 30% distinguishes tall C_3/C_4 Poaceae from short C_4 Poaceae (Alexandre *et al.*, 1997).

Zone C1Z2 is marked by increased abundance of burnt phytolith for Poaceae morphotypes, reaching a maximum of 82% at 49 cm, ca. 700 yr. BP (cal 1244-1393 AD), while those from non-Poaceae sources are rare.

Local zone C1Z2 generally indicates a period of reduced forest vegetation cover at the expense of Pocaeae in the catchment of Munsa II, with marked increases in burnt phytoliths, suggesting increased burning. The latter is also apparent in the charcoal records discussed in chapter nine. Evidence for reduction in forest vegetation cover in the catchment area of Munsa is supported by significant decline (< 4) in *DP* values. A sedge swamp became established as suggested by increased abundance of Cyperaceae morphotypes. In this zone, the I_{ph} values increase in zone C1Z2 to a maximum of 43% at 66 cm, ca 850 yr. BP (cal 1042-1276 AD), indicating C_4 short grasses as the more common occurrence in surrounding vegetation. The I_{ph} values decline, however, to less than 10% towards the upper boundary of the zone C1Z2, suggesting a shift from C_4 short Poaceae (Chloridoideae) to a C_3/C_4 tall Poaceae dominated habitat.

Zone C1Z3 (32 – 0 cm, ca. 190 yr. BP to present). This zone is characterised by an increase in the abundance of the spherical rugose morphotype towards to the top of the core, reaching a maximum of 74%. The Palmae morphotype remains rare in this zone. A general decline in tall C_3/C_4 Poaceae morphotypes occurs towards the top part of the core, while the abundance of the short C_4 Poaceae morphotype remain relatively constant (3%). The Cyperaceae morphotype increases to higher levels (>5%) relative to the upper boundary of zone C1Z2. Musaceae phytoliths, possibly from *Musa*, were recorded in this zone. Phytoliths from *Z. mays* were also recorded (at 14 cm and 18 cm).

Burnt phytoliths from Poaceae morphotype, decline towards the top of the core, while those from non-Poaceae morphotypes are rare in zone C1Z3.

Zone C1Z3 indicates recovery of forest vegetation in the catchment of Munsa II swamp as suggested by high proportions of ligneous dicotyledonous (tree/shrub). This is supported by low abundance of burnt phytoliths, suggesting reduced human activities in the catchment of Munsa. Charcoal data also indicate reduced burning around Munsa (see chapter nine). The *D/P* values (Figure 8.10), however, indicate some slight increase in forests vegetation in Munsa II catchment. The values of I_{ph} decline to relatively low levels (< 20%), suggesting increasing dominance of C_3/C_4 tall grasses in Munsa II catchment. Presences of maize and Musaceae phytoliths in this zone suggest that there was some cultivation in the catchment of Munsa II.

8.4.2 Fossil phytolith stratigraphy for M2C2

Figures 8.5 and 8.6 present the PCA ordination results for samples from M2C2. The two axes account for 66% of the variability in the data in which 54% is contributed by PCA axis 1 and 12% by PCA axis 2. C_3 plants, represented by spherical rugose (-0.9822) and spherical crenate (-0.6873) morphotypes, have the most negative scores on PCA axis 1. Dumbbell bilobate (+0.9221) (tall C_4 Poaceae) and saddle-shaped (+0.6811) (short C_4 Poaceae), have positive scores on the PCA axis 1. On the PCA axis 2, the Cyperaceae (cone/hat shape morphotype) contributes the highest positive scores of +0.6846.

The phytolith assemblages (Figure 8.6) indicate that forest vegetation (C_3 plants) is abundant in zone C2Z1, while zone C2Z2 is dominated by grass vegetation (C_3 plants), correlating with the phytolith assemblage diagram presented in Figure 8.7.

Down-core variation in phytolith morphotypes in M2C2 are presented in Figure 8.7 and are described below.

Zone C2Z1 (176 – 122 cm, ca. >1200 - 840 yr. BP). This zone is characterised by abundant spherical rugose morphotypes, (75% to 98%), while the Palmae morphotype contributes less than 5% of the phytolith sum. The Cyperaceae morphotype has a relatively low abundance (< 10%). Percentages of the C_3/C_4 Poaceae morphotypes are generally low, and mainly comprise the dumbbell bilobate morphotype, with values ranging from 1% to 25%. The dumbbell polylobate morphotype accounts for less than 5% of the total count, while cross-shaped morphotypes are rare. The abundance of C_4 short Poaceae morphotypes is also low, (< 2%). Phytoliths believed to be from the Musaceae family are present in this zone and are mainly of *Ensete* type. Zone C2Z1 is characterised by low burnt phytolith values of < 2% and < 10% for non-Poacaeae and Poacaeae types, respectively.

Zone C2Z1 indicates a predominantly forested vegetation cover in the catchment of Munsa II. *D/P* values (Figure 8.8) are high, thus supporting dominance of forested vegetation in Munsa II catchment. Pollen data (chapter seven) also indicates forest dominance in the catchment of Munsa. In this zone the I_{ph} values are generally below

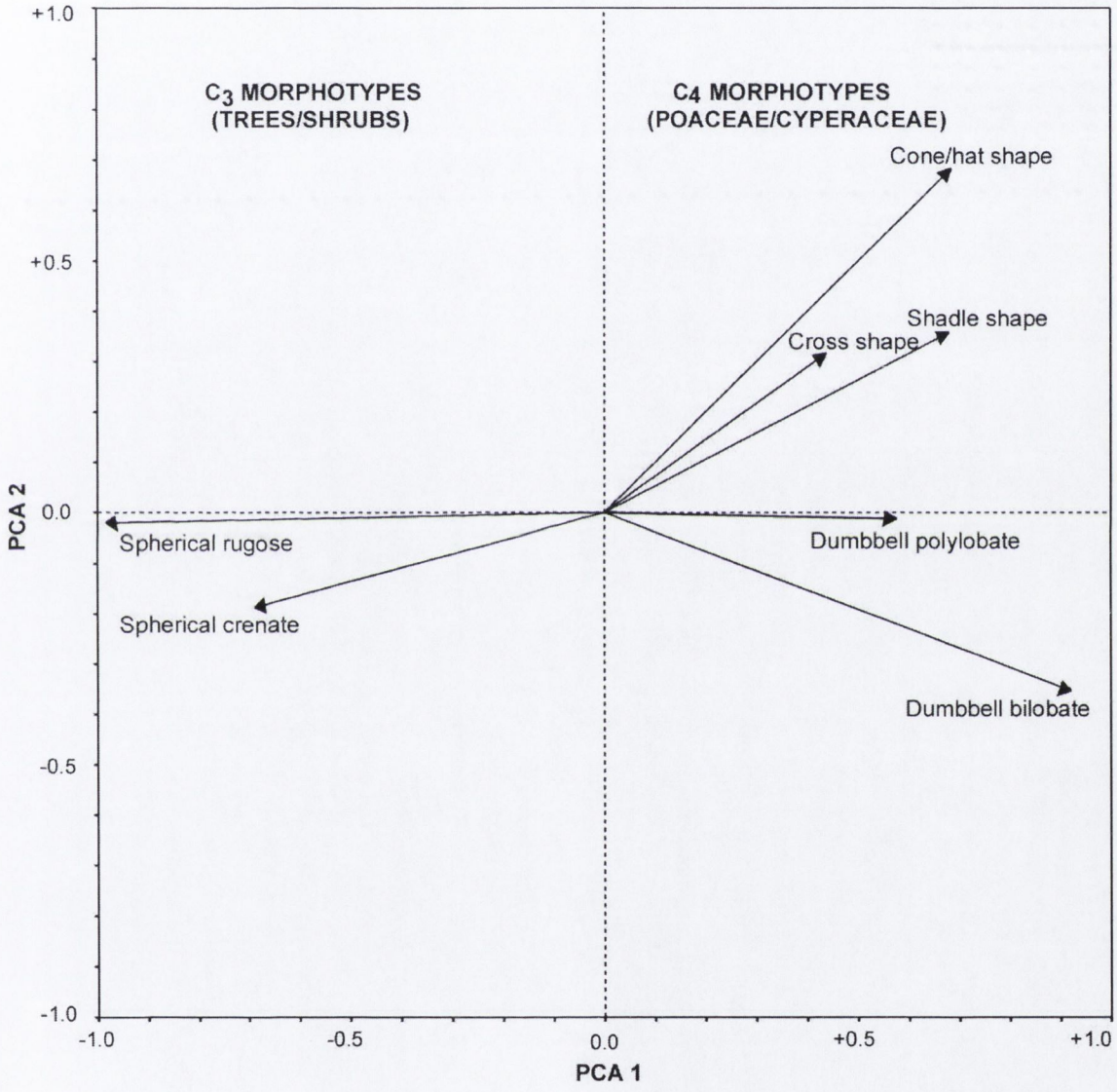

Figure 8.5 M2C2, Biplot distribution of principle component analysis (PCA) loadings of fossil phytolith morphotypes showing the separation of C_3 plants from C_4 tall and short Poaceae.

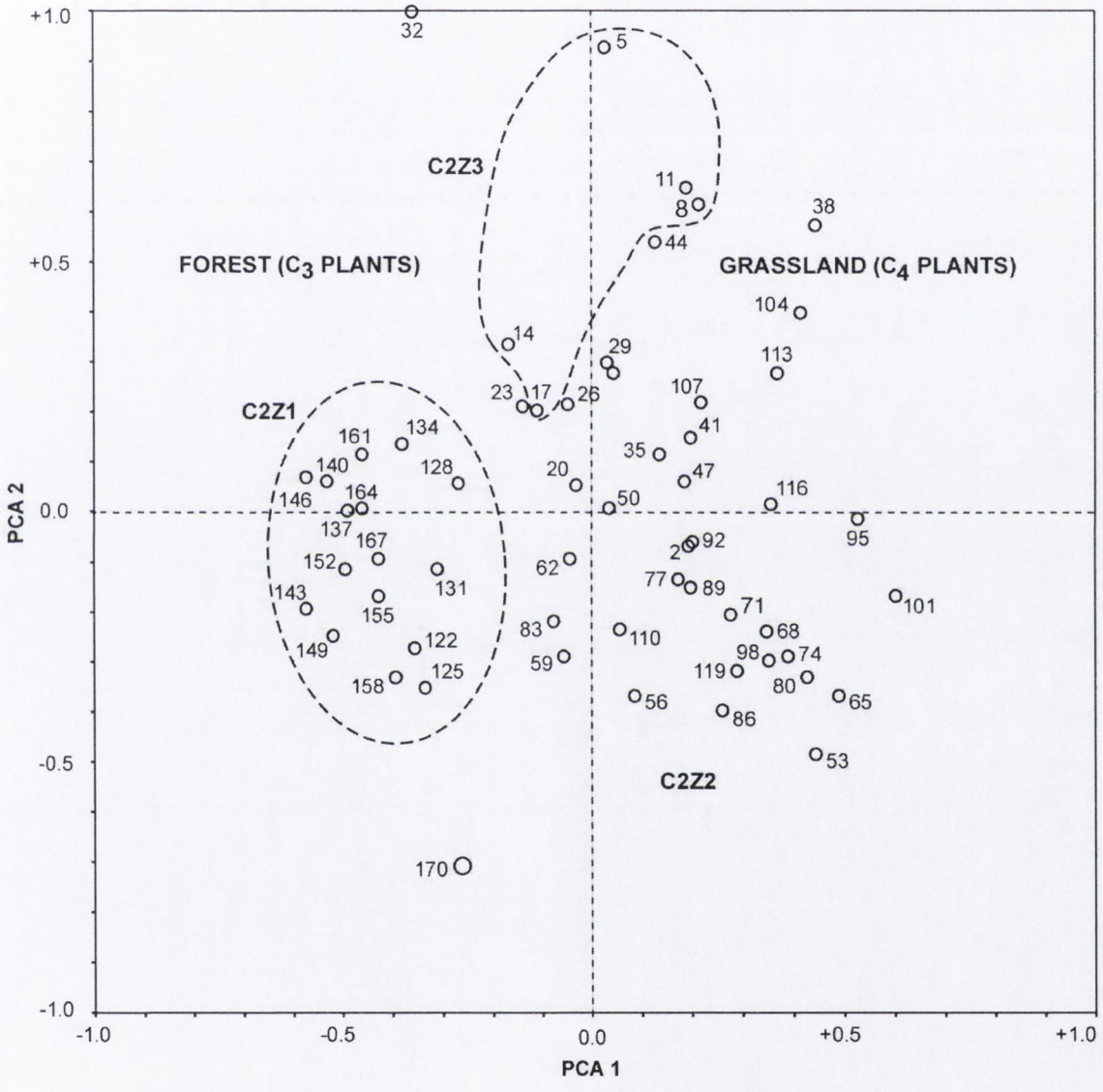

Figure 8.6 M2C2, Biplot distribution of principle component analysis (PCA) of fossil phytolith assemblages showing the relative distribution of forest (C_3 plants) and grassland (C_4 Poaceae) morphotypes in the three zones.

30% suggesting that Panicoideae (C_3/C_4 tall Poaceae) dominates the grass vegetation cover.

Zone C2Z2 (122 – 20 cm, ca. 840 - 190 yr. BP). This zone is marked by a decline in spherical-rugose and crenate morphotypes, with the latter becoming rare. Percentages of the Cyperaceae morphotype increase, reaching 25% at 104 cm, ca. 695 yr. BP (cal 1258-1394 AD), and then decline. This zone is characterised by the dumbbell bilobate morphotype, which accounts for up to 66% of the phytolith morphotypes. The polylobate morphotype contributes up to 20% of the count, while the cross-shaped morphotype represents less than 10%. The short C_4 Poaceae (saddle-shaped morphotype) is relatively constant in zone C2Z2 (< 10%). Musaceae (*Musa* and *Ensete*) phytoliths are absent at the lower apart of this zone, but appear towards the upper boundary. A sharp increase in the burnt phytolith values for Poaceae phytoliths occur in this zone, reaching a peak of 82% at 98 cm, ca. 665 yr. BP (cal 1279-1397 AD). Burnt phytoliths from non-Poaceae phytoliths are relatively low (< 10%) in this zone.

Generally zone C2Z2 represents a period of reduced forest vegetation in the catchment of Munsa II and establishment of sedge vegetation in Munsa II swamp. Relatively low *D/P* values in this zone (Figure 8.8), corresponding to reduced forests vegetation cove in Munsa II catchment. Increased burning in the catchment of Munsa is apparent as suggested by high burnt phytolith values. I_{ph} values are less than 20%, suggesting increased dominance of Panicoideae (C_3/C_4 tall Poaceae) among grass vegetation cover.

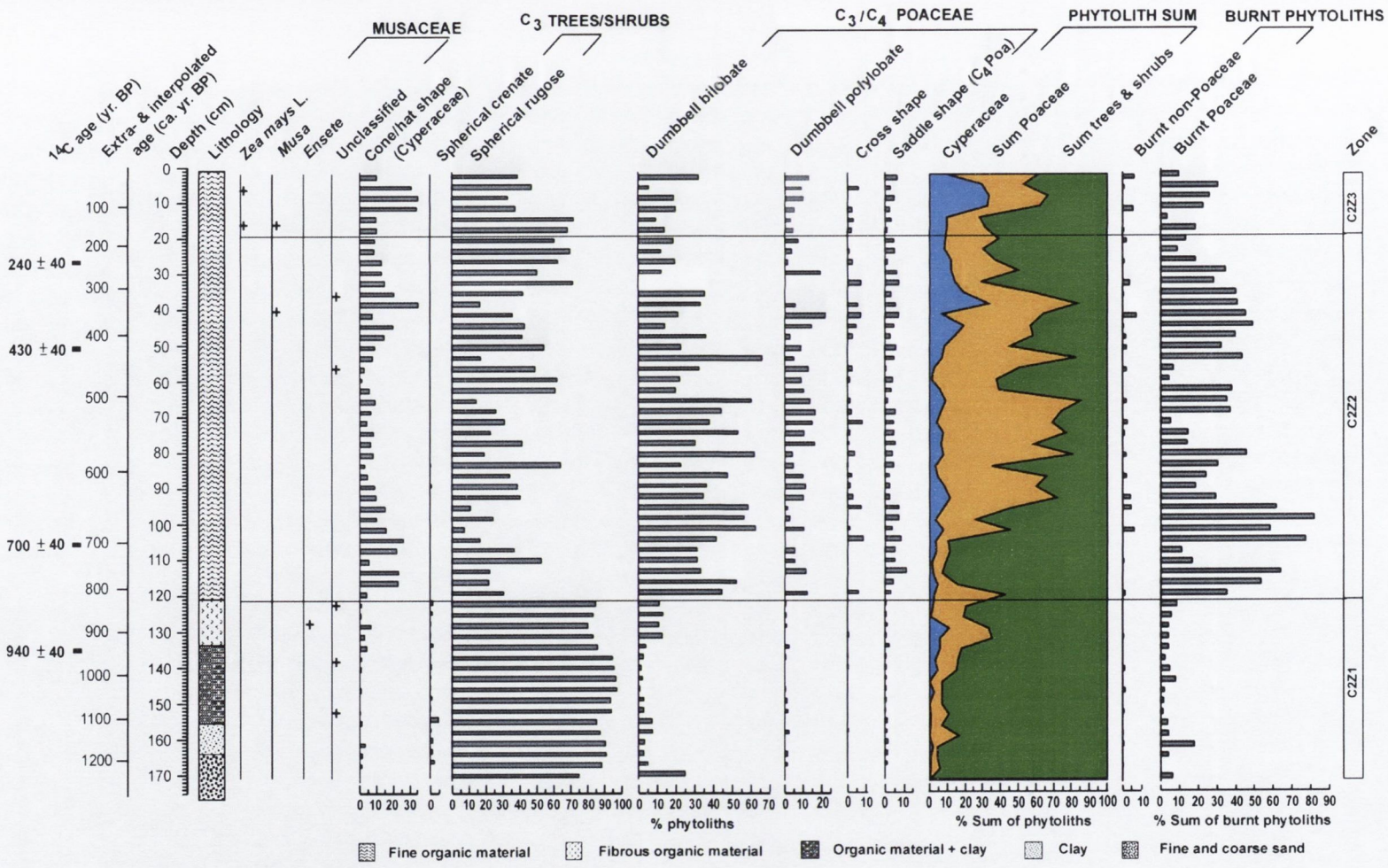

Figure 8.7 M2C2, down-core variations in abundances of subfossil phytoliths. 57 samples were analysed for their phytolith contents and counts ranged from 506 to 759 (mean = 577).

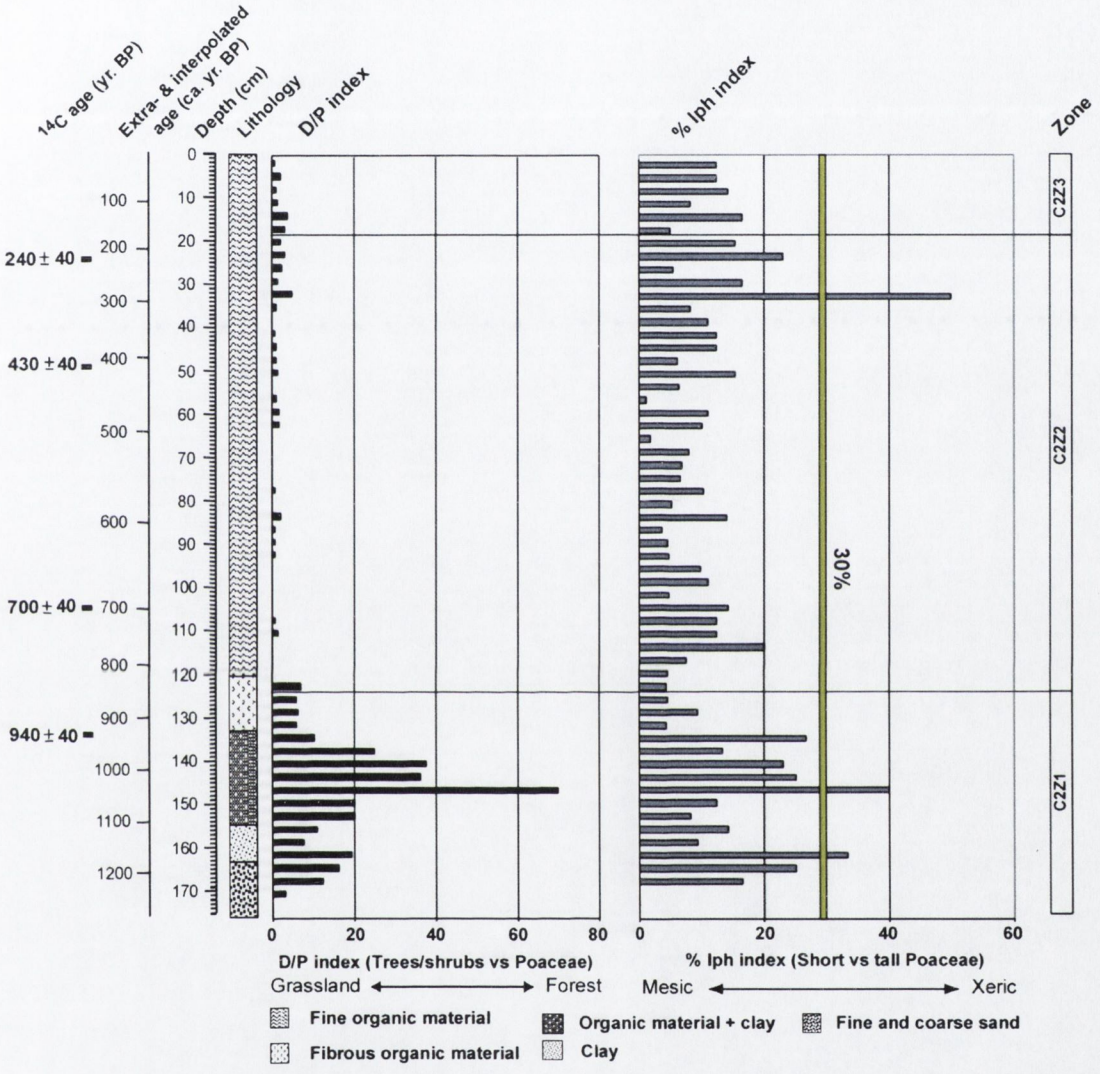

Figure 8.8 M2C2, Phytolith indices, D/P = tree cover density (ligneous dicotyledons/Poacaeae morphotypes) and % Iph = aridity index (Chloridoid / Chloridoid + Panicoid). A minimum value of 30% distinguishes tall C_3/C_4 Poaceae from short C_4 Poaceae (Alexandre *et al.*, 1997).

Zone C2Z3 (20 – 0 cm, ca. 190 yr. BP to present). This zone is characterised by a decline in the proportion of spherical-rugose morphotypes. Spherical-crenate morphotypes disappear from the record in this zone, while the Cyperaceae morphotype reaches a maximum abundance of 33%. Poaceae morphotypes increase gradually towards the upper part of the zone and are mainly dominated by dumbbell bilobate. Cross-shaped phytoliths, possibly from *Zea mays*, appear in the record, while Musaceae phytoliths, possibly *Musa*, are present. The burnt phytolith values for non-Poaceae phytoliths are relatively constant (< 10%), while the abundance of BP from Poaceae sources increase to peak of 31% in the upper most part of the zone.

Forest recovery is not well represented in zone C2Z3 as suggested by low *D/P* values. Among the Poaceae, the I_{ph} values remain below 30% indicating an association in which Panicoideae (C_3/C_4 tall Poaceae) dominates the grass vegetation cover. A sedge-dominated swamp is apparent in this zone as suggested by increased abundance of Cyperaceae morphotypes. Pollen data (see chapter seven) also support dominance of a sedge-dominated at Munsa II.

8.4.3 Phytolith stratigraphy for M2C3C

The PCA ordination results for M2C3C are presented in Figures 8.9 and 8.10. The two axes account for 79% of the variability in the data (PCA axis 1 = 58%, PCA axis 2 = 21%). Spherical rugose morphotypes (C_3 plants) have negative scores on PCA axis 1, while morphotypes produced by C_4 plants were allocated positive scores. The cone/hat-shaped morphotype received a positive score on PCA axis 2, while Palmae has a

negative score. Phytolith assemblages illustrated in Figure 8.10 represent abundance of forest vegetation (C_3 plants) in zone C3Z1, while abundance of grass vegetation (C_4 plants) is apparent in zone C3Z2.

Down-core variations in phytolith assemblages for M2C3C are presented in Figure 8.11. Phytolith zones are described below.

Zone C3Z1 (185 – 94 cm, ca. 5000 - 800 yr. BP). This zone is characterized by abundant spherical rugose morphotypes (60-97%). Abundances of Palmae are low (<5%) at the lower boundary of this zone, between 180cm and 142 cm, but rise to higher levels (5-11%) towards the upper boundary. The Cyperaceae morphotype also has low abundances (<5%) in the zone. Among the C_3/C_4 tall Poaceae morphotypes, the dumbbell bilobate ranges in abundance from 1% to 27%, whereas the dumbbell polylobate and the cross-shaped morphotypes are rare. The abundance of C_4 short Poaceae morphotypes is also relatively low (< 4%) in this zone. Phytoliths from Musaceae, possibly both *Musa* and *Ensete* are present at the lower boundary of this zone. Zone C3Z1 is characterised by very low burnt phytolith values (< 2%) of Poaceae and non-Poaceae morphotypes.

Phytolith assemblages in zone C3Z1 suggest dominance of forest vegetation in the catchment of Munsa II. The *D/P* values are relatively high (Figure 8.12), support dominance of forest vegetation in Munsa II catchment. Among the Poaceae, Panicoideae (C_3/C_4 tall grass) dominates the grass vegetation cover as suggested by generally low I_{ph}

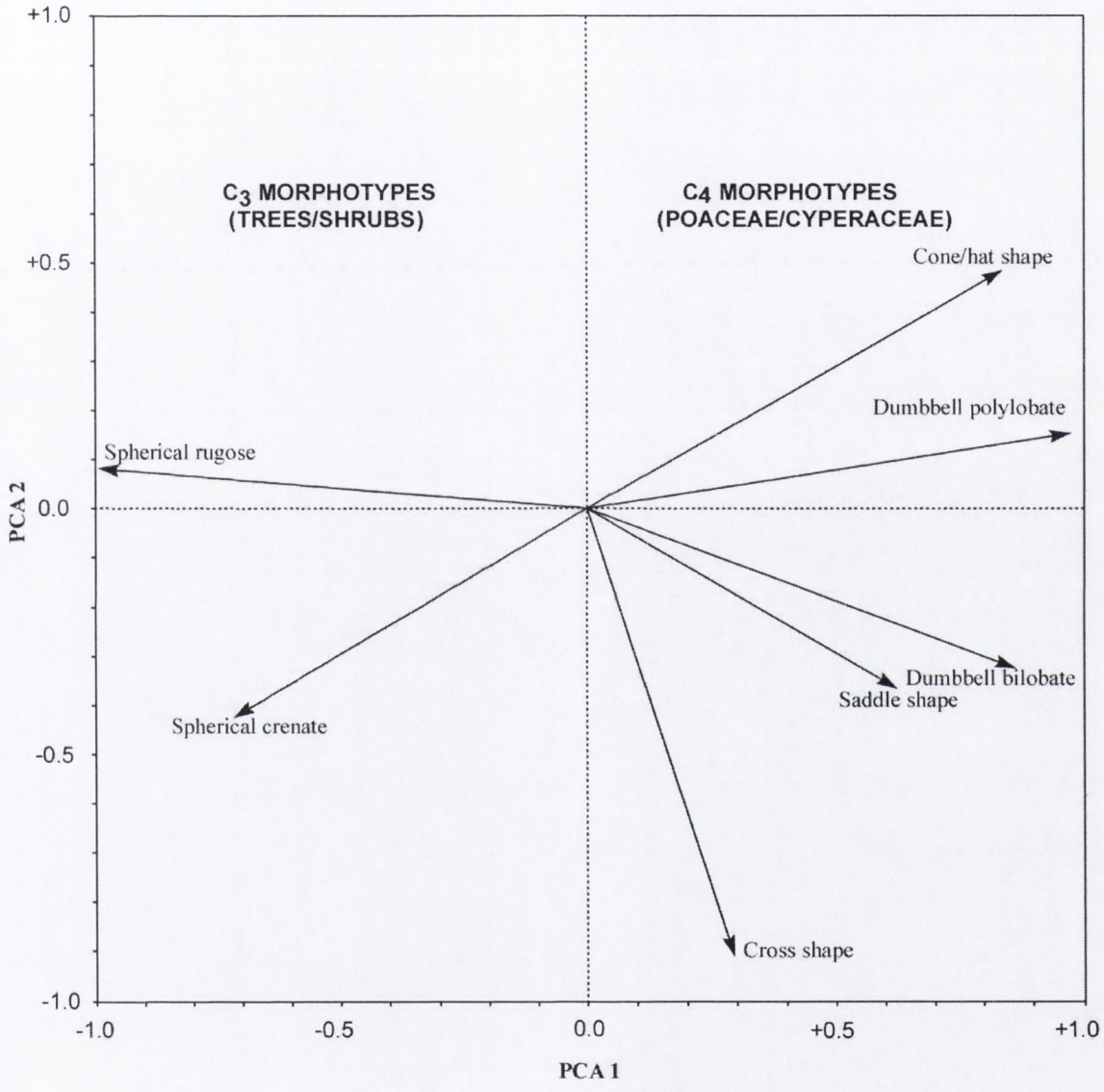

Figure 8.9 M2C3C, Biplot distribution of principle component analysis (PCA) loadings of fossil phytolith morphotypes showing the separation of C_3 plants from C_4 tall and short Poaceae.

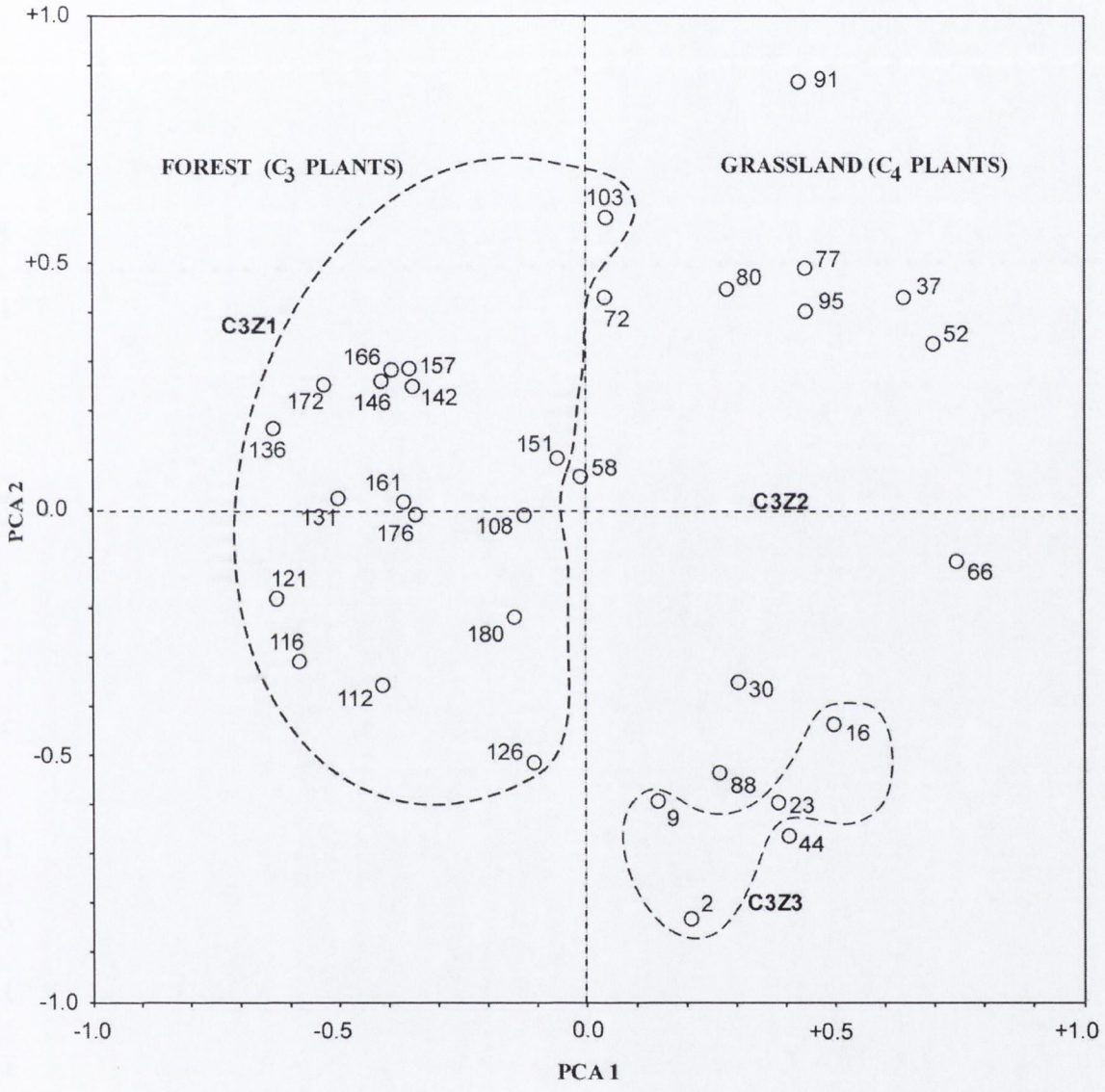

Figure 8.10 M2C3C, Biplot distribution of principle component analysis (PCA) scores for fossil phytolith assemblages, showing the distribution of forest (C_3 plants) and grassland (C_4 Poaceae) in the three zones.

values (< 30%). Presence of Musaceae phytoliths (*Musa* and *Ensete*) suggests some cultivation in the catchment of Munsa II.

Zone C3Z2 (94– 28 cm, ca. 800 – 480 yr. BP). This zone contains lower levels of spherical rugose morphotypes than zone C3Z1. Palmae morphotypes are also rare, while Cyperaceae morphotypes are higher. This zone is also marked by an increase in the proportions of the dumbbell bilobate and polylobate morphotypes, attaining high peaks of 50% at 70 cm and 34% at 60 cm, respectively, relative to zone C3Z1. However, the cross-shaped morphotype is rare in zone C3Z2, while abundances of the C_4 short Poaceae (saddle shaped morphotype) is less than 10%. The burnt phytolith values increase in zone C3Z2, with non-Poaceae phytoliths attaining a peak value of 15% at 50cm. Abundances of burnt phytoliths from Poaceae reach a maximum of 66% at 67 cm, ca. 650 yr. BP (cal 1284-1398 AD).

Local zone C3Z2 indicates a decline in forest vegetation in the catchment of Munsa II, with marked increases in Poaceae vegetation as suggested by relatively low *D/P* values (Figure 8.12) and pollen data (see chapter seven). Increased abundance in burnt phytoliths, suggest increased burning in Munsa catchment. The later is also supported by high abundance of charcoal records (see chapter nine). Establishment of sedge-dominated swamp is apparent in Munsa II as suggested by abundance of Cyperaceae morphotyes (Figure 8.11) and pollen data (see chapter seven).

Zone C3Z3 (28 – 0 cm, ca. 480 to present) is characterised by a rise in the level of spherical crenate morphotype to more than 30%, while the Palmae morphotype remains

rare. The Cyperaceae morphotype drops to less than 5% in this zone. The C_3/C_4 tall Poaceae counts are dominated by dumbbell bilobate morphotypes with values ranging from 39% to 57%, while the dumbbell polylobate morphotype accounts for less than 10%. Abundances of cross-shaped and C_4 short Poaceae morphotypes are relatively low in this zone, representing less than 5%. *Zea mays* phytoliths are present in this zone, while phytoliths from Musaceae are absent. Burnt phytolith values from non-Poaceae phytoliths range from 4% to 9%, while those values for Poaceae phytoliths remain relatively high (> 30%) in this zone.

In zone C3Z1, forest recover is not apparent in Munsa II catchment as suggested by very low *D/P* values (Figure 8.12). Unlike pollen data (chapter seven), which suggest a sedge-dominated in Munsa II catchment, phytolith data indicates reduced sedge vegetation in Munsa swamp. Cultivation is evident at Munsa catchment area as suggested by maize and Musa phytoliths.

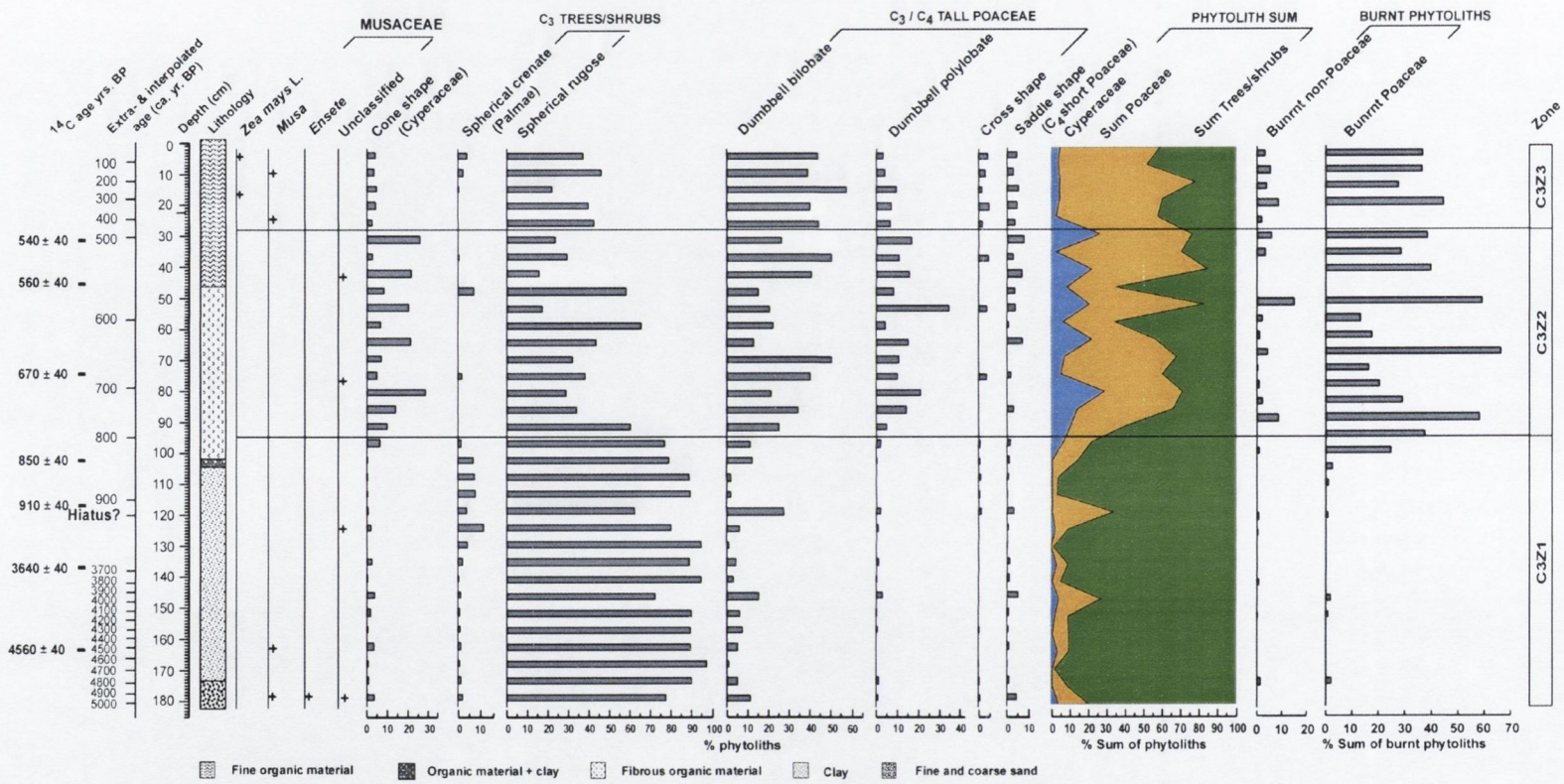

Figure 8.11 M2C3C, down-core variations in abundances of subfossil phytoliths. 32 samples were analysed for their phytolith content and counts ranged from 540 to 1180 (mean = 573).

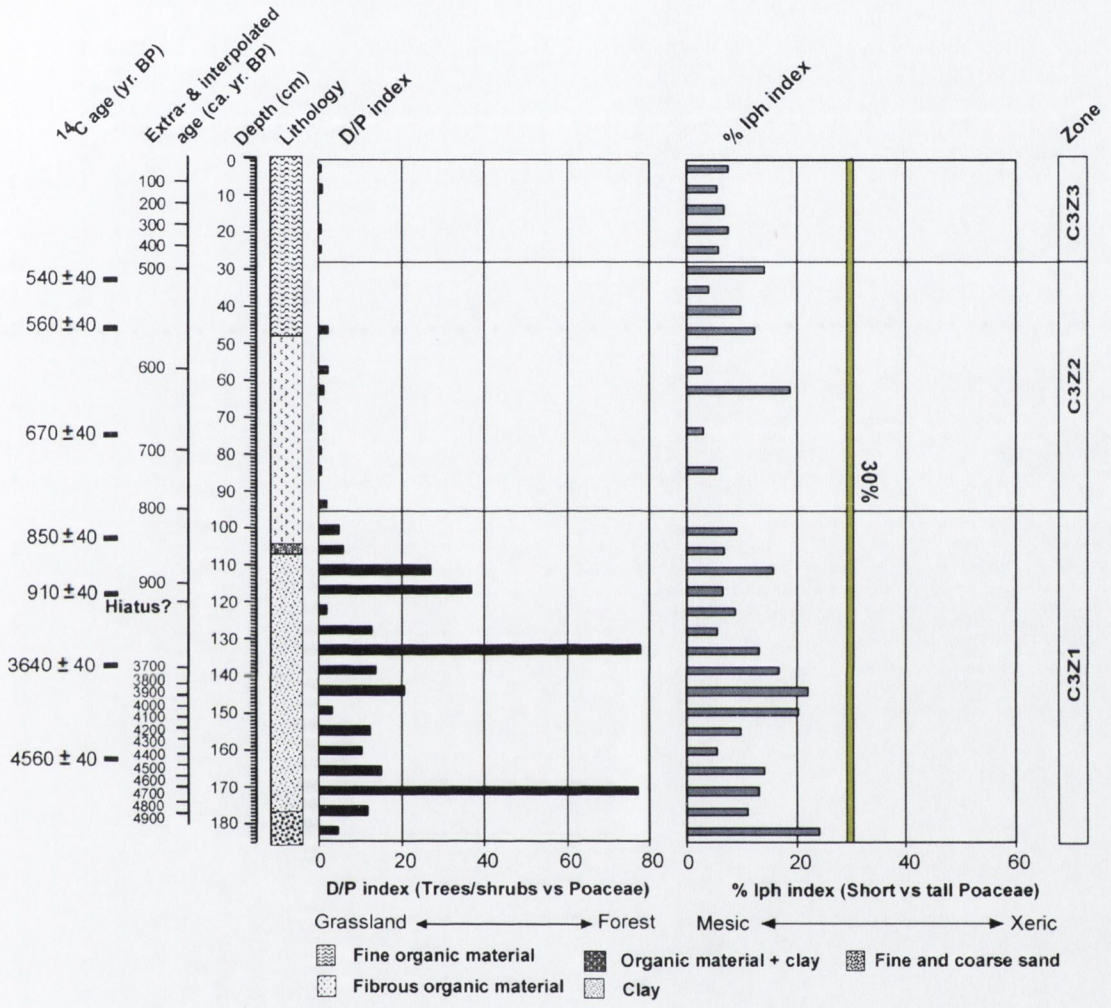

Figure 8.12 M2C3C, Phytolith indices, D/P = tree cover density (ligneous dicotyledons / Poacaeae morphotypes) and % Iph = aridity index (Chloridoid / Chloridoid + Panicoid). A minimum value of 30% distinguishes tall C_3/C_4 Poaceae from short C_4 Poaceae (Alexandre *et al.*, 1997).

8.5 Inter-core comparison of phytolith data from Munsa II sediments

Generally phytolith assemblages indicate similar down-core variations in the local zones, with high *D/P* values suggesting dominance of forested vegetation cover in the catchment of Munsa II pre dating ca. 900 yr. BP. This period corresponds to stratigraphic zones A-C (dominated by inorganic materials) and part of zone D (organic rich matter) in M2C1 and M2C3. The three cores indicate a less developed sedge swamp at Munsa II during this period, though it is moderately well represented in the pollen records (see chapter seven), suggesting the fragility of Cyperaceae phytoliths to physical and chemical process. Abundances of burnt phytoliths are relatively low in the three cores, suggesting that forest fires were rare at Munsa. This period of low incidences of fires is also supported by relatively low abundances of charcoal (see chapter nine).

Decline in forest vegetation (as supported by low *D/P* values) appears to have commenced earlier in M2C1 (ca. 900 yr. BP), and later in M2C2 (820 yr. BP) and M2C3C (ca. 800 yr. BP) probably indicating the sensitivity of M2C1 to its marginal location. This sensitivity is also apparent in the pollen records. Increased forest fires around Munsa are apparent in three cores post ca. 900 yr. BP as reflected by abundances of burnt phytoliths. The three cores indicate an establishment of a sedge-dominated swamp at Munsa II as suggested by abundances of Cyperaceae morphotype, and supported by pollen records in M2C3C, though not well represented in M2C1and M2C2 (see chapter seven).

Forest recovery at Munsa catchment is evident in M2C1 and M2C3C, though not well represented, while M2C2 indicates forest decline at Munsa ca.150 yr. BP as supported by low *D/P*. Decline in forest fires at Munsa is apparent in M2C1 compared to M2C2 and M2C3C.

CHAPTER NINE

RESULTS OF CHARCOAL ANALYSIS

9.1 Introduction

This chapter presents the results of microfossil charcoal analysis for Munsa II sediment cores. It describes down-core variations in charcoal concentrations for M2C1, M2C2 and M2C3 and, where possible provides an interpretation of the results.

9.2 Results of charcoal analysis for Munsa II sediment cores

To ease interpretation of the charcoal results, the zonation of the charcoal diagrams are based on the pollen zones described in chapter five (also see chapter eight)

9.2.1 Charcoal results for M2C1

Figure 9.1 presents results of charcoal analysis for M2C1 derived from the gravimetric (chemical assay) and point-count methods.

9.2.1i Results of chemical assay method

The results show a relatively low abundance of charcoal (< 5%) at the base of the core (C1Z1), between 126 cm and 105 cm. The charcoal content rises to higher levels (9%) and remains relatively constant between 102 cm, ca. 1500 yr. BP (cal 438-642 AD) and 76 cm, ca. 945 yr. BP (cal 1018-1206 AD). The content increases to higher levels (15-

19%) at the upper part of zone C1Z2, between 48 cm and 33 cm, before dropping to lower levels (<15%) in zone C1Z3.

9.2.1ii Results of point count method

(a) Charcoal area

The record of charcoal area is derived from the point count method. The results show a similar trend to that of percentage dry weight charcoal with relatively low values (< 5 $cm^2 g^{-1}$) at the base (zone C1Z1) of M2C1 between 126 cm, ca 2000 yr. BP (cal 104-118 AD) to 120 cm, ca. 1500 yr. BP (cal 438-642 AD). The area of charcoal increases to 9 $cm^2 g^{-1}$ at 83 cm, ca. 1150 yr. BP (cal 782-978 AD) before dropping to 4 $cm^2 g^{-1}$ at the upper boundary of zone C1Z2. The abundance of charcoal remains relatively low (< 10 $cm^2 g^{-1}$) at the lower boundary of zone C1Z2, between 76 cm and 65 cm, rising to higher levels (13-27 $cm^2 g^{-1}$) in the upper part of zone C1Z2. In zone C1Z3, charcoal area declines towards the upper part of the core, reaching a low level of 5 $cm^2 g^{-1}$.

Charcoal influx follows a similar trend to that of charcoal area, with a relatively low rate (< 0.2 $cm^2 yr^{-1}$) at the base of the core (zone C1Z1) between 162 cm and 76 cm. The influx increases steadily in zone C1Z2, reaching a peak of 0.9 $cm^2 yr^{-1}$ at 54 cm, ca. 780 yr. BP (cal 1189- 1292 AD). The influx of charcoal drops to < 0.2 $cm^2 yr^{-1}$ at 50 cm, ca. 700 yr. BP (cal 1244-1393 AD) and remains relatively constant in the upper part of zone C1Z2. The charcoal influx rises sharply at the upper boundary of zone C1Z2, reaching a peak of 1.0 $cm^2 yr^{-1}$ in zone C1Z3 at 30 cm, AMS ^{14}C date 180 ± 40 yr. BP (cal 1654-

1949 AD). The influx drops to 0.2 cm^2 yr^{-1} between 14 cm and 6 cm, before rising to 0.8 cm^2 yr^{-1} towards the top of the core.

(b) Down-core variations in charcoal particle size

The abundance of charcoal particles is relatively low (< 50,000 particles) at the base (C1Z1) of the core, between 126 cm and 95 cm. The total number of particles increases to more than 50,000 towards the upper boundary of C1Z1. Zone C1Z2 is marked by rise in charcoal abundances to higher levels (150,000 to 450,000 particles) towards the upper part of zone C1Z2, before dropping to low levels (70,000 to 200,000 particles) in zone C1Z3.

Figure 9.2 presents the down-core variations in charcoal particle size-classes for core M2C1. The concentration in charcoal particles is generally low (< 25,000 particles) at the base (C1Z1), rising to more than 50,000 particles at the upper part of the core for size-class 25 to < 50 μm. The abundance in zone C1Z2 increased to higher levels, mainly dominated by size-class 25 to < 50 μm (20,000-110,000 particles), followed by size-class 100 to < 125 μm with concentration ranging from 13,000 to 90,000 particles. Charcoal concentration for size-class 7.5 to < 10 μm remains rare in the record. In zone C1Z3 the abundance of charcoal drops to low levels (< 50,000 particles) for all size-classes. The abundance of charcoal particles for size-class range of 7.5 to < 25 μm remains relatively low (< 150,000 particles) throughout the core record, while that for size-class range 25 to < 125 μm dominates with charcoal concentration of up to 270,000 particles.

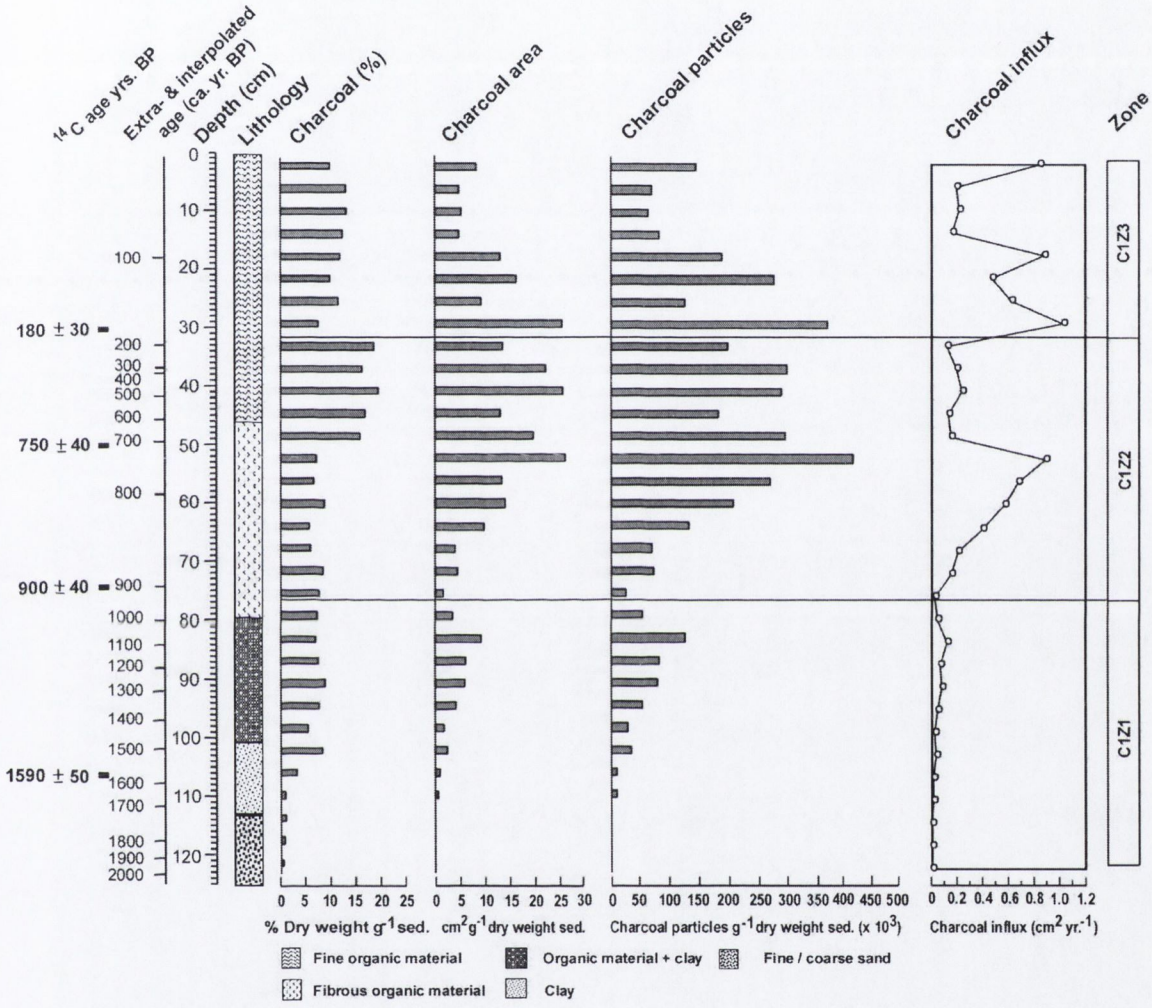

Figure 9.1 Comparison of charcoal results for M2C1

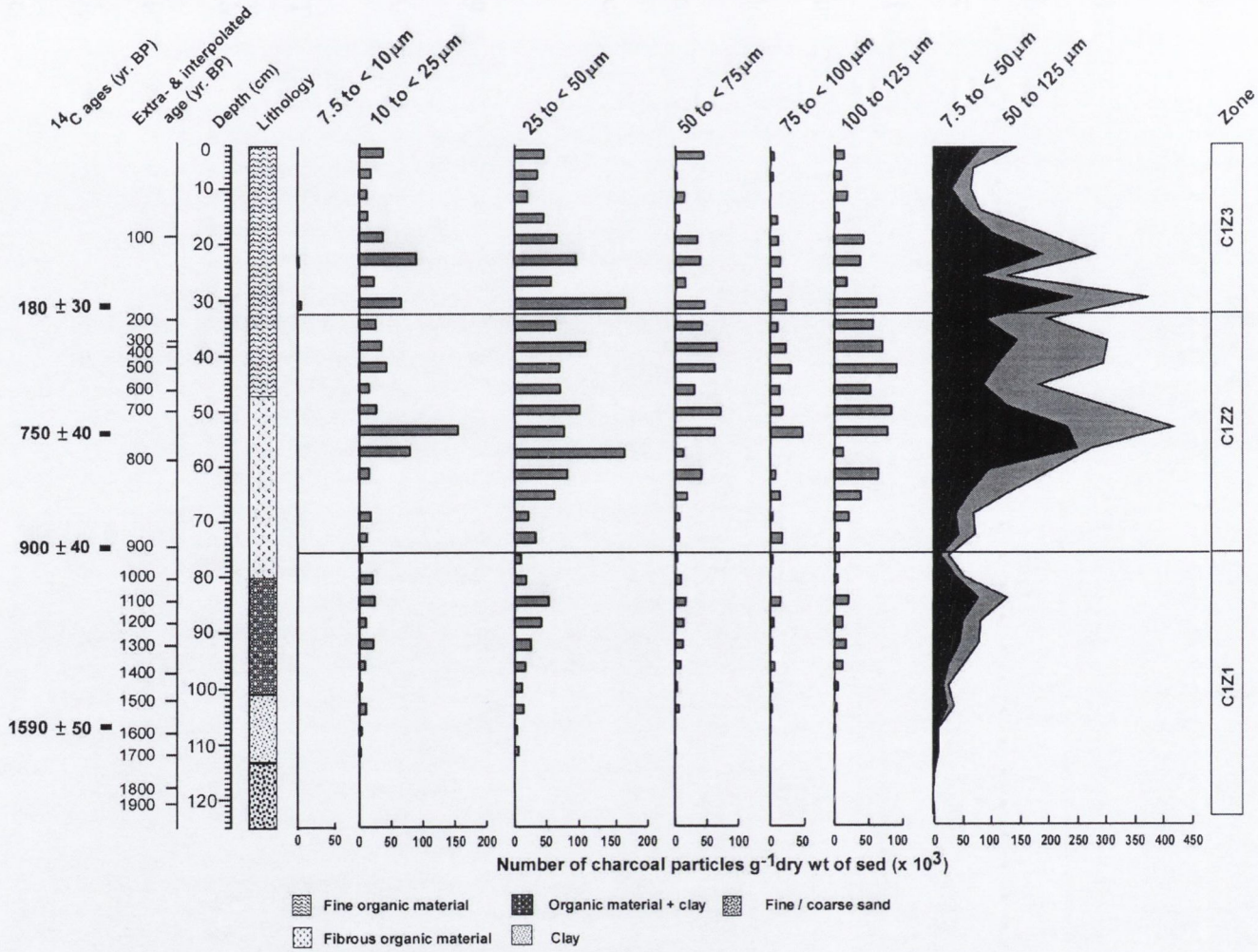

Figure 9.2 M2C1, number of charcoal particles per gram dry weight of sediment recorded for different size-classes

9.2.2 Charcoal results for M2C2

Results of charcoal analysis for M2C2 are presented in Figure 9.3.

9.2.2i Results of chemical assay method

The results illustrate a low charcoal content (< 3%) at the base of the core (zone C2Z1), between 176 cm and 150 cm (ca. 2000 to 1100 yr. BP). However, the abundance of charcoal increases towards the upper boundary of zone C2Z1, reaching a value of 5% at 122 cm, ca. 840 yr. BP (cal 1045-1278 AD). Zone C2Z2 is marked by further increases in charcoal abundance from 6% to 13% between 95 cm and 53 cm, before dropping to less than 5% at the upper part of zone C2Z2. A sharp increase (14%) in charcoal abundance is evident at 26 cm, AMS ^{14}C date 240 ± 40 yr. BP (cal 1519-1948 AD). The charcoal content is relatively constant (7 - 8%) in zone C3Z3.

9.2.2ii Results of point count method

(a) Charcoal area

The abundance of charcoal is generally low (< 10 $cm^2\ g^{-1}$) at the base (zone C2Z1) of M2C2, between 176 cm and 137 cm. The abundance increases in zone C2Z2, attaining a peak of 109 $cm^2\ g^{-1}$ at 92 cm, ca. 620 yr. BP (cal 1295-1404 AD), before dropping to lower levels (< 40 $cm^2\ g^{-1}$) towards the upper boundary of zone C2Z2. In zone C2Z3, the charcoal abundance increases towards the uppermost part of the core, attaining a peak of 42 $cm^2\ g^{-1}$ at 5 cm.

The down-core variations in charcoal influx for M2C2 closely follow the trend of charcoal area. A relatively low influx of charcoal (< 1.0 cm^2 yr^{-1}) occurs in zone C2Z1, but increases from the lower boundary of zone C2Z2, attaining a maximum value of 5.7 cm^2 yr^{-1} at 59 cm, ca. 475 yr. BP (cal 1333-1484 AD). The value of charcoal influx declines to lower levels (< 2.0 cm^2 yr^{-1}) towards the upper boundary of the zone C2Z2 and maintains a relatively low value (< 2.0 cm^2 yr^{-1}) in the top part of the core (zone C2Z3).

(b) Down-core variations in charcoal particle size

The abundance of charcoal particles at the base (zone C2Z1) of core M2C2 (Figure 9.3) is low (< 200,000), but a marked increase to higher levels (300,000 to 1,300,000 particles) occurs in zone C2Z2 between 92 cm and 35 cm. The abundance of charcoal particles drops to less than 60,000 particles, before attaining abundance of 337,500 particles at the upper boundary of the zone. In zone C2Z3, the abundance of charcoal particles range from 90,000 to 300,000 particles.

Figure 9.4 presents the down-core variations in charcoal particle size-classes. Particles of all size-classes are generally rare at the base (zone C2Z1) of the core, but the abundances increase in zone C2Z3. Charcoal particles in the size-class 25 to < 50 μm dominate the record with up to 660,000 particles, followed by size-class 10 to < 25 μm, contributing up to 520,000 particles. The abundance of size-classes 7.5 to < 25 μm and 100 to 25 μm are very low, each contributing less than 550,000 and 700 particles respectively.

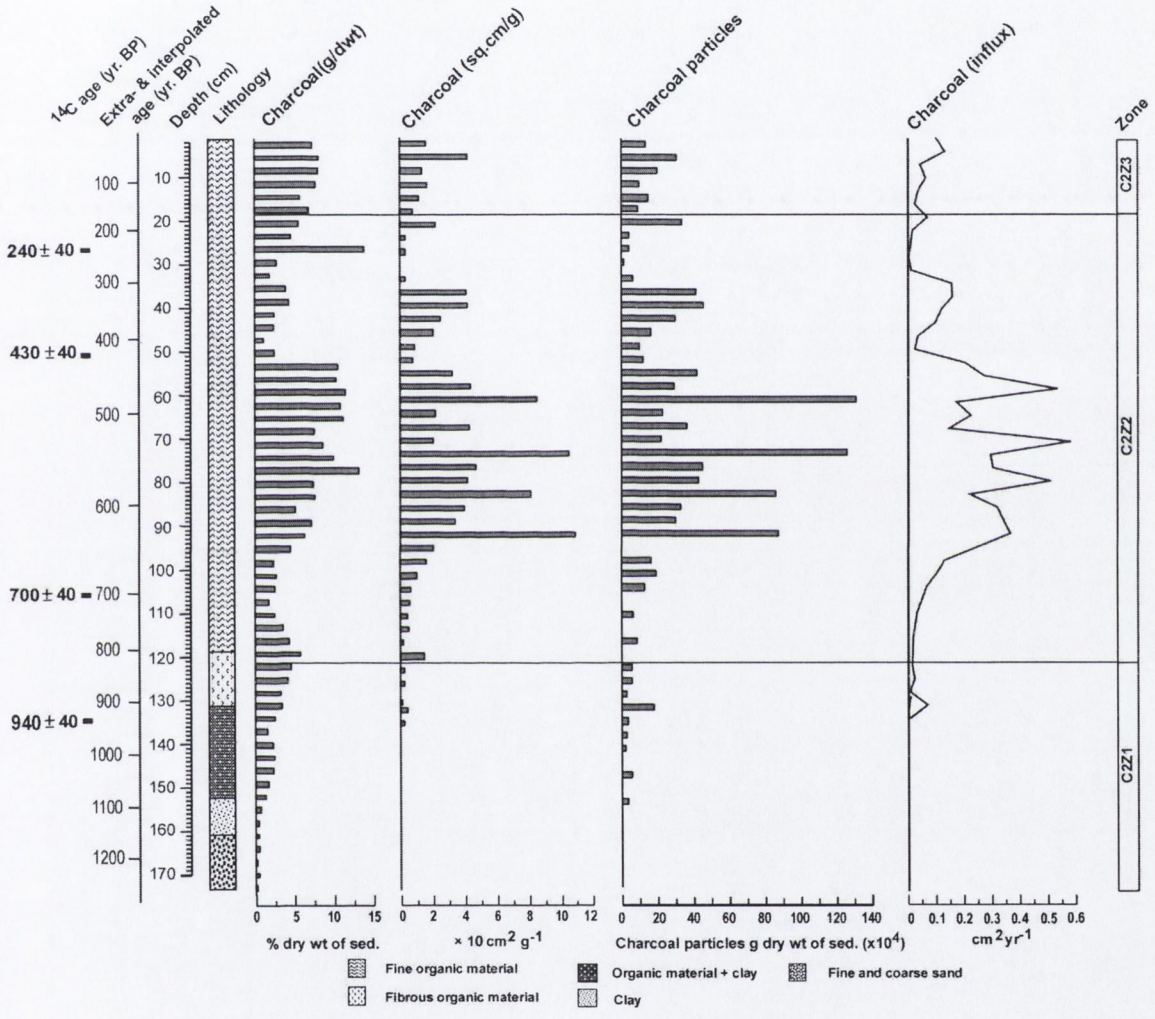

Figure 9.3 Comparison of charcoal results for M2C2

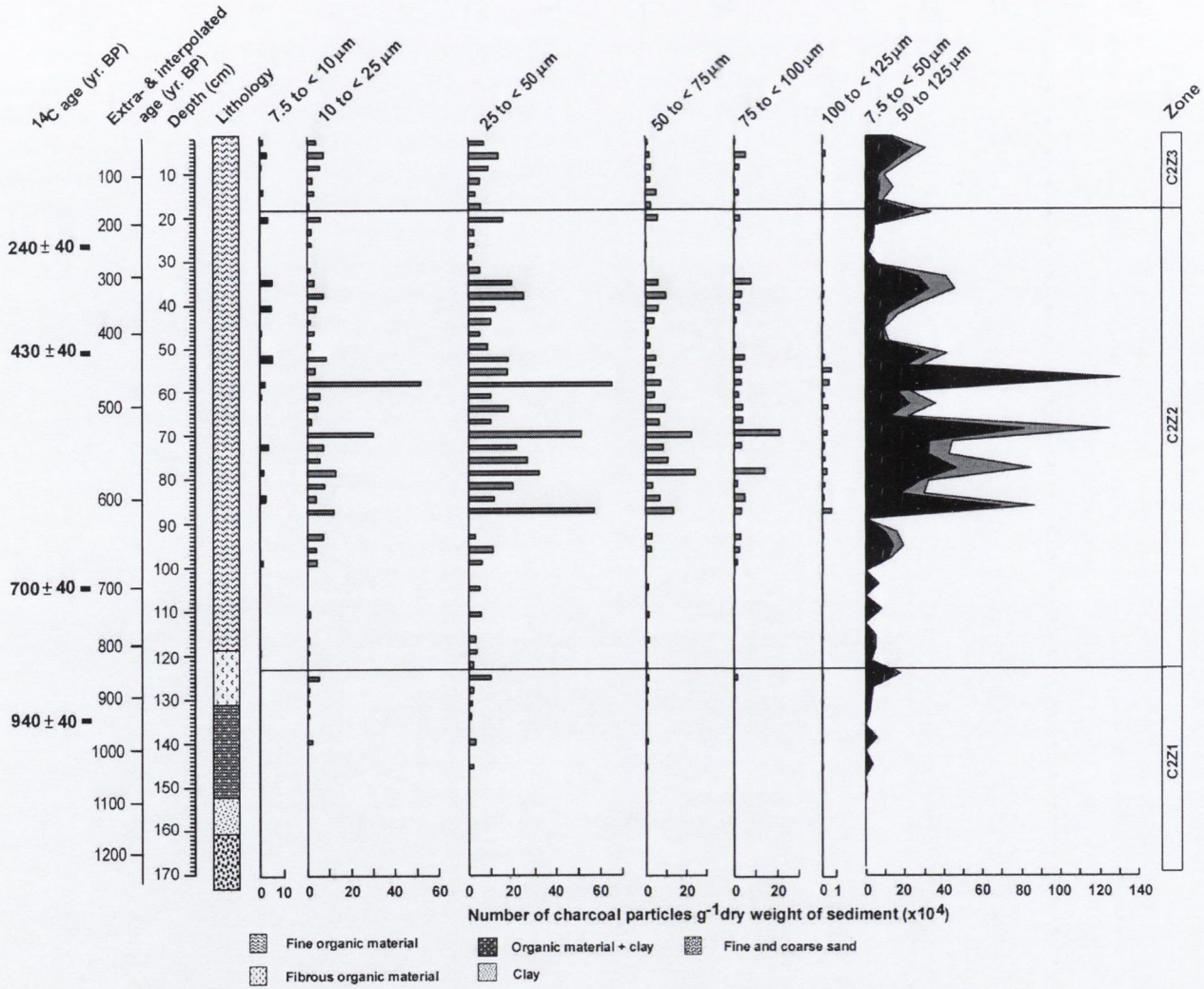

Figure 9.4 M2C2, number of charcoal particles per gram dry weight of sediment recorded for different size-classes

9.2.3 Charcoal results for M2C3C

Charcoal results for M2C3C are presented in Figures 9.5 and 9.6.

9.2.3i Results of chemical assay

As illustrated in Figure 9.5, charcoal abundance in zone Z3C1 range between 1% and 7%. Abundances drop to less than 2% at the lower boundary of zone Z3C2, between 90 cm and 70 cm, before increasing to higher levels (2-8%) towards the upper boundary of this zone. The abundance of charcoal is relatively high and constant (8%) in the uppermost part of the core (C3Z3).

9.2.3ii Results of point-count method

(a) Charcoal area

The abundance of charcoal when expressed as area is relatively low (< 1 cm^2) at the base (C3Z1) of M2C3C (Figure 9.5), attaining a peak of 42 $cm^2 g^{-1}$ at the upper boundary of zone C3Z1, ca. 820 yr. BP (cal 1071-1283 AD). In zone C3Z2, charcoal abundance increases to higher levels (> 1 $cm^2 g^{-1}$), attaining a peak of 112 $cm^2 g^{-1}$ at 38 cm, ca. 550 yr. BP (cal 1305-1437 AD), before dropping to lower levels (25-54%) towards the top of the core.

The influx of charcoal for core M2C3C varies in a similar way to charcoal area, with very low values (< 1.0 $cm^2 yr.^{-1}$) at the base (C3Z1). Charcoal influx increases to 2.8 $cm^2 yr^{-1}$ at 98 cm, ca. 820 yr. BP (cal 1071-1283 AD) before dropping to < 2.0 $cm^2 yr^{-1}$ in zone C3Z2 between 96 and 45 cm. The influx of charcoal attains a peak of 14.0 $cm^2 yr^{-1}$

at 38 cm, ca. 550 yr. BP (cal 1304-1437 AD) before dropping to les than 2 cm^2 $yr.^{-1}$ at the upper boundary of zone C3Z2. The influx drops to lower levels (< 1.0 cm^2 $yr.^{-1}$) towards the top part of the core (zone C3Z3).

(b) Down-core variations in particle size-class

The abundance of charcoal particles is very low (< 150,000 particles) at the base (zone C3Z1) of M2C3C (Figure 9.5), increasing to over 600,000 particles towards the upper boundary of zone C3Z1. Zone C3Z2 is marked by increase to a maximum of 1,400,000 particles at 38 cm, ca. 550 yr. BP (cal 1304-1437 AD). A relatively high abundance of charcoal (300,000-760,000 particles) is maintained in zone C3Z3.

9.3 Summary of charcoal results for Munsa II

The abundances of charcoal results (gravimetric and point-count) for cores M2C1, M2C2 and M2C3C, indicate a similar down-core variations, with relatively low abundances of charcoal, suggesting low incidences of fires. This corresponds to stratigraphic zones A-C (see chapter six) and represents a period of forested conditions as suggested by pollen and phytolth assemblages (see chapters seven and eight) The abundances of charcoal peaked in zone two of each core, mainly dominated by charcoal particles of size-class < 50 μm, suggesting increased incidences of fires in the catchment area. This period of increased charcoal corresponds to declining forest vegetation in the catchment areas of Munsa, thus indicating increased human activities in the catchment areas of Munsa II.

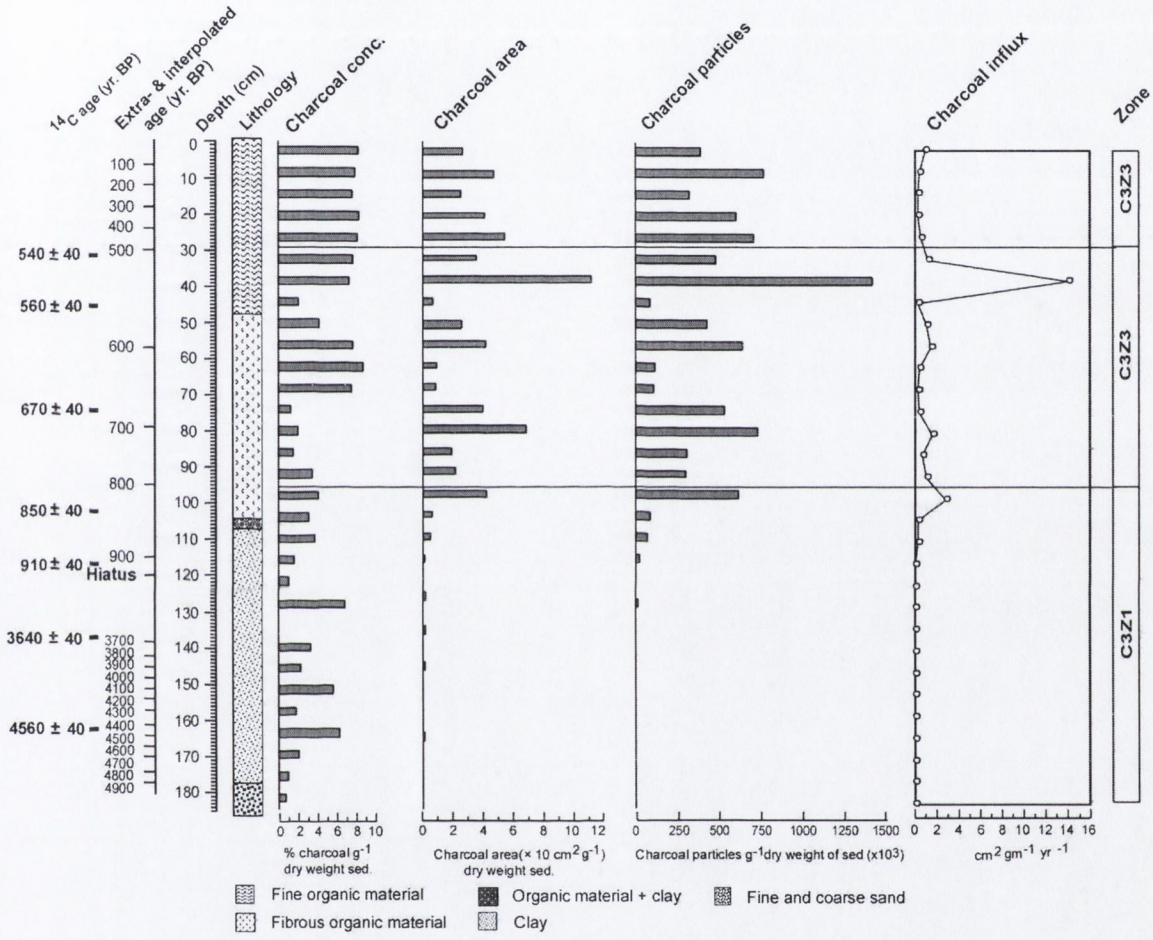

Figure 9.5 Comparison of charcoal results for M2C3C

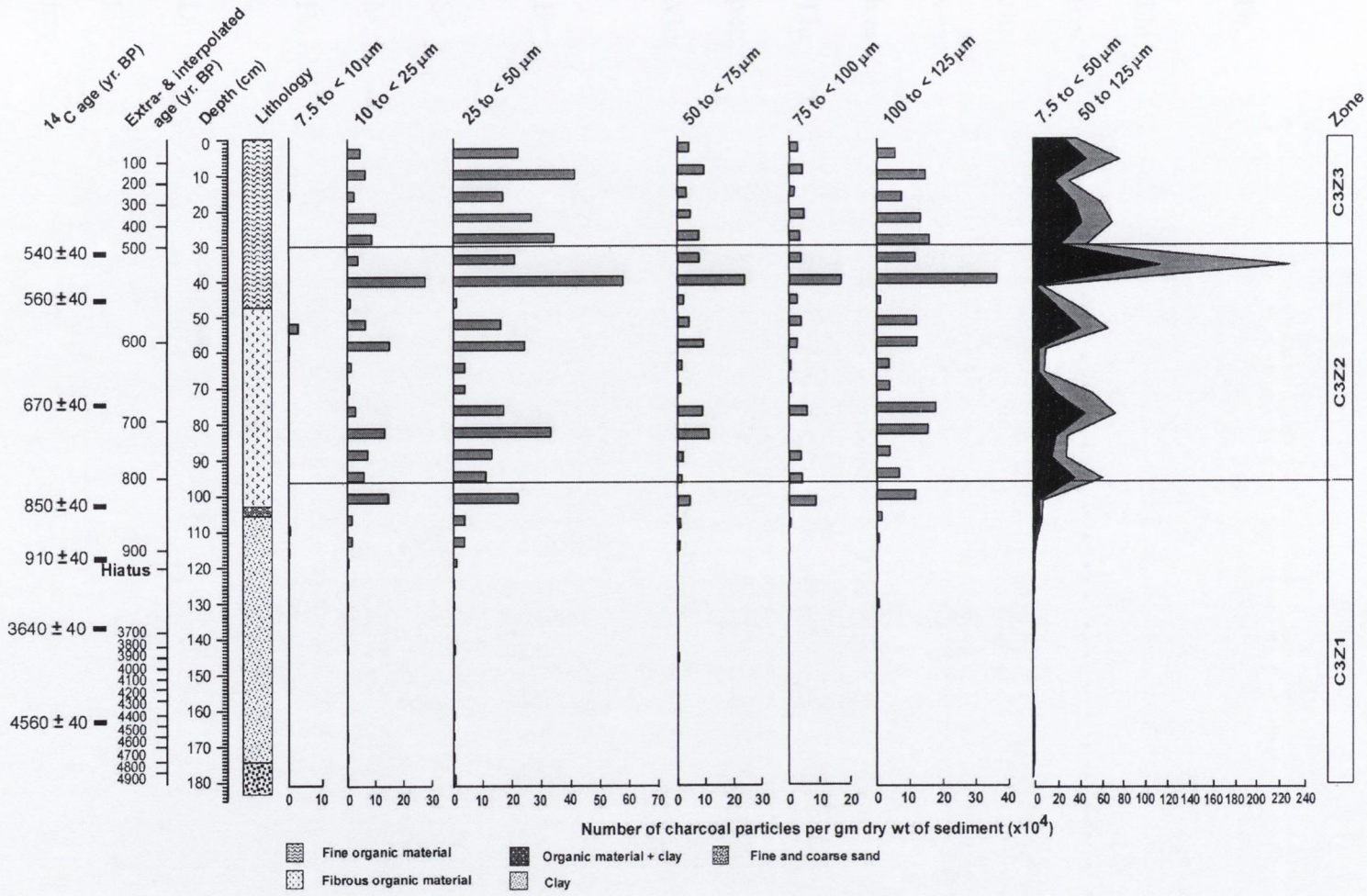

Figure 9.6 M2C3C, number of charcoal particles g^{-1} dry weight of sediment recorded for different size-classes

PART THREE: DISCUSSION AND CONCLUSIONS

CHAPTER TEN: DISCUSSION

DYNAMICS OF MUNSA II, ca. 5000 yr. BP TO THE PRESENT

10.1 Introduction

This chapter summarises the environmental history of Munsa, based on the evidence from proxy records obtained from Munsa II swamp presented in previous chapters. The chapter focuses on changes in the sedimentary composition and distribution of vegetation within the study area, and indicates the possible drivers of these changes, based on the findings from published research in the wider Interlacustrine highlands. The changes in environmental conditions at Munsa are presented in a series of time periods, based on zones used in the description and analysis of sub-fossil data from Munsa II. The time scale covered ranges from ca. 5000 yr. BP to the present.

10.2.1 Sedimentary conditions at Munsa II, ca. 5000 yr. BP to present

Sedimentary information from Munsa II provides a record of environmental history at Munsa dating the mid-Holocene (ca. 5000 yr. BP to the present). The oldest mid-Holocene sediments from Munsa analysed are from the base of M2C3C.

Despite the proximity of the coring sites for M2C1, M2C2 and M2C3C, inter-core comparisons of sedimentary evidence for past environmental conditions reveal several inconsistencies. M2C3C is located in the centre of the swamp and contains the longest sedimentary record (185 cm, ca. 5000 yr. BP). The sedimentary record does not appear to be continuous for M2C3C, but is interrupted by a sedimentation break (hiatus) or

breaks spanning from approximately ca. 3000 to 1000 yr. BP. A second hiatus in the sediment record from M2C3C may be present above the AMS ^{14}C date of 540 ± 40 yr. BP. These hiatuses may be attributed to lack of sediment accumulation, or they may have been caused by erosion process during periods of higher water flow through the swamp or conversely, during periods when the swamp surface dried-out for prolonged periods, causing oxidation of organic-rich sediments. Given the proximity of the M2C3C coring site to the main drainage channel at Munsa II, the breaks in sedimentation, at least towards the base of the core, most likely represent an erosion layer by fluvial activity, possibly under wetter climatic conditions in the local area or this could relate to the transition to more humid climatic regime registered in the region after ca. 2000 yr. BP (Casanova & Hillaire-Marcel, 1992; Barker *et al.*, 2000; Russell *et al.*, 2003).

On the basis of sedimentary characteristics, changes in the amount of organic and inorganic sediments as well as the amount of charcoal, suggest that environmental and anthropogenic factors have influenced the deposition process at Munsa II. The onset of sediment accumulation at Munsa II appears to have been initiated by erosion processes, and largely comprise inorganic material (mainly clay and sand particles) from the surrounding catchments. The basal stratigraphic zone, A, is largely composed of coarse and fine sand material, followed by deposition of clay-rich sediment material represented by stratigraphic zone B. Sediment accumulation appears to have commenced at the centre of the swamp (M2C3C) and the erosional activity could have been influenced by discharge from the stream that runs through the valley and that now contains Munsa II. Changes in sediment composition from inorganic to organic material

are apparent in stratigraphic zones C and D, presumably suggesting changes in hydrological condition in the swamp. The process could have been accelerated by the impeding of drainage, at the coring site.

According to the analysis of results presented in chapter six, the onset of papyrus-dominated swamp conditions at the three coring sites, begins at ca. 2000 yr. BP at M2C1, which is closest to the margin of the swamp and became pronounced at the centre of the swamp at M2C3C by ca. 800 yr. BP. It is likely that the establishment of papyrus-dominated swamp was influenced by reduced discharge from the valley that now contains Munsa II, and may thus represent the onset of lower levels of effective precipitation in the study area registered in the region (Nicholson, 1998; Alin & Cohen, 2003). An expansion of papyrus-dominated swamp conditions at Munsa II could have also been caused, at least in part by human activity, especially given its apparent timing. Increased in-wash of soil to the valley accommodating Munsa II, as a result of the disturbance of vegetation in the catchment, could have led to the impeding of drainage from the valley, and therefore to the spread of the edaphically wet conditions favoured by swamp taxa, such as papyrus. If this was the case then many of the papyrus swamps in the region, which are common at the mid altitudes favoured by agriculturalists, may owe their origin to human activity.

10.3 Vegetation dynamics at Munsa II, and their likely causes

(a) ca. 5000 to 900 yr. BP

Sediment-based evidence from Munsa II for past environmental conditions possibly dating as early as ca. 5000 yr. BP is available from M2C3C. Forested conditions in the catchment for Munsa II appear to have characterised the transition period from mid to late Holocene at Munsa. Sedimentary data from M2C3C suggest that relatively little disturbed by vegetation fires, between ca. 5000 and 900 yr. BP, as evidenced by the generally low abundances in core samples of charcoal and burnt phytoliths.

The coring sites appear to have occupied a relatively well-drained valley, which supported riverine forms of both medium altitude evergreen and semi-deciduous forest. However, some edaphically-wet conditions were present, given the abundances of Cyperaceae pollen, but were presumably not as extensive as today. The pollen record from M2C3C indicates a relatively diverse flora from ca. 5000 yr. BP, becoming less diverse from ca. 4200 yr. BP, characterised by pollen from *Acalypha*, *Artemisia*, *Rapanea*, and *Teclea*. *Acalypha* pollen characterised sediment samples from the base of M2C3C, between ca. 5000 and 4700 yr. BP. *Acalypha* pollen is derived from a wide range of herbs, shrubs and occasionally trees (Langdale-Brown *et al.*, 1964; Livingstone, 1967; Lind & Morrison, 1974). The genus inhabits a wide variety of habitat types and members are reported to be common colonizing species of lowland secondary forests (Lind & Morrison, 1974). The members of this genus are found to be abundant in lower altitude environments on Rwenzori Mountains (Livingstone, 1967). *Acalypha* pollen is reported to be well dispersed (Hamilton, 1972; Lind & Morrison, 1974), and it is

possible that some of this pollen type has been transported from forests elsewhere in the region. Over thirty species of *Acalpha* have been reported in East Africa, most of which occur in forest and forest edges (Smith, 1987). However, *A. villicaulis* is found to be a common species of grassland and woodlands savannas (Kendall, 1969; Lind & Tallantire, 1971). *A. ornata* and *A. neptunica* are reported to be the most abundant forest species of *Acalypha* and the latter is reported to be common in Budongo forest in Bunyoro (Hamilton, 1991).

The presence of *Artemisia* pollen in M2C3C sediments that pre-date ca. 4800 yr. BP, indicates relatively warmer climatic conditions at Munsa to ca. 4800 yr. BP. *Artemisia* pollen is reported by Coetzee (1967), Livingstone (1967), Kendall (1969) and Hamilton (1982) as an indicator of dry conditions in montane forests. This genus is also reported to be associated with upper montane vegetation types (e.g. Afro-alpine conditions) (Livingstone, 1967). *A. afra*, the only known species in East Africa (Livingstone, 1967; Kendall, 1969; Lind & Morrison, 1974), is the probable source of this pollen type. This pollen type is reported to be moderately well dispersed (Hamilton, 1972) and can be over-represented in pollen counts. *Teclea* is an evergreen understorey tree or shrub inhabiting forest habitats (Hamilton, 1991). The pollen type could have originated from two species; *T. nobilis* and *T. grandifolia*, both of which have been reported in Bunyoro (Eggeling, 1947; Hamilton, 1991). *Rapanea* is reported to be a common component of high altitude forests and characterises the *Hagenia - Rapanea* zone (Lind & Morrison, 1974; Hamilton, 1982). The pollen type is derived from two species; *R. rhododendroides* and *R. pulchra.* The former is found to be abundant on swamp forests in Kigezi, western Uganda (Hamilton, 1991). Despite its dominance in montane forest, *R. rhododendroides*

has been recorded in lowland swamps forests in central Uganda and along the shores of Lake Victoria (Lind & Morrison, 1974; Hamilton, 1991).

Pollen records indicate that forested conditions appear to have characterised the catchment for Munsa II to the beginning of the second millennium AD (ca. 900 yr. BP). Forest pollen spectra are characterised by abundant contributions from swamp forest taxa, mainly *Alchornea*, *Cyathea* and *Rapanea*, and moderate levels of *Olea* (M2C2) and *Celtis*, *Croton*, *Neoboutonia* and *Teclea* (M2C1). *Alchornea cordifolia* and *A. laxiflora* are potential sources of *Alchornea* pollen. These species have been recorded in Bunyoro (Eggeling, 1940; Hamilton, 1991). According to Kendall (1969) and Lind & Morrison (1974), *A. cordifolia* is associated with evergreen forests and thickets, while *A. laxiflora* is a component of semi-deciduous forests. The pollen type is reported to be moderately well dispersed (Hamilton, 1972) and can therefore be over-represented in the pollen counts. *Cyathea* and *Rapanea* are common components of swamp forests (Hamilton, 1991). The *Cyathea* spores are presumably derived from *C. maniana,* which is a tree fern (Hamilton, 1991) growing in riverine forest locally. *Cyathea maniana* is also reported to occur on the lower slopes and bottoms of valleys, and in wetter areas at higher altitudes (Lind & Morrison, 1974; Hamilton, 1991). The spores are reported to be poorly dispersed (Hamilton, 1991), and thus can be under-represented in the pollen counts. Taylor (1988) reported that a high level of *Cyathea* spores in a sediment record might not necessarily reflect the common occurrence of the parent taxa, but may be attributed to greater resistance of the spores to physical damage during transportation prior to deposition.

Celtis and *Croton* are common components of lowland moist forests in Uganda today (Livingstone, 1967; Lind & Morrison, 1974; Hamilton, 1982; 1991). *Celtis* is reported to be more abundant in semi-deciduous forests than evergreen forests (Langedale-Brown *et al.*, 1964), and its pollen type in Munsa II sediments is likely to be derived from two potential sources; C. *Africana* and *C. durandii*, which are currently found in the area today. The former is reported to be associated with drier forest types, while the latter is more abundant in moist forest types (Hamilton, 1982). Four species of *Croton* (*C. bukobensis*, *Croton macrostachyus*, *C. sylvaticus* and *C. megalocarpus*) are recorded today in Uganda (Hamilton, 1991). *Croton sylvaticus* is reported to be abundant in Bunyoro, particularly in Budongo forest (Hamilton, 1991). It is a small tree up to 10 m tall, common in secondary forest and on forest edges over a broad altitudinal range (Lind & Morrison, 1974). The pollen is poorly dispersed (Hamilton, 1972) and can therefore be under-represented in the pollen spectra as reflected in Munsa II sediments.

The increase in the amount of *Neoboutonia* pollen in sediments, suggests its establishment in the riverine forest at Munsa. Two species of *Neoboutonia* are currently growing locally in the area; *N. macrocalyx* and *N. melleri.* The former is reported to be a common forest tree in wetter environments between 1400 to 2500 m (Hamilton, 1982; 1991), while the latter is often abundant as a tree in swampy valleys in lower altitudes (Hamilton, 1991). The pollen type has a moderate to low export ability and may be therefore more common in forests in the catchment than suggested in the pollen spectra. *Teclea* is moderately well represented in M2C1 from ca. 1250 to 900 yr. BP, while *Olea* is relatively abundant in M2C2. *Olea* is an important colonizing genus commonly occurring on forest edges (Livingstone, 1967; Kendall, 1969) and is reported to grow in

wide spectra of forest types (Livingstone, 1967; Lind & Morrison, 1974; Hamilton, 1982; 1991). According to Hamilton (1972; 1982), *Olea* pollen has moderate export ability and can therefore be well represented in the pollen counts. This pollen type may have been derived from two species; *O. africana* and *O. capensis*, which are important colonizing species in forest edges, predominantly found between 1500 m to 2500 m and up to 3000 m (Livingstone, 1967; Lind & Morrison, 1974; Hamilton, 1982; 1991). *Olea capensis* is reported by Eggeling (1947), Kendall (1969) and Hamilton (1982) as a common colonizing species of poor and shallow soils on forest edges of Budongo forest in Bunyoro. It is also found to be abundant in the forests of Kibale and Mt Elgon (Hamilton, 1991). While *O. africana* is recorded in forests of western Uganda, and is found to be abundant in drier montane forests of Mt Elgon and Karamoja (Hamilton, 1982; 1991).

Podocarpus pollen in the sediments is derived from three species that exist in Uganda and that are impossible to distinguish in the pollen record; *P. gracilior, P. milanjianus* and *P. usambarensis* (Livingstone, 1967; Lind & Morrison, 1974). *Podocarpus gracilior* occurs in dry montane forest (Lind & Morrison, 1974; Hamilton, 1991). The potential source of this pollen type is perhaps most likely to be *P. milanjianus* and *P. usambarensis,* which are reported to occur across a wide range of altitudes from about 1200 m to 3500 m (Hamilton, 1991). These species have been recorded in lowland seasonal swamp forests near Kagera River (Kendall, 1969; Lind & Morrison, 1974) and along the shores of Lake Victoria (Hamilton, 1991). According to Hamilton (1982), the pollen is well dispersed and may be over-represented in sub-fossil pollen spectra in the Interlacustrine highlands.

Within the sediments of M2C1 and M2C2, the increase in abundance of *Bidens* pollen at ca. 910 yr. BP in M2C2 suggests some disturbance of vegetation habitat. *Bidens* is said to be associated with agricultural activities (Lind & Tallantire, 1971). This pollen type is derived from a varied group of herbs and shrubs (Lind & Tallantire, 1971) and *B. grantii* and *B. pilosa* are common species currently growing locally at the study site.

The fungal spores support the suggestion that the catchment at Munsa II was relatively forested during the mid-Holocene, as indicated by *Ustulina* spores. *Ustulina* is reported to be a mild parasite causing soft-rot of wood on several tree species and, according to van Geel & Anderson (1988), it is associated with forested environments, and its spores are well dispersed. The presence of ascospores of the dung fungi *Cercophora* and *Sporomiella* suggests that herbivores were present at the site. These two fungi are reported to be good indicators of domestic animals (van Geel, 1978; 2001; van Geel *et al.*, 1982-83; Davis, 1987). *Cercophora*-type is coprophilous, commonly occurring on dung of herbivores, and on decaying wood. This fungus has also been recorded on herbaceous stems and leaves, but it is reported to be a good indicator of herbivore dung (van Geel, 1978; 2001; van Geel *et al.*, 1982-83). *Sporomiella* fungus is also reported to be associated with herbivore dung (Davis, 1987), and has been found to be common on the dung of domestic herbivores, such as cattle, sheep, and goats. The spores have also been recorded on dung of wild herbivores and on decaying wood (Ahmed & Cain, 1972). Given the age of the sediments containing fungal spores from plants that may have been growing on herbivore dung, and the absence of archaeological evidence for pastoralism in the western Uganda prior to ca. 3000 yr. BP, it is perhaps more likely that the dung was produced by wild herbivores, such as elephants. Type 181 is present in

sediments from M2C1 between ca. 1800 and 900 yr. BP, presumably suggesting relatively wet conditions. This fungus is reported to be common in stagnant shallow open water and eutrophic conditions (van Geel *et al.*, 1982-83). The presence of relatively wet conditions close to the coring site is also indicated by abundance of *Sordaria*-type 55 spores, which are reportedly associated with damp, mesotrophic to eutrophic environments (van Geel, *et al.*, 1982-83)

Phytolith assemblages from the basal sediments of M2C3C provide additional information on environmental conditions during the mid-Holocene at Munsa. Critically, the phytoliths also provide information on mid Holocene environments at Munsa II for a period that is not covered by pollen and fungal spore data because of the poor preservation of organic material in sediment relating to that time. The phytolith record of vegetation history at Munsa is therefore more complete, although less finely resolved taxonomically in some cases, than the pollen and spore records, at least for the mid to late Holocene. The abundance of ligneous dicotyledon (spherical rugose) morphotypes indicates the local presence of forested conditions from ca. 5000 to 3000 yr. BP. It is probable, that the spherical-rugose morphotypes, which are characteristic of trees and shrubs (Piperno, 1988; Alexandre, *et al.*, 1997; Barboni *et al.*, 1999), are derived from the medium altitude evergreen and semi-deciduous forest taxa that according to the pollen were present in the catchment. Spherical-crenate morphotypes in basal sediments of M2C3C indicate the presence of members of the Palmae family. Palms are reported to occur in a diversity of habitats at different altitudes, but are mostly restricted to wet habitats (Moore, 1973; Tomlinson, 1979). Palmae morphotypes are easily distinguished by distinct projections (spines) from the surface of the sphere (Piperno, 1988). The most

likely source of spherical-crenate morphotype phytoliths in Munsa II sediments is *Phoenix reclinata*, which is currently found in riverine forest locally. Two other species of Palmae, *Raphia farinifera* and *Elaeis guineensis*, are also reported to occur in the swamp forests in western Uganda (Hamilton, 1991), although the latter is predominantly a cultivated species.

The vegetation indices (*D/P* and I_{ph}) provide further evidence of forested conditions at Munsa during the mid-Holocene to ca. 3000 yr. BP. The *D/P* values, which represent the ratio of ligneous spherical-crenate and -rugose phytolith morphotypes to Poaceae phytolith morphotypes (Alexandre, *et al.*, 1997; 1999; Barboni, *et al.*, 1999; Bremond *et al.*, (2005), are generally high at the base of M2C3C, and range from 5 to 78. According to Alexandre *et al.* (1997; 2003) and based on materials from Congo, semi-deciduous forest is represented by a *D/P* value of at least 7, while Alexandre *et al.* (1999) use a minimum *D/P* value of 1.5 to distinguish tree savanna and mesophytic forest in Brazil. Barboni *et al.* (1999) use an even lower value (0.6) to distinguish a riparian forest in Ethiopia. The I_{ph} values represent the proportion of C_4 short and C_3/C_4 tall Poaceae phytolith morphotypes, and are generally lower than the threshold value of 30% that distinguishes tall Poaceae from short Poaceae grassland (Alexandre *et al.*, 1997; Barboni *et al.*, 1999). This suggests that away from forested areas, tall grasslands occur in which both C_3 and C_4 members of the Poaceae are found. According to Alexandre *et al.* (1997), a minimum I_{ph} value of 30% can be used to distinguish tall-grass savannas that are characteristics of more arid parts of Africa. According to work carried out in North America (Kurman, 1985; Fredlund & Tieszen, 1994), I_{ph} values between 40% and 45%

indicate the presence of tall-grass Prairies, whereas 60% represents the occurrence of short-grass Prairies.

Phytoliths from M2C3C also indicate the possible local presence of cultivated plants at Munsa pre ca. 3000 yr. BP, in particular members of the Musaceae (both *Musa*- edible banana and *Ensete*-false banana). Assuming that the phytoliths have been correctly identified, banana could have been cultivated on forest margins and within relatively small forest gaps in the period preceding the main occupation phase at Munsa, although plants found naturally within surrounding areas of forest could have produced the phytoliths identified as *Ensete*. The present-day range of *Ensete ventricosa*, which occurs in forested and riparian forest between 1000 m and 3000 m a.s.l, extends north of the northern shoreline of Lake Victoria (De Langhe *et al.,* 1994-95).

Phytoliths resembling *Musa* were encountered close to the base of the record from Munsa II, predating the AMS ^{14}C date of 4560 ± 40 yr. BP, and thus predate by a considerable length of time the earliest empirical evidence of the genus in Africa. Phytoliths, believed to be from *Musa*, were recovered from a pit deposit at an archaeological site in Cameroon dating to ca. 2500 yr. BP (Mbida *et al.*, 2000; 2001). There is still much debate over the date of the introduction of *Musa* from Asia, where the earliest date for its cultivation, which possibly pre dates ca. 6000 yr. BP, is from the highlands of New Guinea (Wilson, 1985; Denham *et al.*, 2003). There is some evidence that plant domesticates of African origin, including cowpea (*Vigna unguiculata*), pearl millet (*Pennisetum glaucum*) and sorghum (*Sorghum bicolor*), were cultivated in India more than ca. 3000 yr. BP (Fuller, 2003). This indicates some connection existed

between Africa and Asia, and involved the transfer (and possible exchange) of technologies related to food production, pre ca. 3000 yr. BP. The introduction of bananas to eastern and central Africa could presumably have been at least ca. 3000 yr BP. Indeed, De Langhe *et al.* (1994-5) suggests that it is likely that *Musa* reached the coastline of eastern Africa more than 3000 years ago, from where it was transported throughout much of inter-tropical Africa. This early date concurs with the genetic diversity of edible bananas in Africa today, which are reported to be about ten times the number in Asia (Rossel, 1994-5), and with the phytolith evidence from Cameroon in western Africa (Mbida *et al.*, 2000; 2001). According to Rossel (1994-5), the northern shoreline of Lake Victoria was the most likely transportation route from the coast into interior Africa, because extensive tracts of arid and semi-arid conditions elsewhere would have presented a formidable barrier owing to the high moisture requirements of cultivated banana. Clark (1976) and De Langhe *et al.* (1994-5) have also suggested that the spread of *Musa* cultivation may have been facilitated by an existing familiarity with *Ensete* as a source of food. Thus it is possible *Musa* was cultivated in the study area before ca. 3000 yr. BP, and that its early cultivation in the study area was linked to an existing familiarity with the requirements of *Ensete*.

An alternative possibility is that the Musaceae phytoliths at the base of M2C3C are younger than indicated. Bioturbation and vertical movements of water through the sediment profile may have caused downward translocation. Indeed, the effect of phytolith translocation in the soils of equatorial Africa is reported by Alexandre *et al.* (1997) and Runge (1999). Alexandre *et al.* (1997) recorded a high rate of downward translocation of spherical-rugose morphotypes, possibly facilitated by their small size (2-

10 μm). Runge (1999) also noted a high rate of bioturbation in tropical soil profiles, as a result of the activities of termites. Bioturbation and vertical movements of material in the sediment profile could also have impacted the accuracy of the chronological framework based upon the AMS ^{14}C dates. However, any contamination of dated samples in the context of Munsa is most likely to result in younger than actual dates, through, for example, the incorporation of plant roots etc. In any case, the stratigraphic consistency of the dates obtained appears to suggest that the chronological framework is robust. The morphological criteria used to discriminate between *Musa* and *Ensete* presents another problem. According to Vanessa (2003), distinguishing *Musa* from *Ensete* phytoliths is perhaps more difficult than is suggested here and in the recently published literature (e.g., Mbida *et al.*, 2000; 2001), because of the relatively minor differences in phytolith morphotypes produced by members of the two genera; a likely high degree of variation in morphotypes produced by the same plant (according to where the plant phytoliths have been produced; the age of the plant and the ecological conditions under which it is found); and a relatively limited range of reference material upon which criteria used in the identification of Musaceae phytoliths and discrimination of phytoliths produced by component genera are based. Indeed, some light micrographs of *Ensete* morphotypes from Papua New Guinea Asia (Denham *et al.*, 2003) bear close resemblance to SEM micrographs of *Musa* morphotypes from voucher specimens obtained from the study site.

(b) ca. 900 to 200 yr. BP

The date ca. 900 yr. BP marks the onset of forest decline at Munsa. During this period, Poaceae pollen attains maximum levels in the sediment records at the expense of forest taxa, suggesting a change to a more open vegetation type. Poaceae type pollen is produced by a wide range of grasses, which, are currently growing at the study area. The vegetation is currently dominated by *Panicum maximum*, *Pennisetum purpureum*, and *Setaria sphacelata*, which according to Langdale *et al.* (1964) and Lind & Morrison (1974), are associated with human disturbance. Evidence of human disturbance at Munsa is supported by the increases in amounts of *Bidens* pollen, which is often associated with agricultural activities (Lind & Tallantire, 1971).

This period is characterised by increased forest fires as evidenced by relatively abundant charcoal and burnt phytoliths in the sediment records. The relatively more abundant charcoal particles with size less than 50 μm, suggests that the fires may have originated from both adjacent and / or regional areas. According to Clark & Royall (1995) and Clark & Hussey (1996), charcoal particles with size greater than 50 μm reflect local burning, as they are often not transported far, unlike smaller particles (< 50 μm), which are usually transported for longer distances by wind and are often from regional and extra-regional fires. Indeed Thevenon *et al.* (2003) recorded abundance of larger charcoal particles (> 50 μm), which they attribute to local anthropogenic burning around Lake Masako in Tanzania.

A marked increase in the proportions of the spores of the dung-colonising fungi *Cercophora* occurs in sediments of M2C2 and M2C3C, dating to this period of forest decline. This presumably suggests increased number of herbivores in the area, and mostly likely domestic animals, notably cattle, as this period correlates with the occupation of the Munsa archaeological site by communities who, according to the archaeological record, were herding cattle along with other domesticated animals (Robertshaw, 1997). The proportion of *Sordoria*-type 55 fungus remains relatively high in the record, indicating the continued presence of edaphically-wet condition close to coring sites. However, high percentages of Sordoriaceae ascospores in modern and Iron Age cow dung from southern Africa (Carrion *et al.*, 2000) suggest that members of this family of fungi are also indicators of grazing.

The phytolith data support the pollen-based evidence for forest decline at Munsa between ca. 900 and 200 yr. BP, as reflected by increased percentages of Poaceae morphotypes at the expense of ligneous spherical-rugose (trees/shrubs) morphotypes. The Palmae (spherical-crenate) morphotypes became rare during this period. Palms are currently used locally for basketry in the region and may also have been used during the occupation of Munsa. The presence of Musaceae (*Musa* and *Ensete*) during this period may also suggest that it was cultivated locally. *Musa*, which includes the cultivated, edible banana and plantains, was introduced to Africa from Asia. The genus *Ensete*, or false banana, is native to eastern, central and southern Africa is reported to be widely cultivated in Ethiopia and is also collected from the wild in central and eastern Africa as food plant and other purposes (De Langhe *et al.*, 1994-5; Rossel (1994-5: 144)

Phytoliths from the tall C_3/C_4 Poaceae dominate the assemblage between ca. 900 and 200 yr. BP, suggesting relatively moist environmental conditions. The rise in level of C_4 short Poaceae (saddle-shaped) phytoliths in M2C1 between ca. 900 and 700 yr. BP is probably a result of the opening of forest vegetation cover creating a favourable microclimate, as C_4 short grasses are often associated with warmer climatic conditions (Twiss, 1992; Alexandre *et al.*, 1997; Barboni *et al*, 1999).

(c) ca. 200 yr. BP to present

This time period is recorded by sediments from the three cores, although there may have been a minor sedimentary hiatus in M2C3C, post dating the AMS ^{14}C date of 540 ± 40 yr. BP. During this period, some recovery of medium altitude evergreen and semi-deciduous forest is evident dated at M2C1 and M2C2 at ca. 200 and 180 yr. BP respectively. However, forest recovery is less evident at M2C3C, and this may reflect the presence of a hiatus in the upper part of this core. Alternatively, and as was mentioned previously, this inter-core difference may reflect a lower sensitivity of core M2C3C to non-local pollen fluctuation, because of its more central location in the Munsa II swamp. There is a correlation in the timing of forest recovery and apparent decline in the concentration of charcoal and burnt phytoliths, suggesting a period of reduced frequency of fires. The abundance of charcoal particles is dominated by the size-class < 50 μm, probably suggesting that the charcoal originated from both regional and local sources.

Pollen records suggest a period of well developed sedge swamp at Munsa II, dominated by *Cyperus papyrus*. The pollen of forest taxa record indicates an expansion of *Myrica – Neoboutonia - Rapanea* swamp forest at Munsa, with *Syzygium* being moderately well represented. The potential source of *Myrica* pollen is likely to have been *M. kandtiana*. This species is a small tree up to 5m tall growing on swamps, usually found at lower altitudes (Hamilton, 1982; 1991). *Myrica* pollen type is reported to be well dispersed (Hamilton, 1972) and thus can be well represented in the pollen diagram as indicated in M2C3C. Four species of *Myrica* are reported to exist in eastern Africa, but *M. salicifolia* and *M. kandtiana* are reported to be widely distributed in the region (Hamilton, 1972). The proportion of *Neoboutonia* pollen represented by M2C1 and M2C3C could reflect local abundance of *N. macroxalyx* as this taxon is currently found in relatively wet riverine forests in the study area.

Although it has proven impossible to distinguish pollen and phytoliths produced by sorghum and millet from the remains of wild members of the Poaceae preserved in the cores from Munsa II, it has been possible to identify phytoliths from maize. Maize-like, cross-shaped phytoliths were encountered in sediment samples from Munsa II postdating ca. 150 yr. BP. Maize is a crop that is native to central and South America (Wright, 1949). The exact period of maize introduction to eastern Africa is not known; however, according to linguistic evidence, maize may have been introduced to eastern Africa between the sixteenth and seventeenth century AD, and was commonly grown in western Uganda by the mid-nineteenth century when Europeans first ventured into the region (Wright, 1949; Philippson & Bahuchet, 1994-5). The phytolith evidence from

Munsa II for maize would thus appear to accord with the linguistic and historical information relating to the introduction of the crop to eastern Africa.

10.4 Vegetation dynamics at Munsa, ca. 5000 yr. BP to present, within a regional context

The period ca. 5000 to 2000 yr. BP is generally characterised by forested conditions around Munsa, consisting of evergreen and semi-deciduous forest taxa. Climatically this period accommodates a transition to drier conditions, evidenced by a period of low lake levels in tropical central and eastern Africa that commenced in the mid-Holocene. (Adamson *et al.* 1980; Butzer, 1980; Nicholson & Flohn, 1980; Habery & Heckey, 1987; Johnson *et al.*, 1991; Casanova & Hillaire-Marcel, 1992; Stager, 1998; de Menocal *et al.*, 2000; Gasse, 2000; Russell *et al.,* 2003; Stager & Mayewski, 1997; Stager *et al.*, 1997; 2003).

A period of low water levels is registered in Lake Edward between ca. 4000 and 3000 yr. BP (Russel *et al.*, 2003). Diatom records (Stager *et al.* 1997; 2003) and carbon isotopes (Talbot *et al.*, 1989) from Lake Victoria also registered a period of arid climatic conditions in the region dated to ca. 2200 to 2000 yr. BP. Evidence from Nile River sedimentary records indicates a period of relatively low water levels between ca. 4300 and 3300 yr. BP and ca. 2500 to 2000 yr. BP (Adamson *et al.,* 1980; Butzer, 1984; Hassan, 1997). Lake Kivu (Haberyan & Hecky, 1987) and Lake Tanganyika (Casanova & Hilaire-Marcel, 1992; Alin & Cohen, 2003) experienced prolonged low stands between ca. 4000 and 3700 yr. BP.

Although pollen and phytolith records indicates no clear evidence of forest decrease around Munsa during the mid to late Holocene transition to arid dry conditions, apparent changes in forest is registered in other pollen data in central and eastern Africa (see Kendall, 1969; Hamilton, 1982; Taylor, 1988; 1990; 1992; Bonnefille *et al.*, 1991; Jolly & Bonnefille, 1992; 2002; Beuning *et al.*, 1997; Marchant, 1997; Taylor *et al.*, 1999). Pollen data from Lake Victoria (Kendall, 1969; Ssemmanda & Vincens, 2002) indicates a progressive decline in semi-deciduous forest and the establishment of open vegetation round Lake Victoria from about ca. 4100 to 3000 yr. BP. Areas around Lake Albert (Beuning *et al.*, 1997) registered an increase in semi-deciduous forest from ca. 3500 to 3000 yr. BP, while around Rwenzori Mountains, a decline in forest vegetation ca. 3000 yr. BP is evident from the pollen record (Livingstone, 1967) around ca. 3000 yr. BP.

Evidence of changes in forest composition during the mid Holocene is provided by pollen records from swamp sediments in the highlands of western Uganda (Hamilton, 1982; Taylor, 1988; 1990; 1992; Taylor *et al.*, 1999; Marchant, 1997). The records suggest an expansion of drier montane forest types composed of *Celtis*, *Olea* and *Podocarpus*. A reduction in forest vegetation ca. 3800 yr. BP is evident in pollen records from Burundi (Jolly *et al.*, 1994) and in Congo (Elenga *et al.*, 1994) from ca. 3000 yr. BP. Pollen data from Rwanda (Hamilton, 1982), Burundi (Bonnefille *et al.*, 1991; Jolly & Bonnefille, 1992; Jolly *et al.* 1994), and Ethiopia (Bonnefille & Mohammed, 1994), also registered a decline in forest vegetation from around ca. 3000 yr. BP.

The period after ca. 3000 to 2000 yr. BP is marked by a change to grassland vegetation around Lake Victoria (Kendall, 1969). Ssemanda & Vincens (2002) noted an extension

of dry montane forest, mainly *Juniperus procera* and *Podocarpus*, between ca. 3000 and 1700 yr. BP around Lake Victoria. Establishment of semi-deciduous forest was extensive around ca. 2200 yr. BP, but declined between ca. 1700 and 1100 yr. BP followed by increase in abundance of *Trema*-type and grasses, suggesting a shift to an open vegetation environment. In southern Uganda (Hamilton *et al.*, 1986; Taylor, 1988; 1992; 1993), forest degradation was registered at Muchoya swamp ca. 2200 yr. BP, while areas around Lake Kasende (Ssemmanda *et al.*, 2005), registered a progressive decline in forested conditions around ca. 1200 to 900 yr. BP. Pollen data from Lake Tanganyika (Vincens, 1989) after ca. 2500 yr. BP and in Burundi (Jolly *et al.*, 1994; 1997) indicate a decline in forest between ca. 2400 and 1400 yr. BP.

The onset of deforestation at Munsa approximately 900 yr. BP (cal 1032- 1217 AD) generally coincides with the archaeological evidence for the earliest phase of human occupation of the site (Robertshaw, 1997). Major forest clearance at Munsa and associated burning appear to have been part of much more widely felt changes in vegetation cover in western Uganda associated with human induced deforestation early in the second millennium AD. The deforestation at Munsa appears to have commenced about the same time as around Lake Kasenda (Ssemmanda *et al.*, 2005), but earlier than around Kabata swamp, where evidence of increased forest clearance was reported to have occurred around 400 yr. BP (cal 1432-1631 AD) (Taylor *et al.*, 1999; 2000). The timing of deforestation in western Uganda corresponds with archaeological data from major excavations in the region (Reid, 1991; Sutton, 1993; Robertshaw, 1997) and surveys (Reid, 1991; Robertshaw, 1994), as well as with historical linguistic evidence (Schoenbrun, 1993b; 1998), all of which indicate that there was considerable

immigration to the region at this time by people who were reliant on cattle and other forms of food production and thus demanding of land for farming.

The period of forest clearance corresponds with the period when central Africa was experiencing relatively dry climatic conditions (Verschuren *et al.*, 2000; Thompson *et al.*, 2002; Alin & Cohen, 2003). The onset of forest decline coincides with the timing of the Medieval Warm Period (MWP) of higher latitudes (cal 1000 to 1250 AD) (Bradley, 2000; Bradley *et al.*, 2003). Oxygen isotopes from Kilimanjaro ice core registered a period of reduced precipitation in the region, cal 1040 to 1100 AD (Thompson *et al.*, 2002), while ostracod data obtained from Lake Tanganyika (Alin& Cohen, 2003) registered low water levels between cal 1050 and 1250 AD. Lake Naivasha (Verschuren *et al.*, 2000) also experienced low water levels between cal 1000 and 1270 AD. In contrast, evidence of a prolonged period of increased aridity during the early part of the second millennium AD is absent from cores of sediment from Lake Edward (Russell *et al.*, 2003), and not apparent in records of Nile River levels (Herring, 1979; Hassan, 1981; Nicholson, 1998) that largely reflect Lake Victoria levels, and therefore rainfall in the Lake Victoria catchment (Nicholson, 1996a; 1998). Instead, Nile River discharge minima indicate relatively dry climatic conditions from cal 940-1040 AD, followed by a period of enhanced precipitation from approximately 1100 to 1200 AD.

The commencement of forest recovery at Munsa catchment dated to ca. 200 yr. BP (cal 1647-1948 AD) appears to have occurred during or shortly following a period of prolonged drought conditions recorded in many parts of central and eastern Africa (Nicholson, 1996a; 1998; Stager *et al.*, 1997; 1998; 2003; Verschuren *et al.*, 2000;

Thompson *et al.*, 2002; Alin and Cohen, 2003). This period of forest recovery corresponds to the later stages of the Little Ice Age (LIA) in higher latitudes from 1550 to 1850 AD (Bradley, 2000; Bradley *et al.*, 2003). During this period, many parts of central and eastern Africa were marked by recurrent droughts and famines. Webster (1979) and Nicholson (1998) reported the occurrence of severe droughts and famines dated to cal 1560-1625 AD (Nyarubanga) and cal 1760-1840 AD (Lapanarat-Mahlatule), although the precise dating of these droughts and famines has been questioned by some researchers (see Robertshaw *et al.*, 2005). The postulated droughts do appear to correspond to low water levels of the Nile River, however. The Nile River records indicates low water levels between cal 1520 and 1850 AD (Nicholson, 1998), with a brief phase of increased precipitation between cal 1770 and 1800 AD. Nicholson (1998) and Nicholson & Yin (2001) suggest that water levels in Lake Victoria increased from 1850 AD and peaked around 1880 AD, before dropping to lower levels. Lake Victoria water levels remained low until 1960, before rising to high levels as a result of increased precipitation in the region between 1961 and 1962 (Flohn, 1987; Conway, 2002).

The recovery of forest vegetation at Munsa could be due to reduced human impact, as this period appears to coincide with the phase of abandonment of the archaeological site at Munsa. According to archeological records (Robertshaw, 1997; Robertshaw & Taylor, 2000), Munsa archaeological site was abandoned around cal 1600 and 1700 AD, and was possibly part of a more general shift in settlement patterns from nucleated settlements to dispersed homesteads (Robertshaw, 1994). By late in the eighteenth century, much of western Uganda is reported to have been politically united into the kingdom of Bunyoro (Robertshaw, 1999a; Doyle, 2000) and was characterised by a

pastoralist, and mobile, nobility and a more sedentary agricultural peasantry. The exact reason for the abandonment of earthworks and the rise of the later kingdoms is not known (Robertshaw, 1994), and one possibility for the abandonment of the site at Munsa could be related to the death of the chieftain, who was reported to have been killed by his subjects, as recounted in the oral traditions (Lanning, 1959). One possible reason behind the social strife that may have led to the death of the chieftain at Munsa, to abandonment of the site, and to the changes in settlement patterns and socio-economic conditions more generally in the Interlacustrine highlands was increased environmental stress, due to the combined influence of increased frequency/prolonged droughts, over population and environmental degradation, including forest removal and soil exhaustion and erosion (see Taylor *et al.*, 2000).

In western Uganda, large grasslands areas that supported a large population of cattle and Basongora pastoralists was reported to have been abandoned from around 1890 AD (Ssemmanda *et al.*, 2005). This period is marked by recovery of moist semi-deciduous forest as recorded in sediments from Lakes Kasenda and Wandakara (Ssemmanda *et al.*, 2005). During this period, outbreak of local war and rinderpest were reported in the region. This period was followed by epidemics of sleeping sickness and nagana, which were widespread in Bunyoro (Doyle, 2000), reaching its peak from 1910 to 1920.

The presence of phytoliths from bananas and maize suggests that some agricultural activity continued in the catchment for Munsa II during this post-forest recovery period. This agricultural activity was presumably carried out by a relatively small population, when compared to the main period of occupation of Munsa site, of sedentary or shifting

cultivation, who continued to farm the area following the decline in the importance of the hill at Munsa (Bikegete) as a focus of settlement. During the 1800s AD, agriculture practices in Bunyoro were reported to be generally low (Doyle, 2000). Finger millet was the staple food crop cultivated in the region, with few domestic animals (Robertsaw, 1999). Agriculture in Bunyoro became increasingly important during the last century as a mechanism to cope with recurrent famine (Robertshaw *et al.*, 2005).

CHAPTER ELEVEN: CONCLUSIONS

SUMMARY OF DYNAMICS OF MUNSA II, ca. 5000 yr. BP TO THE PRESENT

11.1 Introduction

This chapter summarises the findings from this thesis. It presents the major environmental changes that occurred at Munsa archaeological site during the mid to late Holocene, and highlights the contribution of the findings to the understanding of the past environmental conditions at Munsa and in the wider region. Within this chapter, areas that require future investigations are highlighted.

11.2 Summary of sedimentary and vegetation dynamics at Munsa II, ca. 5000 yr. BP to the present

On the basis of sediment-based multi-proxy data from Munsa II swamp, the evidence suggests that significant environmental changes occurred at Munsa during the last ca. 5000 years.and particularly the last ca. 1000 years. The summary of these findings are presented below:

1. The changes in sedimentary composition (organic and inorganic sediments as well as the amount of charcoal), suggest that the development of papyrus-dominated swamp conditions at Munsa II may have been the result of a combination of factors, including human. Early accumulations of sediment at Munsa II largely comprise fluvial deposits of clay and sand-rich sediments. According to the sediment-based records analysed in this thesis, sedimentation

occurred first towards the centre of the valley (at M2C3C), and presumably in, or close to, the main drainage channel. However, sediment accumulation does not appear to have been continuous, it is likely that a major break (hiatus) in sedimentation between ca. 3000 and 1000 yr. BP was caused by increased discharge from the valley, possibly during a period of locally increased precipitation.

2. The accumulation of sediments rich in organic material, post-dating ca. 1000 yr. BP, marked the onset of a spread of sedge-dominated swamp conditions at Munsa II. It is likely that papyrus was one of the sedges involved in this expansion and that the spread of papyrus was influenced by reduced discharge from the valley, and may thus represent the onset of a lower level of effective precipitation that has been registered in the wider region of central and eastern Africa. It is also likely that human activities in the catchment could have facilitated an expansion of swampy conditions at Munsa II, as the spread of papyrus in the valley appears to correlate with the onset of deforestation, ca. 900 yr. BP (cal 1032 - 1217 AD), and with a major increase in human population levels. Deforestation associated with erosion in the catchment could have impended drainage from Munsa II leading to the spread of waterlogged, peat-accumulating conditions, and thus of papyrus swamp.

3. The pollen and phytolith records for core M2C3C suggest a period of relatively humid climatic conditions during the mid Holocene ca. 5000 yr. BP during which vegetation in the Munsa II catchment was characterised by mixed medium

altitude evergreen and semi-deciduous forest. Notwithstanding a sediment hiatus from ca. 2000 to 1000 yr. BP, little change in catchment vegetation is evident to ca. 900 yr. BP. It is likely that locally Munsa could have experienced climatically relatively wet conditions during this period, since such phases are registered in Nile River sediment records between ca. 5200 and 4400 and from ca. 3200 to 2500 yr. BP (Adamson *et al.*, 1980; Hassan, 1997)

4. The early part of the second millennium AD is marked by significant changes in vegetation in the Munsa II catchment in the form of a decline in forest in association with increased burning, which commenced ca. 900 yr. BP (cal 1032 - 1217 AD). These changes in vegetation coincide with archaeological evidence for major increases in human population levels and activities relating to the production of food and iron. The onset of deforestation at Munsa commenced about the same time as other parts in western Uganda, for instance around Lake Kasenda (Ssemmanda *et al.*, 2005), and the timing corresponds with archaeological data from excavations in the region that suggest formation of several major settlements of farming communities (e.g., Reid, 1991; Schoenbrun, 1993b; 1998; Sutton, 1993; Robertshaw, 1997). Deforestation at Munsa, particularly the burning of vegetation, may have been facilitated by climatic conditions, especially periods of reduced precipitation, as it coincides with the period when central and eastern Africa generally experienced reduced precipitation between ca. 1000 and 1270 AD (Verschuren *et al.*, 2000; Thompson *et al.*, 2002; Alin & Cohen, 2003). However, there is some uncertainty in climate conditions in the region at this time (Lejju *et al.*, in press),

and it is possible that locally Munsa experienced relatively wet climatic conditions, as evidence of a prolonged period of increased aridity during the early part of the second millennium AD is not apparent in Nile River levels (Herring, 1979; Nicholson, 1998). Instead, Nile River levels indicate a period of enhanced precipitation from approximately 1100 to 1200 AD.

5. Major increases in population levels at the site at Munsa, and possibly its first occupation, is marked by archaeological evidence of human activities, such as cultivation, cattle rearing and iron smelting (Robertshaw, 1997) This evidence is supported by sediment core-based information, in the form of the abundant presence of fungal spores (*Cercophora* and *Sporomiella*) associated with herbivore dung.

6. Sediment-based evidence of forest recovery at Munsa from ca. 200 yr. BP (cal 1647-1948 AD) concurs with evidence from archaeology and oral history for the abandonment of the site between cal 1600 and 1700 AD (Robertshaw, 1997). Other major settlements in the region, also appear to have been abandoned about the same time, leading to the emergence of pre-colonial states that were first described by early European visitors to the region in the mid 1800s AD (Robertshaw, 1999; Robertshaw & Taylor, 2000). Abandonment of the settlements may have been partly caused by a period of prolonged drought registered in the region from mid 1500s to 1700s AD. It is also likely that political instability and climate related phenomena such as droughts, famines and

diseases could have interacted to cause what amounted to dramatic changes in settlement and socio-economic conditions.

7. Sedimentary records from Munsa II attest the local presence of food plants as indicated by the occurrence of phytoliths produced by members of the Musaceae (both *Musa* and *Ensete*) from possibly as early as ca. 4500 yr. BP. It could be that bananas were being grown on forest margins and within relatively small forest gaps in the period preceding the main occupation phase at Munsa, although plants found naturally within surrounding areas of forest could have produced the phytoliths identified as *Ensete*. Recent discoveries of *Musa* phytoliths in West Africa, and archaeological evidence of early African cultivars in India as well as of early extra-African domesticates in Africa, provide a basis for tentatively accepting the cultivation of edible bananas of Asian descent at Munsa pre-dating ca. 4000 yr. BP. However, it is possible that phytoliths identified as *Musa* have been mis-identified, as the development of reliable morphological criteria that can be used to separate phytoliths from Musa from those from *Ensete*, to a high level of certainty, are still in their infancy.

8. The appearance of maize phytoliths and the continued presence of Musaceae phytoliths in the sediment records post ca. 150 yr. BP (cal 1667-1950 AD) suggest that some agricultural activity continued in the catchments for Munsa II during the post-forest recovery period, presumably carried out by relatively small populations of humans living in dispersed homesteads. The presence of maize phytoliths in sediment records during this period concurs with the evidence from

historical linguistics for its introduction to central and eastern Africa around 1600 AD (Wright, 1949; Philippson & Bahuchet, 1994-5).

11.3 Implications of the multi-proxy records in palaeoenvironments of central and eastern Africa.

The sediment data from Munsa II discussed in this thesis highlights the potential of a multi-core, multi-proxy approach to the study of environmental changes in the Interlacustrine highlands.

1. Based on the findings from this thesis, it is possible to detect human activities, such as cultivation and herding in the sediment record. These activities often leave no imprint on pollen records; thus the use of multi-proxy sources for future palaeoenvironmental studies in the Interlacustrine highlands of central Africa is highly recommended.

2. The palaeoenvironmental records from Munsa are from sites that are geographically close to archaeological and palaeoclimatic sources of evidence. The benefits of this approach are evident in the result, and in the relative ease of integrating very different sources of information into one interpretation.

3. The presence of Musaceae phytoliths in Munsa sediments merits further investigation, especially to confirm records that predate ca. 4000 yr. BP. This will require improved knowledge of the variability of Musaceae phytolith

morphotypes. For this to be achieved, a much greater range of type material than it has been possible to consult thus far will have to be collected, processed and analysed.

REFERENCES

Adams, M. E. (1996). Savanna environments. **In**: Adams, W. M., Goudie, A. S. & Orme, A. R. (editors), *The physical geography of Africa.* Oxford University Press, 198-210.

Adamson, D. A., Gasse, F., Street, F. A. & Williams, M. A. J. (1980). Late Quaternary history of the Nile. *Nature*, **288**: 50-55.

Ahmed, S. I. & Cain, R. F. (1972). Revision of the genera *Sporormia* and *Sporormiella*. *Canadian Journal of Botany*, **50**: 419-477.

Alexandra, G. (2001). Biomorphic analysis as a part of soil morphological investigation. *Catena*, **43**: 217-230.

Alexandre, A. & Muenier, J. D. (1999). Late Holocene phytolith and carbon record from a latosol at salitre, south-central Brazil. *Quaternary Research,* **51**: 187-194.

Alexandre, A. Meunier, J. D., Lezine, A. M., Vincens, A. and Schwartz, D. (1997). Grassland dynamics in the intertropical Africa during the late Holocene: a phytolith analysis. *Palaeogeography Palaeoclimatology and Palaeoecology*, **136**: 213-229.

Alin, S. R. & Cohen, A. S. (2003). Lake-level history of Lake Tanganyika, East Africa, for the past 2500 years based on ostracode-infferred water-depth reconstruction. *Palaeogeography Palaeoclimatology and Palaeoecology*, **199**: 31-49.

Atlas of Uganda (1967). *Department of lands and survey*. 2nd edition, Kampala, Uganda.

Aucour, A. M., Hillaire-Marcel, C. (1994). Late Quaternary biomass changes from ^{13}C measurements in a highland peatbog from equatorial Africa (Burundi). *Quaternary Research*, **41**: 225-233.

Barker, P., Telford, R., Merdaci, O., Williamson, D., Taieb, M., Vincens, A. & Gibert, E. (2000). The sensitivity of a Tanzanian crater lake to catastrophic tephra input and four millennia of climate change. *The Holocene*, **10**: 303-310.

Barboni, D. Bonnefille, Alexandre, A. & Meunier, J. D. (1999). Phytoliths as palaeoenvironmental indicators, west side Awash Valley, Ethiopia. *Palaeogeography, Palaeoclimatology, and Palaeoecology*, **152**: 87-100.

Bates, C. D., Coxon, P. & Gibbard, P. L. (1978). A new method for the preparation of clay-rich sediment samples for palynological investigation. *New Phytology*, **81**: 459–463.

Bender, M. M. (1971). Variations in the $^{13}C/^{12}C$ ratios of plants in relations to the pathway of photosynthetic carbon dioxide fixation. *Phytochemistry*, **10**: 1239-1244.

Bennet, K. D. (1998). *C programs for plotting pollen diagrams and analysing pollen data*. Quaternary Geology, Uppsala Universitet

Benninghoff, W. S. & Kapp, R. O. (1962). Suggested notation to indicate identification status of fossil pollen. *Pollen & spores*, **4**: 332.

Beuning, K. R. M., Talbot, M. R. & Kelts, K. (1997). A revised 30,000 – year palaeoclimatic and palaeohydrologic history of Lake Albert, East Africa *Palaeogeography Palaeoclimatology and Palaeoecology*, **136**: 259-279.

Bird, M. I. & Grocke, D. R. (1997). Determination of the abundance and isotope composition of elemental carbon in sediments. *Geochimica et Cosmochimica Acta,* 1**6:** 3413 – 3423.

Birks, H. J. B. (1986). *Numerical zonation, comparison and correlation of Quaternary pollen and stratigraphic-pollen data.* **In**: Berglund, B. E. (editor), *Handbook of Holocene Palaeoecology and Palaeohydrology*. Wiley and Sons, Chichester, 743-774.

Birks, H.J.B. & Birks, H. H. (1980). *Quaternary Palaeoecology*. 1st edition. Edward Arnold, London.

Birks, H. J. B. & Gordon, A. D. (1985). *Numerical methods in Quaternary pollen analysis*. Academic Press, London.

Bonnefille, R., Mohammed, U. (1994). Pollen-inferred climatic fluctuations in Ethiopia during the last 3000 years. *Palaeogeography, Paleoclimatology and Palaeoecology,* **109**: 331–343.

Bonnefille, R., Riollet, G. & Buchet, G. (1991). Nouvelle séquence pollinique du'une tourbière de la crête Zaïre-Nil (Burundi). *Review of Palaeobotany and Palynology*, **67**: 315-330.

Benninghoff, W. S & Kapp, R. O. (1962). Suggested notation to indicate identification status of fossil pollen *Pollen and Spores*, **4**: 332

Boutton, T. W., Archer, S. R., Midwood, A. L. Zitzer, S. F. & Bol, R. (1998). $\delta^{13}C$ values of soil organic carbon and their use in documenting vegetation change in a subtropical savanna ecosystem. *Geoderma*, **82**: 5-41.

Bowdery, D. (1989). *Phytolith analysis: introduction and applications, plants in Australian archaeology and material culture studies in anthropology*, Watson, Ferguson and Company, Brisbane.

Bowdery, D. (1998). *Phytolith analysis applied to Pleistocene- Holocene archaeological sites in the Australian arid zone*. BAR International series 695, Oxford OX2 7BP.

Boyd, M. (2002). Identification of anthropogenic burning in the palaeoecological record of the Northern Prairies: a new approach. *Annals of the Association of American Geographers*, **92**: 471-487.

Bradley, R. S. (2000). 1000 years of climate change. *Science*, **288**: 1353-1355.

Bradley, R. S., Hughes, K. & Diaz, H. F. (2003). Climate in Medieval time. *Science*, **302**: 404-405.

Bremond, L., Alexandre, A., Peyron, O. & Guiot, J. (2005). Grass water stress estimated from phytoliths in west in West Africa. *Journal of Biogeography*, **32**: 311-327.

Brown, D. A. (1984). Prospects and limits of a phytolith key for grasses in the central United States. *Journal of Archaeological Science*, 11: 345-368.

Butzer, K. W. (1980). The Holocene Lake plain of North Rudolph, East Africa. *Physical Geography*, **1**: 42-58.

Butzer, K. W. (1984). Long-Term Nile Flood variation and political discontinuities in Pharaonic Egypt. In Clark, J. D. & Brandt, S. A. (editors), *From hunters to farmers, the causes and consequences of food production in Africa.* Berkeley, University of California Press, 102-112.

Carrion, J. S., Scott, L. Huffman, T. & Dryer, C. (2000). Pollen analysis of Iron Age cow dung in southern Africa. *Vegetation History and Archaeology*, **9**: 239-249.

Casanova, J. & Hillaire-Marcel, C. (1992). Late Holocene hydrological history of Lake Tanganyika, East Africa, from isotopic data on fossil stromatolites. *Palaeogeography, Palaeoclimatology and Palaeoecology*, **91**: 35– 48.

Cerling, T. E. (1999). Palaeorecords of C_4 plants and ecosytems. **In** Saga, R. F. & Monson, R. K. (editors). *C_4 plant Biology*. Academic Press, London.

Clark, J. D. (1976). The domestication process in sub-Saharan Africa with special reference to Ethiopia. *Origine de l'élevage et de la domestication.* IXe Congrès UISPP: Nice, 56-115.

Clark, J. S. (1988a). Particle motion and theory of charcoal analysis: source area, transport, deposition and sampling. *Quaternary Research*, **30**: 67-80.

Clark, J. S. (1988b). Stratigraphic charcoal analysis on petrographic thin sections: application to fire history in northwestern Minnesota. *Quaternary Research*, **30**: 81-91.

Clark, J. S. & Hussey, T. C. (1996). Estimating the mass flux of charcoal from sedimentary records: effects of particle size, morphology and orientation. *The Holocene,* **6**: 129-144.

Clark, J. S. & Royall, P. D. (1995). Particle–size evidence for source areas of charcoal accumulation in the late Holocene sediments of Eastern North America lakes. *Quaternary Research*, **43**: 80-89.

Clark, R. L. (1982). Point - count estimation of charcoal in pollen preparations and thin section of sediments. *Pollen et Spores* **24**: 523–535.

Clark, R. L. (1984). Effects on charcoal of pollen preparation procedures. *Pollen et spores*. **26**: 599–576.

Coetzee, J. A. (1967). Pollen analytical studies in East and Southern Africa. *Palaeoecology of Africa*, **3** : 1-146.

Cohen, A. S. Talbot, M. R. & Awramik, S. M. Dettman, D. L. Abell, P. (1997). Lake level and palaeoenvironmental history of Lake Tanganyika, Africa, as inferred from late Holocene and modern stromatolites. *Geological Society of American Bulletin*, **109**: 444-460.

Collatz, G. J., Berry, J. A. & Clark, J. S. (1998). Effects of climate and atmospheric CO_2 partial pressure on the global distribution of C_4 grasses: present, past and future. *Oecologia*, **114**; 411-454.

Conway, D. (2002). Extreme rainfall events and lake level changes in East Africa: Recent events and historical precedents. *In* Odada, E. O. and Olago, D. O. (editors), *The East African Great Lakes: Limnology, Palaeolimnology and Biodiversity*. Kluwer Academic Publishers, Netherlands, 63-92.

Davis, O. K. (1987). Spores of the dung fungus *Sporormiella*: increased abundance in historic sediments and before Pleistocene megafaunal extinction. *Quaternary Research,* **28**: 290-294.

Davis, T. D., Brimblecombe, P. & Vincent, C. E. (1977). The daily cycle of weather on Mount Kenya. *Weather*, **32**: 406-417.

De Langhe, E., Swennen, R. & Vuylsteke D. (1995). Plantain in the early Bantu world. *Azannia*, **15**: 147-160.

de Menocal, P., Ortiz, J., Guilderson, T. and Sarnthein, M. (2000). Coherent high- and low-latitude climate variability during the Holocene Warm Period. *Science*, **288**: 2198-2202.

Denham, T. P., Haberle, S. G., Lentfer, C., Fullagar, R., Field, J., Therin, M., Porch, N., Winsborough, B. (2003). Origins of agriculture at Kuk Swamp in the highlands of New Guinea. *Science*, **301**: 189-193.

Doyle, S. (2000). Population decline and delayed recovery in Bunyoro, 1860-1960. *Journal of African History*, **41**: 429-458.

Eggeling, W. J. (1940). *The indigenous trees of the Uganda Protectorate*. Government Printer, Entebbe, 296pp.

Eggeling, W. J. (1947). Observations on the ecology of the Budongo rainfall forest, Uganda. *Journal of Ecology*, **34**: 20-87.

Elbaum, R. & Weiner, S. (2003). Detection of burning of plant material in the archaeological record by changes in the refractive indices of siliceous phytoliths. *Journal of Archaeological Science*, **30**: 217-226.

Elenga, H., Schwartz, D. & Vincens, A. (1994). Pollen evidence of late Quaternay vegetation and inferred climate changes in Congo. *Palaeogeography, Palaeoclimatology and Palaeoecology*, **109**: 345-356.

Ehleringer, J. R., Cerling, T. E. & Helliker, B. R. (1997). C_4 photosynthesis, atmospheric CO_2, and climate. *Oecologia*, **112**; 285-299.

Faegri, K. & Iverson, J. (1989). *Textbook of pollen analysis*. 4th edition, John Wiley & Sons, Chichester.

Fearn, M. L. (1998). Phytoliths in sediment as indicators of grass pollen source. *Review of palaeobotany and Palynology*. **103**: 75-81.

Ficken, K. J., Woller, M. J., Swain, D. L. Stree-Perrott, F. A. & Eglinton, G. (2002). Reconstruction of a subalpine grass-dominated ecosystem, Lake Rutundu, Mount Kenya: a novel multi-proxy approach. *Palaeogeography, Palaeoclimatology and Palaeoecology*, **177**: 137 – 149.

Flohn, H. (1987). East African rains of 1961/62 and the abrupt changes of the White Nile discharge. *Palaeoecology of Africa*, **18**: 3-18.

Flohn, H. & Nicholson, S. (1980). Climatic fluctuations in the arid belt of the Old World since the last glacial maximum; possible causes and future implications. *Paleoecolgy of Africa and the last surrounding islands*, **12**: 3-21.

Fredlund, G. G. & Tieszen, L. T. (1994). Mordern phytolith assemblages from the North American Great Plains. *Journal of Biogeography*, **21**: 321-335.

Fuller, D.Q. (2003). African crops in prehistoric South Asia: a critical review. **In**:. Neumann, K., Butler, A. and Kahlheber, S. (editors), *Food, Fuel and Fields: Progress in African Archaeobotany*. Africa Praehistorica 15. Cologne: Heinrich Barth Institute, 239-271.

Gasse, F. (2000). Hydrological changes in the African tropics since the Last Glacial Maximum. *Quaternary Science Reviews*, **19**: 189-211.

Geis, J. W. (1973). Biogenic silica in selected species of deciduous angiosperms. *Soil Science*, **116**: 113-119.

Gauch, H. G., Whittaker, R. H. & Wentworth, T. R. (1977). A comparative study of reciprocal averaging and other ordination techniques. *Journal of Ecology,* **65**: 157-174.

Gordon, A. D. (1982). Numerical methods in Quaternary palaeoecology, V. Simultaneous graphical representation of the levels and taxa. *Review of Palaeobotany and Palynology*, **37**: 155-188).

Gordon, A. D. & Birks, H. J. B. (1972). Numerical methods in Quaternary palaeoecology, 1 Zonation of pollen diagrams. *New Phytologist*, **73**: 221-249.
Goudie, A. S. (1996). Cliamte: past and present. **In**: Adams, W. M., Goudie, A. S. & Orme, A. R. (editors), *The physical geography of Africa,* Oxford University Press, 34-59.

Grove, A. T. (1986). Geomorphology of the African Rift System. **In**: Fronst, L. E., Renault, R. W., Reid, I. & Tiercelin, J. J. (editors), *Geological Society Special Publication* No. 25.

Haberyan, K. A. & Hecky, R. E. (1987). The late Pleistocene and Holocene stratigraphy paleolimnology of lakes Kivu and Tanganyika. *Palaeogeography, Paleoclimatology and Palaeoecology*, **61**: 169-197.

Hamilton, A. (1972). The interpretation of pollen diagrams from highland Uganda. *Palaeoecology of Africa*, **7**: 45-149.

Hamilton, A. C. (1976). Identification of East Africa Urtricaceae pollen. *Pollen et Spores*, **18**: 27-66.

Hamilton, A. (1982). *Environmental history of East Africa. A study of the Quaternary.* Academic Press, London, 328pp.

Hamilton, A. (1991). A field guide to Ugandan forest trees. Makerere University, Kampala, 279pp.

Hamilton, A. C., Taylor, D. & Vogel, J. (1986). Early clearance and environmental degradation in southwest Uganda. *Nature*, **320:** 164-167.

Hart, D. M. (1990). Occurrence of the 'Cyperaceaea-type' phytolith in dicotyledons. *Australian Systematic Botany*, **3**: 745-750.

Harrop, J. P. (1960). *The soils of the western province of Uganda*. Memoir No. 6. Research division of the Department of Agriculture, Uganda Series 1.

Hassan, F. A. (1981). Historical Nile Floods and their implications for climatic change. *Science*, **212**: 1142-1144.

Hassan, F. A. (1997). The dynamics of a riverine civilization: a geoarchaeological perspective on the Nile Valley, Egypt. *World Archaeology*, **29**: 51-74.

Hastenrath, S. 2001: Variations of East African climates during the past two centuries. *Climatic Change*, **50**: 209-217.

Hastenrath, S., Nicklis, A. and Greischar, L. 1993: Atmosptheric-hydrospheric mechanisms of climate anomalies in the western equatorial Indian Ocean. *Journal of Geophysical Research-Oceans*, **98** (C11): 20219-20235.

Henderson, J. P. (1949). Some aspects of climate in Uganda, with special reference to rainfall. *Uganda Journal*, **13**: 154-170.

Herring, R. S. (1979). Hydrology and chronology: The Rhodah Nilometer as an arid dating Interlacustrine History. **In**: Webster, J. B. (editor), *Chronology, Migration and Drought in Interlacustrine Africa*, 39-86.

Hillaire-Marcel, C., Aucour, A. M., Bonnefille, R., Riollet, G., Vincens, A. & Williamson, D. (1989). ^{13}C / Palynological evidence of differential residence times of organic carbon prior to its sedimentation in east African rift lakes and peat bogs. *Quaternary Science Reviews*, **8**: 207-212.

Hume, M. (1996). Climate change within the period of meteorological records. **In**: Adams, W. M., Goudie, A. S. & Orme, A. R. (editors), *The physical geography of Africa,*. Oxford University Press, 88-102.

Innes, J. B. & Blackford, J. J. (2003). The ecology of late Mesolithic woodland disturbances: model testing with fungal spore assemblage data. *Journal of Archaeological Science*, **30**: 185-194.

International code for phytolith nomenclature (ICPN, 1.0), (2003). *The Phytolitharien*, **15**: 1-10.

Johnson, T. C., Halfman, J. D. & Showers, W. J. (1991). Palaeoclimate of the past 4000 years at Lake Turkana, Kenya, based on the isotopic composition of authigenic calcite. *Palaeogeography, Palaeoclimatology and Palaeoecology,* **85**: 189-198.

Jolly, D. & Bonnefille, R. (1992). Histoire et dynamique du macrécage tropical de la Ndurumu (Burundi), données polliniques. *Review of Palaeobotany and Palynology*, **75**: 133-151.

Jolly, D. Bonnefille, R. & Roux, M. (1994). Numerical interpretation of a high resolution of Holocene record from Burundi. *Palaeogeography, Palaeclimatology and Palaeoecology,* **109**: 357-370.

Jolly, D. Taylor, D., Marchant, R., Hamilton, A., Bonnefille, R., Buchet, G. & Riollet, G. (1997). Vegetation dynamics in central Africa since 18,000 yr BP: Pollen records from the Interlacustrine highlands of Burundi, Rwanda and western Uganda. *Journal of Biogeography*, **24**: 495-512.

Kalgutker, R. M. & Jansonius, J. (1999). *Synopsis of fossil fungal spores, mycelia and fructifications*. ASSP Foundation, Dallas, USA.

Kealhofer, L. & Penny, D. (1998). A combined pollen and phytolith record for fourteen thousand years of vegetation change in northeastern Thailand. *Review of Palaeobotany and Palynology*, **103**: 83-93.

Kelly, E. F. Becker, S. W., Yonker, C. M. Olson, C. G. Wohl, E. E. & Todd, L. C. (1998). Stable isotope composition of soil organic matter and plant phytoliths as paleoenvironmental indicators. *Geoderma,* **82***:* 59-81.

Kendall, R. L. (1969). An ecological history of the Lake Victoria basin. Ecological *Ecological Monographs*, **39**: 121-176.

Kent, M. & Coker, P. (1992). *Vgetetaion description and analysis. A practical approach.* Belhaven Press, London, 363pp.

Kurmann, M. H. (1985). An opal phytolith and palynomorph study of extant and fossil soils in Kansas (USA). *Palaeogeography, Palaeoclimatology and Palaeoecology*, **49**: 217-235.

Kutzbach, J. E. & Stree-Perrott, F. A. (1985). Milankovitch forcing of fluctuations in the level of tropical lakes from 18 to 0 kyr BP. *Nature*, **317**: 130-134.

Laerdal, T., Talbot, M. R. & Russell, J. M. (2002). Late Quaternary sedimentation and climate in the lakes Edward and George area, Uganda-Congo. **In**: Odada, E. O. & Olago D. O. (editors). *The East African Great Lakes: Limnology, Palaeoliminology and Biodiversity*. Kluwer Academic Publishers. The Netherlands, 429-470.

Langdale-Brown, I. (1960). *The vegetation of the Western Province of Uganda.* Uganda Department of Agriculture Memoirs, Series 2, No. 4, 111pp.

Langdale-Brown, I., Osmaston, H. A. & Wilson, J. G. (1964). *The vegetation of Uganda and its bearing on land use*. Government of Uganda, 159pp.

Lanning, E. C. (1953). Ancient earthworks in Uganda. *Uganda Journal*, **17**: 51-62.

Lanning, E. C. (1955). The Munsa earthworks. *Uganda Journal*, **19**: 177-182.

Lanning, E. C. (1959). The death of chieftain Kateboha. *Uganda Journal*, **23**: 186-188.

Lanning, E. C. (1970). Ntusi: an ancient capital site of western Uganda. *Azania*, **5**: 39-54.

Lejju, B. J., Taylor, D. & Robertshaw, P. (in press). Holocene environmental variability at Munsa archaeological site, Uganda: a multi-core, multi-proxy approach. *The Holocene*.

Lentfer, C. J. & Boyd, w. B. (1999). An assessment of techniques for the deflocculation and removal of clays from sediments used in phytolith analysis. *Journal of Archaeological Science*, **26**: 31-44.

Lind, E. M. & Morrison, M. E. S. (1974). *East African Vegetation*, Longman ltd. London, 257pp.

Lind, E. M. & Tallantire, A. C. (1971). *Some common flowering plants of Uganda*. 2nd edition. Oxford University press. Nairobi, Kenya, 259pp.

Livingstone, D. A. (1967). Post-glacial vegetation of the Rwenzori mountains in equatorial Africa. *Ecological Monographs*. **37**: 25-32.

Livingstone, D. A. & Clayton, W. D. (1980). An altitudinal cline in tropical grass floras and its palaeoecological significance. *Quaternary Research*, **13**: 392-402.

Lowe, J. J & Walker, M. J. C. (1997). *Reconstructing Quaternary environments*. 2nd edition. Longman Group Ltd.

Maher, L. J. (1981). Statistics for microfossil concentration measurements employing samples spiked with marker grains. *Review of Palaeobotany and Palynology*, **64**: 153-191.

Maitima, M. J. (1997). Prehistoric fires and land-cover change in western Kenya: evidence from pollen, charcoal, grass phytoliths and grass cuticle analysises. *The Holocene*, **7:** 409-417.

Marchant, R. (1997). *Late Quarternary vegetation dynamics in Bwindi-Impenetrable forest, Central Africa.* Ph.D thesis, University of Hull, London.

Mbida, C. M., Doutrellepont, H., Vrydaghs, L., Swennen, R. L., Swennen, R. J., Beeckman, H., Langhe, E. & Maret, P. (2001). First archaeological evidence of banana cultivation in central Africa during the third millennium before present. *Vegetation History and Archaeobotany*, **10**: 1-6.

Mbida, C. M. (2000). Evidence for banana cultivation and animal husbandry during the first millennium BC in the forest of southern Cameroon. *Journal of Archaeological Science*, **27**: 151-162.

Mercader, J., Runge, F., Vrydaghs, L., Doutrelepont, H., Ewango, C. E. N. & Juan-Tresseras, J. (2000) : Phytoliths from archaeological sites in the tropical forest of Ituri. Democratic republic of Congo. *Quaternary Research*, **54**: 102-112.

Mistry, V. V. & Conway, D. (2003). Remote forcing of the East African lakes and relationships with fluctuations in levels of Lake Victoria. *International Journal of Climatology.* **23**: 67-89.

Moore, H. E. (1973). Palms in the tropical forest ecosystems of Africa and South America. In B. J. Meggers, E. S. Ayensu and W. D. Duckworth (editors), *Tropical forest ecosystems in Africa and South America: a comparative review,* Washington, D.C. Smithsonian Institution, 63-88.

Moore, P. D.; Webb, J. A. & Collinson, M. E. (1991). *Pollen analysis.* 2nd edition. Blackwell Scientific Publications, Oxford.

Morrison, K. D. (1994). Monitoring regional fire history through size-specific analysis of microscopic charcoal: The last 600 years in the south India. *Journal of Archaeological Science*, **21**: 675-685.

Morrison, M. E. S. (1968). Vegetation and climate in the uplands of south-western Uganda during the Later Pleistocene Period, 1. Muchoya swamp, Kigezi District. *Journal of Ecology*. **56**: 363-383.

Morrison, M. E. S. & Hamilton, A. C. (1974). Vegetation and climate in the uplands of south-western Uganda during the later Pleistocene period. *Journal of Ecology*, **62**: 1-31.

Munsell Colour Charts (2000). Revised edition. GretagMacbeth, New Windsor, New York.

Mulholland, S. C. (1992). A morphological classification of grass silica bodies, In Rapp, G., Mulholland, S. C. (editors), *Phytolith systematics. Enmerging Issue*s. Plenum Press, New York, 129-147.

Nichols, G. J.; Cripps, J. a.; Collinson, M. E. & Scott, A. C. (2000). Experiments on water logging and sedimentology of charcoal: results and implications. *Palaeogeography, Palaeoclimatology and Palaeoecology*, **164**: 43-56.

Nicholson, S. E. (1996a). A review of climate dynamics and climate variability in eastern Africa. **In**: Johnson, T. C. & Odada, E. O. (editors), *The limnology, Climatology and Paleoclimatology of the East African Lakes*. Gordon and Breach Publishers, The Netherlands.

Nicholson, S.E. (1996b). Environmental change within the historical period. **In**: W.A. Adams, A.S. Goudie and A.R. Orme (editors), *The Physical Geography of Africa*. Oxford, Oxford University Press, 60-87.

Nicholson, S.E. (1998): Historical fluctuations of Lake Victoria and other lakes in the northern Rift Valley of East Africa **In**: Lehman, J. T. (editor), *Environmental Change and Response in East African Lakes*. Dordrecht: Kluwer Academic, 7-35.

Nicholson, S.E. (2000). The nature of rainfall variability over Africa on the time scales of decades to millennia. *Global Planetary Change*, **26**: 137-158.

Nicholson, S. E. & Entekhapi, D. (1986). The quasi-periodic behaviour of rainfall variability in Africa and its relationship to southern oscillation. *Journal of Climate and Applied meteorology* **34**: 311-348.

Nicholson, S.E. & Flohn, H. (1980). African environmental and climatic changes and the general atmospheric circulation in late Pleistocene and Holocene. *Climatic Change*, **2**: 313-348.

Nicholson, S.E. & Kim, J. Y. (1997). The relationship of the El Nino Southern Oscillation to African rainfall. *International Journal of Climatology*, **17**: 117-135.

Nicholson, S.E. & Yin, X. (2001). Rainfall conditions in equatorial East Africa during the nineteenth century as inferred from the record of Lake Victoria. *Climatic Change* **48**: 387-398.

Nyamweru, C. K. (1996). The African Rift System. **In** Adams, W. M., Goudie, A. S. & Orme, A. R. (editors), *The physical geography of Africa.* Oxford University Press, 18-33.

Parker, R. & Epstein, S. (1960). Carbon isotope fractionation during photosynthesis. *Geochemica et Cosmochimica Acta*, **21**: 110-126.

Parr, J. F., Dolic, V., Lancaster, G. & Boyd, W. E. (2001). A microwave digestion method for the extraction of phytoliths from herbarium specimens. *Review of Palaeobotany and Palynology*, **116**: 203-212.

Patterson III, W.A., Edwards, V.J. and Maguuire, D.J (1987). Microscopic charcoal as an indicator of fire. *Quaternary Science Reviews,* **6**: 3-23.

Pearsall, D. M. (1978). Phytolith analysis of archaeological site: Evidence for maize cultivation in formative Ecuador. *Science*, **199**: 177 – 178.

Pearsall, D. M. (1989). *Palaeoethnobotany: A hand book of procedures*. 1st edition. Academic Press, San Diego.

Pearsall, D. M. (2000). *Paleoethnobotany. A handbook of procedures*. 2nd Edition. Academic Press. NY.

Pearsall, D. M. & Trimble, M. K. (1984). Identifying past agricultural activity through soil phytolith analysis: A case study from the Hawaiian Islands. *Journal of Archaeological Science*, **11**: 119-133.

Philippson, G. & Bachuchet, S. (1995). Cultivated crops and Bantu migration in central and eastern Africa: A linguistic approach. *Azania*, **30**: 103-120.

Phillips, J. & McIntyre, B. (2000). ENSO and interannual rainfall variability in Uganda: implications for agriculture management. *International Journal of Climatology*, **20**: 171-182.

Piperno, D. R. (1984). A comparison and differentiation of phytolitic from maize and wild grasses: Use of morphological criteria. *American Antiquity*, **49**: 361-381.

Piperno, D. R. (1985). Phytolitic analysis of geological sediments from Panama. *Antiquity*, **59**: 13-19.

Piperno, D. R. (1988). *Phytolith Ananlysis: An archaeological and Geological Perspective*. Academic Press Inc. California.

Posnansky, M. (1969). Bigo by Mugenyi. Uganda *Jouranal*, **33**: 125-150.

Reid, D. A. M. (1990). Ntusi and its hinterland: further investigations of the Later Iron Age and pastoral ecology in southern Uganda. *Nyame Akuma,* **33**: 26-28.

Reid, D.A.M. and Meredith, J. (1993). Houses, pots and more cows. The 1991 excavation in season at Ntusi: *Nyame Akuma,* **40**: 58-61.

Rhodes, A. N. (1998). A method for the preparation and quantification of microscopic charcoal from terrestrial and lacustrine sediment cores. *The Holocene*, **8**: 11-117.

Robertshaw, P. T. (1994). Archaeological survey, ceramic analysis, and state formation in Western Uganda. *African Archaeological Review,* **12**: 105-131.

Robertshaw, P. T (1997). Munsa Earthworks: A preliminary report on recent excavations. *Azania,* **32:** 1-20.

Robertshaw, P.T. (1999a). Women, labour, and state formation in Western Uganda. **In**: Bacus, E. and Lucero, L. (editors), *The development and organization of socio-political complexity in tropical environments.* Washington, Archaeological Papers of the American Anthropological Association Vol. 9, 51-65.

Robertshaw, P. T. (1999b). Seeking and keeping power in Bunyoro-Kitara, Uganda. **In**: McIntosh, S. K. (editor), *Beyond Chiefdoms: Conceptualising African Middle-Range Societies.* Cambridge, Cambridge University Press.

Robertshaw, P. & Taylor, D. (2000). Environmental change and the rise of political complexity in Western Uganda. *The journal of African History,* **41**: 1-28.

Taylor, D. and Robertshaw, P. (2001) Sedimentary sequences in western Uganda as records of human environmental impacts. *Palaeoecology of Africa*, **27**: 63-76.

Robertshaw, P., T Taylor, D., Doyle, S. & Marchant, R. (2005). Famine, climate and crisis in western Ugnada. **In**: Battarbee, R., Gasse, F. & Stickley, C. (editors), *Past climate variability through Europe and Africa. Developments in palaeoenvironmental research* Vol. 6. Kluwer, Amsterdam. 610pp.

Rossel, G. (1995). *Musa* and *Ensete* in Africa: taxonomy, nomenclature and uses. *Azannia*, **15**: 130-146.

Rovner, I. (1971). Potential of opal phytoliths for use in paleoecological reconstruction. *Quaternary Research*, **1**: 343-359.

Rovner, I. (1983). Plant opal phytolith analysis: Major advances in archaeological research. *Advances in Archaeological Methods and Theory*, **6**: 155-163.

Runge, F. P. (1995). Potential of opal phytoliths for use in palaoecolgical reconstruction in the humid tropics of Africa. *Z. Geomorph. N. F.* **99**: 53 - 64.

Runge, F. (1999). The opal phytolith inventory of soils in central Africa – quantities, shapes, classification and spectra. *Review of Palaeobotany and Palynology*, **107**: 23-53.

Russell, J. M., Johnson, T. C., Kelts, K. R., Laedal, T. & Talbot, R. M. (2003). An 11,000 -year lithostratigraphic and paleohydrologic record from Equatorial Africa: Lake Edward, Uganda-Congo. *Palaeogeography, Palaeoclimatology and Palaeoecology*, **193**: 25-49.

Schmidt, P. R. (1997). Archaeological views on a history of landscape change in East Africa. *Journal of African History*. **38**: 393-421.

Schmidt, P. R. & Childs, S. T. (1985). Innovation and industry during the Early Iron Age in East Africa: KM_2 and KM_3 sites in Northwest Tanzania. *African Archaeological Review*, **3**: 64-67.

Schoenbrun, D. L. (1993a). We are what we eat: Ancient agriculture between the Great Lakes. *Journal of African History,* **34**: 1-31.

Schoenbrun, D.L. (1993b): Cattle herds and banana gardens: the historical geography of the western Great Lakes region, ca. AD 800-1500. *African Archaeological Review*, **11**: 39-72.

Schoenbrun, D. L. (1998). *A green place, a good place. Agrarian change, gender and social identity in the great lakes region to the 15th century*. Heinemann Inc. Portsmouth, NH.

Scott, A. C., Cripps, J. A., Collinson, M. E., & Nichols, G. J. (2000). The taphonomy of charcoal following a recent heathland fire and some implications for interpretation of fossil charcoal deposits. *Palaeogeography, Palaeoclimatology and Palaeoecology*, **164**: 1-31.

Simmonds, N. W. (1966): *Banana*. London: Longman.

Smith, A. R. (1987). Euphorbiaceae (Part 1). In: Polhill, E. R. (editor) *Flora of Tropical East Africa*. Balkem, Rotterdam-Boston.

Smith, B. N. & Epstein, S. (1971). Two categories of $^{13}C/^{12}C$ ratios for higher plants. *Plant physiology*, **47**: 380-384.

Ssemmanda, I. & Vincens, I. (2002). Vegetation changes and their climatic implications for the lake Victoria region during the late Holocene. **In**: Odada, E. O. & Olago, D. O. (editors). The East African lakes: *Limnology, Palaeoliminoloy and Biodiversity*. Kluwer Academic Publisher. London.

Ssemmanda, I., Ryves, D., Bennike, O. & Appleby, P.G. (2005). Vegetation history in western Uganda during the last 1200 years: a sediment-based reconstruction from two crater lakes. *The Holocene,* **15**: 119-132.

Stager, J. C. (1998). *Ancient analogue for recent environmental changes at Lake Victoria, East Africa.* **In.** Lehman, J. T. (editors). *Environmental change and response in East African Lakes*. Kluwer Academic Publishers, Dordrecht, The Netherlands.

Stager, J. C. (2002). Cooling cycles, Heinrich event 1, and the desiccation of Lake Victoria. *Palaeogeography, Palaeoclimatology and Palaeoecology*, **183**: 169-178.

Stager, J. C., Cumming, B. & Meeker, L. (1997). A high resolution 11,400 – Yr diatom record from Lake Victoria, East Africa. *Quaternary Research*, **47**: 81-89.

Stager, J. C., Cumming, B. F. & Meeker, D. L. (2003). A high resolution record from Pilkington Bay, Lake Victoria, east Africa. *Quaternary Research*, **59**: 172-181.

Stockmarr, J. (1971). Tablets with spores used in absolute pollen analysis. *Pollen et Spores*, **13**: 615-621.

Stuiver, M., Reimer, P. J., Bard, R. E., Beck, J. W., Burr, G. S., Hughen, K. A., Kromer, B., McCormac, G., van der Plicht, J. and Spurk, M. (1998). INTCAL98 Radiocarbon age calibration, 24,000 -0 cal BP. *Radiocarbon*, **40** (3): 1041-1083.

Summerfield, M. A. (1996). Tectonics, geology and long-term landscape development. **In** Adams, W. M., Goudie, A. S. & Orme, A. R. (editors), *The physical geography of Africa.* Oxford University Press, 1-17.

Sutton, J. E. G. (1993). The antecedents of the Interlacustrine Kingdoms. *Journal of African History,* **34**: 33-64.

Sutton, J. E. G. (2000). Ntusi and Bigo. Farmers, cattle-herders and rulers in western Uganda, AD 1000 - 1500. British Institute in Eastern Africa, Nairobi, 34pp.

Talbot, M. R. & Livingstone, D. A. (1989). Hydrological index and carbon isotopes of lacustrine organic matter as lake-level indicators. *Palaeogeogrgaphy, Palaeoclimatology and Palaeoecology,* **80**: 283-300.

Taylor, D. (1988). *Environmental history of Southwest Uganda.* PhD. Thesis, University of Ulster, Colraine, UK.

Taylor, D. (1990). Late Quaternary pollen diagrams from two Uganda mires: evidence for environmental change in the Rukiga Highlands of Southwest Uganda. *Palaeogeogrgaphy, Palaeoclimatology and Palaeoecology,* **80**: 283-300.

Taylor, D. (1992): Pollen evidence from Muchoya swamp, Rukiga highlands (Uganda) for abrupt changes in vegetation during the last ca. 21,000 years. *Bulletin of Social Geography. France*, **163**: 77-82.

Taylor, D. (1993): Environmental change in montane southwest Uganda: pollen record for the Holocene from Ahakagyezi Swamp. *The Holocene,* **3**: 324-332.

Taylor, D.; Marchant, R. A. & Robertshaw, P. (1999). A sediment-based history of medium altitude forest in central Africa: a record form Kabata swamp, Ndale volcanic field, Uganda. *Journal of Ecology,* **87**: 303-315.

Taylor D., Robertshaw, P. & Marchant, R, A. (2000). Environmental change and socio-economic upheaval in pre-colonial, Western Uganda. *The Holocene,* **10**: 437-446.

ter Braak, C. J. F. (1990). *"Update Notes: CANOCO version 3.10" Agricultural Mathematics Group*. Wageningen, The Netherlands.

ter Braak, C. J. F. & Smilauer, P.(1998). *"Canoco Reference Manual and User's Guide to Canoco for Windows: Software for Canoco Community Ordination", Version 4. Microcomputer Power*, Ithaca, New York.

Thevenon, F., Williamson, D., Vicens, A., Taieb, M., Merdaci, O., Decobert, M. and Buchet, G. (2003). A late-Holocene charcoal record from Lake Masoko, SW Tanzania: climatic and anthropogenic implications. *Holocene*, **13**: 785-792.

Thompson, K. & Hamilton, A. C. (1983). Peatlands and swamps of the African continent. **In**: Gore, A. J. P. (editor) *Ecosystems of the world. Mires: swamp, bog, fen and moor. Regional studies*. Elsevier Scientific publishing Company, Amsterdam. 4B, 331-373.

Thompson, L. G., Mosley-Thompson, E., Davis, M. E., Henderson, K. A. Brecher, H. H., Zagorodnov, V. S., Mashiotta, T. A., Lin, P. N., Hardy, D. R., Beer, J. (2002). Kilimanjaro ice core records: evidence of Holocene climate change in tropical Africa. *Science,* **298**: 589-593.

Tinga, I. P. & Gibbs, M. (1982). *Crassulacean Acid Metablolism*. Waverly, Baltimore

Thorn, V. C. (2004). Phytolith evidence for C_4-dominated grassland since the early Holocene at Long Pocket, northeast Queensland, Australia. *Quaternary Research*, **61**: 168-180.

Tiercelin, J. J. & Lezzar, K. E. (2002). A 300 million years history of rift lakes in central and East Africa: An updated broad review. **In**: Odada, E.O. & Olago, D. O. (editors), *The East African Great Lakes: Liminology, Palaeoliminology and Biodiversity.* Kluwer Academic Publishers, Netherlands, 3-60.

Tieszen, L., Senyimba, M. M., Imbamba, S. K. (1979). The distribution of C_3 and C_4 grasses and carbon isotope discrimination along am altitudinal and moisture gradient in Kenya. *Oecologia*, **37**: 337-350.

Tomlinson, P. B. (1979). Systematics and ecology of the Palmae. *Annual Review and Systematics*, **10**: 85-107

Troel-Smith, J. (1955). Karakterisering af lose jordarter. Dan. Geol. *Unders. IV Raekke*, **3**: 1-73.

Twiss, P. C., Suess, E. & Smith, R. (1969). Morphological classification of Grass phytoliths. Proceedings: *Soil Science Society of America* **33**: 109-115.

Twiss, P. C. (1992). Predicted world distribution of C_3 and C_4 grass phytoliths. **In**: Rapp, G. Jr., Mulholland, S. C. (editors), *Phytolith Systematics. Emerging Issues.* Plenum New York, NY, 113-128.

van Geel, B. 1978. A palaeoecological study of Holocene peat bog sections in Germany and the Netherlands, based on the analysis of pollen, spores and macro- and microscopic remains of fungi, algae, cormophytes and animals. *Review of Palaeobotany and Palynology*, **25:** 1-120.

van Geel, B. (1986). Application of fungal and algal remains and other microfossils in palynological analysis. **In**: Berglund, B. E. (editor), *Handbook of Holocene Palaeoecology and Palaeohydrology,* Chichester: John Wiley, 497-505.

van Geel, B. (2001). Non-pollen palynomorphs. **In**: Smol, J. P., Birks, H. J. B. & Last, W. M. (editors), *Tracking environmental change using lake sediments. Volume 3: Terrestrial, algal and siliceous indicators*. Kluwer Academic Publishers, Dordrecht, The Netherlands. pp 1-21.

Van Geel, B. & Anderson, S. T. (1988). Fossil ascospores of the parasitic fungus Ustulina deusta in Eemian deposits in Denmark. *Review of Palaeobotany and Palynology*, **56**: 89-93.

van Geel, B., Hallewas, D. P. & Pals, J. P. (1982-83). A late Holocene deposit under the westfriese zeedijk near Enkhuizen (Province of Noord-Holland, the Netherlands): Palaeoecological and archaeological aspects. *Review of Palaeobotany and Palynology*, **38**: 269-335.

van Norton, F. (1979). The Early Iron Age in the Interlacustrine region. The diffusion of iron technology. *Azania*. **14**: 61-80.

Vansina, J. (1984). Western Bantu expansion. *Journal of African History*. **25**: 129-145.

Vansina, J. (2004). Banana in Cameroun ca. 500 BCE? Not proven. *Azania*, **38**: 174-176.

Vincens, A. (1989). Paléoenvironments du basin Nord-Tanganyika (Zaïre, Burundi, Tanzania) au cours des 13 derniers mille ans: apport de la palynologie. *Review of Palaeobotany and Palynology,* **61**: 69-88.

Verschuran, D., Laird, K. R. & Cumming, B. F. (2000). Rainfall and drought in equatorial east Africa during the past 1,100 years. *Nature*, **403**: 410-414.

Vrydaghs, L. & De Langhe, E. (2003). Phytoliths: an opportunity to rewrite history. INIBAB Annual Report, 14-17.

Waddington, J. C. B. (1969). A stratigraphic record of the pollen influx to a lake in the Big woods of Mimnnesota. *Geological Society of America, Special paper*, **123**: 263-282.

Walling, D. E. (1996). Hydrology and rivers. **In** Adams, W. M., Goudie, A. S. & Orme, A. R. (editors), *The physical geography of Africa.*. Oxford University Press, 103-121.

Webster, J. B. (1979). Noi! Noi! Famines as an aid to Interlacustrine chronology. **In** Webster, J. B. (editor), *Chronology, Migration and Drought in Interlacustrine Africa*. Longman Group Ltd, London, 1-37.

Website: http://www.geo.arizona.edu/palynology/apd.html. Access date: 24/12/2002.

Website: http://www.radiocarbon.com/analytic.htm. Access date: 04/11/2004).

Website: http://www.radiocarbon.com/labmethods.htm. Access date: 04/11/2004.

White, F. (1983). *The vegetation map of Africa. A descriptive memoir to accompany the UNESCO/AETFAT/UNSO vegetation map.* UNESCO, Paris, 356pp.

White, J. (1999). *Pollen, its collection and preservation for the microscope*. 2nd edition. Northern Biological Supplies Ltd. Martlesham Heath, Ipswich.

Whitlock, C. & Larsen, C. (2001). Charcoal as a fire proxy. **In**: Smol, J. P., Birks, H. J. B, & Last, W. M (editors), *Tracking environmental change using lake sediments. Volume 3: Terrestrial, algal and siliceous indicators*. Kulwer Academic Publishers, Dordrecht, The Netherlands, 75-97.

Wigboldus, J. S. (1995): The spread of crops into sub-equatorial Africa during the Early Iron Age. A 'minimalist' view based primarily on documentary evidence from the Indian Ocean side. *Azannia*, **15**: 121-129.

Willis, L. (2003). An overview of leaf phytolith production patterns in selected northern Australian flora. *Review of Palaeobotany and Palynology*, **125**: 201-248.

Wilson, S. M. (1985). Phytolith analysis at Kuk, an early agricultural site in Papua New Guinea. *Archaeology in Oceania*, **20**: 90-97.

Winkler, M. G. (1985). Charcoal analysis for paleoenvironmentlal interpretation: a chemical assay. *Quaternary Research*, **23**:313-326.

Wooller, M. J. (2002). Fossil grass cuticles from lacustrine sediments: a review of methods applicable to the analysis of tropical African lake cores. *The Holocene*, **12**: 97-105.

Wolf, F. A. (1966). Fungus of East African Lake sediments. *Bulletin of the Torrey Botanica Club*; **93**: 104-113.

Wright, A. C. A. (1949). Maize names as indicators of economic contacts. *Uganda Journal*, **13**: 61-81.

Young, H. & Young, T. (1983). Local distribution of C3 and C4 grasses in sites of overlap on Mount Kenya. *Oecologia*, **58**: 373-377.